



University of Kentucky
UKnowledge

University of Kentucky Doctoral Dissertations

Graduate School

2010

OPIOID-CANNABINOID CODRUGS WITH ENHANCED ANALGESIC AND PHARMACOKINETIC PROFILE

Harpreet Kaur Dhooper
University of Kentucky, hkdh002@uky.edu

[Right click to open a feedback form in a new tab to let us know how this document benefits you.](#)

Recommended Citation

Dhooper, Harpreet Kaur, "OPIOID-CANNABINOID CODRUGS WITH ENHANCED ANALGESIC AND PHARMACOKINETIC PROFILE" (2010). *University of Kentucky Doctoral Dissertations*. 98.
https://uknowledge.uky.edu/gradschool_diss/98

This Dissertation is brought to you for free and open access by the Graduate School at UKnowledge. It has been accepted for inclusion in University of Kentucky Doctoral Dissertations by an authorized administrator of UKnowledge. For more information, please contact UKnowledge@lsv.uky.edu.

ABSTRACT OF DISSERTATION

Harpreet Kaur Dhooper

College of Arts & Sciences

University of Kentucky

2010

OPIOID-CANNABINOID CODRUGS WITH ENHANCED ANALGESIC AND
PHARMACOKINETIC PROFILE

ABSTRACT OF DISSERTATION

A dissertation submitted in partial fulfillment of the requirement for the degree of Doctor of
Philosophy in the College of Arts & Sciences at the University of Kentucky

By

Harpreet Kaur Dhooper

Lexington, Kentucky

Director: Dr. Peter A. Crooks, Professor of Pharmaceutical Sciences

Lexington, Kentucky

2010

Copyright © Harpreet Dhooper 2010

ABSTRACT OF DISSERTATION

OPIOID-CANNABINOID CODRUGS WITH ENHANCED ANALGESIC AND PHARMACOKINETIC PROFILE

The central hypothesis of the dissertation is that “the design and synthesis of a codrug of an opiate and a cannabinoid can be achieved which is stable in the gastrointestinal tract and shows a superior pharmacological and pharmacokinetic profile when compared to a physical mixture of the two parent drugs.” To prove the hypothesis, a series of novel codrugs were prepared by conjugation of the opiate drug codeine with Δ^9 -tetrahydrocannabinol (Δ^9 -THC), cannabidiol, abn-cannabidiol and an opiate prodrug 3-O-acetylmorphine with Δ^9 -THC. Codeine-cannabinoid codrugs were evaluated for analgesic activity in the rat after oral administration. The Cod-THC codrug showed greater effectiveness as well as prolonged pain management properties as compared to the parent drugs. The stability of Cod-THC codrug in aqueous solutions from pH 1-9, in simulated gastrointestinal fluids, in brain homogenate and the hydrolysis of the carbonate ester linkage in rat plasma suggested that after oral administration, the codrug would be absorbed intact from the GI tract and then hydrolyze in the plasma to generate both parent drugs. The enzymes present in rat brain homogenate were incapable of cleaving the codrug into the parent drugs.

The pharmacokinetic profiles of the Cod-THC codrug and an equimolar physical mixture of the parent drugs were evaluated in rats. The plasma concentrations of codeine and Δ^9 -THC were much higher after codrug administration compared to the plasma concentrations of these drugs after oral administration of an equimolar physical mixture. The parent drugs were also present in the plasma for longer period of time compared to

the physical mixture, probably due to the sustained release of the parent drugs from codrug in the plasma. The concentrations of codeine and Δ^9 -THC were much higher in rat brain after oral administration of the Cod-THC codrug as compared to brain concentrations of these drugs after oral administration of the physical mixture. Thus, the design and synthesis of an opiate and a cannabinoid codrug was achieved which was stable in the gastrointestinal tract, showed enhanced analgesic effects as compared to the parent drugs, and also showed a superior pharmacokinetic profile when compared to a physical mixture or the two parent drugs.

KEYWORDS: Opioid, Cannabinoid, Codrug, Antinociception, Pharmacokinetics

Harpreet Dhooper

Date

OPIOID-CANNABINOID CODRUGS WITH ENHANCED ANALGESIC AND
PHARMACOKINETIC PROFILE

By

Harpreet Kaur Dhooper

Director of Dissertation

Director of Graduate Studies

Date

DISSERTATION

Harpreet Kaur Dhooper

College of Arts and Sciences

University of Kentucky

2010

OPIOID-CANNABINOID CODRUGS WITH ENHANCED ANALGESIC AND
PHARMACOKINETIC PROFILE

DISSERTATION

A dissertation submitted in partial fulfillment of the requirement for the degree of
Doctor of Philosophy in the College of Arts & Sciences at the University of
Kentucky

By

Harpreet Kaur Dhooper

Lexington, Kentucky

Director: Dr. Peter A. Crooks, Professor of Pharmaceutical Sciences

Lexington, Kentucky

2010

Dedication

To my parents

ACKNOWLEDGEMENTS

Foremost, I would like to express my sincere gratitude to my advisor Dr. Peter A. Crooks for the continuous support of my Ph.D study and research, for his patience, motivation, enthusiasm, and immense knowledge. His guidance helped me in all the time of research and writing of this thesis. I could not have imagined having a better advisor and mentor for my Ph.D study. I would like to thank all my advisory committee members, Dr. Stephen Testa, Dr. Abeer Al-Ghananeem, Dr. Joseph Holtman, Dr. Boyd Haley and Dr. Mark Watson for their time, and suggestions in designing some of the experiments.

I am grateful to Dr. Zaineb Albayati and Dr. Elzbeita Wala for helping me with all the animal work. I thank Dr. Malkawi for his help with the HPLC studies of the drugs. I would like to thank Dr. Jamie Horn and John May for their help with the LC-MS/MS studies. I am thankful to Dr. Peter Wedlund for helping me with pharmacokinetics. I would also like to thank my friend, Ujjwal Chakraborty for his constant support. He has always been a constant source of encouragement during my graduate study. Additionally, I am very grateful for the friendship of all of the members of Crooks' research group with whom I worked closely and puzzled over many problems.

I want to thank my father-in-law Dr. Surjit Singh Dhooper without whom I would never have been able to achieve so much. He has always been one of my best counselors. I also want to thank my mother-in-law, my husband and my kids, Mantegh and Sachleen for their moral support.

I am extremely thankful to my parents, the reason for my existence. I would like to dedicate this dissertation research to them. Without their sacrifice, blessings and encouragement it would have been impossible to reach this stage. I have no suitable words that can fully describe their everlasting love to me. Although they are no longer with me, they are forever remembered. I am sure they share our joy and happiness in the heaven. The support of my brother and sisters is also greatly appreciated.

TABLE OF CONTENTS

Acknowledgements	III
List of Figures	VIII
List of Schemes	XIV
List of Tables	XVI
Chapter 1. Objects of the Study and Literature Review	
1.1 Hypothesis	1
1.2 Overall Aim	1
1.3 Methodology to be utilized in this study	2
1.4 Literature Review	
1.4.1 Codrugs/Hybrid Drugs	3
1.4.2 Marketed Codrug	9
1.4.3 Codrug for the Treatment of Proliferative Diabetic Retinopathy	10
1.4.4 Codrug for the Simultaneous Treatment of Alcohol Abuse and Tobacco Dependence	15
1.4.5 L-DOPA Codrugs	23
1.5 Codrug strategy in pain management	
1.5.1 Opioids and Cannabinoids	28
1.5.2 Pharmacokinetics and Pharmacodynamics of Opioids	28
1.5.3 Pharmacokinetics and Pharmacodynamics of Cannabinoids	31
Chapter 2. Synthesis of Codrugs and Parent drugs	
2.1 Synthesis of Δ^9 -Tetrahydrocannabinol (Δ^9 -THC)	35
2.2 Synthesis of (-)-Cannabidiol (CBD)	36
2.3 Codeine- Δ^9 -Tetrahydrocannabinol (Cod-THC) Codrug Synthesis	47
2.4 Synthesis of the Codeine-(-)-Cannabidiol (Cod-CBD)	60

2.5 Synthesis of the Codeine-abnCannabidiol (Cod-abnCBD)	61
2.6 Synthesis of the 3- <i>O</i> -acetylmorphine- Δ^9 -tetrahydrocannabinol (AcMor-THC)	63
2.7 Experimental Section	7
Chapter 3. The Analgesic activities of Codrugs and their Parent Compounds	
3.1 Introduction	79
3.2 Methods and Materials	84
3.2.1 Animals	84
3.2.2 Drugs	84
3.2.3 Tail Flick test (Measure of analgesia/antinociception)	84
3.2.4 Chronic Constriction nerve injury (CCI, Neuropathic pain model)	86
3.2.5 Statistical analysis	86
3.3 Results	
3.3.1 Cod-THC codrug antinociception (tail flick tests)	87
3.3.2 Cod-THC codrug antihyperalgesic effect (CCI model)	92
3.3.3 ED ₅₀ values	99
3.3.4 Codeine-cannabidiol (Cod-CBD) codrug antinociception (tail flick test)	100
Chapter 4. In-vitro Stability Study of Cod-THC Codrug	
4.1 Introduction	102
4.2 Materials and Methods	
4.2.1 Drugs	104
4.2.2 Sample preparation	104

4.2.3 HPLC analysis	106
4.3 Results	
4.3.1 Assay Validation	107
4.3.2 Chemical and enzymatic stability study	109
4.3.3 Stability study in brain homogenate	110
Chapter 5. Pharmacokinetic Analysis of Cod-THC Codrug	
5.1 Introduction	114
5.1.1 Pharamacokinetic profile of Codeine and Δ^9 -THC	117
5.2 Materials and Methods	
5.2.1 Chemicals and reagents	119
5.2.2 Animals	119
5.2.3 Instrumentation	120
5.2.4 HPLC and mass spectrometric conditions	120
5.2.5 Plasma Pharmacokinetics	121
5.2.6 Standard curve and Quality control Validation Solutions	121
5.2.7 Extraction procedure	122
5.2.8 Brain Uptake study	122
5.2.9 Assay Validation	123
5.2.10 Pharmacokinetic Analysis	123
5.3 Results	124
5.3.1 Assay Validation	124

5.3.2 Dose-response curve analysis of Cod-THC codrug in plasma samples	130
5.3.3 Codrug and physical mixture data comparison after oral administration	136
5.3.4 Brain Uptake Study Results	140
Chapter 6. Summary	141
References	147
Vita	159

LIST OF FIGURES

Fig. 1.1 Examples of bipartate and tripartate codrugs	4
Fig. 1.2 Parenteral routes of drug administration	6
Fig. 1.3 Sultamicillin codrug and the <i>in vivo</i> hydrolysis products generated from the codrug	10
Fig. 1.4 Structures of THS, 5FU and the THS-BIS-5FU codrug	11
Fig. 1.5 Hydrolytic behavior of the THS-BIS-5FU codrug	14
Fig. 1.6 Cumulative release of THS and 5FU from neat pellets containing 2 mg of the THS-BIS-5FU codrug in bovine vitreous humor	14
Fig. 1.7 Structures of parent drugs NTX, NTXOL, BUP, BUPOH and codrugs NTX-BUPOH and CB-NTXOL-BUPOH	16
Fig. 1.8 Hydrolytic behavior of the NTX-BUPOH codrug	20
Fig 1.9 Hydrolytic profile of the carbonate drug hybrid, NTX-BUPOH, in isotonic phosphate buffer at pH 7.4	21
Fig 1.10 Hydrolytic profile of the carbonate drug hybrid, CB-NTXOL-BUPOH, in Guinea Pig Plasma at 37°C	22
Fig 1.11 Mean (\pm S.D.) plasma concentration profiles in guinea pigs after topical application of a gel formulation containing either CB-NTXOL-BUPOH or 6- β -Naltrexol	22
Fig.1.12 L-Dopa ester of entacapone	23
Fig. 1.13 (a) L-Dopa and α -lipoic acid codrug	24

(b) Dopamine and α -lipoic acid codrug	24
Fig. 1.14 (a) L-Dopa and Glutathione codrug	25
(b) Dopamine and Glutathione codrug	25
Fig. 1.15 Structures of (a) 3, 4-diacetyloxy-L-dopa methyl ester with caffeic acid (b) 3, 4-diacetyloxy-L-dopa methyl ester with carnosine	26
Fig. 1.16 Codrugs of L-Dopa linked to cysteine, methionine and bucillamine	26
Fig. 1.17 Codrug of L-Dopa with benserazide	27
Fig. 1.18 Structures of Morphine, Codeine and Endogenous Opioids	28
Fig. 1.19 Possible metabolic oxidation sites of Δ^9 -THC	32
Fig. 2.1 Single crystal X-ray structure of the selenoxide intermediate in the synthesis of Δ^9 -THC	35
Fig. 2.2 GC-MS of Δ^9 -THC	37
Fig. 2.3 GC-MS of (+)-Limonene oxide	38
Fig. 2.4 GC-MS of reaction mixture for the synthesis of 4-isopropenyl-1- methyl-2-(4-oxy-morpholin-4-yl)-cyclohexanol after 6 hrs and 24 hrs	40
Fig. 2.5 GC-MS of 4-isopropenyl-1-methyl-2-(4-oxy-morpholin-4-yl)- -cyclohexanol	41
Fig. 2.6 GC-MS of (<i>1S,4R</i>)-p-mentha-2,8-dien-1-ol	42
Fig. 2.7 GC-MS of the crude mixture from (-)-cannabidiol synthesis	43
Fig. 2.8 GC of synthesized (-)-cannabidiol	44
Fig. 2.9 MS of (a) synthesised (-)-cannabidiol	

(b) MS of a reference standard of (-)-cannabidiol	44
Fig. 2.10 GC of abn-cannabidiol	45
Fig. 2.11 (a) MS of abn-cannabidiol (b) MS of standard (-)-cannabidiol	46
Fig. 2.12 Structures of Morphine, Codeine (1), 3-Ethylphenol (2) and Δ^9 -THC (3)	47
Fig. 2.13 MALDI spectrum of codeine- <i>p</i> -nitrophenol carbonate	54
Fig. 2.14 HPLC chromatograms of different analytes (<i>p</i> -nitrophenol, codeine, Δ^9 -THC, codeine- <i>p</i> -nitrophenol carbonate)	54
Fig. 2.15 MALDI analysis of the Cod-THC codrug	58
Fig. 2.16 High resolution electron impact ionization mass spectrum of Cod-THC codrug	59
Fig. 2.17 HPLC chromatogram of Cod-THC codrug	59
Fig. 2.18 High-resolution electron impact ionization mass spectrum of Cod-CBD codrug	61
Fig. 2.19 LC-MS analysis of the Cod-CBD codrug	62
Fig. 2.20 High resolution electron impact ionization mass spectrum of cod-abnCBD Codrug	63
Fig. 2.21 GC-MS of 3-O-acetylmorphine (AcMor)	64
Fig. 2.22 ESI-MS of 3-O-acetylmorphine- <i>para</i> -nitrophenol carbonate (AcMor-PNP)	66
Fig. 2.23 High resolution electron impact ionization mass spectrum of 3-O-acetylmorphine- Δ^9 -tetrahydrocannabinol codrug	66

Fig. 2.24 ESI-MS of 3-O-acetylmorphine- Δ^9 -tetrahydrocannabinol codrug	67
Fig. 3.1 Nociceptive pain transmission	80
Fig. 3.2 Tail-Flick test	81
Fig. 3.3 Chronic Constriction Injury pain model	82
Fig. 3.4 Tail-Flick Latencies for Codeine and Cod-THC Codrug	88
Fig. 3.5 Antinociceptive Effect of Codeine and Cod-THC Codrug (5, 10, 20 mg/kg doses) in the Tail-Flick Pain Model	89
Fig. 3.6 Time-response Curves for the Cod-THC Codrug in the Tail-Flick Test	89
Fig. 3.7 Time-response (a) and dose-response (b) curves for Codeine in the Tail-Flick Pain Model	90
Fig. 3.8 Dose-Response Curves for the Antinociceptive Effects of Codeine-THC Codrug and Codeine Alone in the Tail-Flick Test	92
Fig. 3.9 Time-response (a) and dose-response (b) curves for codeine in the CCI model	94
Fig. 3.10 Antihyperalgesic effect of the Cod-THC codrug in the CCI Model	96
Fig. 3.11 Time-Action Curves for the Cod-THC Codrug in the Chronic Constriction Nerve Injury (CCI) Model	97
Fig. 3.12 Antihyperalgesic Effect of the Cod-THC Codrug in the Chronic Constriction Nerve Injury (CCI) Model	98
Fig. 3.13 Antihyperalgesic Effect of Codeine, THC and the Cod-THC Codrug in the Chronic Constriction Nerve Injury (CCI) Model	98

Fig. 3.14 Time-Response Curves for the Cod-CBD Codrug in the Tail-Flick Test	100
Fig. 3.15 Antinociceptive Effects of Codeine, Cannabidiol and the Cod-CBD Codrug in the Tail-Flick Test	101
Fig. 4.1 Standard curves for (a) Cod-THC codrug (b) Δ^9 -THC and (c) Codeine	107
Fig. 4.2 Hydrolysis of the Cod-THC codrug at different pHs (non-enzymatic hydrolysis)	109
Fig. 4.3 Hydrolysis of the Cod-THC codrug in different enzymatic solutions	110
Fig. 4.4 Hydrolysis of the Cod-THC codrug in rat plasma	111
Fig. 4.5 Hydrolysis of the Cod-THC codrug at pH 9.7	112
Fig. 5.1 Pharmacokinetic Parameters and their importance for dose regimen and dose size	115
Fig. 5.2 Concentration versus time curve in general	117
Fig. 5.3 Morphine, codeine, naltrexone, Cod-THC codrug and Δ^9 -THC Chromatograms	125
Fig. 5.4 Calibration curves for codeine, Δ^9 -THC and Cod-THC codrug in rat plasma	126
Fig. 5.5 Calibration Curves of codeine, Δ^9 -THC, Cod-THC codrug and morphine in rat trunk plasma	128
Fig. 5.6 Calibration Curves for codeine, Δ^9 -THC, Cod-THC codrug and morphine in brain homogenate	131

Fig. 5.7 Morphine peaks with concentrations 3000, 300 and 3 ng/mL	134
Fig. 5.8 Plasma concentration vs. time curve after oral administration of Cod-THC codrug (5, 10 and 20 mg/kg doses)	135
Fig. 5.9 Plasma concentration vs. time curve after oral administration of physical mixture of codeine (4.9 mg) and Δ^9 -THC (5.1 mg); Codrug 10 mg/kg	138
Fig. 5.10 Brain samples showing Codeine and Δ^9 -THC parent drugs	139

LIST OF SCHEMES

Scheme 1.1: (a) Synthesis of the chloroformate analogue of THS	12
Scheme 1.1: (b) Synthesis of THS-BIS-5FU codrug	13
Scheme 1.2: Syntheses of NTX-BUPOH and CB-NTXOL-BUPOH codrugs	17
Scheme 2.1: Synthesis of Δ^9 -THC	36
Scheme 2.2: Synthesis of (1 <i>S</i> ,4 <i>R</i>)- <i>p</i> -mentha-2,8-dien-1-ol	38
Scheme 2.3: Synthesis of (-)-cannabidiol and <i>abnormal</i> -cannabidiol	43
Scheme 2.4: Synthesis of a symmetrical carbonate of 3-ethylphenol	47
Scheme 2.5: Conjugation of two different phenolic compounds utilizing triphosgene	48
Scheme 2.6: Synthesis of an unsymmetrical carbonate of 4-ethylphenol and 5,6,7,8-tetrahydro-2-naphthol	49
Scheme 2.7: Synthesis of an unsymmetrical carbonate of 4-ethylphenol and 5,6,7,8-tetrahydro-2-naphthol utilizing triethylamine	49
Scheme 2.8: Synthesis of an unsymmetrical carbonate of 4-ethylphenol and 3-quinuclidinol	50
Scheme 2.9a: Synthesis of carbonate of 3-quinuclidinol and <i>p</i> -nitrophenol	51
Scheme 2.9b: Synthesis of unsymmetrical 3-quinuclidinol-codeine carbonate	51
Scheme 2.10: Synthesis of unsymmetrical carbonate of codeine and 3-quinuclidinol via the intermediacy of codeine- <i>p</i> -nitrophenol carbonate	52

Scheme 2.11: Formation of carbonate of codeine and <i>p</i> -nitrophenol using triethylamine	52
Scheme 2.12: Formation of carbonate of codeine and <i>p</i> -nitrophenol using DMAP	53
Scheme 2.13: Synthesis of carbonate of codeine and Δ^9 -THC	55
Scheme 2.14(a): Synthesis of unsymmetrical carbonate of codeine and 4-ethylphenol utilizing microwave irradiation	55
Scheme 2.14(b): Synthesis of unsymmetrical carbonate of codeine and 5,6,7,8-tetrahydro-2-naphthol utilizing microwave irradiation	56
Scheme 2.14(c): Synthesis of unsymmetrical carbonate of codeine and Δ^9 -THC utilizing microwave irradiation	57
Scheme 2.15: Synthesis of unsymmetrical carbonate of codeine and Δ^9 -THC utilizing a stronger base (NaH)	58
Scheme 2.16: Synthesis of carbonate of codeine and (-)-cannabidiol	60
Scheme 2.17: Synthesis of carbonate of codeine and <i>abnormal</i> -cannabidiol	61
Scheme 2.18(a): Synthesis of 3- <i>O</i> -acetylmorphine	65
Scheme 2.18(b): Synthesis of 6- <i>O</i> -carbonate of 3- <i>O</i> -acetylmorphine and <i>para</i> -nitrophenol	65
Scheme 2.18c: Synthesis of 3- <i>O</i> -acetylmorphine- Δ^9 -tetrahydrocannabinol carbonate	65

LIST OF TABLES

Table 1.1 Physicochemical Properties of NTX (1), NTXOL (2), BUPOH (4) and the carbonate codrugs, NTX-BUPOH (25) and CB-NTXOL-BUPOH (26)	19
Table 1.2 Pharmacokinetic parameters of NTXOL in the Guinea pig after application of a gel formulation containing either CB-NTXOL-BUPOH or NTXOL base	21
Table 3.1 AUCs for 5, 10, and 20 mg/kg doses of Cod-THC Codrug	91
Table 3.2 AUCs for 2.5, 5 and 10 mg/kg Cod-THC Codrug (CCI model)	98
Table 3.3 ED ₅₀ values for the Cod-THC codrug and codeine	99
Table 4.1 Rate constants for the hydrolysis of the Cod-THC codrug in pH 9.7 buffer and 80% Rat plasma at 37 °C	111
Table 5.1 (a) Pharmacokinetic parameters for the Cod-THC codrug, codeine and Δ^9 -THC after 5, 10, 20 mg/kg oral dosing	136
Table 5.1 (b) Calculated clearance values for the Cod-THC codrug, codeine and Δ^9 -THC	136

Chapter 1

Object of the Study and Literature Review

1.1 Hypothesis

The hypothesis to be tested in this dissertation work is as follows: *the design and synthesis of a codrug comprising an opiate drug and a cannabinoid drug can be achieved which is stable in the gastrointestinal tract, and exhibits a superior pharmacological and pharmacokinetic profile when compared to an equimolar physical mixture of the two parent drugs.*

1.2 Overall Aim

There is a continuing need for analgesic medications that are able to provide high efficacy pain relief while providing more favorable pharmacokinetics and reducing the possibility of undesirable side effects. Enhancement of the analgesic effect of opioids by combination with cannabinoids has been previously described (Cichewicz et al., 1999). These opioid and cannabinoid drugs target opioid and cannabinoid receptors, which are found throughout the central and peripheral nervous system (Cichewicz et al., 1999; Cichewicz and McCarthy, 2002). In addition, these two classes of drugs produce similar effects on calcium levels and cyclic AMP accumulation through G protein-mediated pathways (Bloom and Dewey, 1978). However, appropriate dosing of these active agents to deliver the drug(s) to the site of action, e.g., the brain or spinal column, can be difficult because of their differential pharmacokinetics. Therefore, there is a need to devise a way of administering opioids and cannabinoids concomitantly to provide a more favorable pharmacokinetic profile for optimizing the enhancement of the analgesic effects.

1.3 Methodology to be Utilized in this Study

- To synthesize codrugs comprising one opioid molecule, and one cannabinoid molecule, both covalently bound via a linker that is capable of cleaving to the parent drugs in the body. The two drugs will be connected by means of a cleavable covalent linker (e.g. ester, carbonate, amide, carbamate, etc.), which should hydrolyze in vivo to generate the active parent drug entities.
- To evaluate the chemical and enzymatic stabilities of one of the codrugs, in order to determine its stability to hydrolysis in aqueous media over a range of pHs, and its stability in simulated gastric and intestinal fluids, rat plasma, and rat brain, utilizing a stability-indicating HPLC-UV assay.
- To provide a codrug with improved drug stability, as well as improved targeting of parent drugs to the site of action (central nervous system) as compared to a physical mixture of the parent drugs.
- To provide a codrug with more desirable pharmacokinetic properties, in particular for drugs with different physicochemical properties (e.g. differences in lipid solubility, water solubility, polarity, etc.). To determine rat plasma and brain concentrations of codrug and parent drugs after oral administration of one of the codrugs. To determine the bioavailability of the codrug, and to compare these properties with those of a physical mixture of the parent drugs after oral and iv administration, utilizing an LC-MS/MS analytical methodology.
- To provide a codrug that has the potential for treating patients in pain with an opioid analgesic, that affords prolonged and effective pain management, while at the same time providing the opportunity to reduce the side effects, dependence, and tolerance that patients usually experience when subjected to prolonged treatment with opioids.
- To provide a codrug which, after oral administration, produces a superior analgesic response to pain (acute, chronic and/or cancer-related) as compared to the response from a physical mixture of the two parent drugs.

1.4 Literature Review

1.4.1 Codrugs/Hybrid Drugs

There are instances in prodrug design where the prodrug molecule incorporates two identical or non-identical drugs into a single chemical entity. This is often desirable when two synergistic drugs have different physicochemical and pharmacokinetic properties, and it is desirable to have the parent drugs released concomitantly at the site of action to obtain a synergistic pharmacodynamic effect that is not attainable by delivering a physical mixture of the two drugs. Also, one of the drugs in the codrug structure may be incorporated to counterbalance the known side-effects associated with the other parent drug, or may amplify the pharmacodynamic effect of the other parent drug through an action at another biological target. Thus, codrugs can be designed to overcome various barriers to drug formulation and delivery, such as poor aqueous solubility, chemical instability, insufficient oral absorption, rapid pre-systemic metabolism, inadequate brain penetration, toxicity and local irritation. Structurally, a codrug (also known as a mutual prodrug, or hybrid drug) comprises two or more different drugs within a single chemical entity where the drugs must each contain an appropriate chemical functionality to enable them to be connected together, either directly or by means of a cleavable, biolabile covalent linker (Hamad et al., 2006). Such codrugs can be either bipartate or tripartate in nature (Silverman, 2004) (Fig.1.1).

Thus, a codrug strategy can be useful when:

- Synergistic drugs need to be given concomitantly to act at the same time, either at the same or different biological targets.
- The physicochemical properties of two synergistic drugs are not favorable for delivery of the two drugs as a physical mixture, but can be improved by chemical combination of the two drugs.

- Improved pharmacokinetics results from a chemical combination of two synergistic drugs compared to those of a physical mixture of the two drugs.

As with prodrugs, the codrug structure can incorporate two drugs joined together by linker moieties such as ester, carbonate, amide, carbamate, etc., which are then cleaved enzymatically *in vivo* to release the active drugs at a required site in the body. By appropriate structural design of these linkers, it may be possible to control the release kinetics of one or both drugs. When the two drugs are chemically combined together, the resulting codrug will usually have different physicochemical properties to those of the individual parent drugs, which may provide superior properties for delivery of the two drugs when compared to delivery of a physical mixture of the drugs (Howard et al., 2007).



Fig. 1.1 Examples of bipartate and tripartate codrugs: A) conjugation of a carboxylic drug with an alcoholic drug to form a bipartate codrug where the two drugs are connected by an ester linkage which cleaves *in vivo* to release only the two parent drugs; B) conjugation of two alcoholic drug molecules via a carbonate ester linker to form a tripartate codrug which cleaves *in vivo* to form the two parent drugs and an equivalent of carbonic acid.

An ideal codrug will generate the parent drugs with high recovery rates, and will incorporate linkers that give rise to non-toxic linker residues upon *in vivo* cleavage. There may be other advantages in delivering of two drugs as a single chemical entity *versus* a physical mixture. These include, for example, improved chemical stability of the formulation (i.e. no chemical interaction of the two parent drugs within the formulation), improved metabolic stability (especially with regard to possible protection of either drug from high first pass metabolism), as well as improved targeting of drugs to the site of

action (e.g., the central nervous system), and more desirable pharmacokinetic properties, in particular for drugs with different physicochemical properties (e.g., differences in lipid solubility or polarity).

There are also certain disadvantages that are associated with a codrug strategy. One disadvantage is that codrugs are usually large molecules with molecular weights that are often greater than 500. Thus codrugs with large molecular weights may well violate Lipinsky's rule of five (Lipinski et al., 2001) as favorable molecules for oral or topical dosage form development, or for CNS delivery. In addition, by the very nature of their structural design, these cleavable molecules may possess poor stability profiles for formulation development. Thus, it must be initially established that the codrug is resilient enough to withstand the rigors of formulation development, but must not be too stable that it will not efficiently cleave to the parent drugs *in vivo*.

Another important aspect of codrug design is the toxicological significance of delivering a codrug to an individual. Since codrugs are novel chemical entities (although the parent drugs they generate may or may not be novel), they will have to be treated as new xenobiotics by the FDA, as are all new drugs entities that have never been previously administered to humans. Thus, there are important toxicological and safety issues associated with the development of codrugs as they move toward clinical status.

Several important criteria are required for codrugs to be effective. The codrug must be well absorbed and distribution, metabolism and elimination of the codrug should be superior to the physical mixture of the parent drugs. Both parent drugs should be released concomitantly and quantitatively after absorption, and the maximal effect of the drug combination should occur when a simple molar ratio, i.e. 1:1, 2:1, or 3:1, is utilized.

Before designing the codrug, one needs to know the route of administration. Routes of administration can be broadly divided into topical, enteral and parenteral routes. The topical route has a local drug effect. The drug is directly applied where the action is desired, e.g. asthma medications, eye or eardrops, and decongestant nasal

sprays. In the enteral route, drug administration involves any part of the gastrointestinal tract. The effect is non-local. Sublingual, oral and rectal are all enteral routes. In sublingual administration, the drug is placed under the tongue, is rapidly absorbed and avoids first-pass metabolism. The first-pass effect term refers to the hepatic metabolism of a drug when it is absorbed from the gastrointestinal tract and delivered to the liver via the hepatic portal circulation. The greater the first-pass effect, the lower the concentration of drug that reaches the systemic circulation. In the oral (p.o., per os) route, the drug is swallowed. It passes through the whole gastrointestinal tract. Drugs taken orally are usually cheaper than ones administered by any other route, and can easily be self-administered (minimal invasiveness) by the patient. The disadvantage of oral delivery is that the drug has to be absorbed from the gastrointestinal tract and go through the first pass effect. Sometimes this route of administration is inefficient because only part of the drug may be absorbed; also a significant first-pass effect may occur. In addition, some orally administered drugs can cause irritation of the gastric mucosa, and cause nausea and vomiting.

The different parenteral routes for drug administration are intravenous, intraarterial, intramuscular and subcutaneous, and more rarely, intracerebral (i.e. directly into the brain), intraosseous (into the bone marrow), or intradermal (into the skin itself). These different parenteral routes are depicted in Fig. 1.2 (Copeland, 2009).

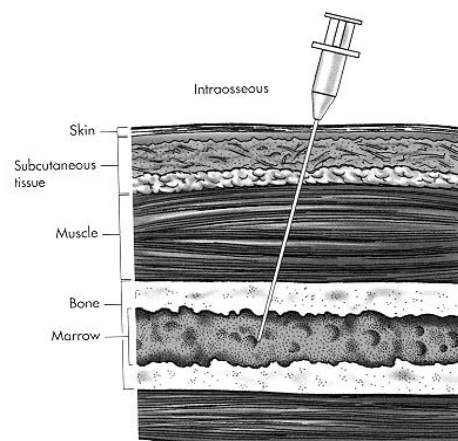


Fig. 1.2 Parenteral routes of drug administration (Copeland, 2009)

Times taken by drugs to show effect in different routes of administration are given below:

- intravenous 30-60 seconds
- inhalation 2-3 minutes
- sublingual 3-5 minutes
- intramuscular 10-20 minutes
- subcutaneous 15-30 minutes
- rectal 5-30 minutes
- ingestion 30-90 minutes

Note: drugs given orally take more time than any other route to show a pharmacological response, but the oral route is considered to be the safest, pain free and cheapest method of drug administration. Other routes are used if there is an emergency situation where the effect of the drug is needed in seconds (Silverman, 2004).

Several important criteria are required for codrugs to be effective as compared to a physical mixture of the parent drugs, or either of the parent drugs alone. The codrug must be well absorbed. When a drug enters the body, it encounters a wide range of pHs. A drug given orally faces low pHs in the range 1-2 in the stomach, pHs around 4-6 in the intestine, and pHs in the range 5-9 in the colon. These pH values vary in the body, depending on the presence of an empty stomach or a fed stomach. The pH values generally increase after food is ingested. For example, if the pH of the empty stomach is around 1-2, then after the food is taken, it will increase to around 2.5-4. If a codrug can survive in this pH range and reach the plasma without being hydrolyzed, it can reach the plasma intact, and with appropriate design can release the parent drugs after hydrolysis by plasma enzymes. The codrug will also be exposed to various enzymes in the gastrointestinal tract which may hydrolyze the codrug to release the parent drugs before the codrug reaches the systemic circulation. Therefore, important insights can be obtained from incubating the codrug with simulated gastrointestinal fluids in *in vivo* stability

studies before carrying out more expensive and time-consuming *in vivo* pharmacokinetic studies. These include stability in simulated gastric fluid (SGF) and simulated intestinal fluid (SIF). These fluids are specified in the United States Pharmacopeia (USP). The SGF components are pepsin (an acidic protease) and NaCl, and the pH is adjusted to 1.2 with HCl. SGF simulates stomach fluid and incorporates both acidic and enzymatic hydrolysis conditions. The SIF components are pancreatin (a mixture of amylase, lipase and protease from hog pancreas) in monobasic phosphate buffer and the pH is adjusted to 6.8 with NaOH. SIF mimics the pH and hydrolytic enzymes in the intestine. The main purpose of these stability studies is to predict stability of the codrug after oral dosing. The codrug's stability in these two fluids can often be a guide on how to structurally modify the codrug to improve gastrointestinal stability. This information helps in optimizing codrug bioavailability and prioritization of compounds for subsequent *in vivo* pharmacokinetic studies.

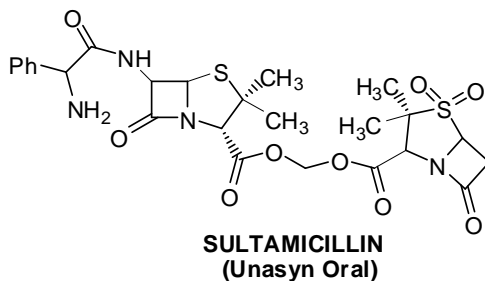
Once the drug reaches the systemic circulation, it encounters a large number of hydrolytic enzymes, such as cholinesterase, aldolase, lipase, dehydropeptidase, and alkaline and acid phosphatase in the blood. If the drug has affinity for one of these enzymes and it has the correct hydrolysable group in an appropriate position in the molecule, it can be degraded in the plasma to generate the parent drugs. In a codrug strategy, *in vitro* plasma stability studies are important and help identify a codrug with the optimal properties for releasing the active parent drugs after absorption from the g.i. tract. Therefore, it is very important to carry out the *in vitro* plasma stability studies before embarking on the *in vivo* pharmacokinetic study. This will ensure that compounds are subsequently investigated *in vivo* that are most likely to be successful therapeutics (Kern and Di, 2008).

Also, both conjugated drugs should be released concomitantly and quantitatively after absorption from the gastrointestinal tract. The maximal effect of the combination of the two drugs should occur at a simple ratio, i.e. 1:1, 2:1, or 3:1, and the distribution and elimination of the codrug should be superior to the physical mixture of the parent drugs (Cynkowska et al., 2005).

The codrug can exert its action in two different ways. One way is absorption from the gastrointestinal tract into the systemic circulation as a single chemical entity followed by cleavage in the plasma and release of the two parent drugs. The other way is to reach the site of action first, e.g. the brain, and then undergo cleavage to the parent drugs via the action of site-specific enzymes present in the target tissue. With regard to brain delivery, small codrug molecules with high lipid solubility and a low molecular mass of less than 400–500 Daltons will cross the blood-brain barrier (Pardrige, 2001), and such codrugs can be designed to contain a linker that can be cleaved specifically by brain enzymes. Alternatively, a codrug can be designed in such a way (i.e. molecular weight exceeding 500) that it will not be able to cross the blood-brain barrier, but can deliver the parent drugs to the brain after release from the codrug in the plasma.

1.4.2 Marketed Codrug

A good example of an effective and marketed codrug is the antibiotic sultamicillin (Unasyn Oral), a tripartate codrug of ampicillin and penicillanic acid sulfone (Fig. 1.3) (Baltzer et al., 1980; Hartley and Wise, 1982). Ampicillin is a well-known β -lactam antibiotic, but suffers from ineffectiveness against resistant bacteria that excrete high concentrations of the bacterial enzyme, β -lactamase. β -Lactamase degrades penicillins such as ampicillin by hydrolysis of the β -lactam ring with consequent loss of antibacterial activity. Subsequent co-administration of a β -lactam antibiotic with a β -lactamase inhibitor was utilized as a strategy for treating resistant strains of bacteria. For example, the antibiotic Augmentin is a mixture of the β -lactam penicillin, amoxicillin and the β -lactamase inhibitor, potassium clavulinate (Fig. 1.3). One of the problems of administering the two synergistic drugs together (as a physical mixture) is that they may not have similar pharmacokinetic profiles, and thus may not arrive at the target site at the same time or at the same concentration. The codrug sultamicillin incorporates a labile linker, which on hydrolysis by a plasma esterase affords the two synergistic parent drugs in equimolar amounts together with a molar equivalent of formaldehyde.



A DRUG HYBRID OF AMPICILLIN AND PENICILLANIC ACID SULFONE

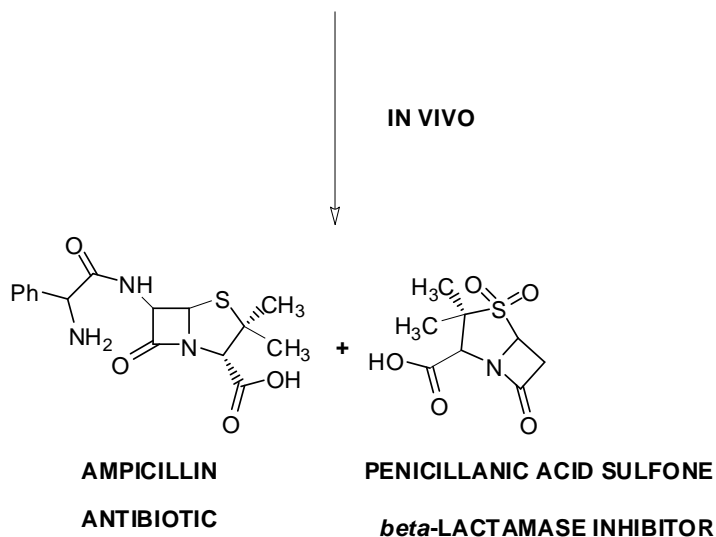


Fig.1.3 Sultamicillin codrug and the *in vivo* hydrolysis products generated from the codrug (Baltzer et al., 1980; Hartley and Wise, 1982).

1.4.3 Codrug for the Treatment of Proliferative Diabetic Retinopathy

The codrug strategy has previously been utilized when the physicochemical and/or pharmacokinetic properties of two synergistic drugs are not favorable for delivery of the two drugs as a physical mixture, but can be improved by chemical combination of the two drugs. For example, 5-fluorouracil (5-FU) is a polar, water-soluble antiviral and cytotoxic drug that is rapidly cleared from the vitreous when delivered topically to the eye. In a topical drug combination treatment consisting of 5-FU and the lipophilic, water-insoluble, anti-inflammatory drug, trihydroxy steroid (THS), a codrug strategy was utilized which provided a superior sustained release delivery of the two synergistic parent drugs for the treatment of diabetic retinopathy (Howard et al., 2005). The individual

physicochemical properties of 5-FU and THS are not favorable for sustained release of a physical mixture of the two drugs. However, utilizing a codrug approach, the chemical combination of 5FU and THS in a 2:1 molar ratio, respectively (for optimal synergistic activity) afforded a molecule with greatly improved physicochemical characteristics for sustained delivery compared to formulations of the two drugs as a physical mixture (Howard et al., 2005). Fig. 1.4 shows the structure of THS, 5-FU and the THS-BIS-5-FU codrug. THS was synthesized from Reichstein's substance S as depicted in Scheme 1.1. The 5-FU-THS codrug was synthesized via the intermediacy of a chloroformate analogue, as shown in Scheme 1.1 (a) and 1.1 (b).

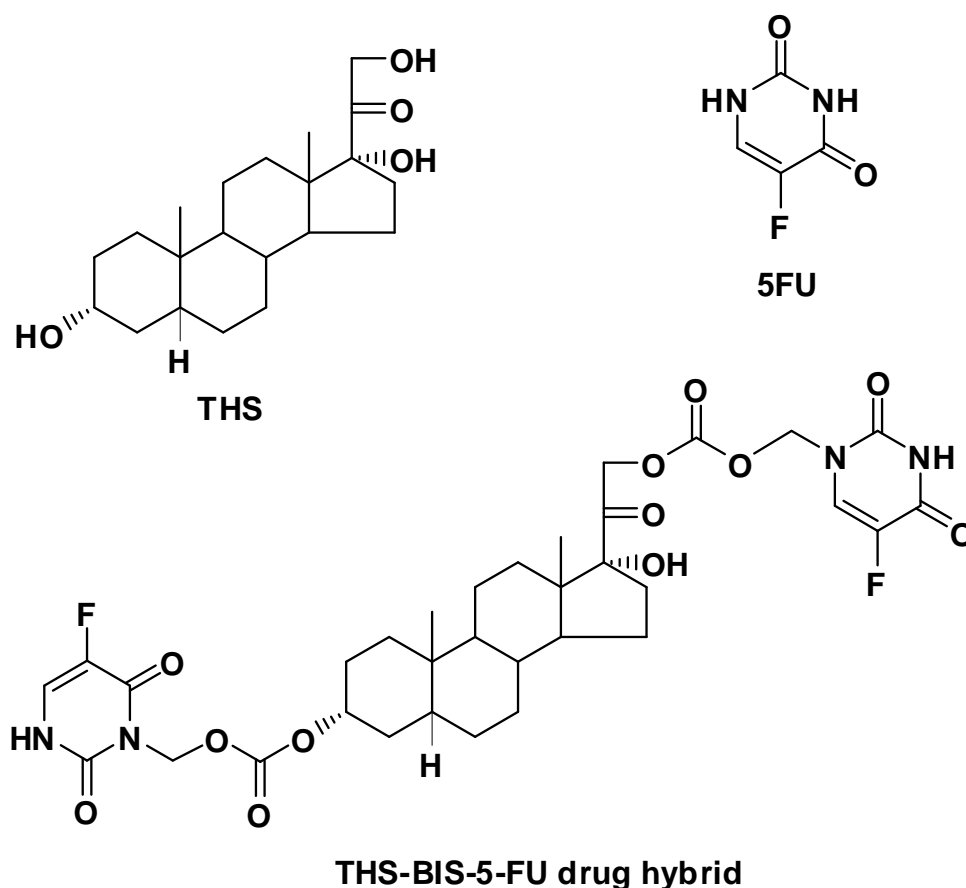
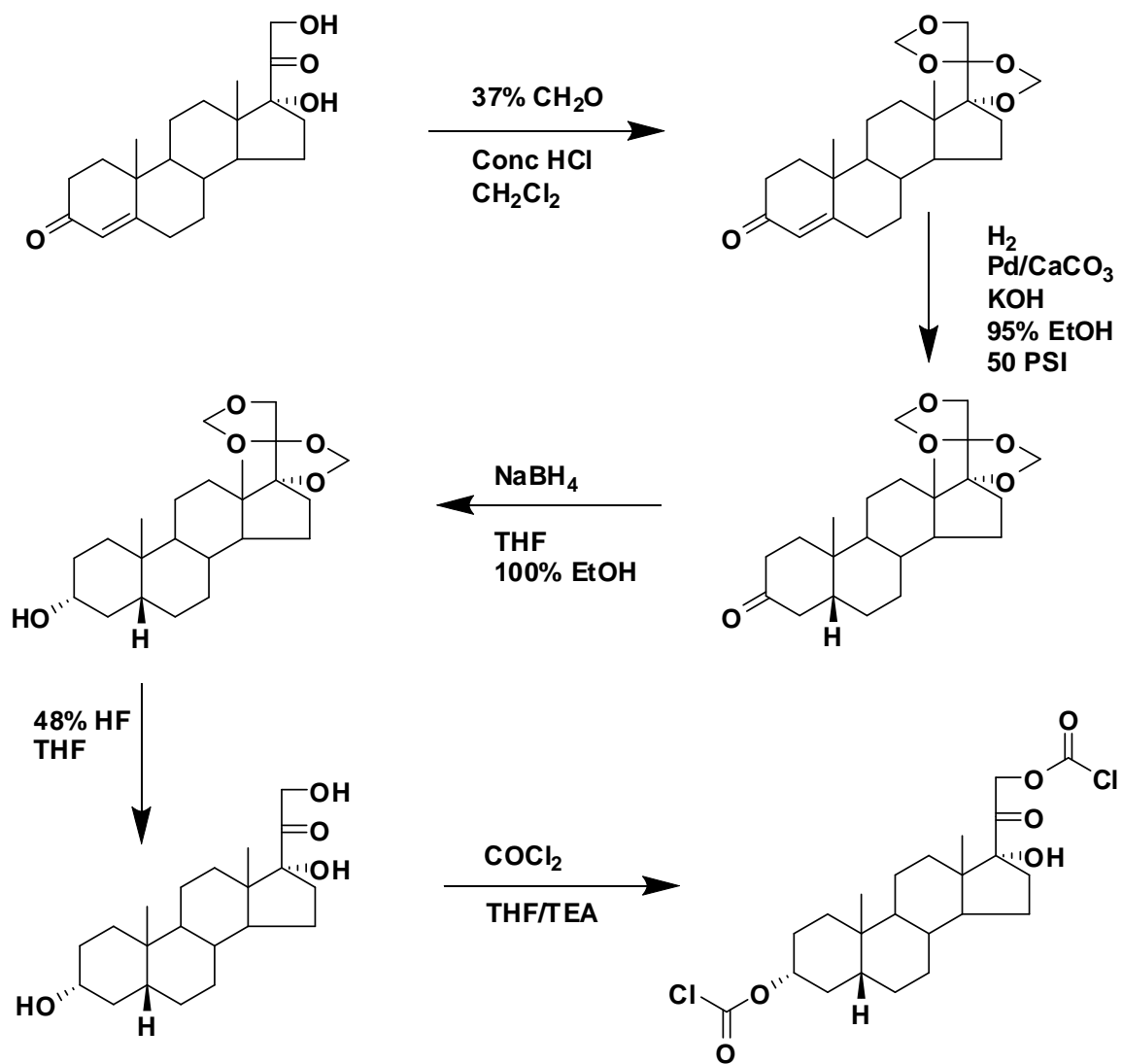
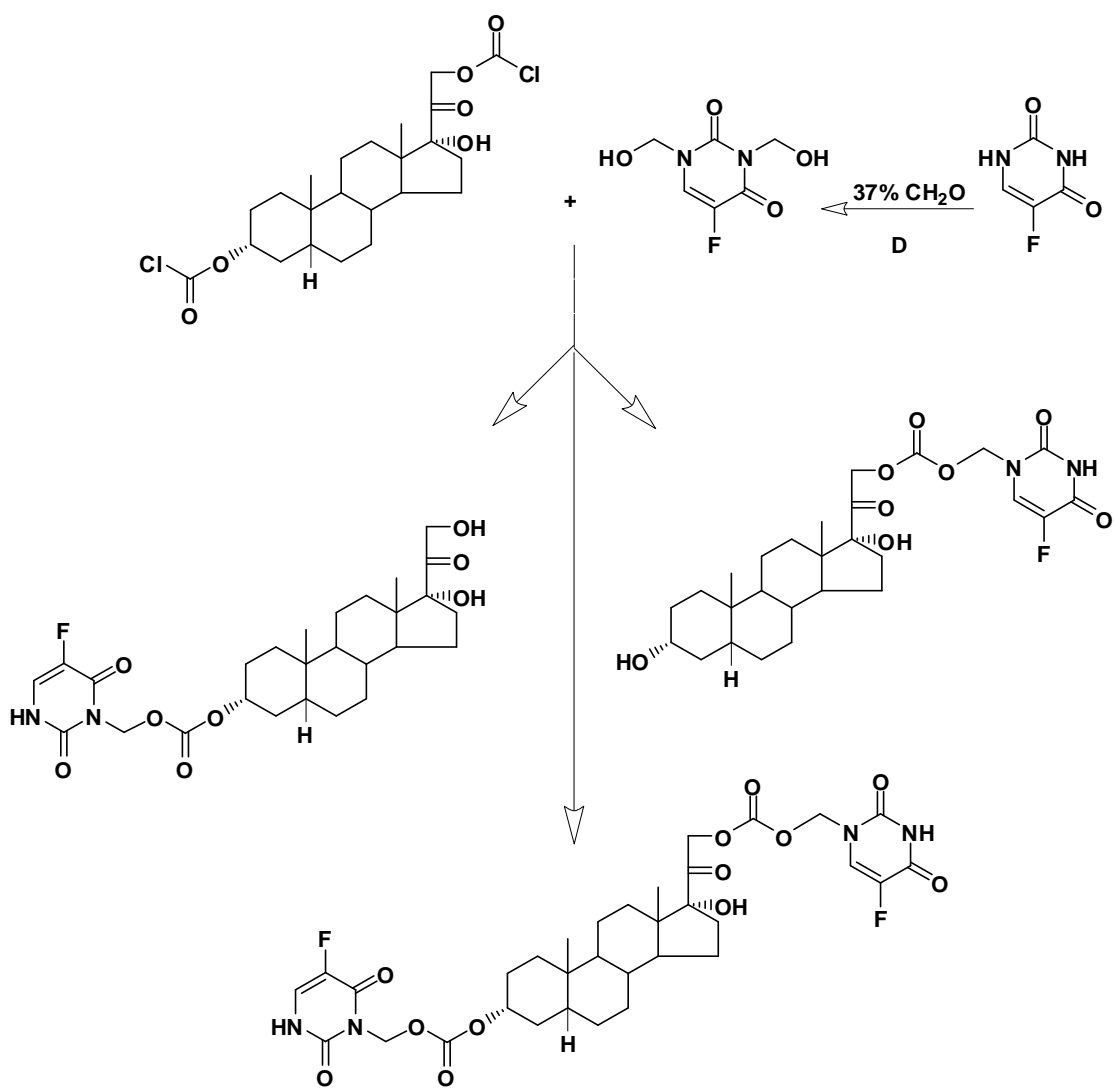


Fig. 1.4 Structures of THS, 5FU and the THS-BIS-5FU codrug
 (Reprinted from Journal of Enzyme Inhibition and Medicinal Chemistry, Howard et al., 2005, copyrighted by Informa Healthcare, used by permission”)

Scheme 1.1: (a) Synthesis of the chloroformate analogue of THS



Scheme 1.1: (b) synthesis of THS-BIS-5FU codrug



(Reprinted from Journal of Enzyme Inhibition and Medicinal Chemistry, Howard et al., 2005, copyrighted by Informa Healthcare, used by permission”)

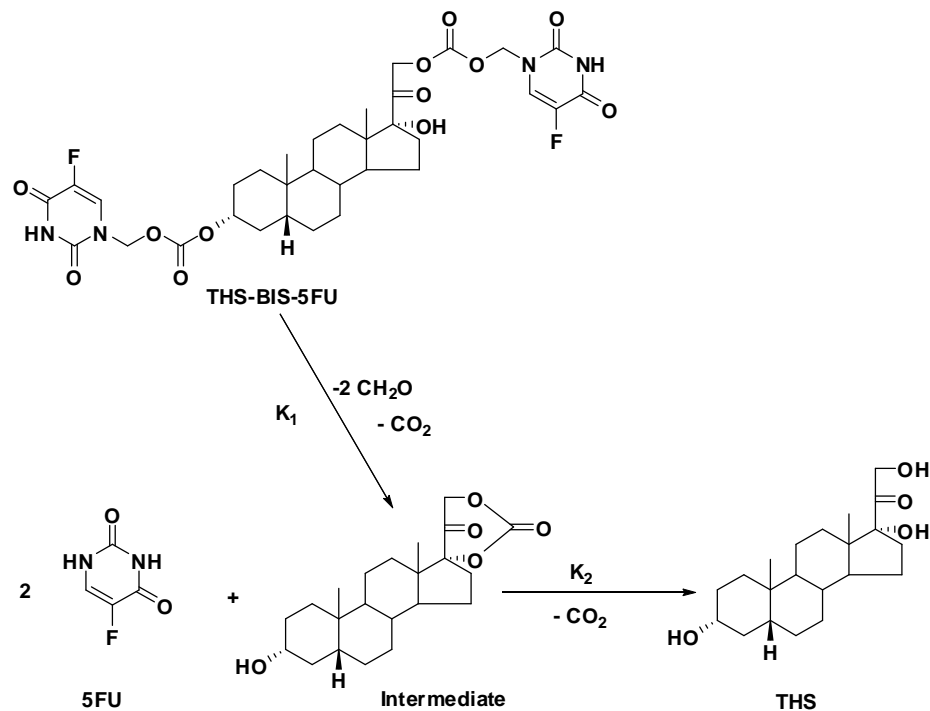


Fig. 1.5 Hydrolytic behavior of the THS-BIS-5FU codrug (Reprinted from Journal of Enzyme Inhibition and Medicinal Chemistry, Howard et al., 2005, copyrighted by Informa Healthcare, used by permission”)

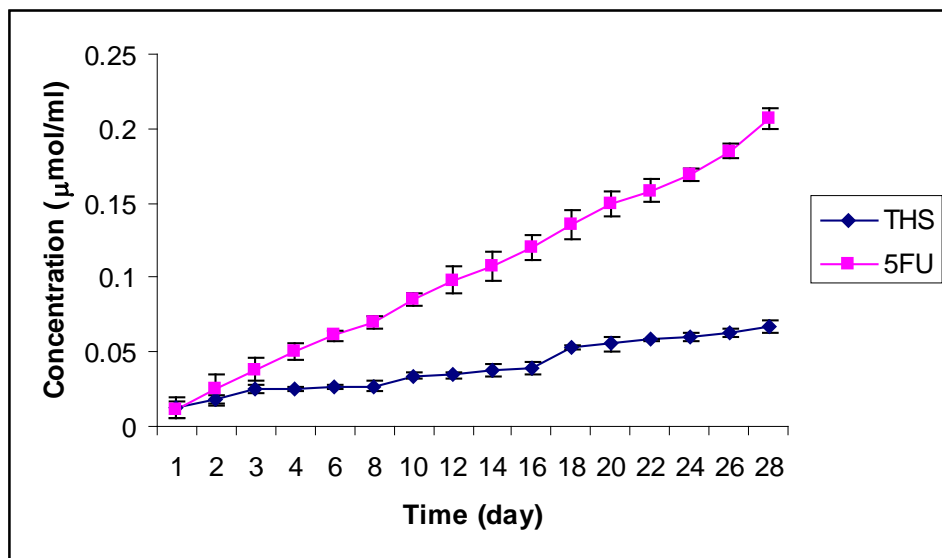


Fig. 1.6 Cumulative release of THS and 5FU from neat pellets containing 2 mg of the THS-BIS-5FU codrug in bovine vitreous humor (Reprinted from Journal of Enzyme Inhibition and Medicinal Chemistry, Howard et al., 2005, copyrighted by Informa Healthcare, used by permission)

The 5-FU-THS codrug was designed as a “chemical delivery” system (Howard et al., 2005) which joined together the two drugs via a labile linker moiety. The physicochemical properties of the codrug were favorable for both formulation as a sutured ophthalmic pellet, and for slow dissolution of the codrug pellet in the vitreous humor. The labile linker was specifically designed to undergo rapid hydrolysis once the codrug pellet had dissolved, providing sustained release of the parent drugs, which was dependent on the rate of dissolution of the codrug pellet. Fig. 1.5 illustrates the hydrolytic behavior of the codrug. According to the figure, one molar equivalent of the codrug produces one molar equivalent of THS, two molar equivalents of 5FU, and two molar equivalents of both formaldehyde and carbon dioxide. Another important consideration in the design of the 5-FU-THS codrug was the structure of the labile linker. The two drugs were linked together via a linker that afforded hydrolysis products that were considered to be non-toxic. The pellets containing the THS-BIS-5FU codrug simultaneously released THS and 5FU in 0.1 M phosphate buffer, (pH=7.4), human serum and in bovine vitreous humor. Fig. 1.6 depicts the release of THS and 5FU from the codrug in bovine vitreous humor. The results demonstrate that a neat pelleted THS-5FU codrug can be utilized as a sustained release ocular delivery form of the parent compounds, and that the unique physicochemical properties of the codrug allow both a slow dissolution and a rapid release of the two parent drugs (Fig. 1.6).

1.4.4 Codrug for the Simultaneous Treatment of Alcohol Abuse and Tobacco Dependence

Naltrexone (NTX) is a useful drug for the treatment of alcohol abuse (Volpicelli et al., 1992), and cigarette smoking is known to be a social cue for alcoholics. Thus, many alcoholics are also chronic smokers. Naltrexol (NTXOL) is the active metabolite of NTX (Rukstalis et al., 2000; Wang et al., 2001). NTX produces severe gastrointestinal effects, has low bioavailability, and is a hepatotoxin. Also, poor patient compliance via the oral route is observed, and neither NTX nor NTXOL is deliverable in therapeutic concentrations via the transdermal route (Kiptoo et al., 2006). A codrug approach was applied to attempt to solve these problems. Hydroxybupropion (BUPOH) is the active

metabolite of the orally active smoking cessation agent, bupropion (Zyban) (Cooper et al., 1994; Ascher et al., 1995; Sanchez and Hyttel 1999, Slemmer et al., 2000). A transdermal NTX-BUPOH or CB-NTXOL-BUPOH codrug should have improved transdermal delivery characteristics, lower toxicity, and afford better patient compliance than either NTX or NTXOL. This single codrug entity has the potential to treat both alcohol and nicotine abusers when delivered transdermally. Fig. 1.7 shows the structure of NTX, NTXOL, BUP, BUPOH and the two codrugs of BUPOH covalently linked to either NTX or NTXOL.

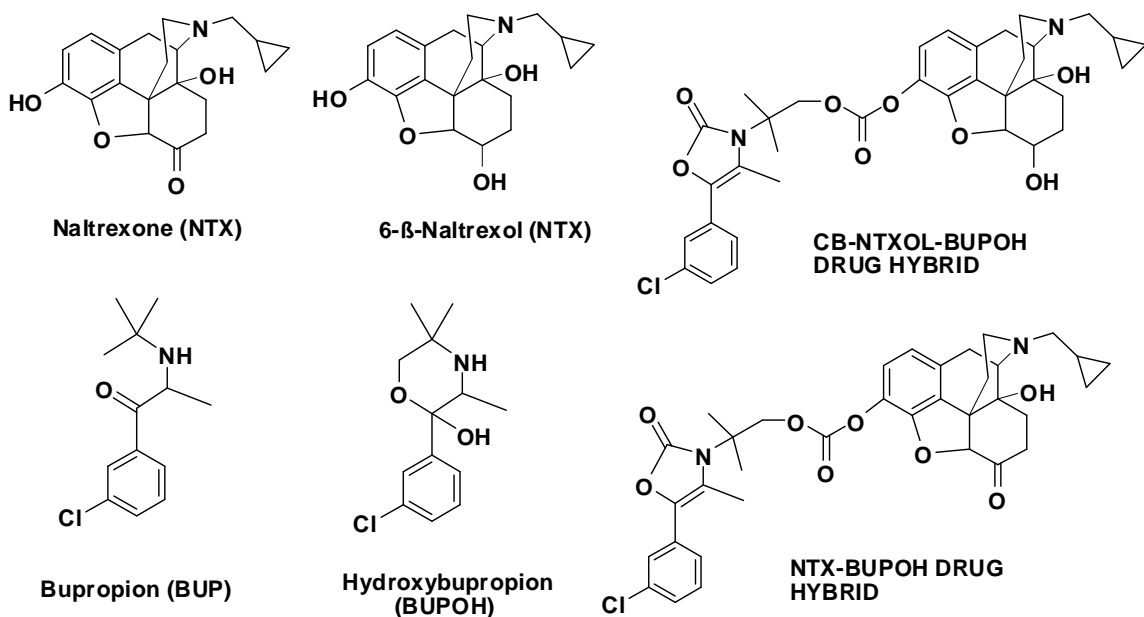
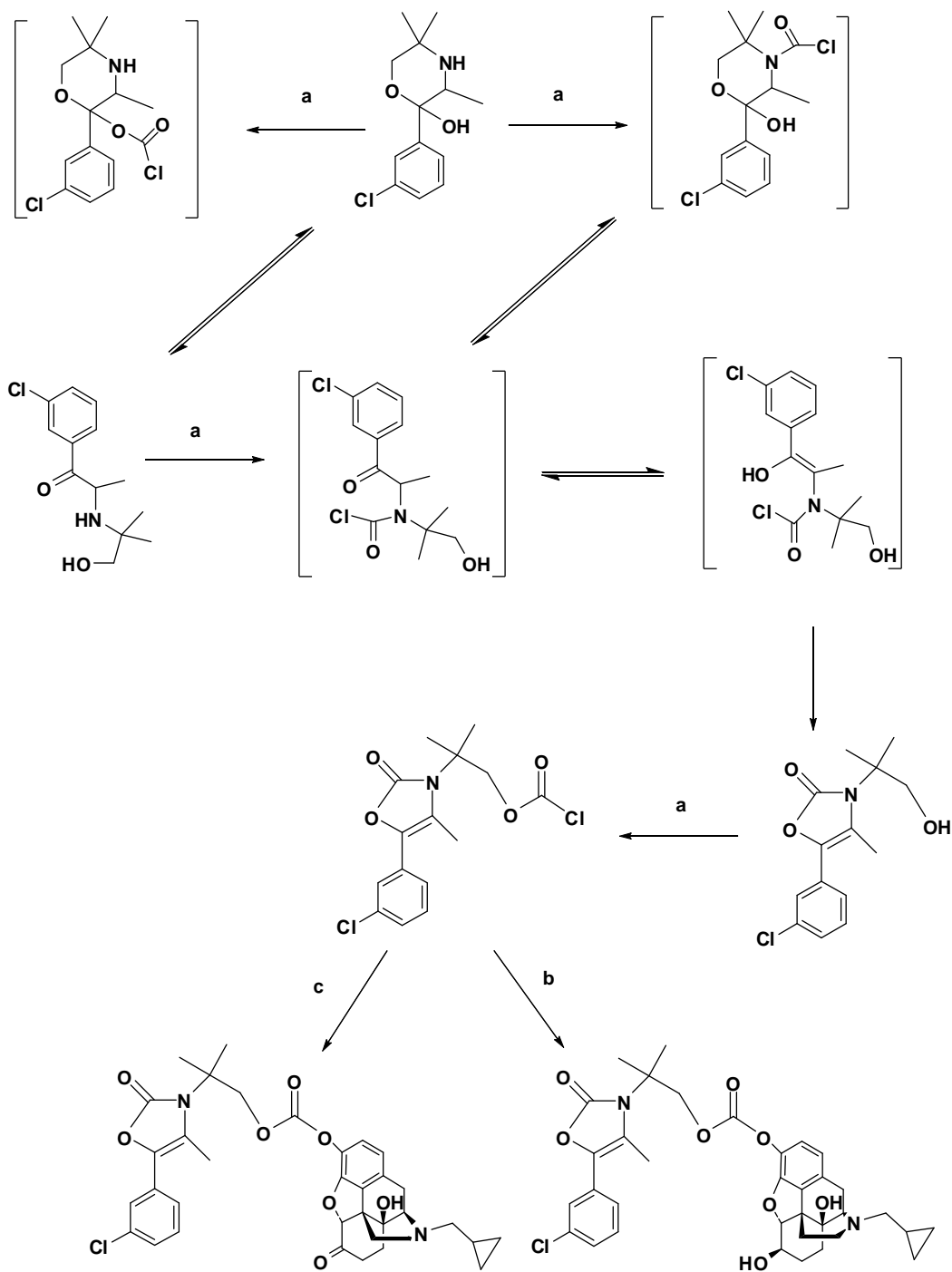


Fig. 1.7 Structures of parent drugs NTX, NTXOL, BUP, BUPOH and codrugs NTX-BUPOH and CB-NTXOL-BUPOH

Scheme 1.2: Syntheses of NTX-BUPOH and CB-NTXOL-BUPOH codrugs humor
 (Reprinted from Journal of Bioorganic and Medicinal Chemistry Hamad et al., 2006,
 copyrighted by Elsevier, used by permission)



(a) COCl₂, CH₂Cl₂, TEA, 0 °C, argon. (b) NTX, CH₂Cl₂, TEA, 0 °C, argon. (c) NTXOL, CH₂Cl₂, TEA, 0 °C, argon.

The syntheses of the two codrugs were achieved by initial formation of a chloroformate derivative of BUPOH followed by coupling of this intermediate with NTX and NTXOL. The step-wise syntheses of the codrugs are shown in scheme 1.2 (Hamad et al., 2006).

In order to determine the stability of the codrugs, hydrolytic studies were carried out in isotonic phosphate buffer at pH 7.4 (physiological pH). The results showed that the codrugs were susceptible to hydrolysis and produced the parent drugs at physiological pH. Table 1.1 summarizes the results of hydrolytic study performed on the two synthesized codrugs and the parent drugs. The proposed hydrolytic conversion of the NTX-BUPOH codrug to the parent drugs is shown in detail in Fig. 1.8. The NTX-BUPOH codrug undergoes cleavage of the carbonate bond to generate NTX, and a stable cyclic carbamate intermediate of BUPOH, which then undergoes hydrolysis to subsequently generate BUPOH. The chemical stability of the NTX-BUPOH codrug was studied in isotonic phosphate buffer at pH 7.4 over 4 days. The disappearance of the codrug and the appearance of the two parent drugs over time are shown in Fig. 1.9. The rate of appearance of NTX was identical to the rate of disappearance of the codrug. On the other hand, the rate of formation of BUPOH was found to be slower than the rate of disappearance of the codrug, involving the formation of a relatively stable intermediate. That intermediate was identified as the 5-membered cyclic carbamate analogue of BUPOH (Hamad et al., 2006).

The stability of the carbonate codrug of 6- β -naltrexol and hydroxubupropion was also evaluated in Guinea pig plasma after transdermal delivery. Fig. 1.10 illustrates the hydrolytic profile of the carbonate codrug (CB-NTXOL-BUPOH) and the time course of formation of the two active parent drugs in the plasma. The release of 6- β -naltrexol from the codrug was a one-step process, as confirmed by rate of appearance of 6- β -naltrexol being the same as the rate of disappearance of the carbonate codrug. The release of BUPOH involved the initial formation of the cyclic carbamate analogue of BUPOH, which was then converted subsequently to the parent drug, BUPOH. The rate of

hydrolysis of the CB-NTXOL-BUPOH codrug in plasma was 3 times faster compared to the rate of hydrolysis in isotonic phosphate buffer at pH 7.4 (Kiptoo et al., 2008).

The CB-NTXOL-BUPOH codrug and 6- β -naltrexol were administered transdermally to hairless Guinea pigs and the concentrations of the parent drugs in the plasma were determined by LC-MS/MS. The plasma concentration profile of the analytes following topical application of either CB-NTXOL-BUPOH or 6- β -naltrexol is shown in Fig. 1.11. The results showed a fivefold enhancement in the transdermal delivery of 6- β -naltrexol when given in the form of the codrug. Also, the codrug delivered a significant amount of BUPOH to the plasma when administered transdermally. The cyclic carbonate intermediate of BUPOH was not detected in the plasma of codrug-treated Guinea pigs. The calculated pharmacokinetic parameters for the CB-NTXOL-BUPOH codrug and 6- β -naltrexol are listed in Table 1.2 (Kiptoo et al., 2008).

Table 1.1 Physicochemical Properties of NTX (1), NTXOL(2), BUPOH(4) and the carbonate codrugs, NTX-BUPOH (25) and CB-NTXOL-BUPOH (26)

Compound	MW	Mp (°C)	clog P ^a	Half-life, <i>t</i> _{1/2} (h) ^b
1	341.40	175.7 ± 1.20	0.36	Stable
2	343.42	187.76 ± 2.62	0.83	Stable
4	255.74	124.40 ± 1.60	2.87	Stable
25	649.13	137.00 ± 1.41	3.23	36.68 ± 2.88
26	651.15	159.50 ± 2.12	3.71	28.88 ± 2.82

^a Derived from Daylight[®] Software.

^b Studied in isotonic phosphate buffer, pH 7.4, at 32 °C.

(Reprinted from Journal of Bioorganic and Medicinal Chemistry Hamad et al., 2006, copyrighted by Elsevier, used by permission)

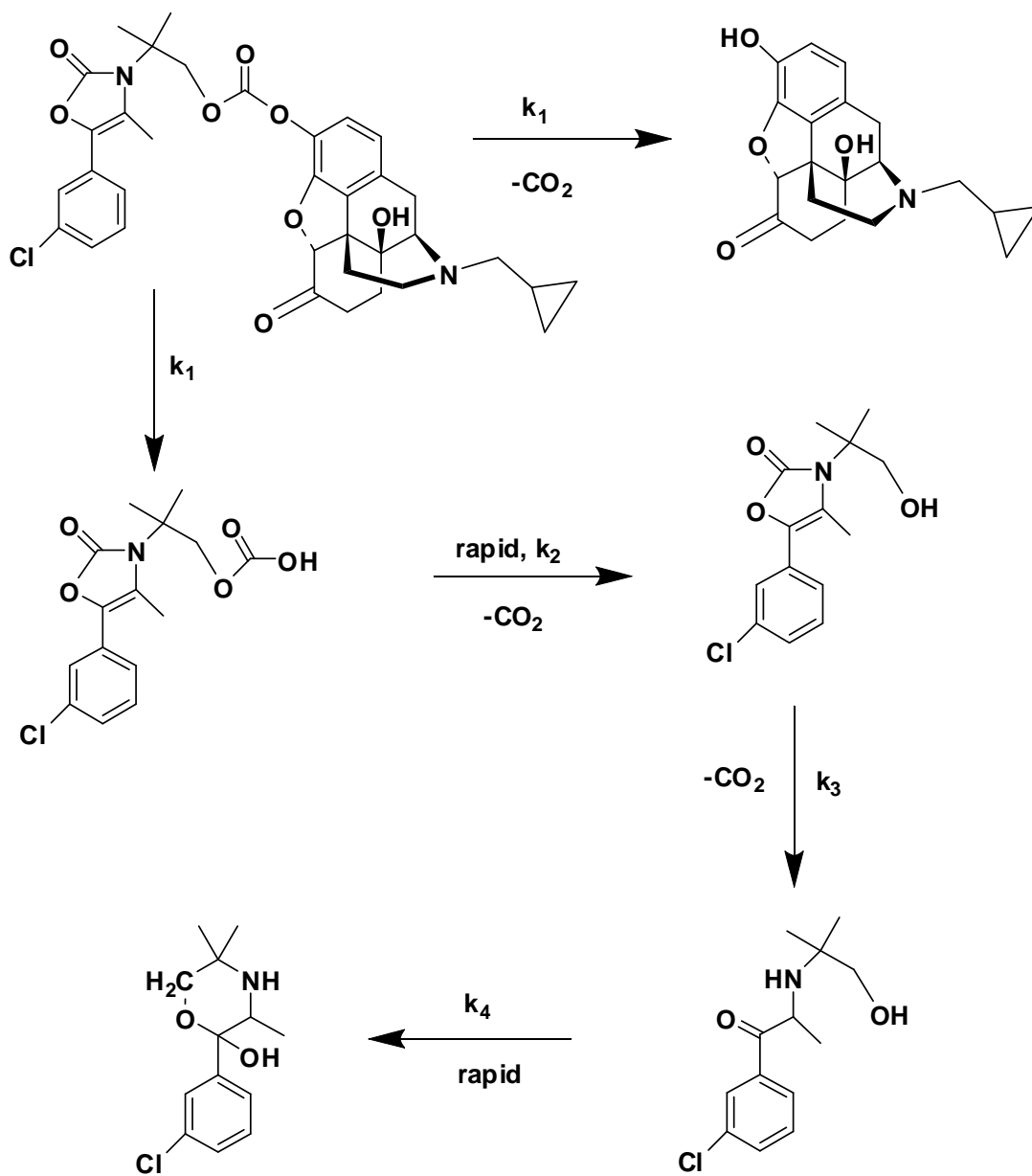


Fig. 1.8 Hydrolytic behavior of the NTX-BUPOH codrug
 (Reprinted from Journal of Bioorganic and Medicinal Chemistry Hamad et al., 2006,
 copyrighted by Elsevier, used by permission)

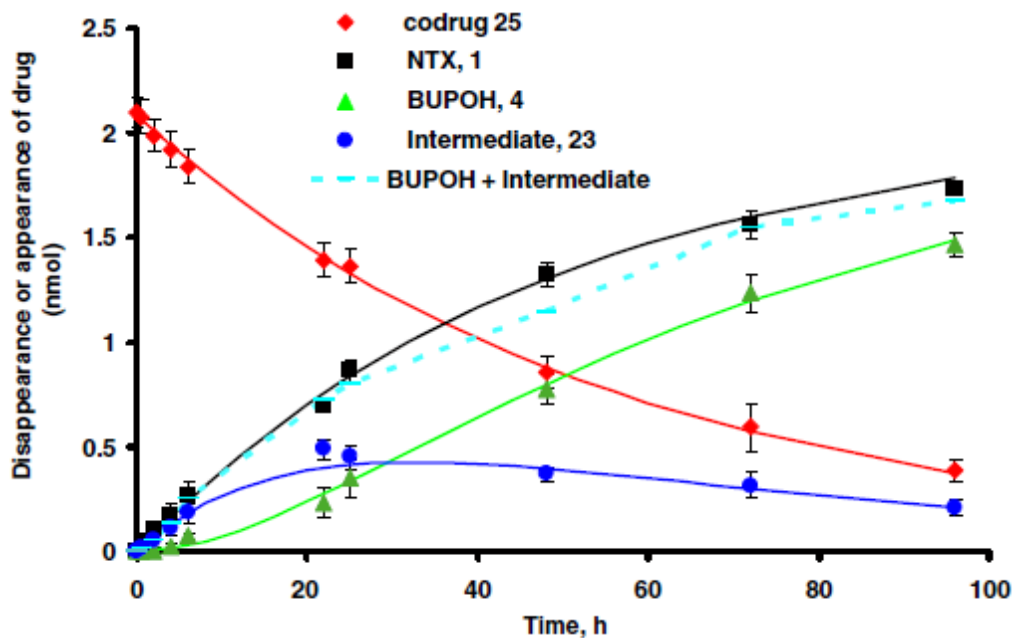


Fig 1.9 Hydrolytic profile of the carbonate drug hybrid, NTX-BUPOH, in isotonic phosphate buffer at pH 7.4 (Reprinted from Journal of Bioorganic and Medicinal Chemistry Hamad et al., 2006, copyrighted by Elsevier, used by permission)

Table 1.2 Pharmacokinetic parameters of NTXOL in the Guinea pig after application of a gel formulation containing either CB-NTXOL-BUPOH or NTXOL base. (Reprinted from European Journal of Pharmaceutical Sciences, Kiptoo et al., 2008, copyrighted by Elsevier, used by permission)

Parameter	NTXOL	NTXOL from CB-NTXOL-BUPOH
AUC ₀₋₄₈ (ng/ml h)	66.4 ± 7.9	282.0 ± 14.5
C _{max} (ng/ml)	1.5 ± 0.2	6.6 ± 0.4
T _{max} (h)	28.1 ± 1.5	10.1 ± 0.9
T _{lag} (h)	5.1 ± 0.7	5.0 ± 1.1
Observed C _{SS} (ng/ml)	1.3 ± 0.5	6.4 ± 0.9
Predicted C _{SS} (ng/ml) ^a	0.2 ± 0.1	0.7 ± 0.3
Enhancement factor	1	5.3

Data is represented as mean ± S.D. n = 5 for NTXOL and n = 6 for CB-NTXOL-BUPOH.

^a Predicted from *in vitro* human skin diffusion data.

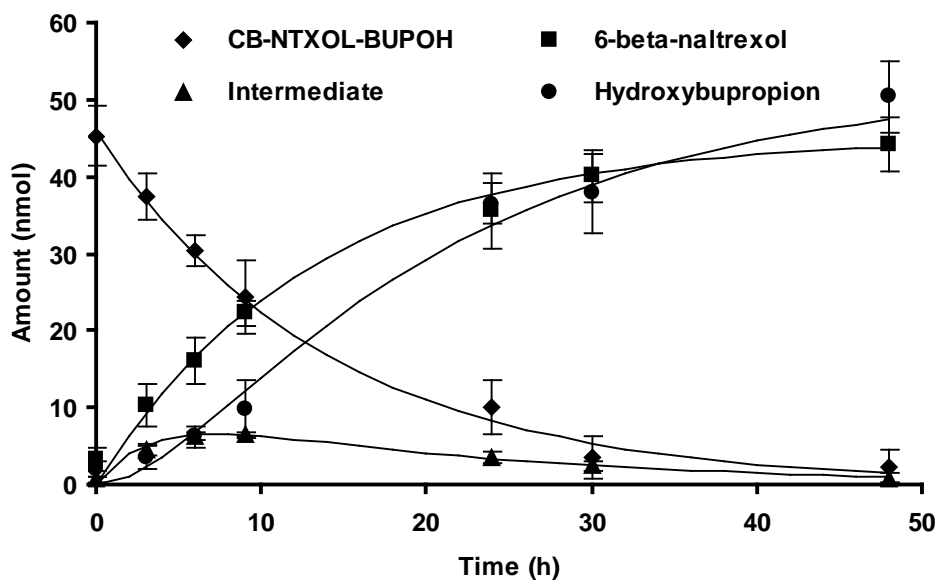


Fig 1.10 Hydrolytic profile of the carbonate drug hybrid, CB-NTXOL-BUPOH, in Guinea Pig Plasma at 37°C (Reprinted from European Journal of Pharmaceutical Sciences, Kiptoo et al., 2008, copyrighted by Elsevier, used by permission)

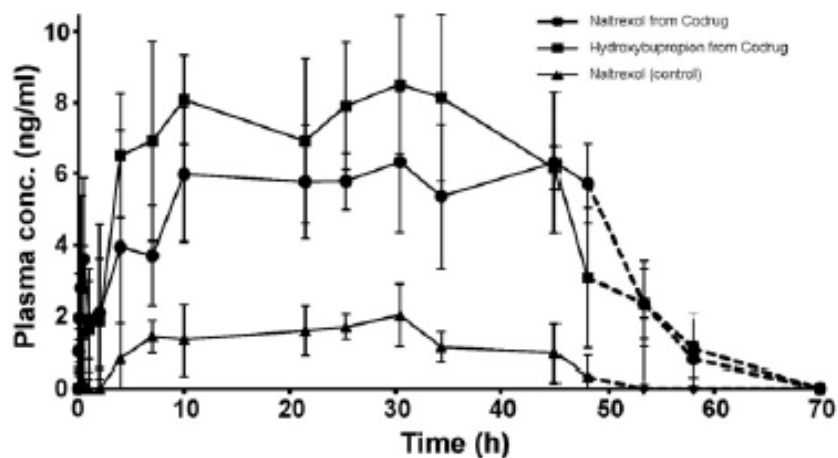


Fig 1.11 Mean (\pm S.D.) plasma concentration profiles in guinea pigs after topical application of a gel formulation containing either CB-NTXOL-BUPOH or 6- β -Naltrexol (control). The dotted line (----) indicates the plasma concentration after the removal of the formulation. . (Reprinted from European Journal of Pharmaceutical Sciences, Kiptoo et al., 2008, copyrighted by Elsevier, used by permission)

1.4.5 L-DOPA Codrugs

Dopamine is deficient in the brains of patients suffering from Parkinson's disease. Unfortunately, dopamine cannot be given as a drug for this disease because it cannot cross the blood-brain barrier. L-Dopa is a precursor of dopamine, and is used in the treatment of Parkinson's disease. L-Dopa crosses the blood-brain barrier via facilitated transport, and is then converted to dopamine in the brain by the enzyme DOPA decarboxylase. For the treatment of Parkinson's disease, L-Dopa is given in combination with a peripheral dopa decarboxylase inhibitor such as carbidopa, to prevent degradation of L-Dopa in the systemic circulation. Entacapone is another L-Dopa decarboxylase inhibitor, which is currently used with L-Dopa to treat Parkinson patients. Since oral L-Dopa bioavailability is low, a codrug approach was utilized, by combining L-Dopa and entacapone via an ester linkage to improve L-Dopa brain delivery (Fig.1.12). The codrug showed stability in aqueous media at different pHs and was hydrolysed to the parent drugs in liver homogenate, fulfilling the codrug criteria (Leppanen et al., 2002).

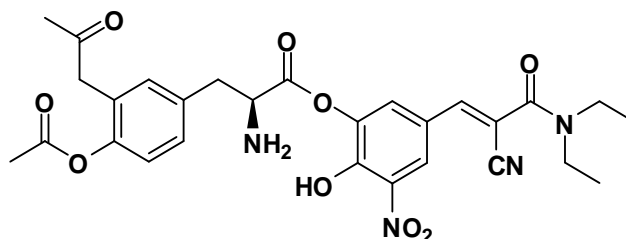


Fig.1.12 L-Dopa ester of entacapone

A series of codrugs have also been designed by linking L-Dopa and dopamine with antioxidant compounds such as α -lipoic acid, glutathione, caffeic acid, carnosine, benserazide and *N*-acetylcysteine (Stefano et al., 2006 [1]; Stefano et al., 2007; Piera et al., 2008; Stefano et al., 2006 [2]; Pinnen et al., 2009).

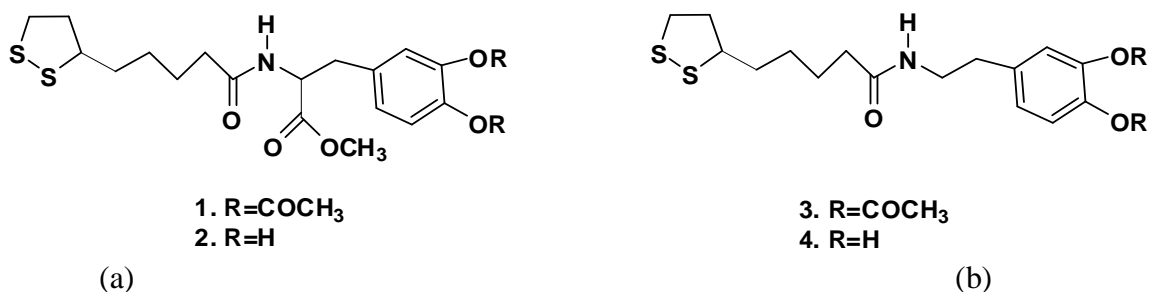
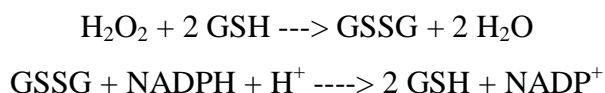


Fig. 1.13 (a) L-Dopa and α -lipoic acid codrug (b) Dopamine and α -lipoic acid codrug

As shown in Fig.1.13, L-Dopa and dopamine can be linked to α -lipoic acid and glutathione via an amide linkage (Stefano et al., 2006). α -Lipoic acid is an effective antioxidant. It exists as dihydrolipoate *in vivo*, which can regenerate (reduce) antioxidants such as glutathione, vitamin C and vitamin E (Biewenga et al., 1997; Packer et al., 1995). The strained 5-membered ring conformation of lipoic acid contributes to its good scavenging activity (Haenen and Bast, 1991). All the four codrugs in Fig. 1.13 showed good stability in the gastrointestinal tract and cleaved enzymatically in rat and human plasma to release the parent drugs. The prolonged release of L-Dopa showed the effectiveness of the L-DOPA codrugs. Codrugs 1 and 2 were used to test antioxidant efficacy using superoxide dismutase (SOD) and glutathione peroxidase (GPx) markers. These enzymes have a central role in the control of reactive oxygen species (ROS). SOD dismutates highly reactive superoxide into oxygen and hydrogen peroxide. GPx reduces hydrogen peroxide to water by oxidising GSH. The oxidised form of GSH (GSSG) is reduced back to GSH by glutathione reductase, as shown in the equations below:



Codrugs 1 and 2 showed increased GPx activity as compared to L-DOPA alone, which could indicate a decreased production of free radicals. Also, these codrugs induced decreased activity of SOD as compared to L-DOPA alone, indicating a reduced production of superoxide anions.

Similar results were obtained when codrugs of L-Dopa and glutathione were constructed with amide linkages (Stefano et al., 2007). Glutathione helps in the decomposition of toxic peroxide molecules, protects enzymes by maintaining their SH groups in a reduced state, and is also involved in the repair of oxidized iron-sulfur centers of the mitochondrial complex. No hydrolysis of these codrugs was observed in gastrointestinal fluids and L-DOPA was released in plasma via enzymatic hydrolysis. The codrugs also showed an antioxidant effect using SOD and GPx markers (Fig. 1.14).

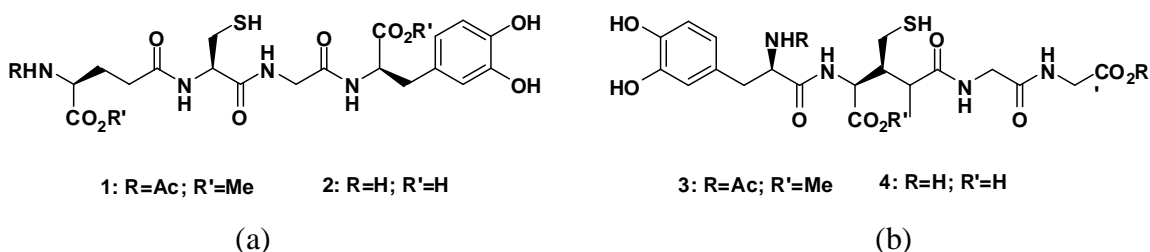


Fig. 1.14 (a) L-Dopa and Glutathione codrug (b) Dopamine and Glutathione codrug

Like glutathione or α -lipoic acid, the other two antioxidants, caffeic acid and carnosine, were conjugated with L-Dopa (Fig. 1.15) and assessed by evaluating plasmatic activities of SOD and GPx in rats (Piera et al., 2008). These codrugs were devoid of significant antioxidant activity, although the literature is full of reports that caffeic acid and carnosine act as natural antioxidants with hydroxyl radical-scavenging and lipid-peroxidase activities.

To overcome the pro-oxidant effects of L-Dopa, the other antioxidants used were sulfur containing, such as *N*-acetyl cysteine (NAC), methionine and bucillamine (Fig. 1.16). *N*-acetylation of cysteine speeds up cysteine absorption and distribution when given orally. NAC helps in increasing the intracellular concentration of glutathione via elevating intracellular cysteine levels. NAC is rapidly absorbed, enters cells, and is rapidly hydrolyzed to cysteine. Methionine is also an intermediate in the synthesis of cysteine, and helps PC 12 cells against DA-induced nigral cell loss in Parkinson's disease by binding to oxidative metabolites of dopamine (Grinberg et al., 2005; Offen et al., 1996; Martínez et al., 1999). Bucillamine is a synthetic cysteine derivative used for

the treatment of rheumatoid arthritis (Horwitz, 2003). It contains two thiol groups, which makes it a more powerful antioxidant as compared to NAC and methionine. It can be easily transported into cells to restore GSH under conditions of oxidative stress and GSH depletion (Hammond et al., 2001).

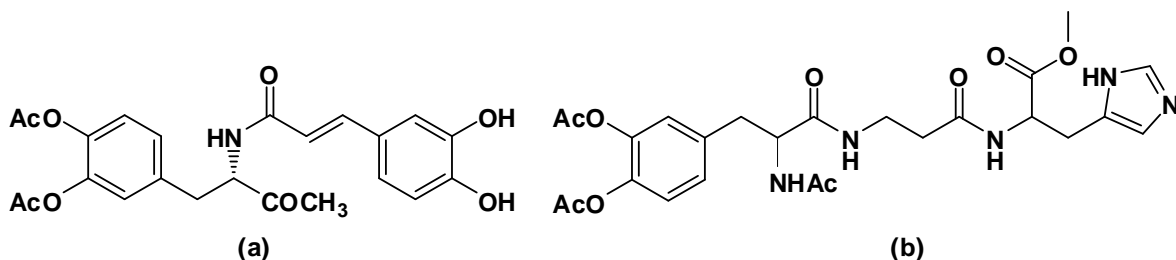


Fig. 1.15 Structures of (a) 3, 4-diacetyloxy-L-dopa methyl ester-caffeic acid codrug (b) 3, 4-diacetyloxy-L-dopa methyl ester-carnosine codrug

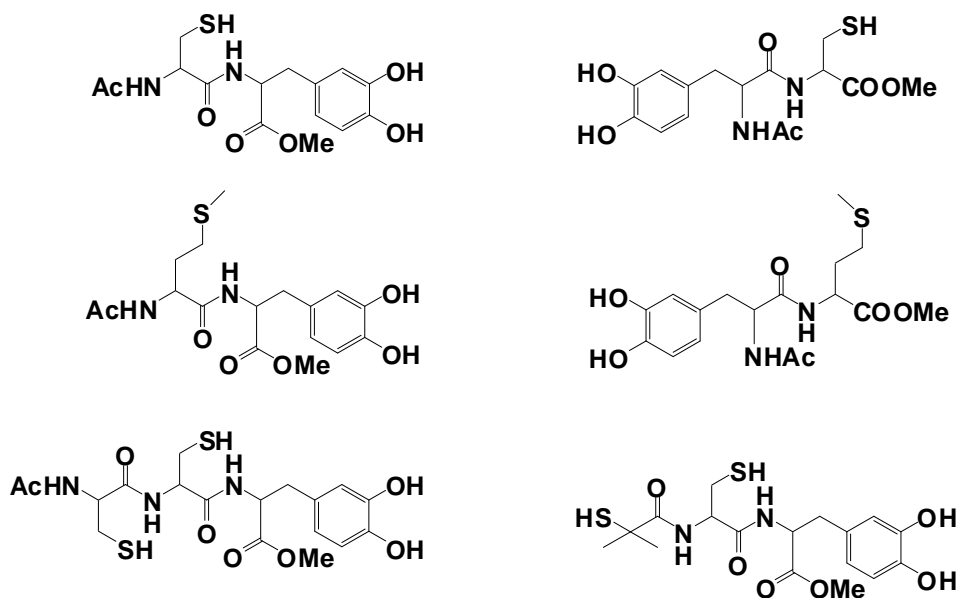


Fig. 1.16 Codrugs of L-Dopa linked to cysteine, methionine and bucillamine

Six codrugs were constructed using L-Dopa as one of the parent drugs and NAC/methionine/bucillamine as the other parent drug (Stefano et al., 2006 [2]). All the codrugs showed good lipophilicity and water solubility for optimal intestinal absorption.

The stability study at pH 1.3 and in SGF indicated that the codrugs would be stable enough to pass un-hydrolyzed through the stomach after oral administration. At pH 7.4, they were stable enough to be absorbed intact from the intestine. In rat and human plasma, the codrugs hydrolyzed to release the parent drugs, although the release of L-Dopa from the codrugs was very slow. Next, the antioxidant efficacy of codrugs was evaluated using a chemiluminescent assay. The comparison was made using NAC; all the codrugs showed a better antioxidant effect as compared to NAC. The physicochemical and pharmacokinetic data showed high levels of L-Dopa in the plasma and brain, even 12 h after administration. Codrugs 3 and 4 were able to induce a sustained release of L-Dopa and dopamine in rat striatum with respect to equimolar doses of L-Dopa. Codrug 4 was injected intracerebroventricularly, and it resulted in levels of dopamine in the striatum that were higher than those in L-Dopa-treated rats. This indicated that the codrug had a longer half-life in brain than L-Dopa (Stefano et al., 2006 [2]).

Benserazide is a Dopa-decarboxylase inhibitor. An L-Dopa codrug with benserazide had good lipophilicity as compared to either L-Dopa or benserazide (Fig. 1.17). The codrug was stable in aqueous buffer solutions. In plasma, the catechol esters and amide bonds were efficiently cleaved, releasing the parent drugs in one step (Stefano et al., 2006 [2]).

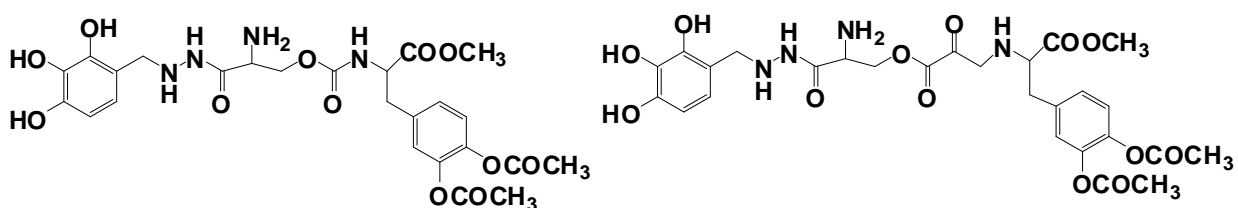


Fig. 1.17 Codrug of L-Dopa with benserazide

1.5 A Codrug strategy in pain management

1.5.1 Opioids and Cannabinoids

Opioid and cannabinoid interaction in the prevention of pain is very significant, especially in the case of chronic pain, where higher doses with greater side effects are encountered. Combination of these two drug types produced an analgesic effect, even with inactive doses of either drug alone, which suggests the possibility of utilizing smaller doses yielding fewer side effects and less addiction potential (Cichewicz, 2004). In addition, opioids exert their analgesic effect on nociceptive pain while cannabinoids are effective in modulating neuropathic pain. Thus, an opioid-cannabinoid codrug might be able to cover a broader range of pain. Several articles have been published on the interaction of opioids with cannabinoids, which are explained further in this chapter. Keeping the interactions between these two classes of analgesics in mind, various codrug combinations of opioids and cannabinoids were synthesized in this dissertation work. These syntheses are discussed in the next chapter.

1.5.2 Pharmacokinetics and Pharmacodynamics of Opioids

Opioids are compounds having morphine-like pharmacological activity. The term opiate refers to any natural or synthetic agent derived from, or structurally related to morphine (Thorn, 2009). The endogenous enkephalin peptides and the endorphins are, therefore, opioids because they are not structurally related to morphine, but have the same pharmacological activity.

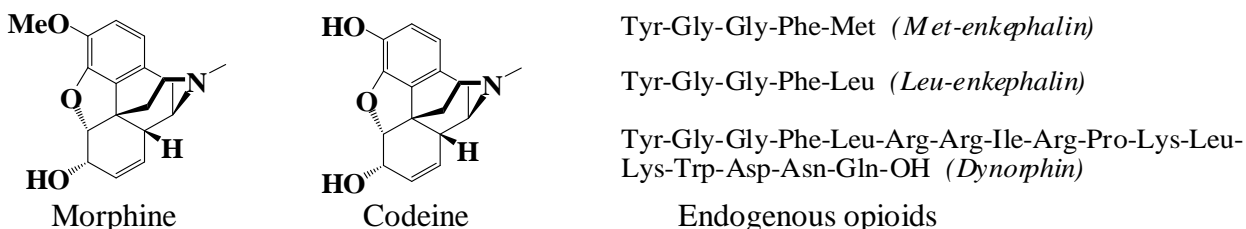


Fig. 1.18 Structures of Morphine, Codeine and Endogenous Opioids

Fig. 1.18 shows the structures of morphine, codeine and a selection of endogenous opioids. Codeine and morphine are the major pain relief drugs in the opiate family. Both drugs are found naturally in the poppy plant, *Papaver somniferum*, but for commercial use, codeine is usually synthesized from morphine, which is more abundant

in nature (Thorn, 2009). In addition to their analgesic effects, both drugs have antitussive effects and antidiarrheal activity. Side effects include respiratory depression, constipation, sedation and addiction. Codeine is a less potent agonist at the mu opioid receptor (OPRM1) compared to morphine, and is considered a safer alternative in an outpatient setting.

The principal pathways for the metabolism of codeine occur in the liver, although some metabolism occurs in the intestine and brain. Approximately 50-70% of codeine is converted to codeine-6-glucuronide by the UGT2B7 glucuronyl transferase enzyme. Codeine-6-glucuronide has a similar affinity for the *mu* opioid receptor as codeine. Approximately 10-15% of codeine is *N*-demethylated to norcodeine by CYP3A4 (Thorn, 2009). Norcodeine also has a similar affinity to codeine for the *mu* opioid receptor. Between 0-15% of codeine is *O*-demethylated to morphine, the most active metabolite, which has 200 fold greater affinity for the *mu* opioid receptor compared to codeine. This metabolic reaction is performed by CYP2D6. Approximately 60% of this morphine is glucuronidated to morphine-3-glucuronide (M3G) while 5-10% is glucuronidated to morphine-6-glucuronide (M6G). These reactions are principally catalyzed by UGT2B7 in the liver.

Opioids exert their antinociceptive effects via interaction with opioid receptors (Pan et al., 2008). There are four major opioid receptors, which have already been cloned: *mu*, delta, kappa and nociceptin/orphanin FQ receptors (opioid receptor-like 1[ORL1]) (Pan et al., 2008). There is good evidence for the existence of subtypes of *mu*-, delta- and kappa-receptors. These receptors are located in brain and spinal cord tissues and each receptor plays a role in the mediation of pain. The *mu* receptor is morphine-selective and is the principal pain-modulating site in the central nervous system. There are two subtypes of mu receptor: *mu1* and *mu2*. Subtype *mu1* is mainly the analgesic site, while subtype *mu2* is responsible for respiratory depression. Opioid receptors belong to the G-protein-coupled receptor (GPCR) superfamily, and are heterodimeric receptors with ligand binding and signaling capabilities. These GPCRs possess seven cell membrane-spanning domains with extracellular ligand binding sites for specific molecules.

Interactions with those sites result in modulation of signal transduction pathways involving second messengers such as cAMP, inositol phosphate, or calcium, which is ultimately translated into cellular responses. Opioid binding can increase calcium ion release from intracellular calcium ion stores via activation of the second messenger, phospholipase C.

Chronic opiate administration leads to tolerance and a desensitization of opioid receptors. In many, but not all instances, a down-regulation of opioid receptors *in vivo* occurs following chronic opioid administration (Rotha et al., 1998).

The expression level of different opioid receptors is influenced by different pain conditions. Pain can be broadly divided into two categories: nociceptive pain, in which the free peripheral nerve endings are activated by noxious stimuli such as heat, pressure, etc. This is manifested as a kind of constant, dull and aching pain. Neuropathic pain occurs as a result of damage to the peripheral or central nervous system. Examples are diabetic neuropathy, multiple sclerosis, or spinal cord injury. This pain is often described as “burning and tingling”. It is characterized by hyperalgesia (increased painful response to noxious stimulus) and allodynia (pain to a previously non-noxious stimulus) (Pan et al., 2008).

Pain is inadequately managed with currently available drugs, especially for patients suffering with chronic pain conditions such as cancer or AIDS. Opioids are considered to be most effective for treatment of nociceptive pain but show little or no effect in neuropathic pain. In the case of nerve injury, or in diabetic neuropathy, *mu* receptor expression is reduced in the spinal dorsal horn, which reduces the antinociceptive effect of *mu* receptor agonists (Rotha et al., 1998). Also, long-term use of opioids such as morphine or oxycodone results in the development of tolerance to the analgesic effect, and causes drug abuse and dependence, as well as significant side effects such as respiratory depression, constipation, and cognitive impairment.

Anticonvulsant drugs such as GABA-pentin (Neurotin[®]) and pregablin (Lyrica[®]) are often used to treat neuropathic pain, but have limited efficacies. An antidepressant, Duloxetine (Cymbalta[®]) has been recently approved for the treatment of diabetic neuropathy, but this drug is also associated with significant side-effects (Patacchioli, 2004).

The limitations of currently available treatments for nociceptive and neuropathic pain clearly indicate the need for new approaches. One approach to address this problem is to consider combining analgesic drugs from other classes with opioids. The theory behind this is to lower the dose to avoid side effects, in addition to covering a broad spectrum of pain, i.e., to treat both nociceptive and neuropathic pain. The two combined drugs should produce a synergistic effect rather than just an additive effect. In this regard, one group of drugs that appears particularly promising for combination with the opioids is the cannabinoids (Patacchioli, 2004).

1.5.3 Pharmacokinetics and Pharmacodynamics of Cannabinoids

Cannabinoids are useful for the treatment of pain, spasticity, glaucoma and other disorders. But they have numerous side-effects too, such as increase in heart rate, lowering of blood pressure, appetite stimulation, dry mouth and dizziness (Patacchioli, 2004). The *Cannabis* plant contains several cannabinoids, one of which is Δ^9 -tetrahydrocannabinol (Δ^9 -THC) which possesses most of the characteristic pharmacological effects (Patacchioli, 2004). Fig. 1.15 shows the chemical structure of Δ^9 -THC. It is yellow resinous oil, sticky at room temperature, which hardens upon refrigeration; it is without smell and has bitter taste. The molecular weight of Δ^9 -THC is 314.45, and the molecular formula is $C_{21}H_{30}O_2$. Δ^9 -THC is highly insoluble in water but soluble in ethanol/methanol.

Oral administration of Δ^9 -THC leads to erratic uptake of the drug as a result of degradation by stomach acids and extensive liver first-pass metabolism (Howelett and Barth, 2002). The measured bioavailability of Δ^9 -THC after oral administration (Marinol) is only 10-20%. Since it is highly lipophilic, high concentrations of the drug are found in

highly vascularized tissues shortly after oral administration of the drug, which is reflected in a high volume of distribution of about 10 L/kg. Δ^9 -THC also binds strongly to plasma proteins, only about 3% of the drug being in the unbound form. The major biotransformation product of Δ^9 -THC is the monohydroxy metabolite, 11-hydroxy- Δ^9 -THC (THC-OH), which also binds to plasma proteins very strongly (Howelett and Barth, 2002).

More than 100 metabolites of Δ^9 -THC have already been identified. Due to its high lipid solubility Δ^9 -THC is a good substrate for cytochrome P450 mixed-function oxidases (Rotha et al., 1998; Patacchioli, 2004; Howelett and Barth, 2002). Δ^9 -THC is hydroxylated at both C11 and C8, and at all the positions of the alkyl side-chain. Fig. 1.19 shows the possible oxidation sites for Δ^9 -THC.

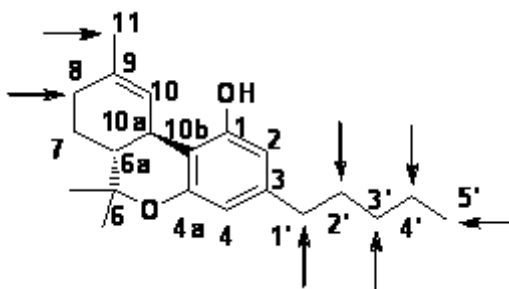


Fig. 1.19 Possible metabolic oxidation sites of Δ^9 -THC

Δ^9 -THC, like any other very lipophilic drug, has long terminal half-life, due to its deposition in tissues. The complete elimination time is very difficult to estimate, due to the slow equilibration of plasma and tissue concentrations. The literature half-life value varies between 1-4 days, while complete elimination may well take up to 5 weeks (Rotha et al., 1998; Patacchioli, 2004; Howelett and Barth, 2002). Δ^9 -THC is excreted both in urine and feces as metabolites. Most urinary metabolites are acids. The main metabolite found in urine is the THC-COOH glucuronide, which, when normalized to the creatinine concentration, can be used for the detection and monitoring of *Cannabis* drug abuse. Δ^9 -THC also undergoes extensive enterohepatic recycling, which also contributes to its slow elimination (Rotha et al., 1998; Patacchioli, 2004; Howelett and Barth, 2002).

Cannabinoid receptors have been identified in both the brain and the immune system. They are denoted by the abbreviation CB, and numbered in the order of their discovery by a subscript (Howelett and Barth, 2002). Two distinct cannabinoid receptors, CB₁ and CB₂ have been cloned. The CB₁ receptor is a GPCR receptor located in the central nervous system. It is expressed strongly in the basal ganglia, cerebellum, hippocampus and in the dorsal primary afferent spinal cord region (Howelett and Barth, 2002; Williams et al., 2006). The localization of CB₁ receptors clearly indicates their effectiveness in memory impairment, analgesia and addiction. The CB₂ receptor exhibits 48% homology with the CB₁ receptor. CB₂ receptor mRNA is found mainly in immune tissues, and is notably absent from normal nervous tissue (Howelett and Barth, 2002). Δ⁹-THC and other cannabinoid receptor agonists show therapeutic effects as analgesics, lessen feelings of nausea and vomiting in cancer chemotherapy, cause appetite stimulation in wasting syndromes, and provide relief from muscle spasms. The main side-effects are alterations in cognition and memory, dysphoria/euphoria, and sedation. Synthetic agonists that bind to cannabinoid receptors are usually Δ⁹-THC analogs and aminoalkylindole compounds. Most notable endogenous cannabinoid ligands are anandamide (arachidonylethanolamide), 2-arachidonoylglycerol, and 2-arachidonoylglycerol ether. Anandamide and 2-arachidonoylglycerol function as neurotransmitters or neuromodulators, and act as retrograde synaptic messengers (Howelett and Barth, 2002). They are synthesized by neurons on demand, and undergo depolarization-induced release from neurons and after their release they are rapidly removed from the extracellular space by a membrane transport system process. This process still remains to be fully characterized. Once within the cell, anandamide is hydrolyzed to arachidonic acid and ethanolamine by fatty acid amide hydrolase (FAAH).

When agonists bind to cannabinoid receptors, they activate a number of signal transduction pathways via the G_{i/o} family of G proteins. Free G_{i/o} proteins regulate adenylyl cyclase, leading to an inhibition of cyclic AMP production. This inhibits phosphorylation by protein kinase A, leading to modulation of signaling pathways, especially ion channels (Williams et al., 2006). An interaction between CB₁ receptors and phospholipase C was demonstrated in cultured cerebellar granule neurons, in which cannabinoid agonists

augmented the Ca^{2+} signal in response to NMDA receptor stimulation of K^+ depolarization (Howelett and Barth, 2002).

A body of evidence suggests the existence of independent but interacting mechanisms of modulation of antinociception by cannabinoid and opioid systems (Hohman et al., 1999). It has been shown previously that Δ^9 -THC and morphine show synergistic effects in the production of antinociception (Williams et al., 2006). There is a similar distribution of CB_1 cannabinoid and *mu* opioid receptors in the dorsal horn of the spinal cord and in central nervous system (Bidaut-Russell and Howlett, 1988). Opioids and cannabinoids also produce similar effects on calcium levels and cyclic AMP accumulation through G protein receptors (Reche et al., 1996). Importantly, cannabinoids have been shown to produce analgesia through interaction with kappa opioid receptors in the spinal cord by releasing endogenous opioids (Hohman et al., 1999).

A synergism between morphine and Δ^9 -THC has also been observed in the spinal cord of mice. Inactive doses of both morphine and Δ^9 -THC showed a greater than additive effect when given by i.v. administration (Bidaut-Russell and Howlett, 1988; Reche et al., 1996). A mixture of these two drugs produced an analgesic effect through *mu* opioid receptor- as well as CB_1 cannabinoid receptor-mediated pathways.

Since, a codrug strategy has been reported useful for improving the physicochemical and pharmacokinetic properties of the parent drugs; the next chapter reports the synthesis of opioid and cannabinoid codrugs. Later on, their pharmacological and pharmacokinetic evaluation has been carried to compare their efficacies with parent drugs and physical mixtures of the parent drugs.

Chapter 2

Synthesis of Codrugs and Parent drugs

2.1 Synthesis of Δ^9 -Tetrahydrocannabinol (Δ^9 -THC)

Δ^9 -THC synthesis was carried out in two steps. In the first step, (+)-limonene oxide (mixture of *cis* and *trans* isomers) was added to a stirred suspension of sodium borohydride and diphenyldiselenide in dry ethanol under a nitrogen atmosphere. The mixture was refluxed for 2 hrs and then after cooling, hydrogen peroxide was added drop-wise. After work up, the solvent was evaporated under reduced pressure and column chromatography was carried out using hexanes:diethyl ether gradient to obtain pure (1*S*,4*R*)-*p*-mentha-2,8-dien-1-ol (Rickards and Watson, 1980). The selenoxide intermediate was characterized by X-ray diffraction (Fig. 2.1) and (1*S*,4*R*)-*p*-mentha-2,8-dien-1-ol was characterized by GC-MS (Fig 2.2) and NMR spectroscopy.

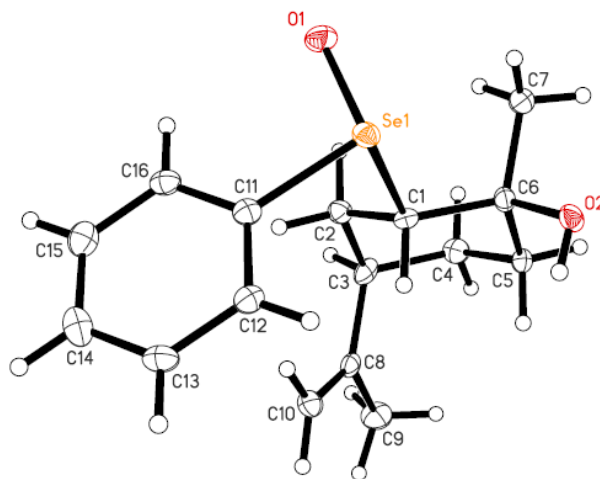
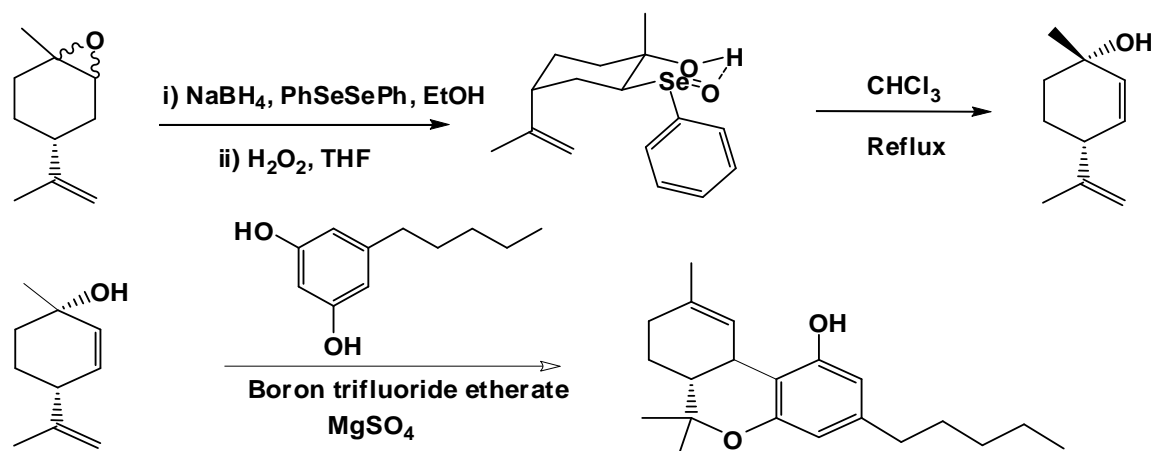


Fig. 2.1 Single crystal X-ray structure of the selenoxide intermediate in the synthesis of Δ^9 -THC

In the second step, $\text{BF}_3 \cdot \text{Et}_2\text{O}$ was added drop-wise to a stirred suspension of (1*S*,4*R*)-*p*-mentha-2,8-dien-1-ol, olivetol and anhydrous magnesium sulfate in methylene chloride at 0 °C under a nitrogen atmosphere. The mixture was stirred for 2 hrs at 0 °C, and then anhydrous sodium bicarbonate was added. After workup, column chromatography over silica was carried out using a hexanes:diethyl ether gradient to obtain pure Δ^9 -THC (Scheme 2.1) (Razdan et al., 1974). The final product was characterized by GC-MS (Fig. 2.2) and NMR spectroscopy.

Scheme 2.1: Synthesis of Δ^9 -THC



2.2 Synthesis of (-)-Cannabidiol (CBD)

A GC-MS of (+)-limonene oxide (mixture of *cis* and *trans* isomers) was recorded before starting this synthesis, to check the purity of the compound, and also to help in monitoring the progress of the initial reaction. In Fig. 2.3, a GC of (+)-limonene oxide is illustrated which shows the peaks attributed to *cis* and *trans* limonene oxides having 90 % matches in the Wiley database.

In the first step of the synthesis of (-)-cannabidiol, morpholine was added to a stirred solution of LiCl and limonene oxide in ethanol and the reaction mixture was

heated at 70 °C (Scheme 2.2). The progress of the reaction was monitored by GC-MS. Fig. 2.4, shows the GC-MS of the reaction after 6 hrs, and after 24 hrs. The GC-MS after 24 hrs showed complete disappearance of the *trans*-(+)-limonene oxide peak. Longer reaction times allowed the *cis*-(+)-limonene oxide to react with morpholine. Thus, the reaction was stopped after 24 hrs. The solvent was evaporated under reduced pressure after work up; the product, 4-isopropenyl-1-methyl-2-morpholin-4-yl-cyclohexanol, was obtained as a yellow oil. The GC-MS of this product is shown in Fig. 2.5 (Gu et al., 2004).

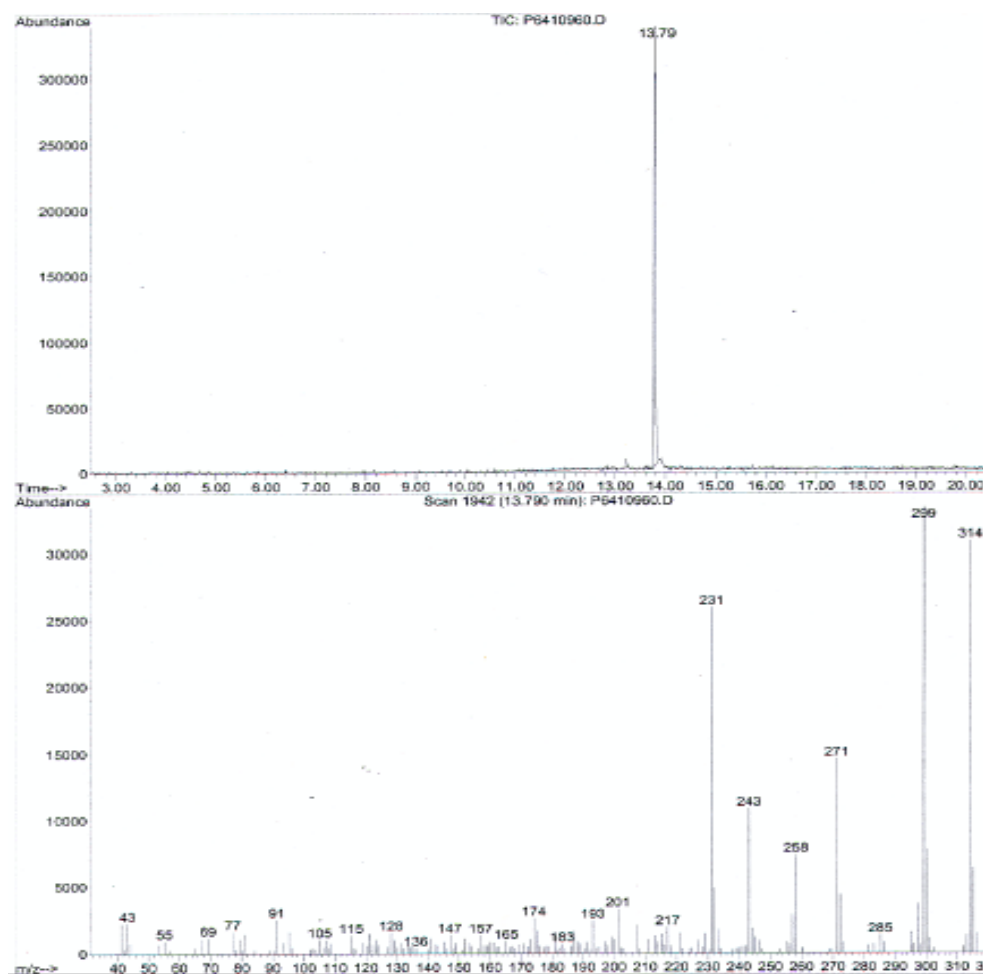


Fig. 2.2 The GC-MS of Δ^9 -THC

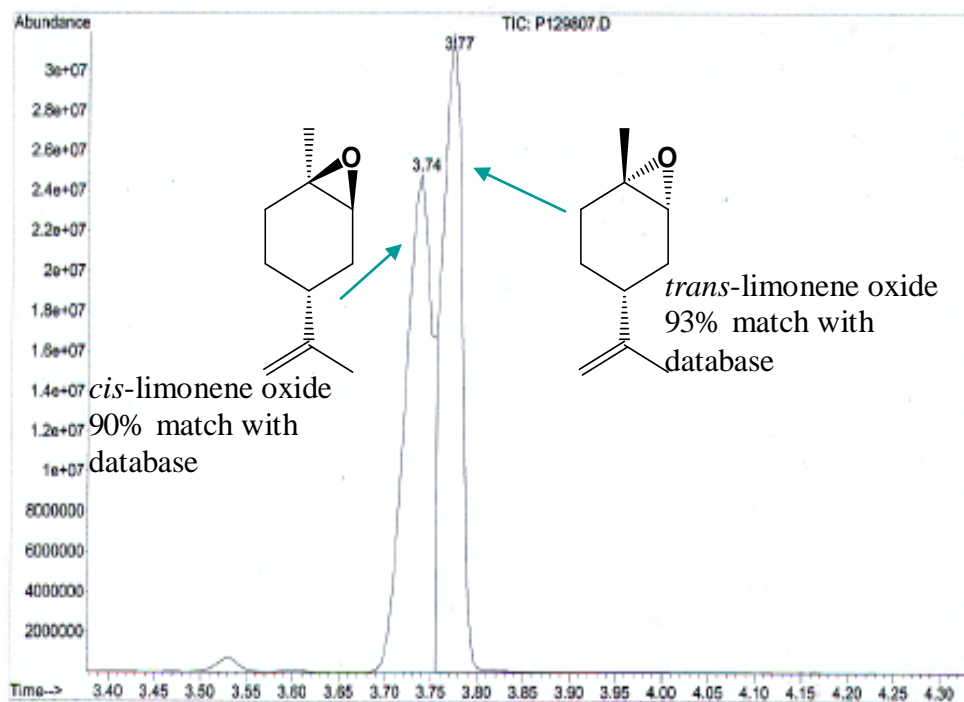
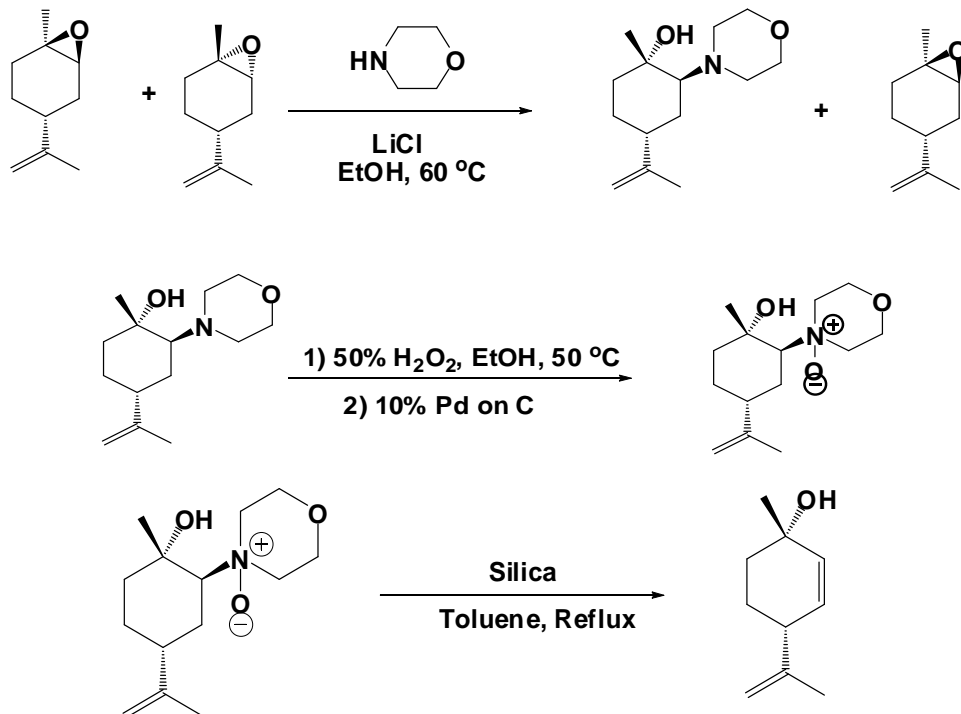


Fig. 2.3 The GC-MS of (+)-limonene oxide

Scheme 2.2: Synthesis of (1*S*,4*R*)-*p*-mentha-2,8-dien-1-ol



In the second step of synthesis of (-)-cannabidiol, hydrogen peroxide was added to the yellow oil resulting from the first step of the synthesis, and the resulting solution was heated for 4 hrs. 10 % Pd on C was then added to decompose the remaining hydrogen peroxide, and the reaction mixture was filtered through a pad of celite. The filtrate was evaporated under reduced pressure to afford yellow oil. Silica gel column chromatography was carried out to purify the compound using a hexanes:ethyl acetate gradient followed by elution with methanol, to afford a pure fraction of 4-isopropenyl-1-methyl-2-(4-oxy-morpholin-4-yl)-cyclohexanol.

4-Isopropenyl-1-methyl-2-(4-oxy-morpholin-4-yl)-cyclohexanol was dissolved in toluene and silica was added. The resulting mixture was heated to reflux with stirring. The literature procedure recommends the use of a Dean and Stark apparatus, but product formation was observed when under these conditions. As an alternative, the solution was refluxed overnight and the silica was then removed by filtration. The filtrate was evaporated under reduced pressure to afford a brown oil, which consisted of the product, (1*S*,4*R*)-*p*-mentha-2,8-dien-1-ol and a small amount of (1*R*,4*R*)-*p*-mentha-2,8-dien-1-ol as a byproduct. The crude (1*S*,4*R*)-*p*-mentha-2,8-dien-1-ol was purified by silica gel column chromatography using a hexanes:diethyl ether gradient and the final product was characterized by GC-MS (89% match with Wiley database) (Fig. 2.6) and NMR spectroscopy (Chen et al., 2007).

In the last step of the synthesis, a mixture of olivetol, zinc chloride, water and dichloromethane was refluxed and (1*S*,4*R*)-*p*-mentha-2,8-dien-1-ol was added drop-wise (Scheme 2.3). It is advisable to add (1*S*,4*R*)-*p*-mentha-2,8-dien-1-ol very slowly to avoid the formation of side-products. The progress of the reaction was monitored by GC-MS. After the completion of the reaction, the solvent was evaporated, and the crude mixture was characterized by GC-MS, which indicated that it contained (-)-cannabidiol, *abnormal*-cannabidiol (*abn*-CBD), olivetol and traces of ⁹-THC (Fig. 2.7). Column chromatography over silica gel was carried out on the crude product using a hexanes:diethyl ether gradient. The fractions obtained were characterized by GC-MS and NMR spectroscopy (Choi et al., 2004). A pure fraction of (-)-cannabidiol was obtained

and was characterized by GC-MS (Fig. 2.8). An NMR spectrum of the synthesized (-)-cannabidiol compared favorably with that of (-)-cannabidiol reported by Gutman et al., 2006.

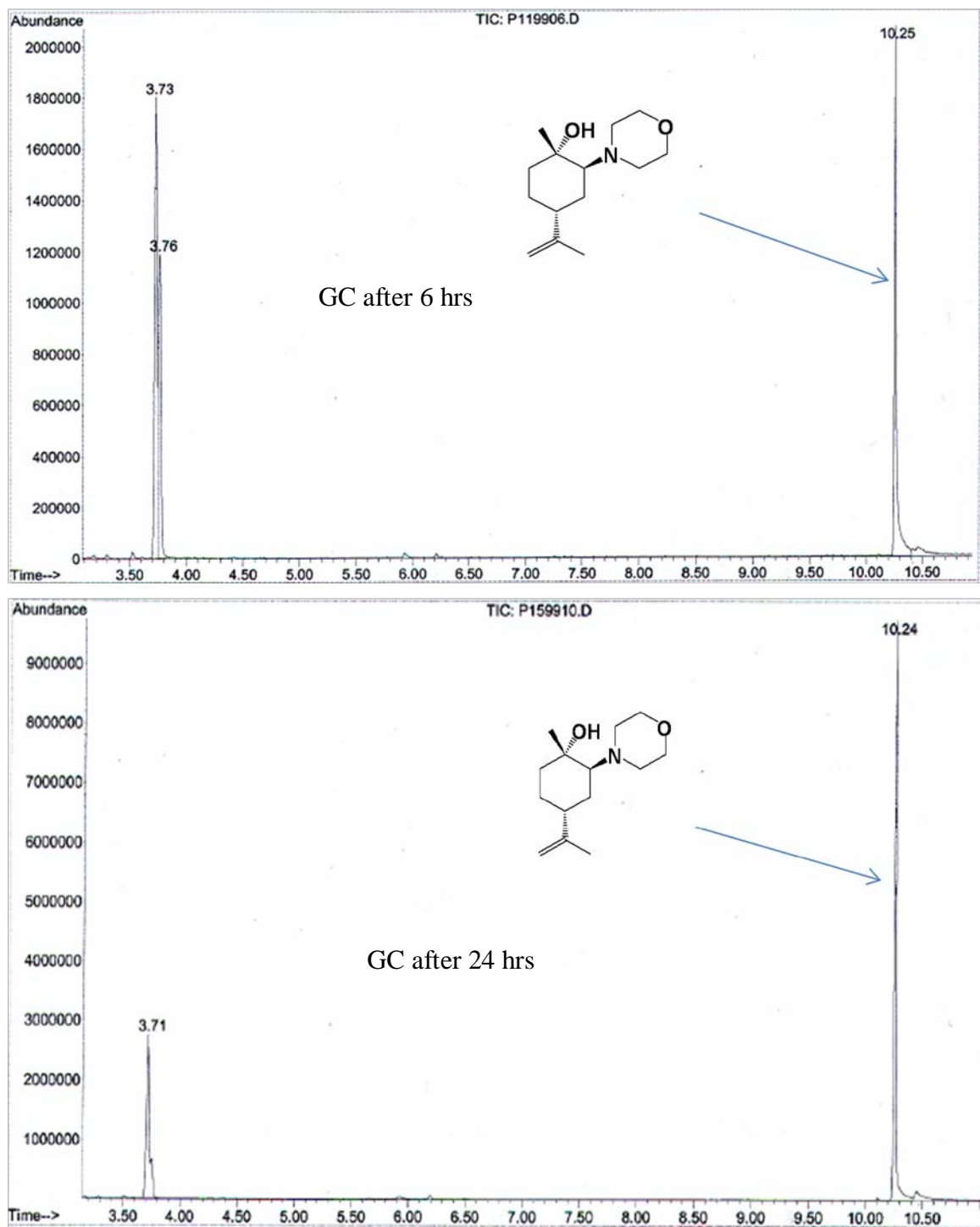


Fig. 2.4 GC-MS of reaction mixture for the synthesis of 4-isopropenyl-1-methyl-2-(4-oxy-morpholin-4-yl)-cyclohexanol after 6 hrs and 24 hrs

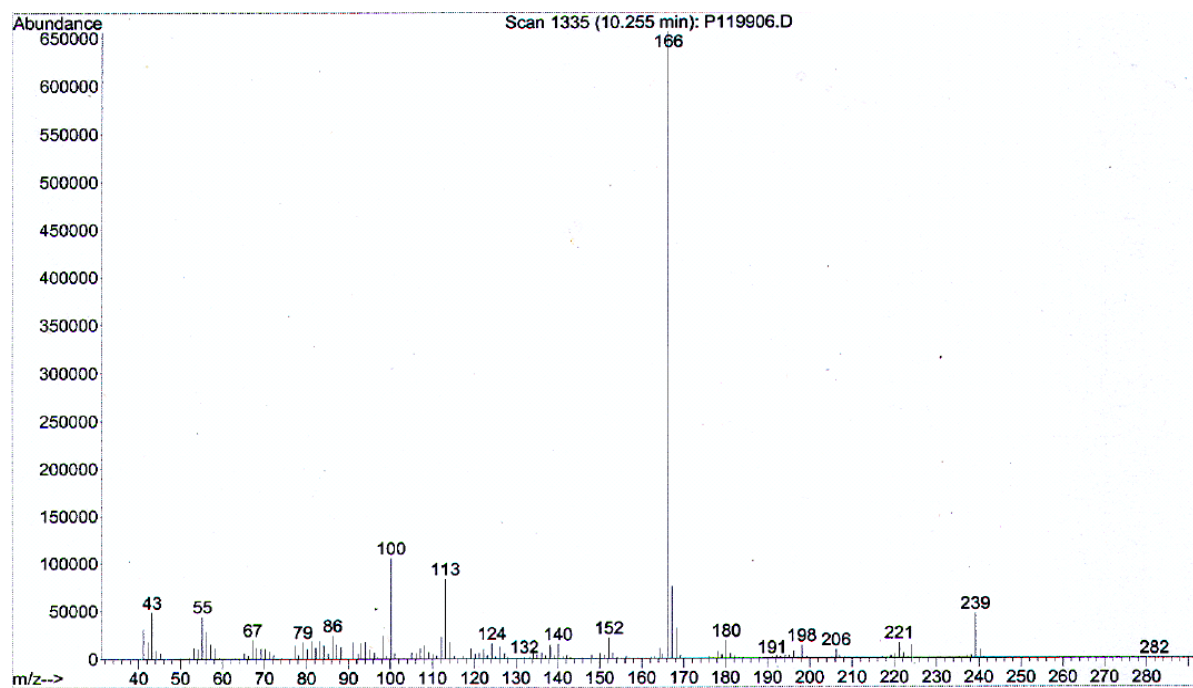
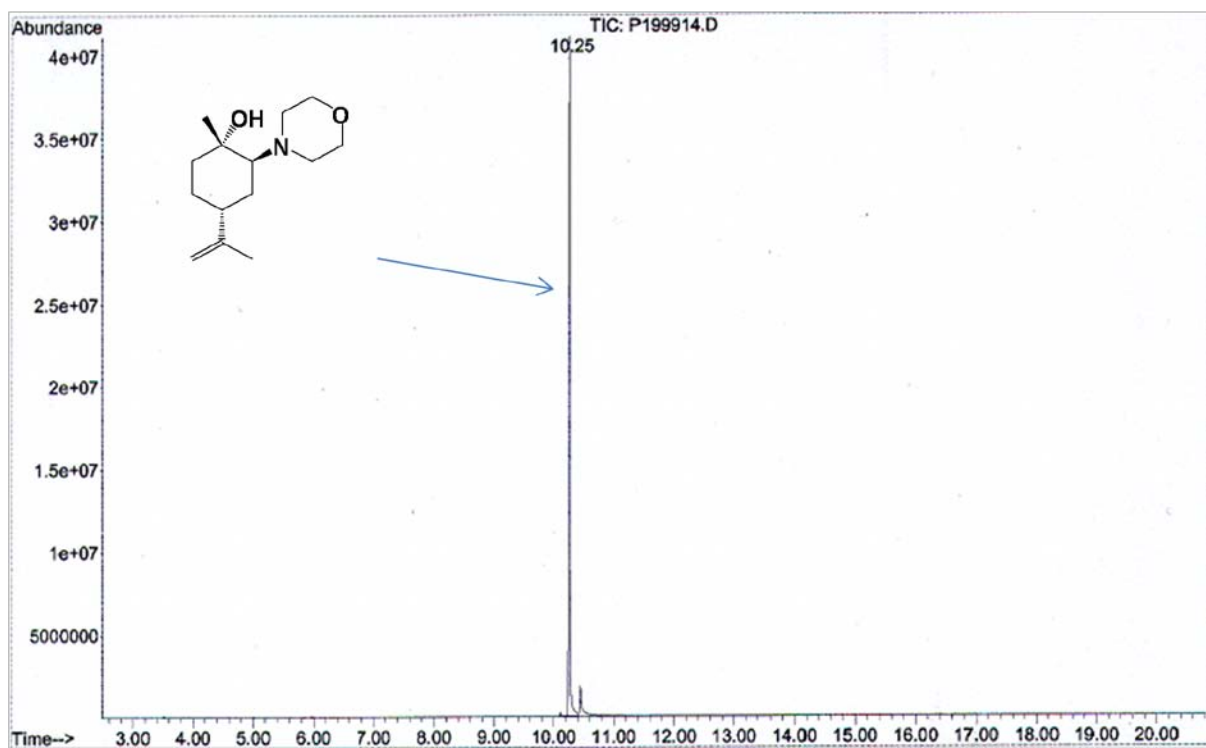


Fig. 2.5 The GC-MS of 4-isopropenyl-1-methyl-2-(4-oxy-morpholin-4-yl)-cyclohexanol

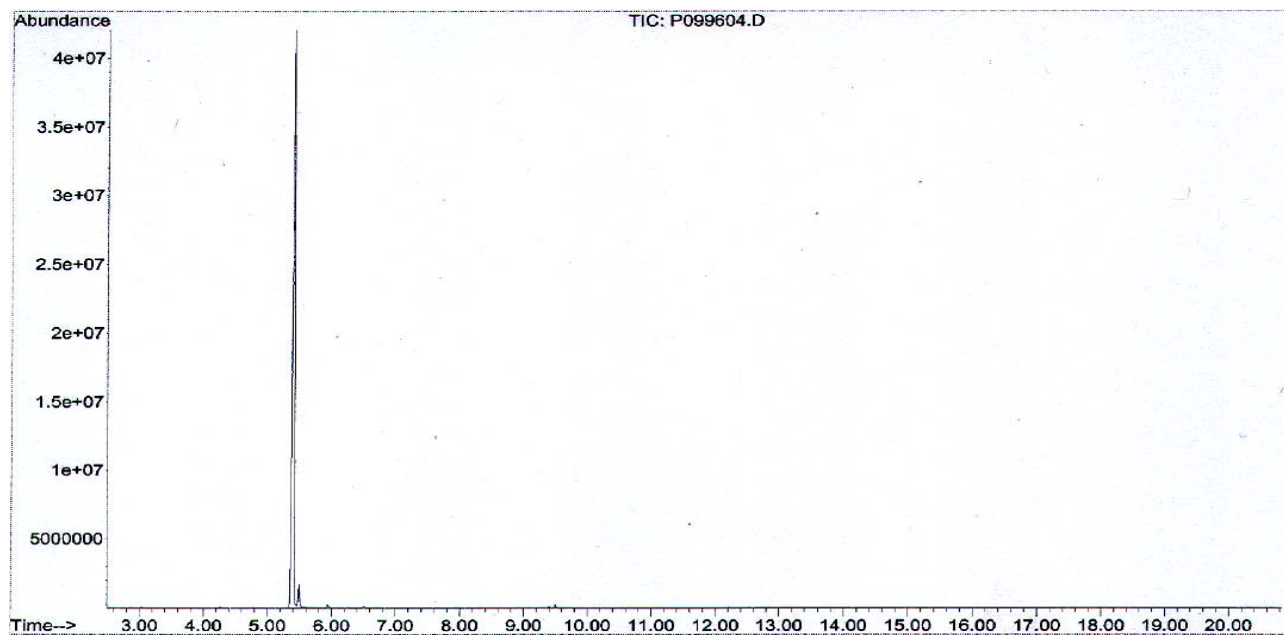
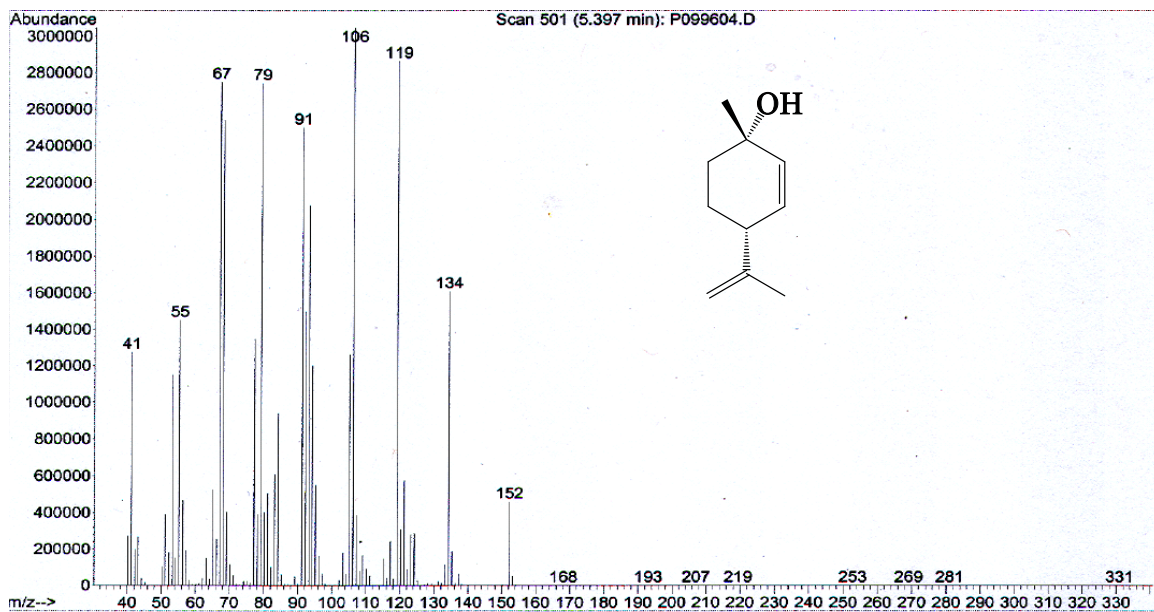


Fig. 2.6 The GC-MS of (1*S*,4*R*)-*p*-mentha-2,8-dien-1-ol

Scheme 2.3: Synthesis of (-)-cannabidiol and *abnormal*-cannabidiol

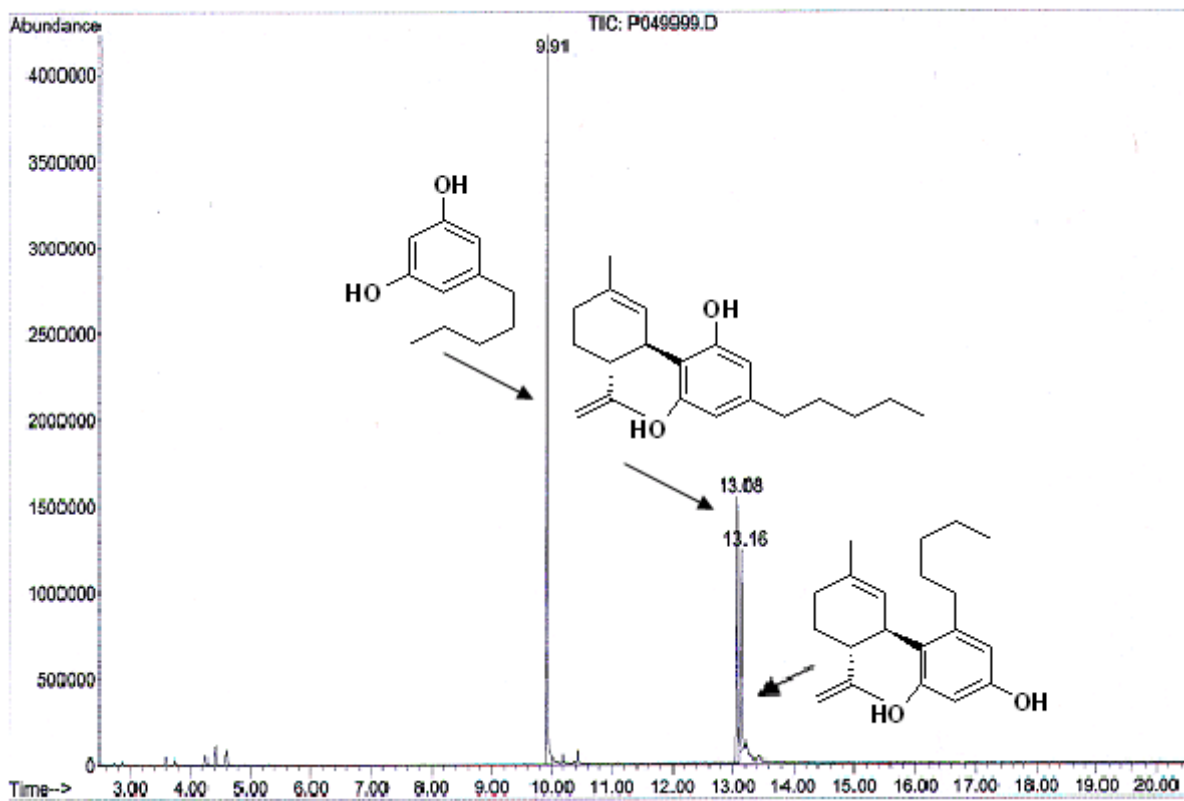
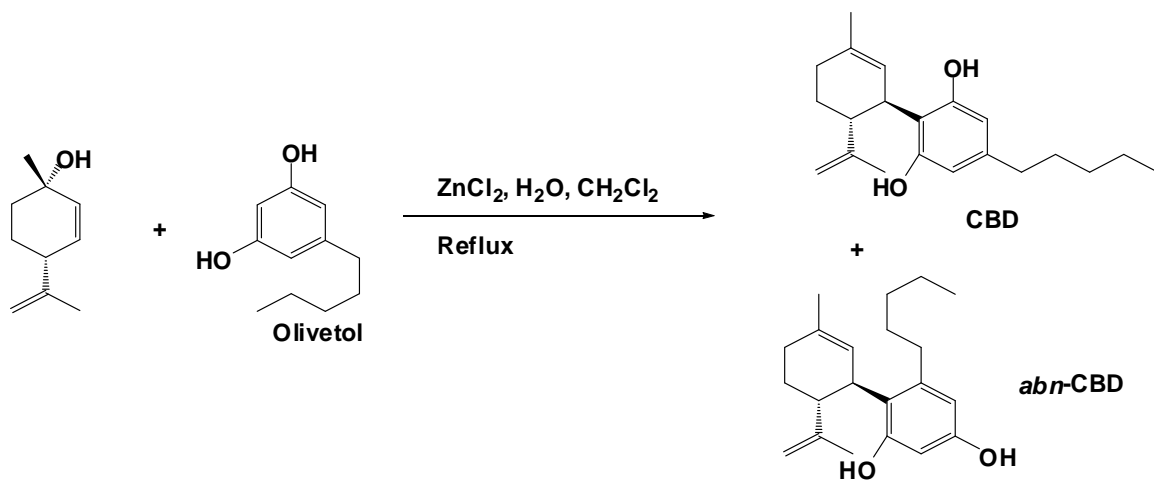


Fig. 2.7 The GC-MS of the crude mixture from (-)-cannabidiol synthesis

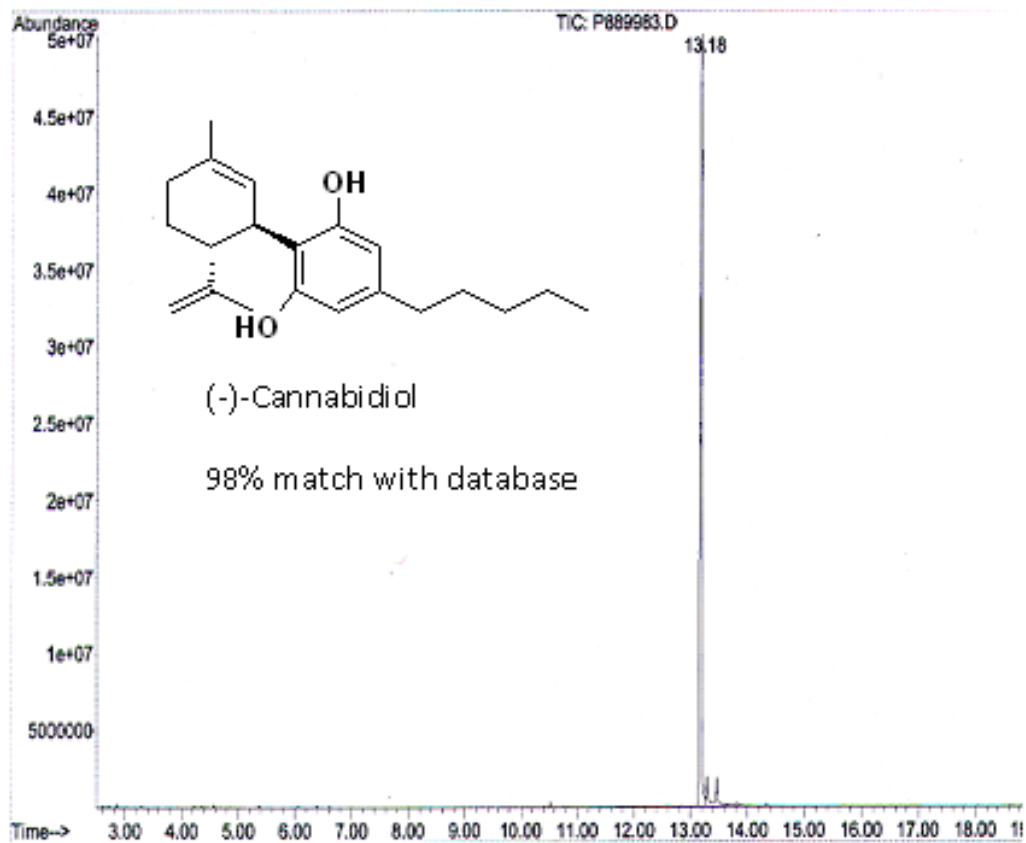


Fig. 2.8 The GC of synthesized (-)-cannabidiol

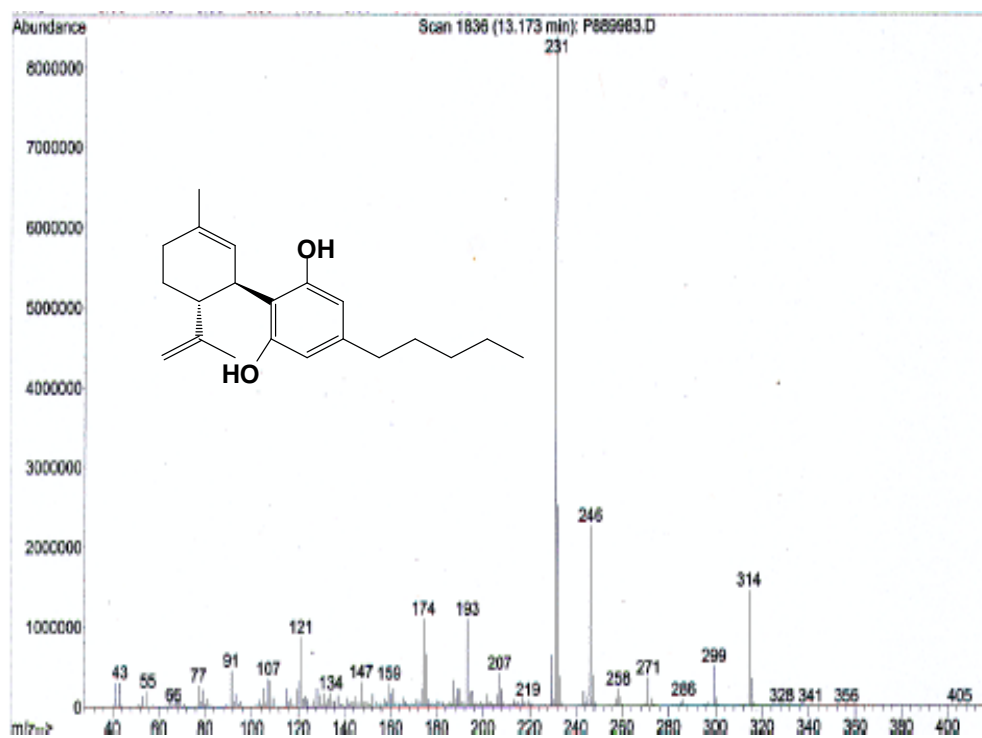


Fig. 2.9(a) The MS of synthesised (-)-cannabidiol

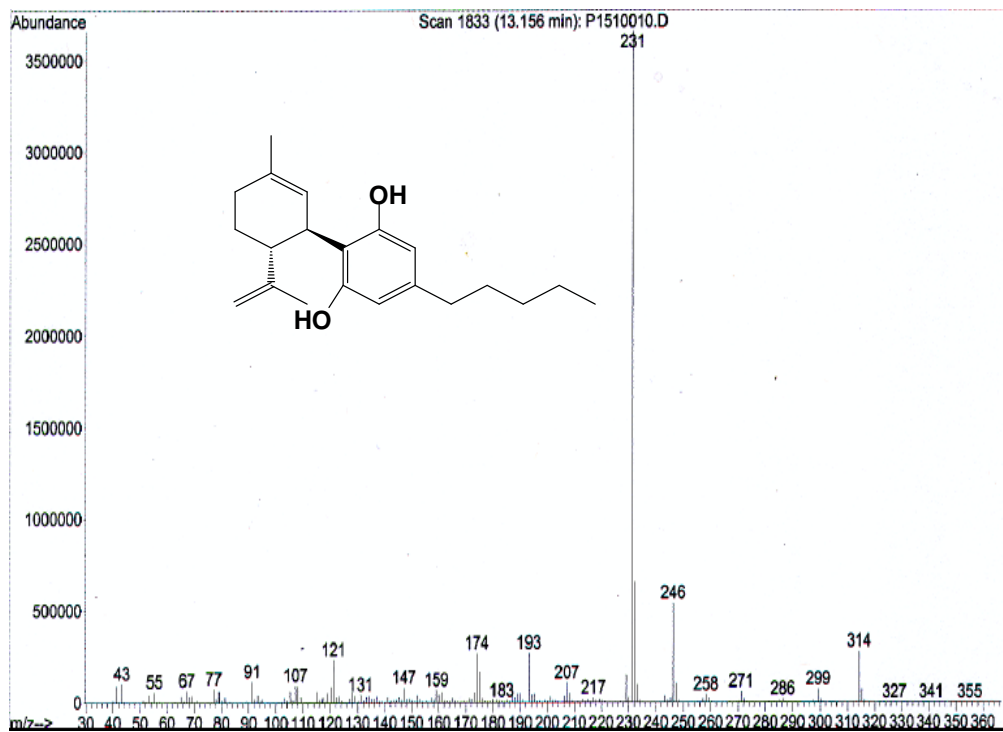


Fig. 2.9 (b) The MS of a reference standard of (-)-cannabidiol

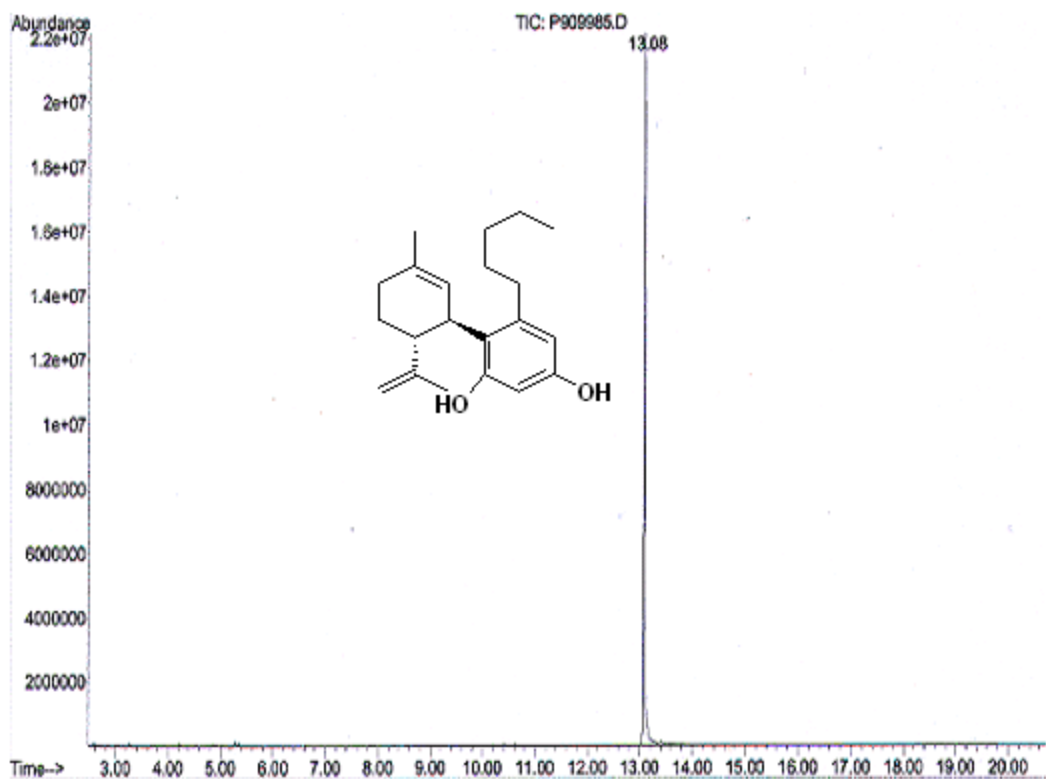


Fig. 2.10 The GC of *abn*-cannabidiol

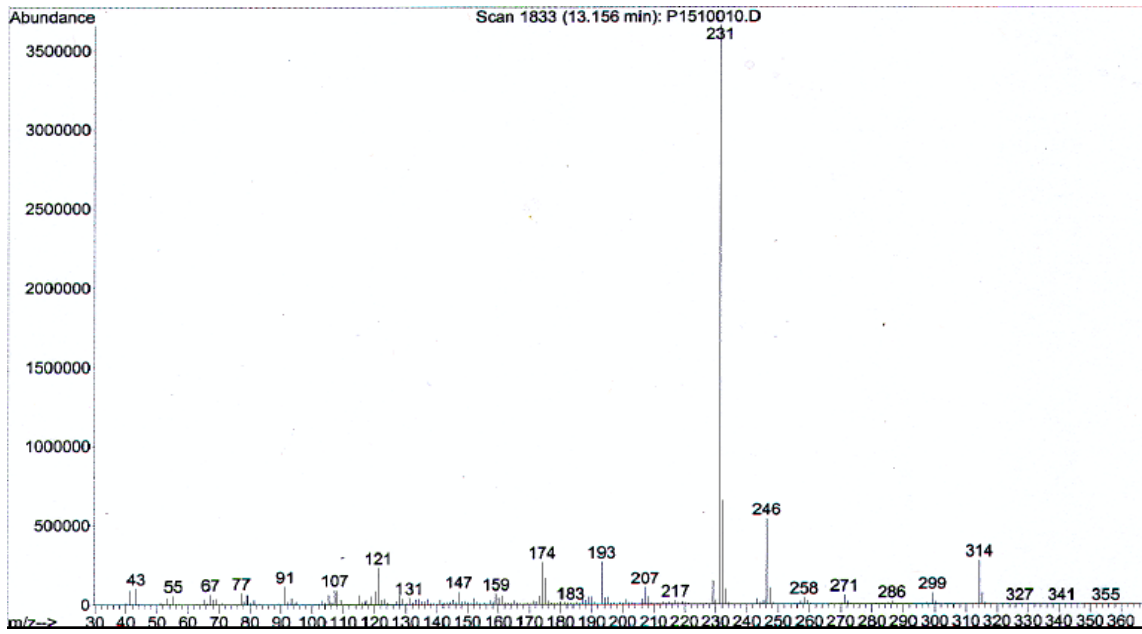
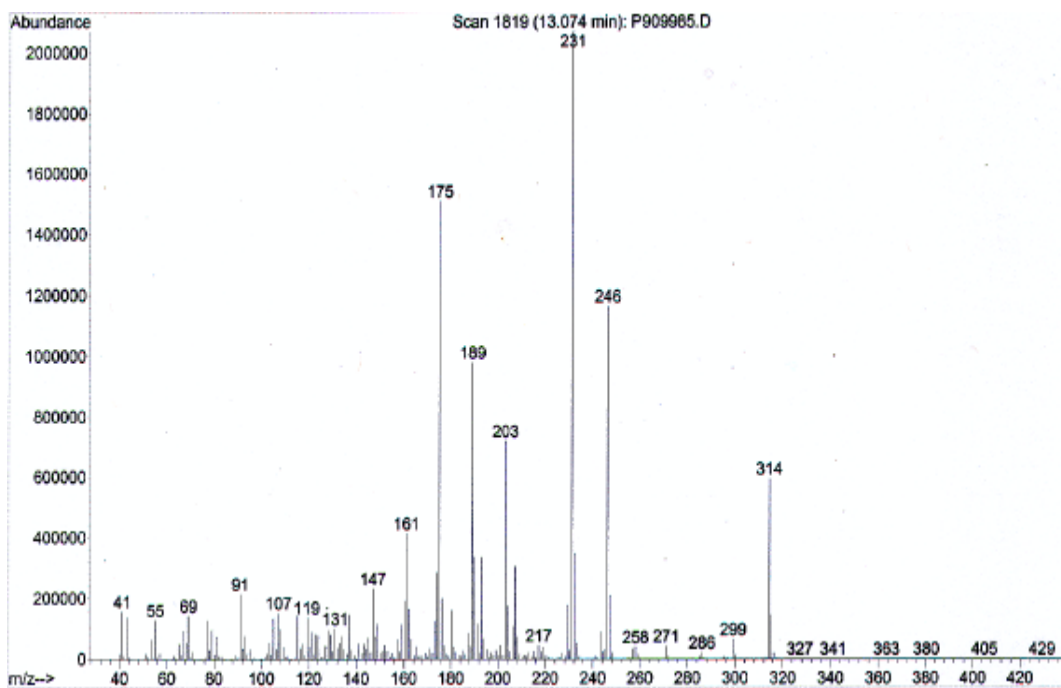


Fig. 2.11 (a) MS of *abn*-cannabidiol and (b) MS of a reference standard of (-)-cannabidiol

2.3 Codeine- Δ^9 -Tetrahydrocannabinol (Cod-THC) Codrug Synthesis

Before starting the synthetic work with expensive controlled substances such as codeine and Δ^9 -THC, coupling reactions were initially carried out with model compounds or chemical-mimics of the drug molecules to optimize the desired chemistry. 3-Ethylphenol was chosen as the model compound for both codeine and Δ^9 -THC.

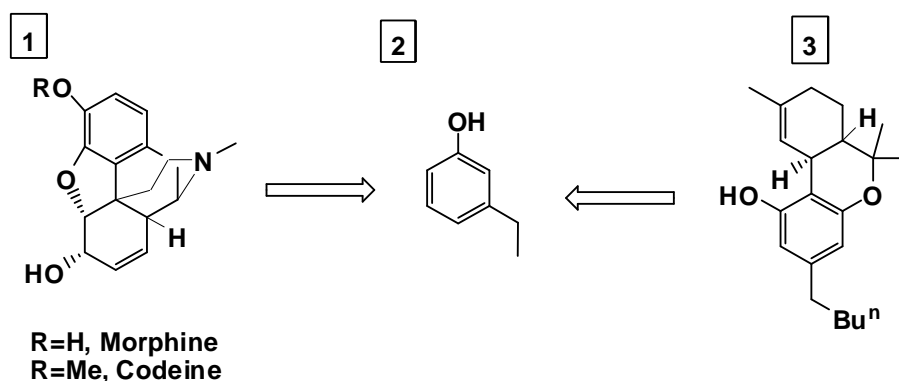
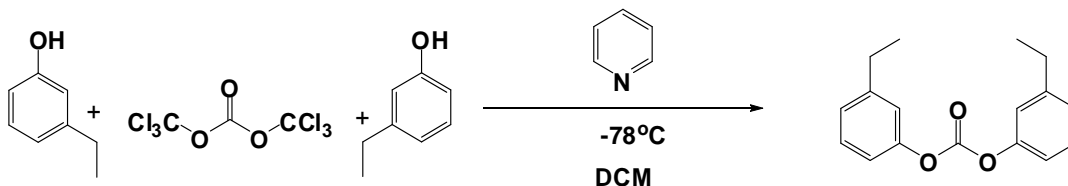


Fig. 2.12 Structures of morphine, codeine (1), 3-ethylphenol (2) and Δ^9 -THC (3)

Since the essential conjugation chemistry in the synthesis of the Cod-THC codrug is the formation of a carbonate linkage, reactions were initiated to generate carbonate linkages with phenols. Initially, a symmetrical carbonate ester of 3-ethylphenol was formed utilizing triphosgene and pyridine (Scheme 2.4) (Burk and Roof, 1993).

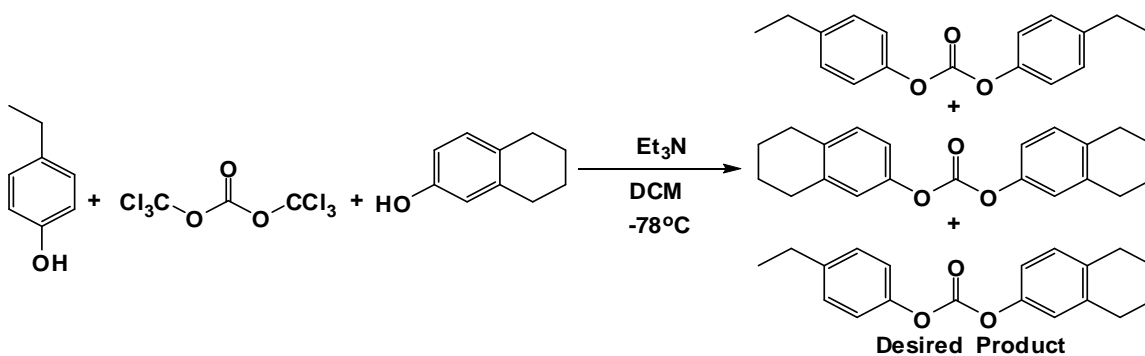
Scheme 2.4: Synthesis of a symmetrical carbonate of 3-ethylphenol



Unfortunately, 3-ethylphenol obtained from Aldrich was only 80% pure, the major of the impurity being 4-ethylphenol, thus a pure sample of desired product was unattainable. Due to this problem, use of 3-ethylphenol in the model reactions was replaced with 4-ethylphenol, since 4-ethylphenol from Aldrich was 98% pure. The same conjugation reaction was carried out with 4-ethylphenol and afforded the desired symmetrical carbonate.

The next aim was to form a carbonate linked product using two different phenols. For this purpose 4-ethylphenol and 5,6,7,8-tetrahydro-2-naphthol were used as model compounds. The reaction between these two phenols in the presence of triphosgene and triethyl amine produced 3 different carbonates, two symmetrical carbonates along with the desired unsymmetrical carbonate. GC-MS analysis showed almost equal quantities of all three carbonates in reaction mixture (Scheme 2.5).

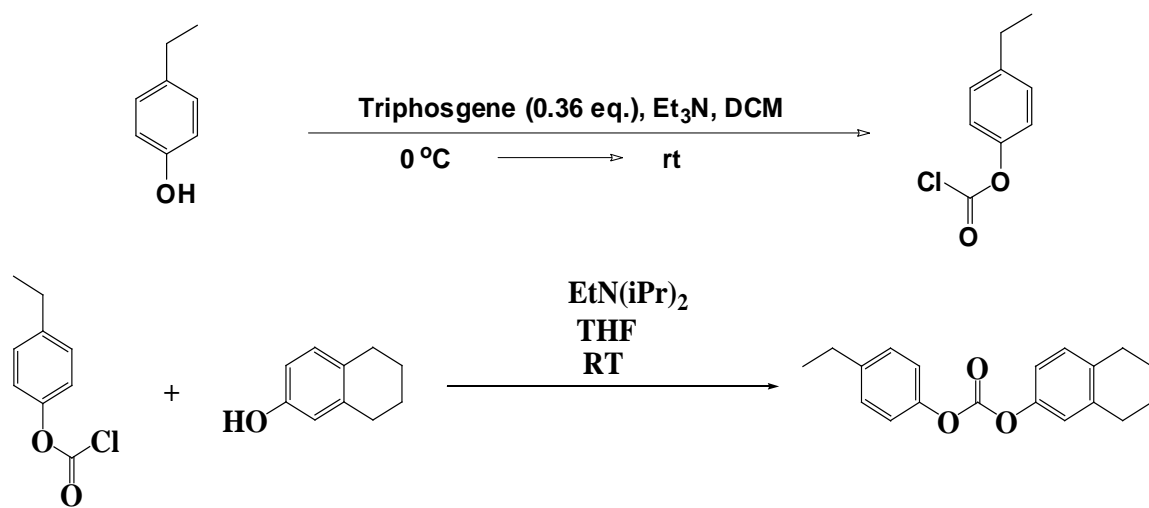
Scheme 2.5: Conjugation of two different phenolic compounds utilizing triphosgene



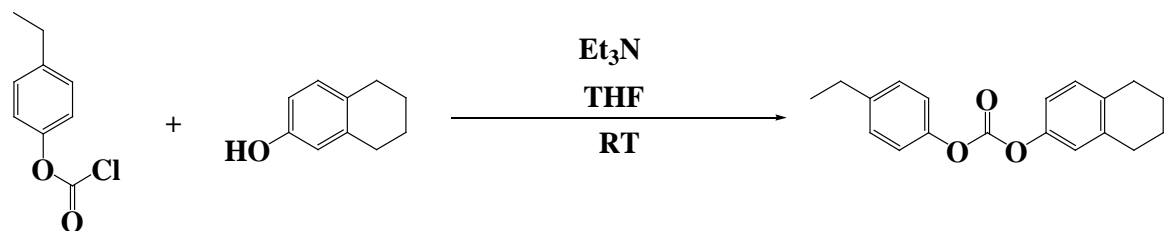
In the above reaction, as there was no selectivity observed for the formation of the desired unsymmetrical carbonate over the two symmetrical carbonates, it was anticipated that purification of the unsymmetrical carbonate would present a difficult challenge. Thus, a different synthetic approach was devised utilizing the intermediacy of a chloroformate analogue. Initially, one of the phenolic starting materials was converted to a chloroformate derivative, and then the other phenolic starting material was reacted with the chloroformate derivative to afford the unsymmetrical carbonate product (Scheme 2.6)

(Martin et al., 2006). Utilizing triethylamine as a base in the second step of the coupling reaction afforded better yield and less amount of side product formation (Scheme 2.7).

Scheme 2.6: Synthesis of an unsymmetrical carbonate of 4-ethylphenol and 5,6,7,8-tetrahydro-2-naphthol



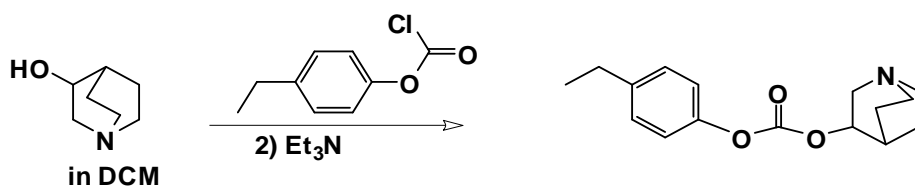
Scheme 2.7: Synthesis of an unsymmetrical carbonate of 4-ethylphenol and 5,6,7,8-tetrahydro-2-naphthol utilizing triethylamine



Since codeine contains an OH group and a basic tertiary *N*-atom, 3-quinuclidinol was chosen as a more appropriate chemical-mimic for codeine. 4-Ethylphenol was retained as the model molecule for ⁹-THC. In the next series of reactions the

chloroformate of 4-ethylphenol was initially formed and then reacted with 3-quinuclidinol to form the carbonate of 4-ethylphenol and 3-quinuclidinol (Scheme 2.8).

Scheme 2.8: Synthesis of an unsymmetrical carbonate of 4-ethylphenol and 3-quinuclidinol

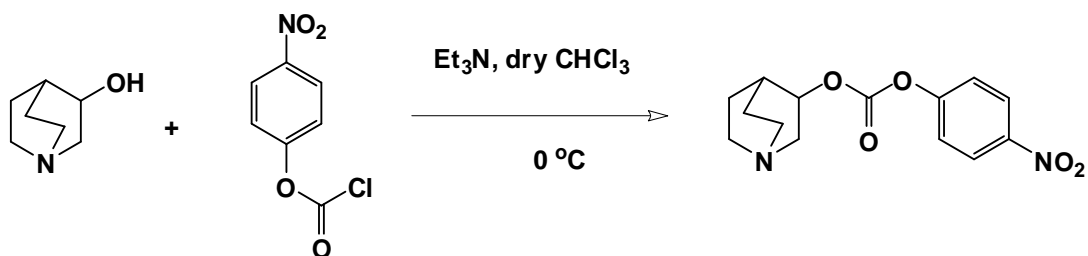


There were some problems associated with the formation of the chloroformate intermediate. The reaction was never clean, and there was always formation of a symmetrical carbonate as a side-product together with the formation of the desired chloroformate. Due to this problem a new synthetic method was sought for the exclusive synthesis of the unsymmetrical carbonate.

p-nitrophenylchloroformate analogues have been described in the literature for the formation of unsymmetrical carbonates and carbamates (Anderson and McGregor, 1957). Initially, an alcohol (A) is reacted with *p*-nitrophenylchloroformate to form the carbonate conjugate of A and *p*-nitrophenol. This intermediate is then reacted with another alcohol/phenol (B) to form the carbonate conjugate of A and B. In the second step, the good leaving group property of *p*-nitrophenol is advantageous in selective formation of the desired unsymmetrical carbonate (Scheme 2.9).

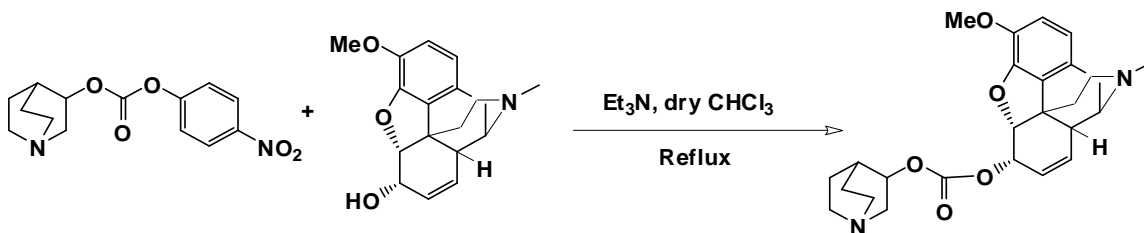
3-Quinuclidinol was allowed to react with *p*-nitrophenylchloroformate in the presence of a base to form the carbonate of 3-quinuclidinol and *p*-nitrophenol (Scheme 2.9a).

Scheme 2.9a: Synthesis of carbonate of 3-quinuclidinol and *p*-nitrophenol



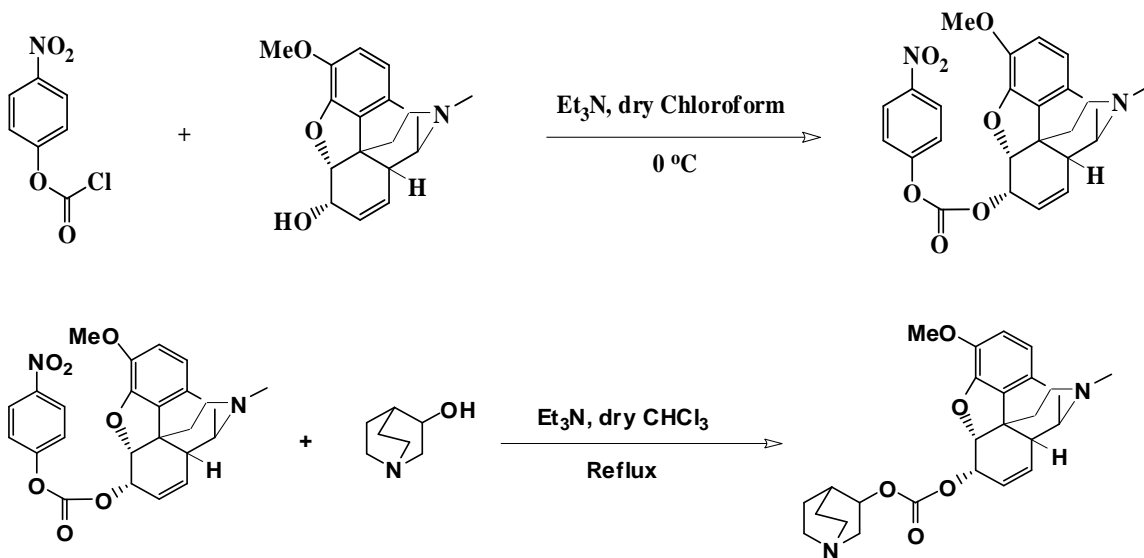
In the next step, the carbonate of 3-quinuclidinol and *p*-nitrophenol was allowed to react with codeine to form the desired unsymmetrical 3-quinuclidinol-codeine carbonate (Scheme 2.9b).

Scheme 2.9b: Synthesis of unsymmetrical 3-quinuclidinol-codeine carbonate



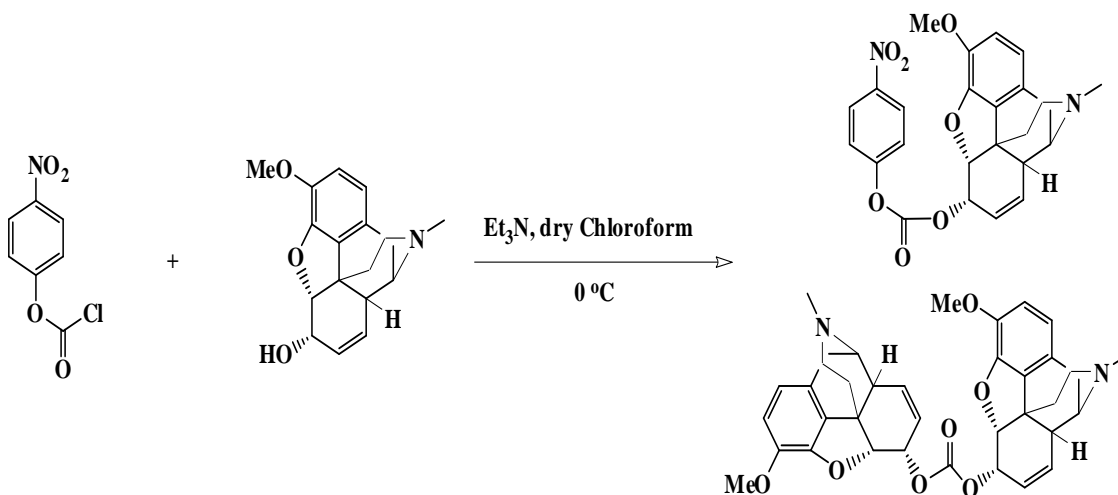
The carbonate ester of 3-quinuclidinol and codeine was also successfully synthesized via the alternative route by first forming the *p*-nitrophenol carbonate of codeine and then reacting this intermediate with 3-quinuclidinol (Scheme 2.10).

Scheme 2.10: Synthesis of unsymmetrical carbonate codeine and 3-quinuclidinol via the intermediacy of codeine-*p*-nitrophenol carbonate



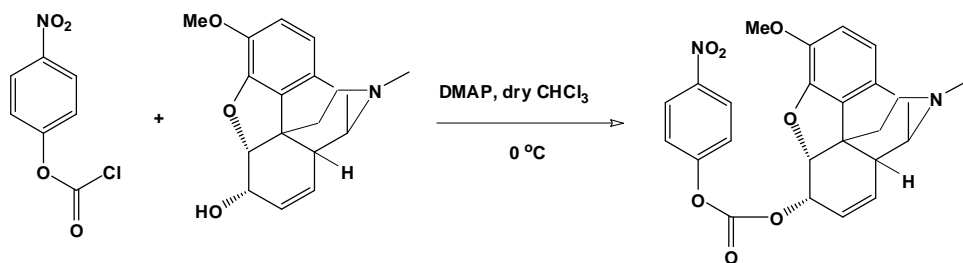
The latter approach was problematic, in that formation of the symmetrical carbonate of codeine was formed along with the desired unsymmetrical carbonate.

Scheme 2.11: Formation of carbonate of codeine and *p*-nitrophenol using triethylamine

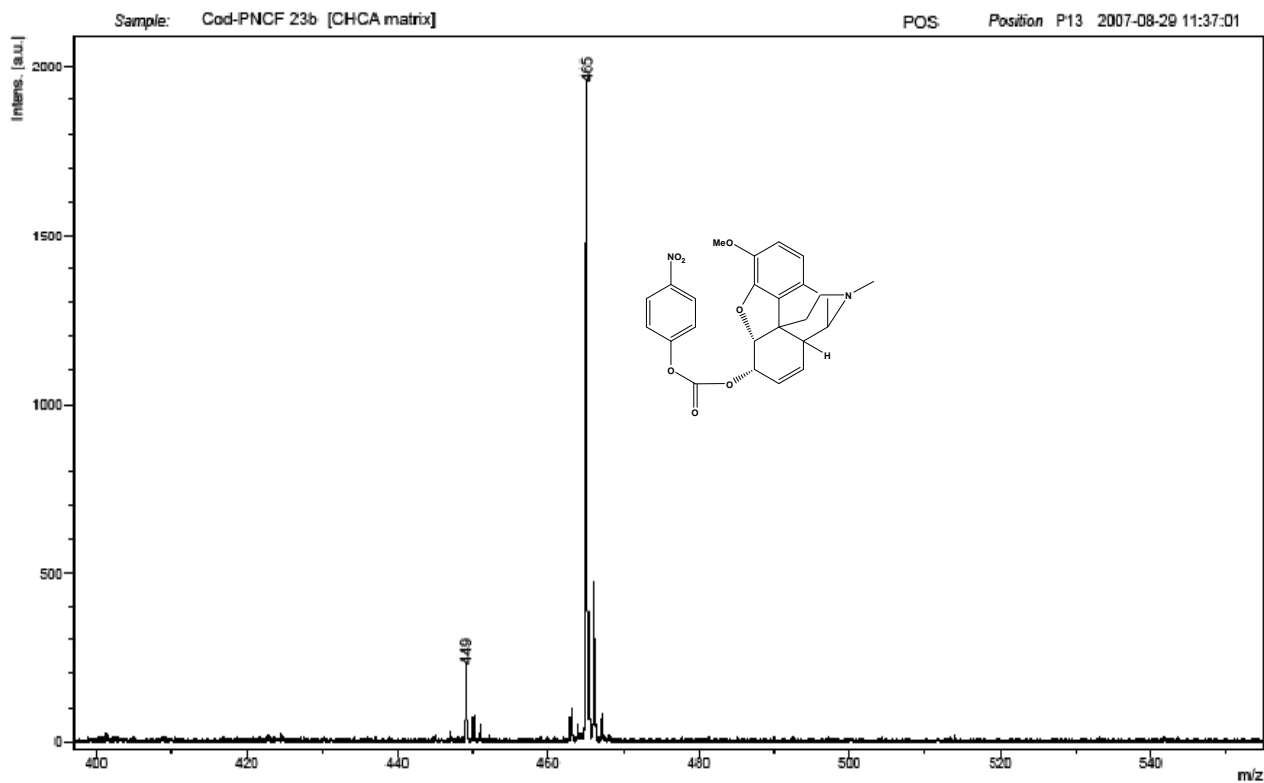
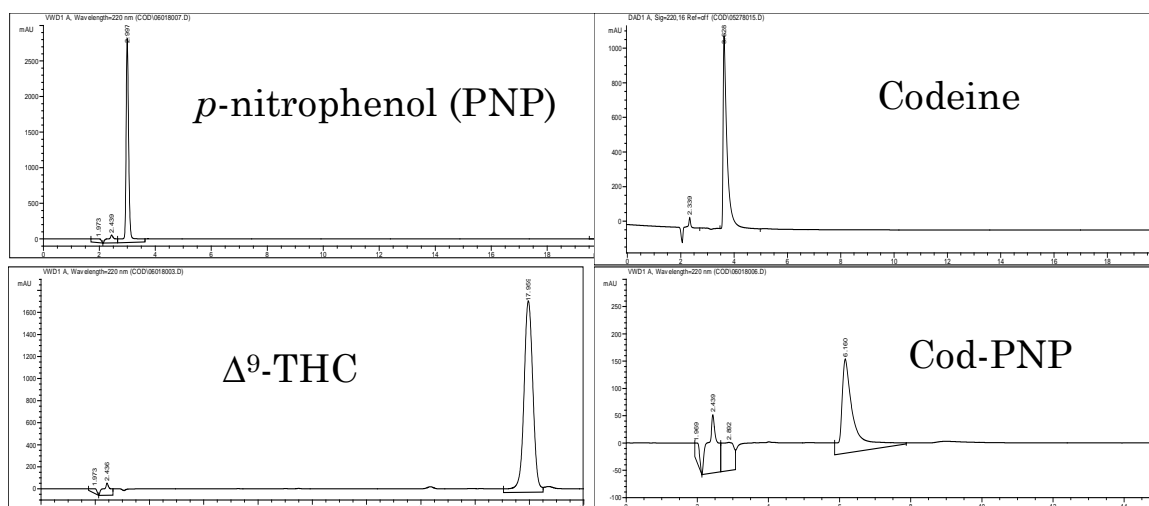


This problem was solved by utilizing a different base (DMAP), and by varying the reaction time and temperature (Scheme 2.12). The purity of the unsymmetrical carbonate was checked by NMR spectroscopy and by analytical HPLC. Fig. 2.14 shows the chromatograms of *p*-nitrophenol, codeine Δ^9 -THC and codeine-*p*-nitrophenol carbonate (Cod-PNP). A UV wavelength of 220 nm was used for the detection. An Apollo C₁₈ reverse phase column was used as the stationary phase, and 80:20 Acetonitrile:NH₄OAc buffer (pH 4.5) was used as the mobile phase with a 1 ml/min flow rate.

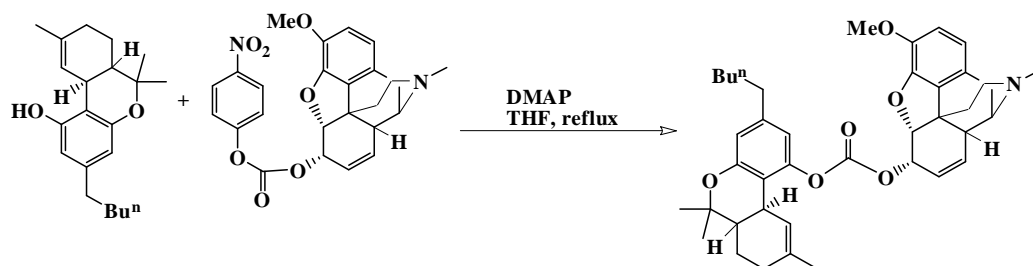
Scheme 2.12: Formation of carbonate of codeine and *p*-nitrophenol using DMAP



The next step was to form the actual codrug by reacting the *p*-nitrophenol carbonate of codeine with Δ^9 -THC. This reaction was carried out in the presence of DMAP as a base, and the reaction mixture was refluxed overnight. Formation of the product was confirmed by recording the MALDI spectrum of the product from the reaction mixture (Scheme 2.13).

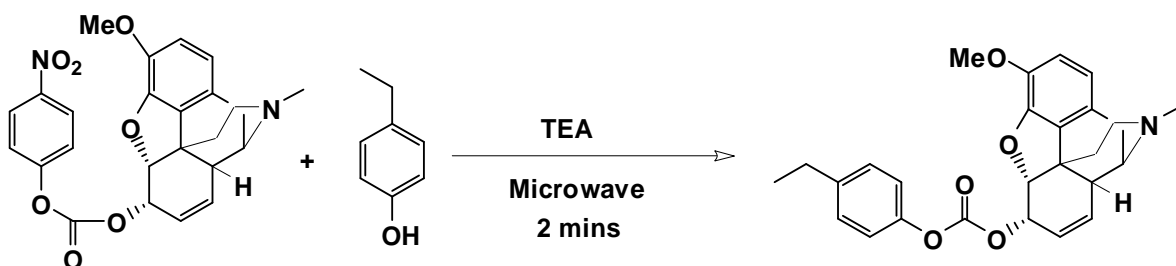
Fig. 2.13 MALDI spectrum of codeine-*p*-nitrophenol carbonateFig. 2.14 HPLC chromatograms of different analytes (*p*-nitrophenol, codeine, Δ^9 -THC, codeine-*p*-nitrophenol carbonate)

Scheme 2.13: Synthesis of carbonate of codeine and Δ^9 -THC



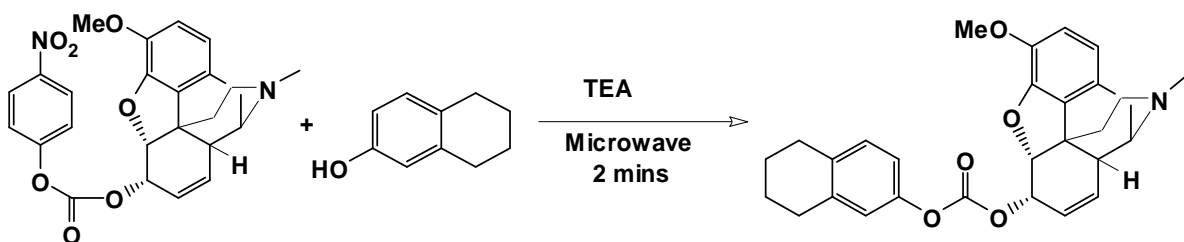
The above reaction was carried out several times by varying the base (DMAP or triethylamine) and varying the reaction temperatures and solvents, but the reaction never went to completion. Although the MADLI spectrum showed evidence for the formation of the desired codrug, TLC monitoring of the reaction mixture showed only a faint spot of the product and intense spots of the starting materials. Since conventional chemical reactions could not solve the problem of incomplete conversion to product, microwave reactions were explored (de la Hoz et al., 2005). In an initial attempt, the carbonate of codeine and *p*-nitrophenol was reacted with 4-ethylphenol in a microwave oven in presence of a base (TEA) and in absence of any solvent (Scheme 2.14a). The reaction mixture was irradiated for 30 seconds followed by TLC monitoring. No further progress of the reaction was noticed after 2 minutes of total microwave irradiation time.

Scheme 2.14 (a): Synthesis of unsymmetrical carbonate of codeine and 4-ethylphenol utilizing microwave irradiation



In another attempt, the reaction between the carbonate of codeine and *p*-nitrophenol and 5,6,7,8-tetrahydro-2-naphthol was performed under microwave conditions. The reaction mixture was irradiated for 30 seconds followed by TLC monitoring. No further progress of the reaction was noticed after 2 mins of total microwave irradiation time (Scheme 2.14b).

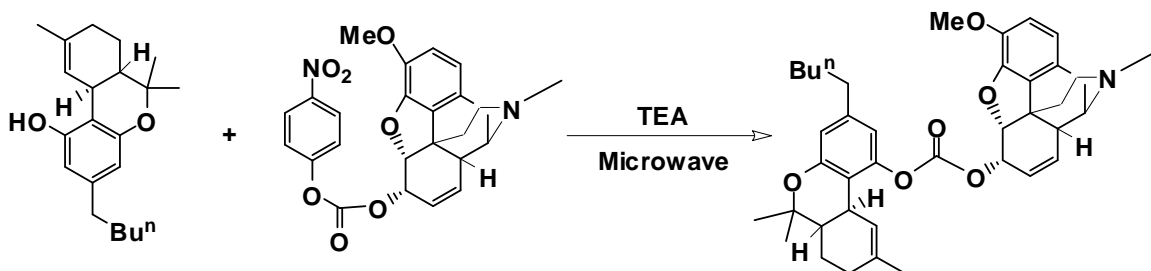
Scheme 2.14(b): Synthesis of unsymmetrical carbonate of codeine and 5,6,7,8-tetrahydro-2-naphthol utilizing microwave irradiation



Both of the model microwave reactions showed positive results and showed the evidence of formation of the desired carbonates (around 20% conversion to product) in both the MALDI and NMR spectra.

Next, the microwave-mediated reaction between the carbonate of codeine and *p*-nitrophenol and Δ^9 -THC was performed. The reaction mixture was heated in the microwave oven for 30 seconds in the presence of TEA and then analyzed by HPLC. The results indicated that the desired product had been formed but the reaction was still incomplete, and in addition to the starting materials, the symmetrical carbonate was also present in the reaction mixture (Scheme 2.14c).

Scheme 2.14(c): Synthesis of unsymmetrical carbonate of codeine and Δ^9 -THC utilizing microwave irradiation

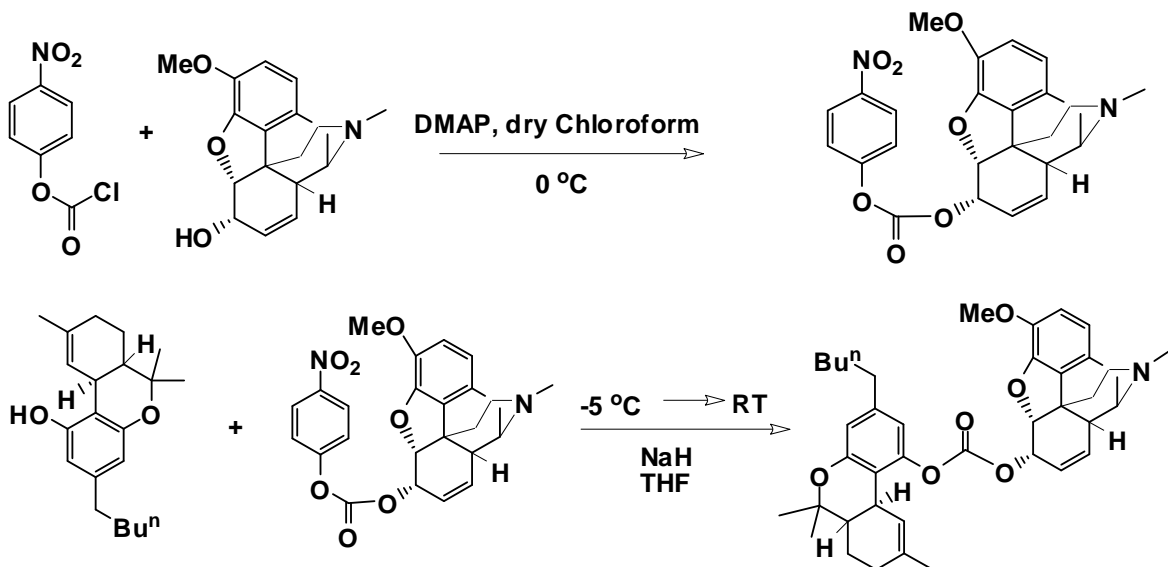


Since microwave-mediated reactions were not a complete success, a conventional approach was again explored, focusing first on the reaction of the *para*-nitrophenol carbonate of codeine with Δ^9 -THC. In this reaction, Δ^9 -THC was treated first with NaH at low temperature, followed by drop-wise addition of the *p*-nitrophenol carbonate of codeine (Scheme 2.15). The product yield obtained was better than the previous attempts (43%). MALDI analysis and NMR spectral analysis showed no sign of formation of the symmetrical carbonate of codeine.

Silica gel column chromatography of the reaction product using a dichloromethane-methanol gradient was performed to purify the compound. MALDI, HRMS and NMR spectral analysis confirmed structure of the pure Cod-THC codrug (Fig. 2.15, 2.16).

The analysis of the Cod-THC codrug by HPLC-UV assay was carried out. Detection was at 220 nm and an Apollo ® C₁₈ (5 μ m, 3.9 x 150 mm) column, equipped with a guard column (Nova-Pak® C₁₈; 3.9 x 20 mm; 4 μ) was used as the stationary phase; methanol/6mM phosphate buffer containing 0.025% heptafluorobutyric acid (HFBA), pH adjusted to 6.9 with triethylamine, was used as the mobile phase. A gradient program with a flow rate of 1mL/min was used for the elution of the Cod-THC codrug molecule. Fig. 2.17 shows the chromatogram of the Cod-THC codrug.

Scheme 2.15: Synthesis of unsymmetrical carbonate of codeine and Δ^9 -THC utilizing a stronger base (NaH)



\\lcj\data\UKMSF08-0190

04/22/2008 09:20:38 AM

Cod-THC #3

08-0190 #13-35 RT: 0.35-0.92 AV: 23 NL: 7.34E7
T: + p ms [100.00-1200.00]

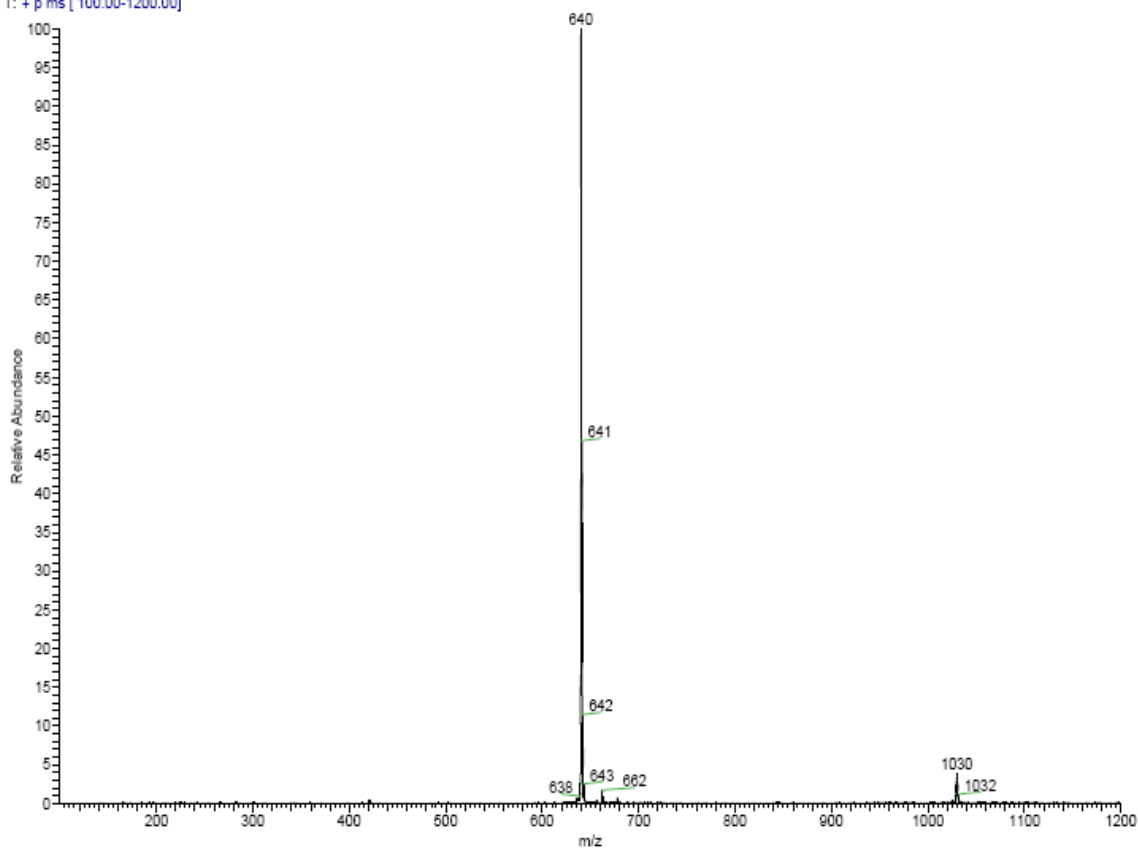


Fig. 2.15 The MALDI analysis of the Cod-THC codrug

09-0798 #158-189 RT: 3.05-3.62 AV: 32 NL: 5.76E6
T: + c Full ms [40.00-750.00]

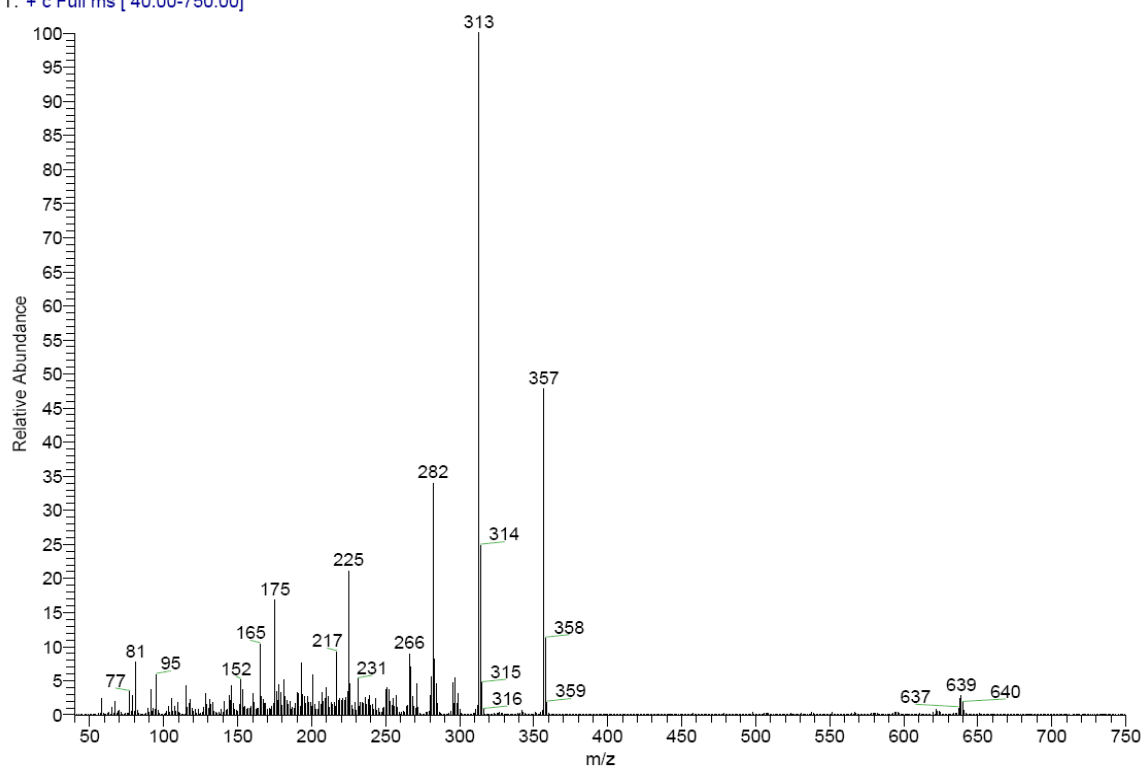


Fig. 2.16 High resolution electron impact ionization mass spectrum of the Cod-THC codrug

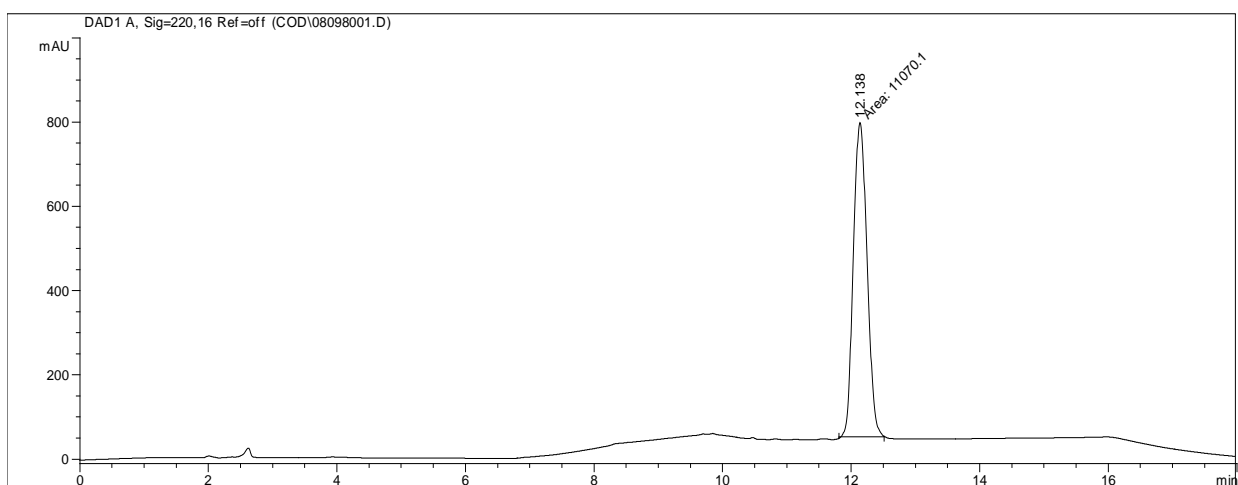
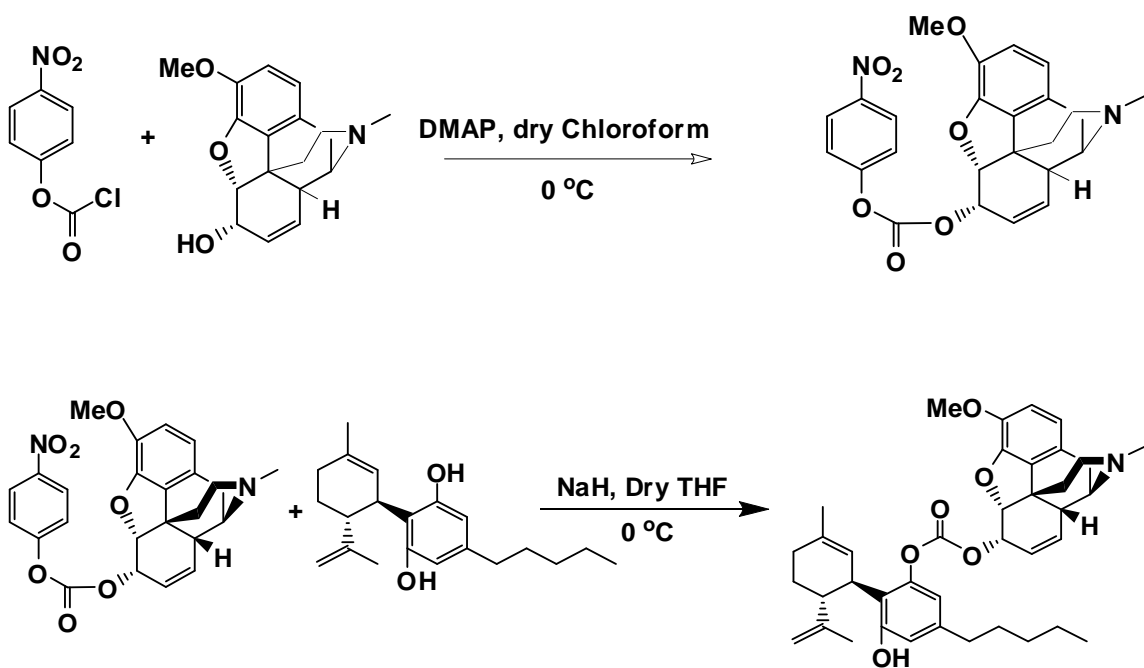


Fig. 2.17 HPLC chromatogram of chromatogram the Cod-THC codrug

2.4 Synthesis of the Codeine-(-)-Cannabidiol codrug (Cod-CBD)

The Cod-CBD codrug was synthesized in a similar manner to the successful synthesis of the Cod-THC codrug. First, the intermediate *para*-nitrophenol carbonate of codeine was prepared. Then, (-)-cannabidiol was treated with NaH and then the *para*-nitrophenol carbonate of codeine was added drop-wise to the reaction mixture. Scheme 2.16 shows the synthesis of the Cod-CBD codrug. Silica gel column chromatography was again carried out in order to purify the desired codrug using a dichloromethane-methanol gradient. The compound was characterized by NMR spectroscopy, HRMS (Fig. 2.18) and LC-MS analysis (Fig. 2.19).

Scheme 2.16: Synthesis of carbonate of codeine and (-)-cannabidiol



2.5 Synthesis of the Codeine-*abn*-Cannabidiol codrug (Cod-*abn*CBD)

The Cod-*abn*CBD codrug was synthesized in a similar manner to the Cod-THC and Cod-CBD codrugs. Scheme 2.17 depicts the synthesis of the Cod-*abn*CBD codrug. Silica gel column chromatography was performed again to obtain a pure sample of the desired codrug using a dichloromethane-methanol gradient. The compound was characterized by NMR and mass spectral analysis (Fig. 2.20).

Scheme 2.17: Synthesis of carbonate of codeine and *abnormal*-cannabidiol

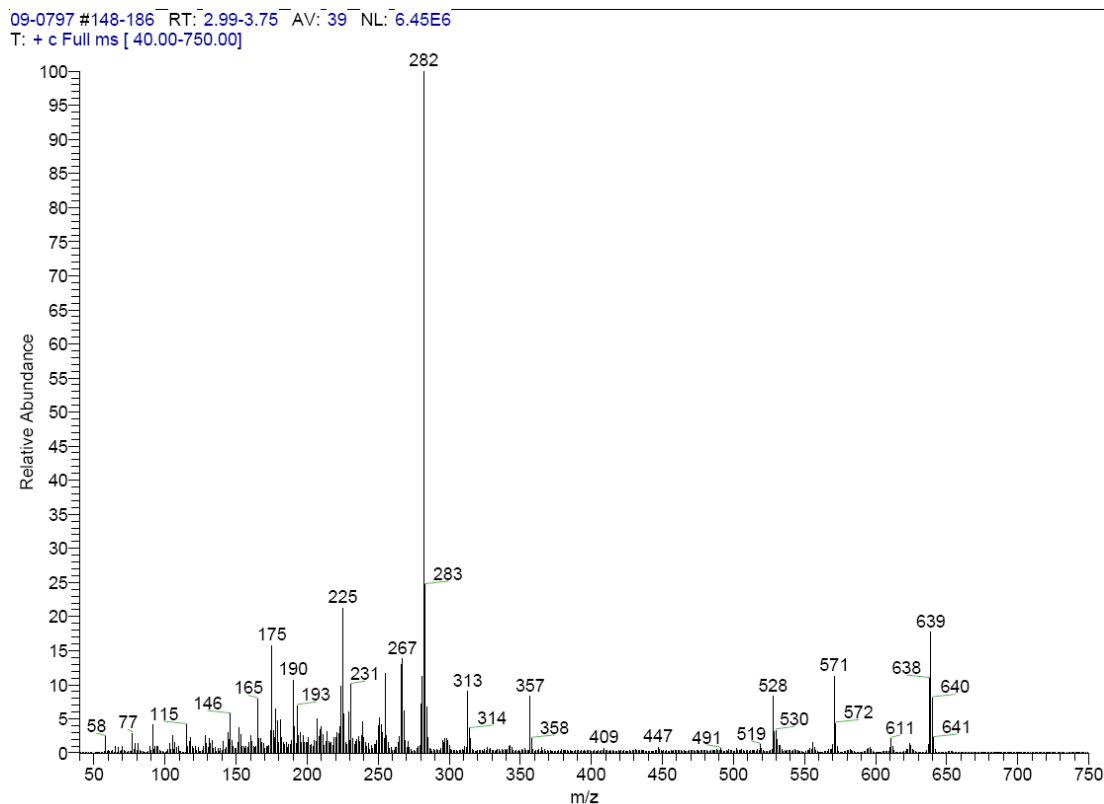
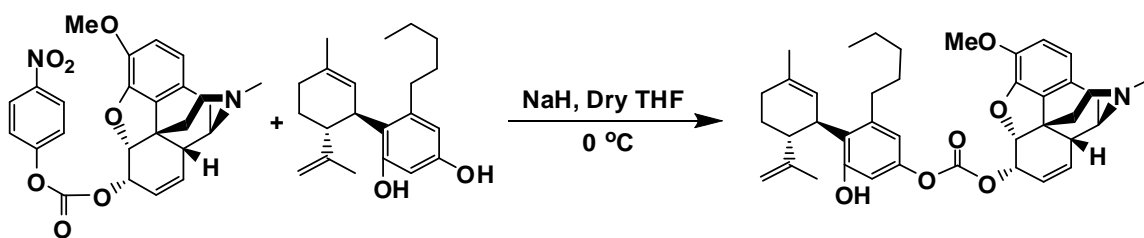


Fig. 2.18 High-resolution electron impact ionization mass spectrum of the Cod-CBD

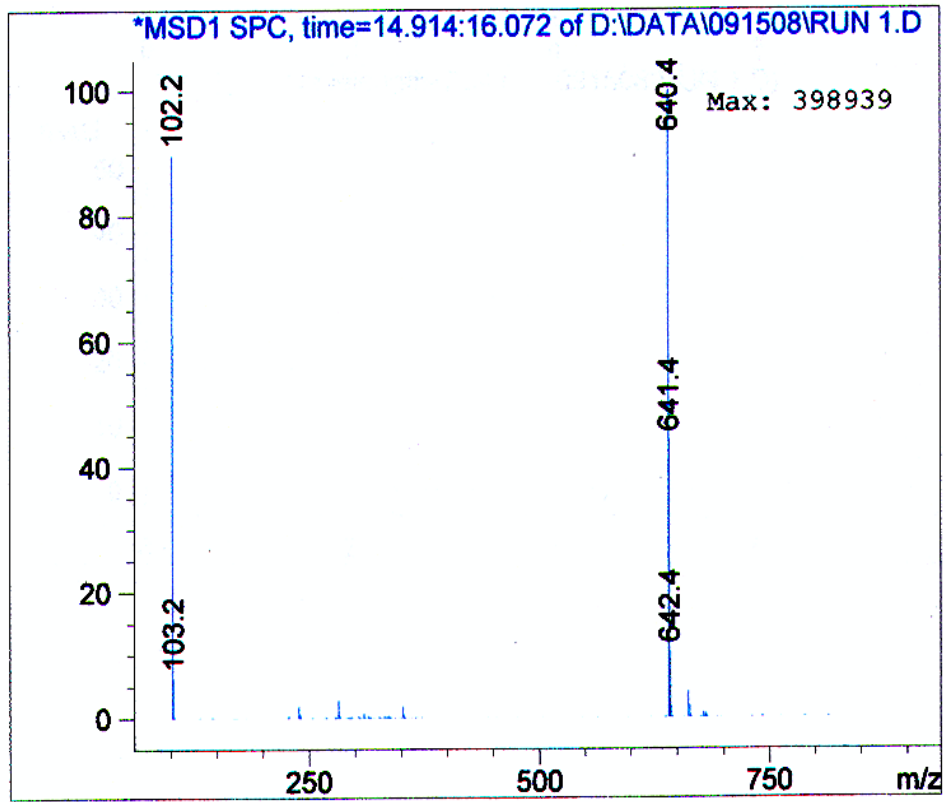
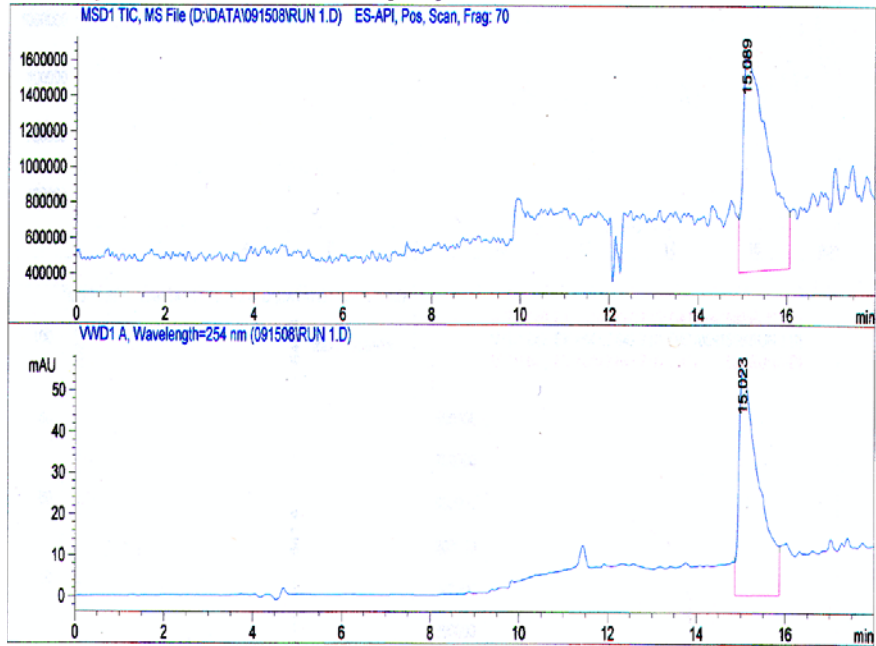


Fig. 2.19 LC-MS analysis of the Cod-CBD codrug

09-0796 #102-135 RT: 1.79-2.45 AV: 34 NL: 7.82E6
T: + c Full ms [40.00-750.00]

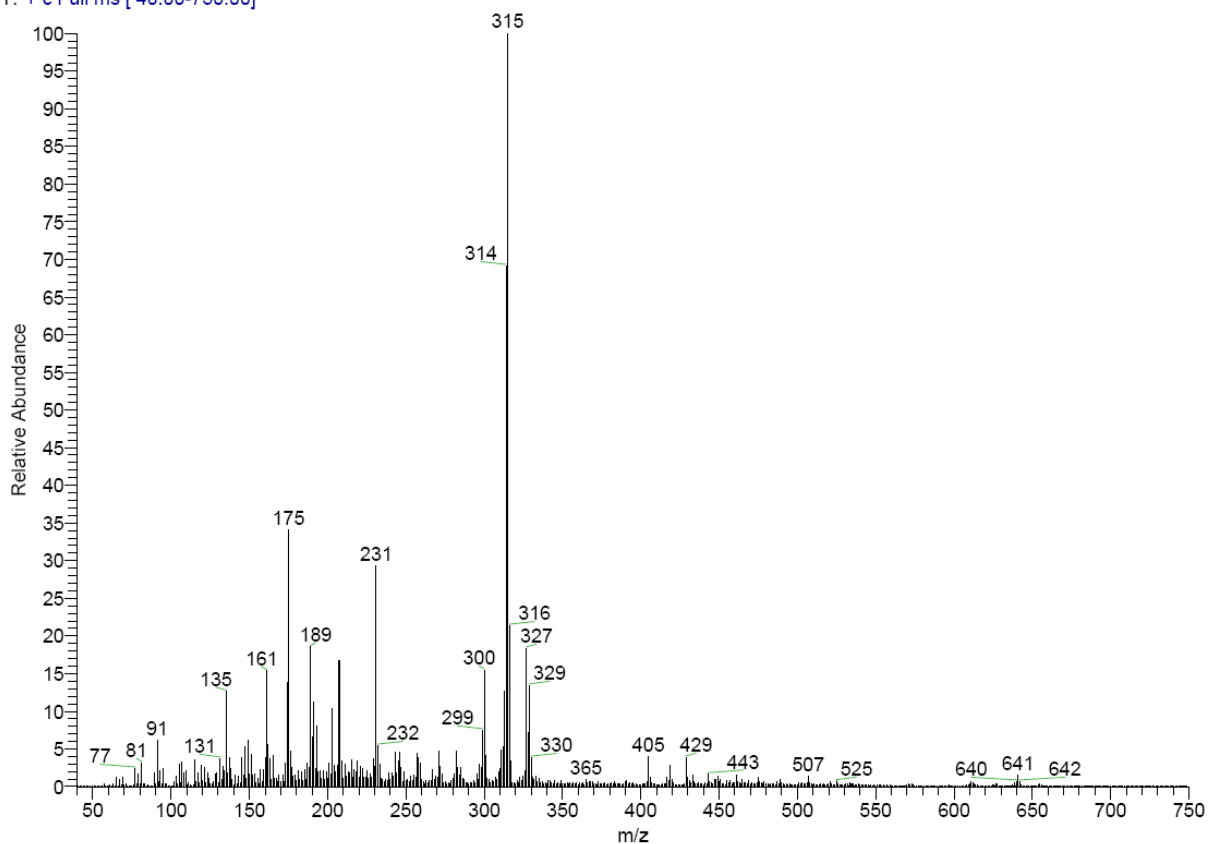


Fig. 2.20 High resolution electron impact ionization mass spectrum of the Cod-*abn*CBD codrug

2.6 Synthesis of the 3-*O*-Acetylmorphine- Δ^9 -tetrahydrocannabinol codrug (AcMor-THC)

AcMor-THC codrug synthesis was carried out in three steps. In the first step, 3-*O*-acetylmorphine was synthesized by regioselective 3-*O*-acetylation of morphine free base using acetic anhydride and sodium bicarbonate. 3-*O*-Acetylmorphine was then allowed to react with *para*-nitrophenylchloroformate to afford the 6-*O*-carbonate of 3-*O*-acetylmorphine and *para*-nitrophenol. Finally, the intermediate carbonate was allowed to react with phenoxide ion of Δ^9 -THC to afford the desired product, 3-*O*-acetylmorphine- Δ^9 -tetrahydrocannabinol carbonate (AcMor-THC). 3-*O*-Acetylmorphine, 3-*O*-acetylmorphine-*para*-nitrophenol carbonate intermediates and the final AcMor-THC

codrug product were all characterized by GC-MS, LC-MS, ESI-MS, and NMR and HRMS analysis (Scheme 2.18) (Crooks et al., 2002).

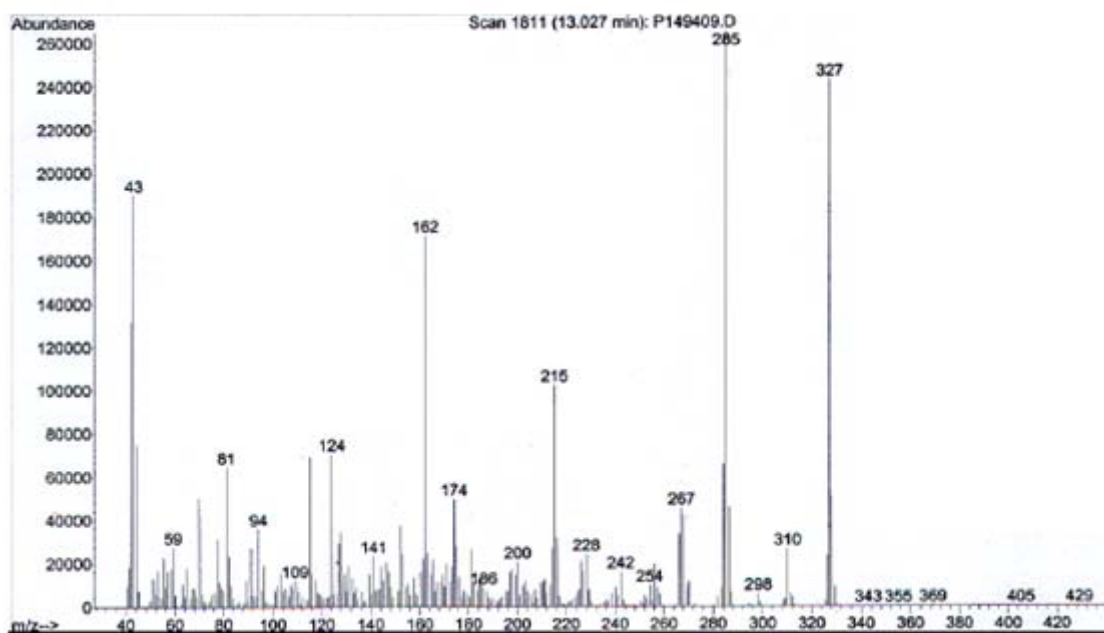
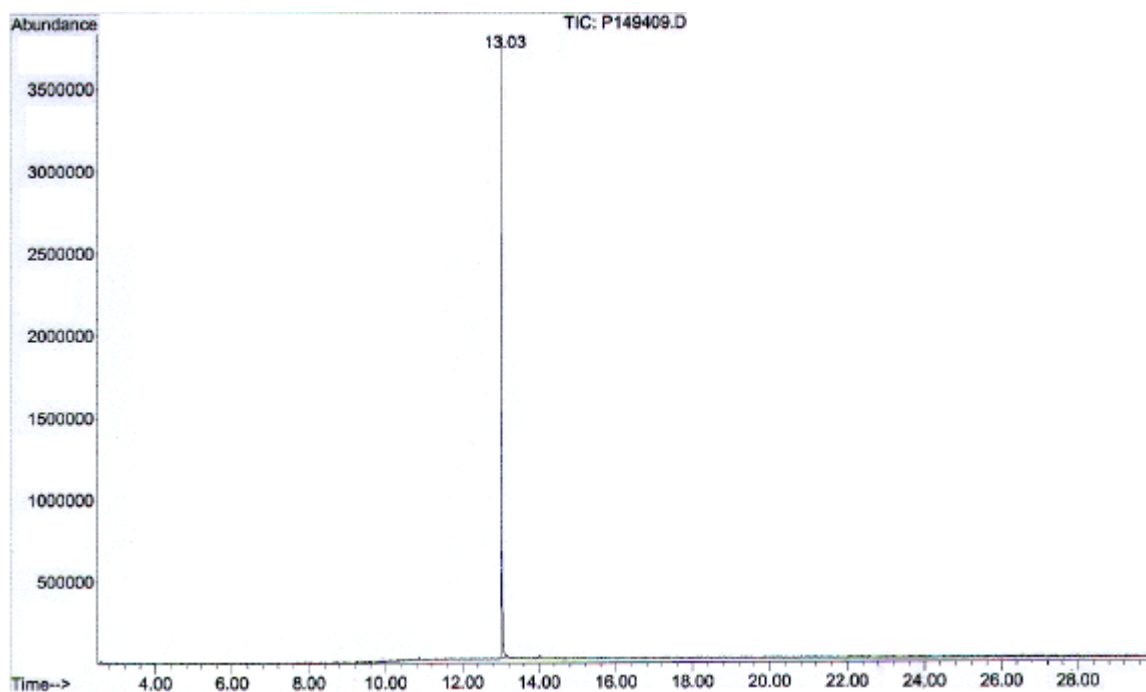
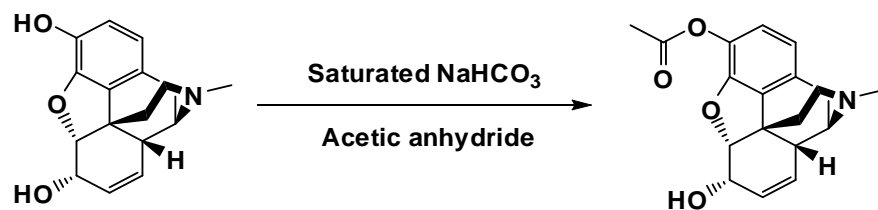
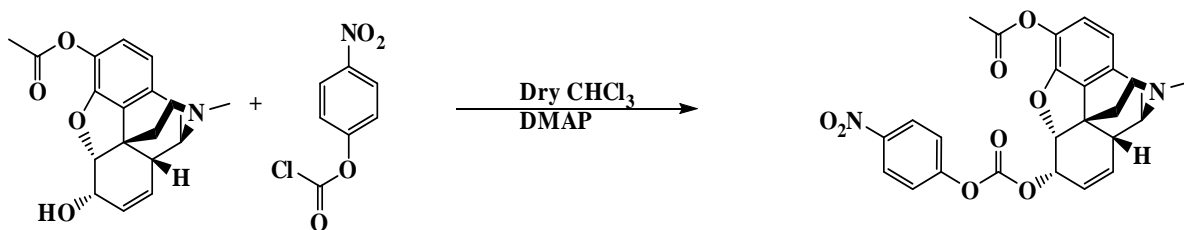


Fig. 2.21 GC-MS spectrum of 3-*O*-acetylmorphine

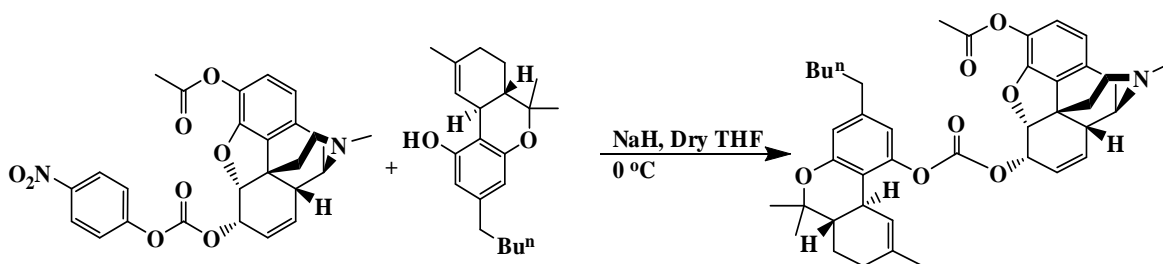
Scheme 2.18a: Synthesis of 3-*O*-acetylmorphine



Scheme 2.18 b: Synthesis of 6-*O*-carbonate of 3-*O*-acetylmorphine and *para*-nitrophenol



Scheme 2.18c: Synthesis of 3-*O*-acetylmorphine- Δ^9 -tetrahydrocannabinol carbonate



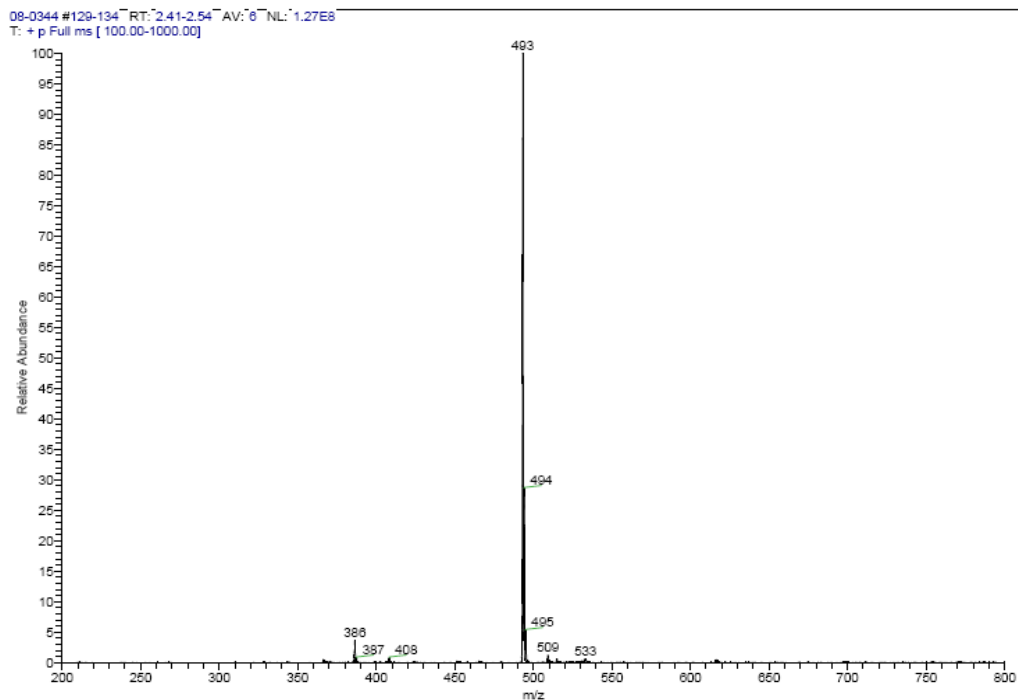


Fig. 2.22 ESI-MS of 3-*O*-acetylmorphine-*para*-nitrophenol carbonate (AcMor-PNP)

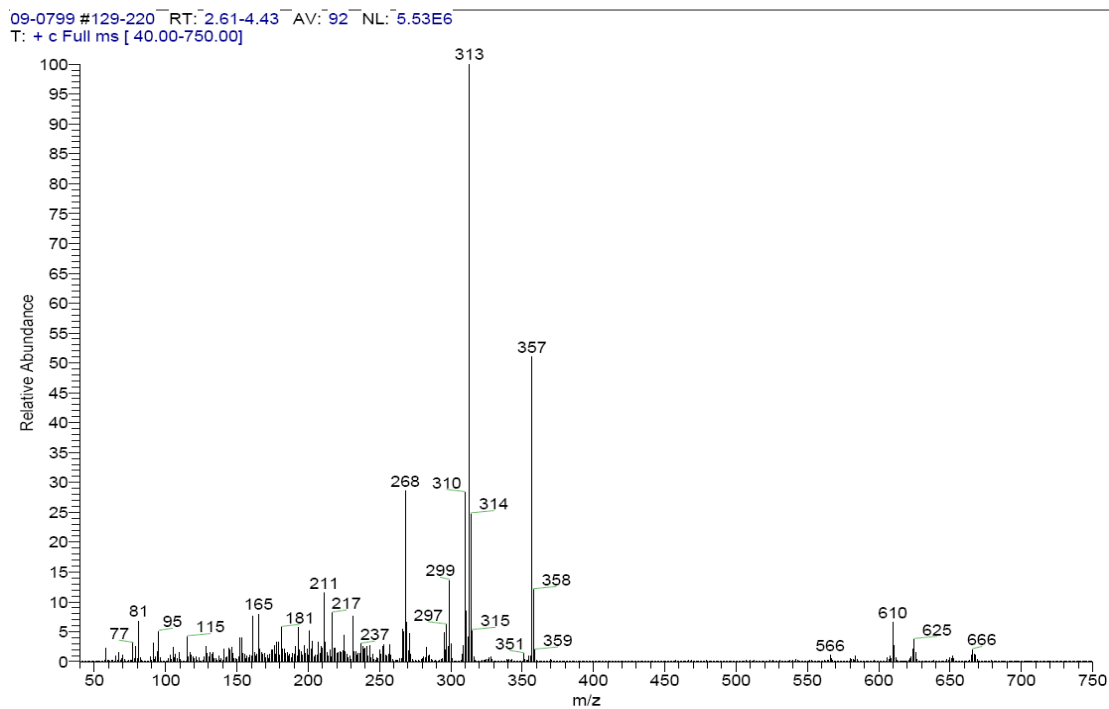


Fig. 2.23 High resolution electron impact ionization mass spectrum of the 3-*O*-acetylmorphine- Δ^9 -tetrahydrocannabinol codrug

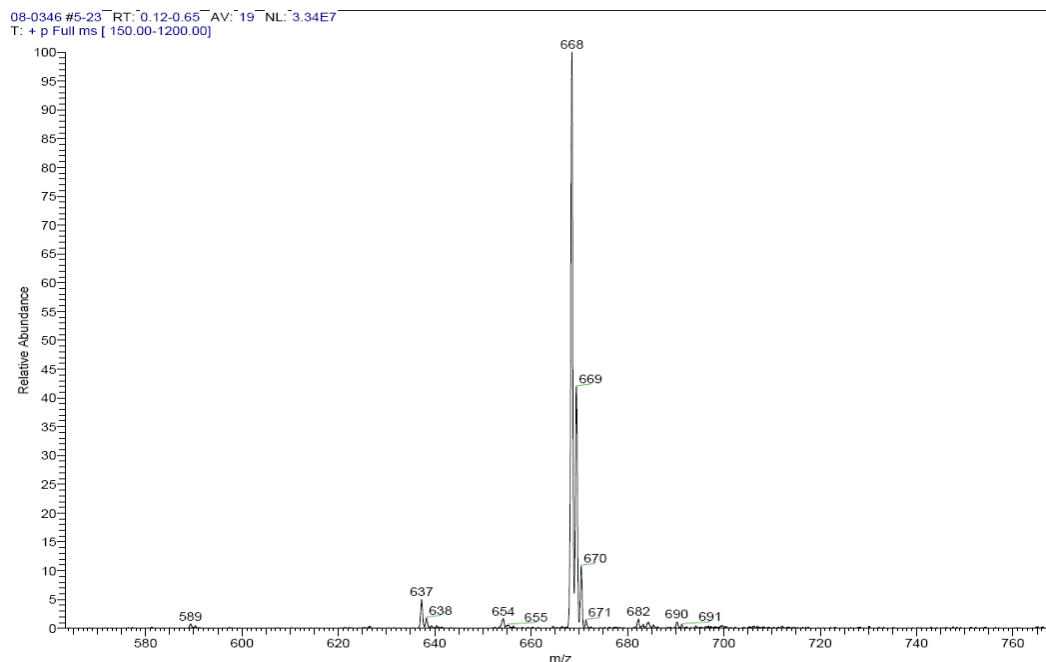


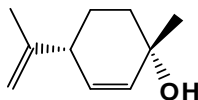
Fig. 2.24 ESI-MS of 3-*O*-acetylmorphine- Δ^9 -tetrahydrocannabinol codrug

Experimental section

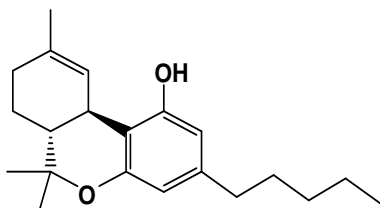
General Procedures. All experimental procedures were carried out under nitrogen and in oven-dried glassware unless otherwise mentioned. Solvents and reagents were obtained from commercial vendors. All solvents were removed by evaporation using a rotary evaporator unless indicated otherwise.

^1H and ^{13}C NMR spectra were recorded on Varian 300MHz and 500MHz spectrometers. HPLC analyses were carried on an Agilent 1100 series Quatpump, equipped with a photodiode array detector and a computer integrating apparatus. GC-MS analyses were carried out on an Agilent 6890 GC instrument attached to a 593 mass-selective detector. Microwave reactions were carried out on a Biotage 355422-AD microwave synthesizer. High-resolution mass spectrometry was performed by the University of Kentucky Mass Spectrometry facility. X-ray crystallography was performed by the University of Kentucky Crystallographic facility.

Synthesis of Δ^9 -Tetrahydrocannabinol.

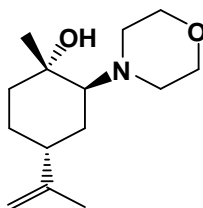


(1S,4R)-*p*-Mentha-2,8-dien-1-ol. Sodium borohydride (0.266 g, 7.02 mmol) was added portion-wise to a stirred suspension of diphenyldiselenide (1.0 g, 3.2 mmol) in dry ethanol (16 mL) under nitrogen atmosphere. A mixture of *cis*- and *trans*- limonene oxide (0.870 g, 5.72 mmol) was added, and the resultant mixture was refluxed for 2 h. After cooling in an ice-bath, THF (15 mL) was added followed by drop-wise addition of 35% v/v hydrogen peroxide (1.7 mL). The solution was allowed to warm to ambient temperature and stirred for 5 h, and then diluted with water (40 mL). The organic layer was separated. The aqueous layer was extracted with methylene chloride, and the combined organic liquors were washed with 10% aqueous sodium carbonate, water, and saturated brine, dried over anhydrous sodium sulfate and concentrated on a rotary evaporator. The residue containing the selenoxide intermediate was utilized in the next step without any further purification. The selenoxide intermediate was heated for 8 h in refluxing chloroform (13.5 mL) under a nitrogen atmosphere. After cooling, the solvent was evaporated and the residue was extracted with diethyl ether. The solvent was evaporated and the crude product was purified through silica gel column chromatography to afford pure (1S,4R)-*p*-mentha-2,8-dien-1-ol (0.213 g, 25%). The elution was carried out with hexanes and increasing portions of diethyl ether up to 5:1 of hexanes:diethyl ether. ^1H NMR (300 MHz, CDCl_3): δ 5.63 (2H, m), 4.70 (2H, m), 2.59 (1H, m), 1.41-1.90 (7H, m), 1.25 (3H, s) ppm; ^{13}C NMR (300 MHz, CDCl_3): δ 148.1, 133.9, 132.1, 110.6, 67.4, 43.4, 36.7, 29.4, 24.9, 20.8 ppm; GC-MS M^+ 152 *m/z*.



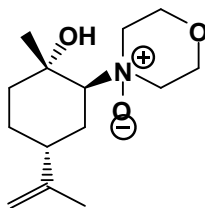
Δ^9 -Tetrahydrocannabinol. Boron trifluoride etherate (0.09 mL) was added dropwise to an ice-cold stirred suspension of (1*S*,4*R*)-*p*-mentha-2,8-dien-1-ol (0.213 g, 1.4 mmol), olivetol (0.263 g, 1.38 mmol) and anhydrous magnesium sulfate (0.185 g) in methylene chloride (9.25 mL) under nitrogen. The mixture was stirred for 2 h at 0 °C, and then anhydrous sodium bicarbonate (0.462 g) was added. Stirring was continued until the color faded to a light brown, and the reaction mixture was then filtered and evaporated to provide a brown gum. The crude product of Δ^9 -THC was purified using silica gel column chromatography. Elution was carried out with hexanes with increasing portion of diethyl ether in hexanes (up to 30:1 hexanes:diethyl ether) to afford a pure fraction of Δ^9 -THC (100 mg, 22%). ¹H NMR (300 MHz, CDCl₃): δ 6.29 (1H, br s), 6.25 (1H, d, J=1.2 Hz), 6.12 (1H, d, J=1.2 Hz), 4.78 (1H, s), 3.18 (1H, br d), 3.42 (2H, t, J=7.2 Hz), 1.20-2.21 (17H, m), 1.07 (3H, s), 0.86 (3H, t, J=7.2 Hz) ppm; ¹³C NMR (300 MHz, CDCl₃): δ 154.8, 154.2, 142.9, 134.5, 123.8, 110.2, 109.2, 107.7, 77.4, 46.0, 35.8, 33.8, 31.8, 31.4, 31.0, 27.9, 25.3, 23.7, 22.9, 19.6, 14.4 ppm; GC-MS M⁺ 314 *m/z*.

Synthesis of (-)-Cannabidiol and *abn*-Cannabidiol.



4-Isopropenyl-1-methyl-2-morpholin-4-yl-cyclohexanol. (+)-Limonene oxide (a mixture of *cis* and *trans* isomers) (5.0 g, 0.033 moles) was dissolved in ethanol (16 mL) and LiCl (2.247 g, 0.053 moles) was added while stirring the solution. Morpholine (4.295 g, 0.049 moles) was added drop-wise and the reaction mixture was heated at 70 °C for 24 hours. The progress of the reaction was monitored by GC-MS. After almost all of the *trans*-(+)-limonene oxide had been consumed solvent was evaporated under reduced pressure and the residue was taken up into methylene chloride solvent (100 mL). The organic solution was washed with water (80 mL) and then extracted into 2M hydrochloric acid (2 x 60 mL) and the aqueous acidic solution was washed with methylene chloride (2 x 50 mL). The aqueous solution was basified to pH 10 by addition of 2M sodium

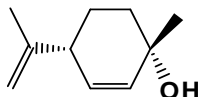
hydroxide. The basic aqueous solution was extracted with diethyl ether (4 x 60 mL) and the organic liquors washed with water (3 x 50 mL). The diethyl ether solution was dried over anhydrous sodium sulfate and the solvent was evaporated under reduced pressure. The desired product was obtained as yellow oil (3.38g, 43%). ¹H NMR (300 MHz, CDCl₃): δ 4.94 (2H, m), 4.85 (1H, m), 3.70 (4H, m), 2.72 (2H, m), 2.52 (4H, m), 2.10 (1H, m), 2.05 (1H, m), 1.98 (1H, m), 1.74 (3H, s), 1.60 (4H, m), 1.21 (3H, s) ppm; ¹³C NMR (300 MHz, CDCl₃): δ 145.6, 111.3, 73.0, 67.9, 67.8, 52.3, 45.8, 39.3, 36.0, 25.3, 24.9, 22.8, 22.7 ppm; GC-MS M⁺ 239 *m/z*.



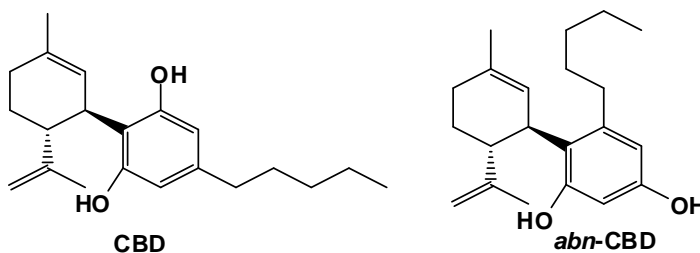
4-Isopropenyl-1-methyl-2-(4-oxy-morpholin-4-yl)-cyclohexanol.

4-

Isopropenyl-1-methyl-2-morpholin-4-yl-cyclohexanol (3.596 g, 0.015 moles) was dissolved in ethanol (21 mL) and 35 % v/v hydrogen peroxide (7.52 mL) was added drop-wise. The solution was heated at 50 °C for 4 h. 10 % Pd on C (20.32 mg) was added at room temperature, the mixture was stirred for 2 h, and the solvent was evaporated under reduced pressure to afford a yellow oil. This oil was submitted to silica gel column chromatography using a hexanes:ethyl acetate gradient with the final elution with methanol to afford the desired product (3.38 g, 88%). ¹H NMR (300 MHz, CDCl₃): δ 4.99 (1H, m), 4.80 (1H, m), 4.48 (2H, m), 3.69 (3H, m), 3.38 (2H, m), 3.20 (1H, m), 2.81 (1H, m), 2.60 (1H, m), 2.20 (1H, m), 1.46-2.00 (12H, m) ppm; ¹³C NMR (300 MHz, CDCl₃): δ 143.9, 112.1, 80.1, 73.7, 65.3, 61.5, 61.3, 59.4, 39.8, 39.3, 28.7, 24.7, 23.6, 22.6 ppm.



(1*S*,4*R*)-*p*-Mentha-2,8-dien-1-ol. 4-Isopropenyl-1-methyl-2-(4-oxy-morpholin-4-yl)-cyclohexanol (5.41 g, 0.021 moles) was dissolved in toluene (94 mL) and silica (1.3 g) was added. The reaction mixture was heated to reflux with stirring overnight. The silica was then removed by filtration. The filtrate was evaporated under reduced pressure to afford a brown oil. This oil was dissolved in methylene chloride (50 mL) and washed with 2M hydrochloric acid (2 x 30 mL). The methylene chloride solution was washed with water (2 x 25 mL) and finally dried over anhydrous sodium sulfate. The solvent was evaporated under reduced pressure to afford the crude product (1*S*,4*R*)-*p*-mentha-2,8-dien-1-ol. The crude product was chromatographed on silica using a hexanes-diethyl ether gradient to afford pure (1*S*,4*R*)-*p*-mentha-2,8-dien-1-ol (0.77 g, 24%). ¹H NMR (300 MHz, CDCl₃): δ 5.63 (2H, m), 4.70 (2H, m), 2.59 (1H, m), 1.41-1.90 (7H, m), 1.25 (3H, s) ppm; ¹³C NMR (300 MHz, CDCl₃): δ 148.1, 133.9, 132.1, 110.6, 67.4, 43.4, 36.7, 29.4, 24.9, 20.8 ppm; GC-MS M⁺ 152 *m/z*.

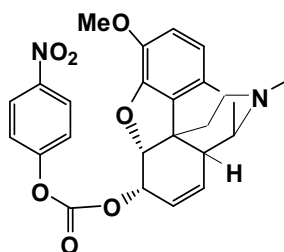


(-)-Cannabidiol and *abn*-Cannabidiol. A mixture of olivetol (1.18 g, 6.55 mmol), zinc chloride (1.35 g, 0.0429 mmol) water (0.115 mL, 0.029 mmoles) and methylene chloride (11.4 mL) was refluxed for 1 h. (1*S*,4*R*)-*p*-Mentha-2,8-dien-1-ol (1.0 g, 6.57 mmol), dissolved in methylene chloride was then added drop-wise and the mixture refluxed for an additional 1 h. the progress of the reaction was monitored by GC-MS. After complete consumption of (1*S*,4*R*)-*p*-mentha-2,8-dien-1-ol, the solution was cooled to ambient temperature, ice cold water (5 mL) was then added and the mixture stirred for 20 min. The organic phase was washed with water (10 mL), 5% sodium bicarbonate (10 mL), and brine (10 mL), dried and concentrated under reduced pressure.

The crude mixture was fractionated on silica gel column using a hexanes/diethyl ether gradient to afford both (-)-cannabidiol (0.64 g, 31%) and *abn*-cannabidiol (0.39 g, 19%). Cannabidiol: ^1H NMR (300 MHz, CDCl_3): δ 6.27 (1H, br s), 6.25 (1H, br s), 6.20 (1H, br s), 5.99 (1H, s), 5.58 (1H, s), 4.66 (2H, m), 4.56 (1H, m), 3.85 (1H, dm), 2.45 (2H, t), 2.21 (1H, m), 2.12 (1H, m), 1.86 (2H, m), 1.80 (3H, s), 1.60 (3H, s), 1.55 (2H, q), 1.31 (4H, m), 0.88 (3H, t) ppm; ^{13}C NMR (300 MHz, CDCl_3): δ 149.5, 143.1, 140.2, 124.2, 113.9, 110.9, 109.8, 108.1, 46.4, 37.5, 35.8, 31.8, 30.9, 30.7, 28.7, 23.9, 22.8, 20.9, 14.4 ppm; GC-MS M^+ 314 m/z .

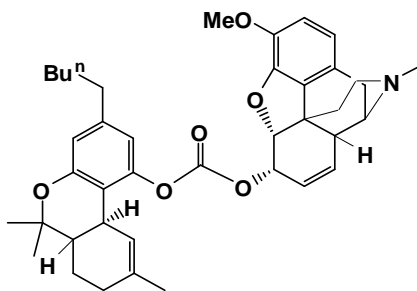
abn-Cannabidiol: ^1H NMR (300 MHz, CDCl_3): δ 6.22 (1H, d), 6.20 (1H, d), 6.06 (1H, s), 5.53 (1H, br s), 4.78 (1H, s), 4.65 (1H, t), 4.47 (1H, br s), 3.53 (1H, dm), 2.58 (1H, m), 2.48 (1H, m), 1.67-2.31 (8H, m), 1.54 (3H, s), 1.47 (2H, m), 1.32 (4H, m), 0.90 (3H, t) ppm; ^{13}C NMR (300 MHz, CDCl_3) δ 156.5, 154.6, 147.7, 144.1, 139.9, 124.8, 120.1, 111.6, 108.7, 102.3, 45.2, 40.3, 34.3, 32.2, 31.4, 30.5, 28.4, 23.9, 22.9, 21.6, 14.4 ppm; GC-MS M^+ 314 m/z .

Synthesis of Codeine- Δ^9 -Tetrahydrocannabinol Codrug.



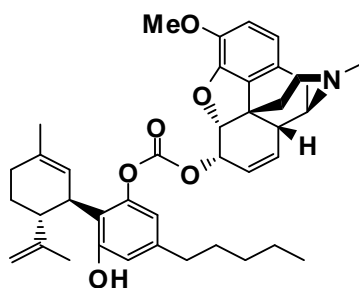
Codeine-*p*-nitrophenol Carbonate. All glasswares were oven-dried and cooled under a nitrogen atmosphere. Codeine (0.05 g, 0.16 mmol) was placed in a round bottom flask under a nitrogen atmosphere and was dissolved in 2 mL of dry chloroform. The solution was cooled to 0 °C. DMAP (0.023 g, 0.192 mmol) was then added to the solution and the mixture stirred for 5 min. *para*-Nitrophenylchloroformate (0.037 g, 0.18 mmol) was dissolved in 3 mL of dry chloroform and the solution was added to the reaction mixture drop-wise, the mixture was allowed to warm to the ambient temperature. The progress of the reaction was monitored by TLC. After completion of the reaction, the

mixture was diluted with chloroform (15 mL). The chloroform layer was washed 5 times with 10 mL 50% NaHCO₃ solution and with brine (10 mL), dried over anhydrous sodium sulfate and concentrated to afford a solid product (0.032 g, 41 %). ¹H NMR (300 MHz, CDCl₃): δ 8.27 (2H, dd), 7.45 (2H, dd), 6.66 (1H, d), 6.56 (1H, d), 5.70 (1H, dd), 5.52 (1H, dd), 5.16 (2H, m), 3.82 (3H, s), 3.36 (1H, m), 3.04 (1H, d), 2.75 (1H, m), 2.58 (1H, dd), 2.43 (3H, s), 2.36 (1H, dt), 2.29 (1H, dd), 2.03 (1H, dt), 1.88 (1H, d) ppm; ¹³C NMR (300 MHz, CDCl₃): δ 156.1, 152.2, 146.7, 145.3, 142.7, 130.4, 127.4, 126.7, 126.6, 125.6, 122.2, 121.9, 119.9, 115.0, 114.5, 87.4, 72.4, 59.5, 56.9, 46.9, 43.1, 42.6, 40.5, 35.3, 20.6 ppm; MS (ESI): (M+1) 465 *m/z*.



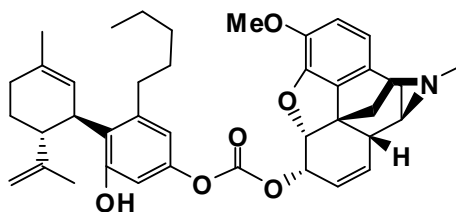
Codeine-Δ⁹-Tetrahydrocannabinol Carbonate. All glasswares were oven dried and cooled under a nitrogen atmosphere. Δ⁹-THC (0.053 g, 0.17 mmol) was placed in a round bottom flask under a nitrogen atmosphere and was dissolved in 2 mL of dry THF. The solution was cooled down to 0 °C. NaH (0.09 g, 0.22 mmol) was added to the solution and allowed to stir for 5 min. Codeine-*p*-nitrophenol carbonate (0.078 g, 0.17 mmol), dissolved in 3 mL of dry THF was added to the reaction mixture drop-wise and the mixture was allowed to warm to the ambient temperature. The progress of the reaction was monitored by TLC. After the completion of the reaction, the mixture was filtered through a pad of celite and then the organic filtrate was concentrated under reduced pressure to afford yellow oil. The organic residue was dissolved in chloroform (20 mL), the organic layer was washed with 50% sodium bicarbonate solution (3 x 10 mL), water (10 mL), and brine (10 mL), dried over sodium sulfate and concentrated under reduced pressure to afford a brownish solid. The crude product was purified using silica gel column chromatography and a methylene chloride-methanol mixture as eluent,

to afford the pure product (0.046 g, 43%). ^1H NMR (300 MHz, CDCl_3): δ 6.71-6.55 (4H, m), 6.06 (1H, br s), 5.76 (1H, d), 5.48 (1H, dt), 5.15 (2H, m), 3.93 (3H, s), 3.38 (1H, m), 3.19 (1H, m), 3.06 (1H, d), 2.74 (1H, m), 2.60-1.29 (27H, m), 1.11 (3H, s), 0.89 (3H, t) ppm; ^{13}C NMR (300 MHz, CDCl_3): δ 154.5, 152.8, 149.9, 146.9, 143.0, 142.4, 134.9, 130.6, 129.9, 127.9, 126.9, 126.5, 123.1, 119.5, 115.9, 115.7, 115.0, 114.7, 113.9, 87.9, 72.2, 59.3, 57.3, 46.9, 45.7, 43.3, 42.9, 40.9, 35.7, 34.4, 31.8, 31.4, 30.8, 27.7, 25.2, 23.6, 22.8, 20.7, 19.7, 14.4 ppm; MS (ESI): ($\text{M}+1$) 640 m/z ; HRMS: calcd. for $\text{C}_{40}\text{H}_{49}\text{NO}_6$ (M^+) m/z 639.3559, found m/z 639.3556.



Codeine-(-)-Cannabidiol Carbonate Codrug. (-)-Cannabidiol (0.175 g, 0.557 mmol) was placed in a round bottom flask under a nitrogen atmosphere and was dissolved in 4 mL of dry THF. The solution was cooled to 0 °C. NaH (0.028 g, 0.72 mmol) was added to the solution and allowed to stir for 5 min. Codeine-*p*-nitrophenol carbonate (0.258 g, 0.56 mmol), dissolved in 4 mL of dry THF was added to the reaction mixture drop wise and the reaction mixture was allowed to warm to the ambient temperature. The progress of the reaction was monitored by TLC. After the completion of the reaction, the mixture was filtered through a pad of celite and concentrated under reduced pressure. Obtained residue was dissolved in methylene chloride (25 mL), washed with 50% sodium bicarbonate solution (3 x 15 mL), water (15 mL), and brine (10 mL), dried and concentrated under reduced pressure to afford a crude solid. The crude mixture was submitted to silica gel column chromatography using a methylene chloride/methanol gradient to afford the pure product (0.164 g, 47%). ^1H NMR (300 MHz, CDCl_3): δ 6.67 (1H, d), 6.62 (1H, d), 6.57-6.51 (2H, m), 5.73 (1H, d), 5.56 (1H, s), 5.48 (1H, dt), 5.00 (1H, dd), 5.09 (1H, m), 4.57 (1H, t), 4.45 (1H, br s), 3.85 (3H, s), 3.78 (1H, dm), 3.39

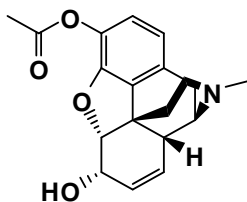
(1H, m), 3.06 (1H, d), 2.76 (1H, m), 1.49-2.64 (23H, m), 1.31 (4H, m), 0.89 (3H, t) ppm; ^{13}C NMR (300 MHz, CDCl_3): δ 155.6, 153.2, 149.7, 147.3, 147.0, 142.9, 142.4, 140.8, 130.7, 130.1, 127.9, 127.0, 123.7, 119.4, 118.6, 114.8, 114.7, 113.7, 111.7, 88.0, 72.2, 59.3, 57.2, 46.8, 46.2, 43.3, 43.1, 41.0, 37.8, 35.7, 31.8, 30.8, 30.7, 28.4, 23.9, 22.8, 20.7, 19.9, 14.4, 14.3 ppm; LC-MS: $(\text{M}+\text{H})^+$ 640.4 m/z ; HRMS: calcd. for $\text{C}_{40}\text{H}_{49}\text{NO}_6$ (M^+) m/z 639.3559, found m/z 639.3558.



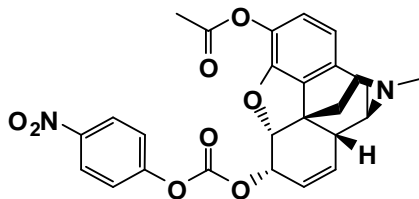
Codeine-*abn*-Cannabidiol Carbonate Codrug. *abn*-Cannabidiol (0.17 g, 0.54 mmol) was placed in a round bottom flask under a nitrogen atmosphere and was dissolved in 3 mL of dry THF. The solution was cooled to 0 °C. NaH (0.024 g, 0.70 mmol) was added to the solution and allowed to stir for 5 min. Codeine-*p*-nitrophenol carbonate (0.251 g, 0.55 mmol), dissolved in 3 mL of dry THF was added to the reaction mixture drop-wise and the reaction mixture was allowed to warm to ambient temperature. The progress of the reaction was monitored by TLC. After the completion of the reaction, the mixture was filtered through a pad of celite and concentrated under reduced pressure. Obtained residue was dissolved in methylene chloride (25 mL), washed with 50% sodium bicarbonate solution (3 x 15 mL), water (15 mL), and brine (10 mL), dried and concentrated under reduced pressure to afford the crude solid. The crude mixture was subjected to silica gel column using a methylene chloride/methanol gradient to afford a pure product (0.13 g, 39%). ^1H NMR (500 MHz, CDCl_3): δ 6.68 (1H, d), 6.59-6.55 (3H, m), 6.15 (1H, s), 5.77 (1H, d), 5.50 (1H, br s), 5.43 (1H, d), 5.20 (1H, d), 5.11 (1H, m), 4.62 (1H, d), 4.32 (1H, s), 3.87 (3H, s), 3.57 (1H, dm), 3.05 (1H, d), 2.63-1.22 (29H, m),

0.87 (3H, t) ppm; ^{13}C NMR (500 MHz, CDCl_3): δ 155.03, 153.4, 150.6, 148.9, 146.6, 144.4, 142.5, 133.6, 130.9, 129.4, 128.2, 126.4, 126.3, 127.7, 119.7, 116.2, 115.4, 110.9, 109.2, 87.3, 71.1, 59.3, 57.6, 46.9, 45.0, 43.0, 41.8, 40.6, 39.9, 34.9, 34.1, 32.1, 31.1, 30.3, 28.9, 23.5, 22.7, 21.3, 20.4, 14.3 ppm; LC-MS: $(\text{M}+\text{H})^+$ 640.4 m/z ; HRMS: calcd. for $\text{C}_{40}\text{H}_{49}\text{NO}_6$ (M^+) m/z 639.3559, found m/z 639.3543.

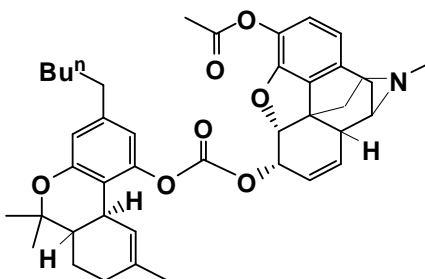
Synthesis of 3-*O*-acetylmorphine- Δ^9 -tetrahydrocannabinol Codrug.



3-*O*-Acetylmorphine. Morphine free base (1.102 g, 3.87 mmol) was suspended in saturated sodium bicarbonate solution (55 mL). To the stirred suspension, 1.1 mL (11.68 mmol) of acetic anhydride was added drop-wise. Reaction mixture was stirred at ambient temperature and the progress of the reaction was monitored by running TLC. After the completion of the reaction, aqueous phase was extracted with chloroform (5 x 20 mL), dried over sodium sulfate and concentrated under reduced pressure to afford a white solid product (1.21 g, 96%). ^1H NMR (300 MHz, CDCl_3): δ 6.73 (1H, d), 6.60 (1H, d), 5.74 (1H, dd), 5.27 (1H, dd), 4.92 (1H, m), 4.16 (1H, m), 3.38 (1H, m), 3.06 (1H, d), 2.60 (1H, m), 2.54 (1H, dd), 2.43 (3H, s), 2.37 (1H, dt), 2.32 (3H, s), 2.29 (1H, dd), 2.05 (1H, dt), 1.88 (1H, d) ppm; ^{13}C NMR (300 MHz, CDCl_3): δ 168.6, 148.7, 134.2, 132.7, 132.3, 131.7, 127.8, 121.1, 119.8, 92.5, 66.0, 59.1, 46.0, 43.3, 42.3, 41.6, 35.4, 21.4, 20.9 ppm; MS (ESI): $(\text{M}+1)$ 328 m/z .



3-*O*-Acetylmorphine-*p*-nitrophenol Carbonate. 3-*O*-Acetylmorphine (2.0 g, 6.12 mmol) was placed in a round bottom flask under a nitrogen atmosphere and was dissolved in dry chloroform (10 mL). The solution was cooled to 0 °C. DMAP (0.9 g, 7.34 mmol) was added to the solution and allowed to stir for 5 min. *p*-Nitrophenylchloroformate (1.48 g, 7.34 mmol) dissolved in dry chloroform (8 mL) was added to the reaction mixture drop-wise and the reaction mixture was stirred at 0 °C. Progress of the reaction was monitored by running TLC. After the completion of the reaction, the mixture was diluted with chloroform (20 mL). The chloroform layer was washed 5 times with 25 mL 50% NaHCO₃ solution and with brine (20 mL), dried over anhydrous sodium sulfate and concentrated under reduced pressure to afford a solid product (1.35 g, 45 %). ¹H NMR (300 MHz, CDCl₃): δ 8.30 (2H, dd), 7.51 (2H, dd), 6.82 (1H, d), 6.64 (1H, d), 5.71 (1H, dd), 5.58 (1H, dd), 5.24 (1H, m), 5.19 (1H, m), 3.42 (1H, m), 3.09 (1H, d), 2.80 (1H, m), 2.62 (1H, dd), 2.45 (3H, s), 2.41 (1H, dt), 2.19 (3H, s), 2.09 (1H, dt), 1.92 (1H, d) ppm; ¹³C NMR (300 MHz, CDCl₃): δ 168.5, 155.9, 151.8, 149.2, 145.6, 132.2, 131.9, 130.4, 127.8, 126.4, 125.5, 122.3, 122.2, 121.8, 119.9, 113.8, 88.2, 72.6, 59.1, 46.7, 43.8, 42.9, 40.7, 35.3, 21.0, 20.8 ppm; MS (ESI): (M+1) 493 *m/z*.



3-*O*-Acetylmorphine- Δ^9 -Tetrahydrocannabinol Carbonate Codrug. Δ^9 -THC (0.053 g, 0.17 mmol) was placed in a round bottom flask under a nitrogen atmosphere and was then dissolved in 2 mL of dry THF. The solution was cooled to 0 °C. NaH (0.09 g, 0.22 mmol) was added to the solution and allowed to stir for 5 min. 3-*O*-Acetylmorphine-*p*-nitrophenol carbonate (0.083 g, 0.17 mmol), dissolved in 3 mL of dry THF was added to the reaction mixture drop-wise and the reaction mixture was allowed to warm to the ambient temperature. The progress of the reaction was monitored by TLC. After the completion of the reaction, the mixture was filtered through a pad of celite and concentrated under reduced pressure. Obtained residue was dissolved in methylene chloride (20 mL), washed with 50% sodium bicarbonate solution (3 x 10 mL), water (10 mL), and brine (10 mL), dried and concentrated under reduced pressure to afford the crude solid. The crude mixture was subjected to silica gel column using a methylene chloride/methanol gradient to afford a pure product (0.057 g, 51%). ¹H NMR (500 MHz, CDCl₃): δ 6.81 (1H, d), 6.61 (1H, d), 6.59 (1H, d), 6.55 (1H, d), 6.07 (1H, br s), 5.75 (1H, d), 5.47 (1H, dt), 5.22 (1H, d), 5.13 (1H, m), 3.40 (1H, m), 3.19 (1H, d), 3.09 (1H, d), 2.75 (1H, m), 2.60 (1H, dd), 2.52 (2H, t), 2.45 (3H, s), 2.39 (1H, dt), 2.32-1.66 (11H, m), 1.65 (3H, s), 1.59 (2H, m), 1.42 (3H, s), 1.32 (4H, m), 1.11 (3H, s), 0.89 (3H, t) ppm; ¹³C NMR (500 MHz, CDCl₃): δ 168.7, 154.7, 152.9, 149.9, 143.0, 135.1, 132.4, 132.2, 131.6, 130.1, 123.2, 123.1, 122.3, 119.6, 115.6, 115.1, 113.9, 113.7, 88.7, 72.2, 59.1, 45.6, 43.3, 43.2, 41.1, 40.9, 35.6, 35.5, 34.3, 34.2, 31.7, 31.3, 30.7, 27.7, 25.1, 23.5, 22.7, 20.9, 20.8, 19.5, 14.3 ppm; MS (ESI): (M+1) 668 *m/z*; HRMS: calcd. for C₄₁H₄₉NO₇ (M⁺) *m/z* 667.3508, found *m/z* 667.3508.

Chapter 3

The Analgesic activities of Codrugs and their Parent Compounds

3.1 Introduction

It is easier to design and synthesize more efficient pain modulating drugs if the type of pain can be better understood. Pain can arise from tissue damage (nociceptive) or from injury to the nervous system (neuropathic). Nociception refers to a withdrawal behavior in response to a dangerous (e.g. sharp or hot) environmental stimulus (Joshi and Honore, 2006). Nociceptive pain occurs when the nociceptive system gets activated by noxious stimuli that can cause mechanically-, chemically-, or thermally-induced damage to tissues (Woolf, 2004; Woolf and Salter, 2000). The nociceptive system originates in peripheral tissues, spans the spinal cord, traverses the brain stem and thalamus, and terminates in the cerebral cortex, where the sensation of pain is perceived. Peripheral tissues are innervated by nociceptors, highly specialized primary sensory neurons, which contain specific receptors or ion channels at their peripheral terminals (Woolf, 2004; Woolf and Salter, 2000). The A-delta fiber and the C-fiber nociceptors are the two main classes of nociceptors. C-fibers are the most common; about 70% of all nociceptors are of the C-fiber type. Activation of these receptors or ion channels by noxious stimuli generates a depolarizing current (or an action potential, or an electrical impulse), which is then relayed to the brain for pain perception (Fig. 3.1) (Scholz and Woolf, 2002). This pain is well localized, and is characterized as dull or aching.

The A-delta fiber and the C-fiber nociceptors are the 2 main classes of nociceptors. C-fibers are the most common; about 70% of all nociceptors are of the C-fiber type.

Neuropathic pain arises from injury to, or abnormal function of the nervous system. The pain can occur even without any physical or chemical stimuli. Unlike nociceptive pain, neuropathic pain can persist for a long time, even after the initiating

injury has been completely healed. This leads to abnormal processing of sensory information by the nervous system. After the nerve injury, changes occurring in the central nervous system can persist indefinitely. Examples of neuropathic pain are: phantom limb syndrome, diabetic pain, shingles, herpes zoster, pain associated with HIV infections, and pain experienced after chemotherapy. The pain is felt in many different ways, such as burning, tingling, prickling, shooting, and spasm (Rotha et al., 1998). Allodynia and hyperalgesia are two hallmarks of neuropathic pain. Allodynia refers to pain due to a stimulus, which does not normally provoke pain e.g., touch, cold, light pressure can be felt as pain. Hyperalgesia refers to an increased response to a stimulus, which is normally painful.

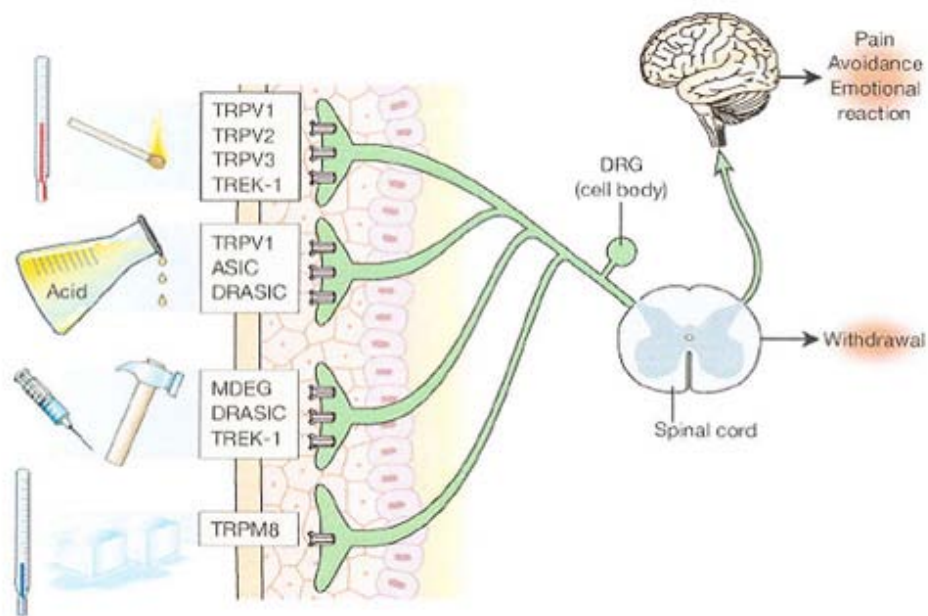


Fig. 3.1 Nociceptive pain transmission (Rotha et al., 1998; Reprinted by permission)

Different animal pain models are used for different kinds of pain. For example models developed to measure responses to acute noxious thermal stimuli use a noxious heat or cold stimulus to the paw or tail of rodents. These models are widely used for

testing opioid analgesics. In these methods, latency to behavioral response is recorded and a cut-off time period is set to avoid any tissue damage to the animal. In the tail-flick test, an intense beam of light is applied to the tail of a rat and the latency period is measured until the tail is flicked out of the path of the light beam (Fig. 3.2). One other assay to determine sensitivity to heat in normal animals, as well as in animals under chronic pain conditions, has been described by Hargreaves et al. and uses a radiant heat source. In this method, the temperature of the heat source is applied to the hind paw and increases over time until it reaches a painful threshold. Latency to of pain to the hind paw is recorded and analyzed. One widely used method to test for reactivity to cold is the application of a drop of cold acetone onto the skin of a rat. Acetone produces a distinct kind of sensation when it evaporates. Normal rats do not respond to this stimulus, while nerve-injured rats show an exaggerated response.



Fig. 3.2 The Tail-Flick test (Reprinted by permission)

Responses to acute noxious mechanical stimuli are measured by stimulating the paw or the tail of rodents. In the Randall Selitto test, increased pressure is applied to the dorsal surface of the hind paw/tail of a rat via a dome-shaped plastic tip. The threshold (in grams) for either paw or tail withdrawal is then recorded. Similarly, responses to acute noxious chemical stimuli can be measured by injecting chemical irritants such as capsaicin, formalin or mustard oil. The animal responds by biting or licking the injected

paw. These observations are recorded at various time points after administration of the drug to be tested.

Different models are used for pain following injury to the nervous system. For example, the chronic constriction injury pain model (Bennett's model). This pain model involves the tying of four loose ligatures around the sciatic nerve of a rat, just tightly enough to touch the nerve (Fig. 3.3) (Expert Rev Proteomics, 2008, Expert Review Ltd.). Subsequent swelling of the nerve constricts the nerve, which develops hyperalgesia and allodynia over 10 to 14 days (Hogon, 2002).

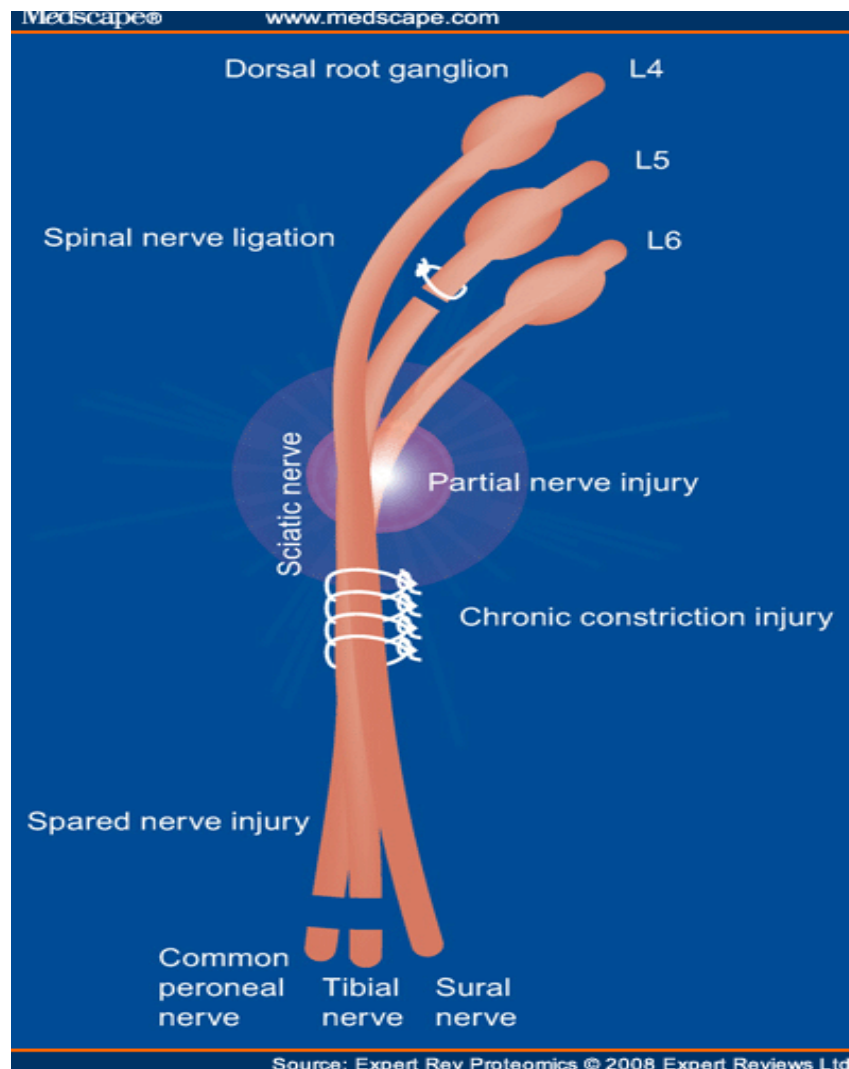


Fig. 3.3 The Chronic Constriction Injury pain model showing tying of four loose ligatures around the sciatic nerve (Expert Rev Proteomics, 2008, Expert Review Ltd., reprinted by permission)

One other most studied neuropathic pain model is L5-L6 spinal nerve ligation (SNL; Chung's model). In this ligation process, the L5 and L6 spinal nerves of the animal are isolated and tightly ligated with silk thread. This induces mechanical allodynia within 7-10 days. Models have also been developed involving cold allodynia and thermal hyperalgesia. Animals exhibit a dynamic mechanical allodynia, which is assessed by gently brushing with a soft brush. In the present chapter, the tail-flick test is used to assess the affect of codrugs on nociceptive pain and the chronic constriction injury pain model is used to assess the effect of codrugs on neuropathic pain.

Codeine is a well known opioid drug commonly used to control pain, whether alone or in combination with an adjunct drug. It produces full efficacy in the tail-flick test for antinociception. Unfortunately, long term use of these types of drugs results in the development of tolerance and physical dependence. This reduces the analgesic effects necessitating the administration of high and potentially harmful doses to achieve effective pain control. The efficacies of physical mixtures of opioids non-antinociceptive doses of cannabinoids have been previously been characterized in rodent models of nociceptive and neuropathic pain (Smith et al., 1998; Cichewicz et al; 2002). These models included acute thermal nociception and peripheral neuropathy (chronic constriction nerve injury, CCI). In the present chapter, we have investigated codrug therapy where two drugs, codeine and Δ^9 -THC are administered as a single chemical entity, whereby the two molecules are covalently linked together via a carbonate ester linkage (Cod-THC). The efficacies of each of the parent drugs as well as a 1:1 physical mixture of the parent drugs, codeine and Δ^9 -THC were compared with the Cod-THC codrug as pain modulators in the above pain models to determine their relative effectiveness. Similarly, a codeine-cannabidiol (Cod-CBD) codrug was also assessed for its analgesic activity and this activity compared to the individual parent drugs.

3.2 Methods and Materials

3.2.1 Animals

Male Sprague-Dawley rats (Harlan, Indianapolis) about 90 days old, weighing 300-350 g were used for all experiments. Rats were housed separately in a transparent cage; with free access to standard laboratory chow and tap water in a humidity- and temperature-controlled facility with lights on between 0600 and 1800 h. Rats were trained in the test situation before initiation of the experimental procedures. Rats were fasted overnight before oral administration of drug. Body weights were determined on the day of experimentation. At the end of the experiment, rats were euthanized with pentobarbital sodium (150 mg/kg, intraperitoneal, IP). A crossover paradigm was used within an experiment (if possible) to minimize the number of rats. All testing was performed in accordance with the guidelines of the National Institute of Health Guide for Care and Use of Laboratory Animals (Publication No. 85-23, revised 1985). The protocol was approved by the University of Kentucky Animal Care and Use Committee.

3.2.2 Drugs

The Cod-THC codrug was evaluated using tail-flick and chronic constriction injury pain model. The parent drugs codeine, Δ^9 -THC and 1:1 physical mixture of codeine and Δ^9 -THC were also assessed using the same pain models. Similarly, Cod-CBD codrug, codeine and cannabidiol parent drugs were evaluated using tail-flick pain model. Drugs were dissolved in 15% PEG saline solution and administered by the oral route using a gavage feeding needle after overnight fasting of the animals. A 15% solution of PEG in saline (vehicle) served as the control.

3.2.3 Tail Flick test (Measure of analgesia/antinociception)

The tail-flick test primarily assesses the spinal antinociceptive (pain relief) response to noxious thermal stimuli (D'Amour and Smith, 1941). An intense beam of

light is applied to the tail of a Sprague-Dawley rat and the latency period is measured until the tail is flicked out of the path of the light beam (Fig. 3.2). Baseline tail-flick latencies were determined prior to drug administration using the tail-flick latency test. During testing, a cutoff time of 10 s was employed to prevent damage to the tail of the rat.

First, rats (6/group) were treated with codeine alone (10 mg/kg), and then with the Cod-THC codrug (10 mg/kg). Drugs were administered via the oral route. Tail flick latencies (TFL) were measured before and after the drug was given. The latency period is the time from onset of stimulation to a rapid flick/withdrawal of the tail from heat source. This time period is also measured before the drug is given to ensure the analgesic effect. Therefore, responsiveness (TFL) was measured prior to (5, 10, 15, and 30 min. apart) and at after oral dosing (Fig. 3.4). Only one dose of codrug was initially examined to confirm the presence of an analgesic action of the codrug. This effect of a single dose of the Cod-THC codrug was compared with the parent drug codeine, to compare the relative analgesic effects of these two drugs.

Second, rats (6/group) were treated with codeine alone (10 mg/kg), and with three doses (5, 10 and 20 mg/kg) of the Cod-THC codrug. Drugs were administered via the oral route. Animals were tested for tail-flick response using the tail-flick apparatus. Intensity of the heat source was adjusted to produce tail-flick latencies of 3 to 4 sec. These baseline latencies of the rats were recorded three times (5, 10, 15, 30 min apart). Responsiveness (TFL) was measured thrice again after oral dosing (5, 10, 15, 30 min apart). Dose response curves can be generated if minimum of three doses of a drug are utilized in this assay. The time-response graphs obtained with the three different doses of codeine-THC codrug are illustrated in Fig. 3.5 and are compared with that of the 10 mg/kg codeine dose.

Third, rats (6/group) were treated with three doses (5, 10 and 20 mg/kg) of codeine administered via the oral route. Responsiveness (TFL) was measured prior to (baseline) and thrice (5, 10, 15, 30 min. apart) after oral dosing as described earlier.

Time-response and dose-response curves were drawn to calculate ED₅₀ values for both codeine and the Cod-THC codrug (Fig. 3.7).

In a similar manner, the codeine-cannabidiol codrug (Cod-CBD) and its parent drugs codeine and cannabidiol were assessed in the tail-flick test. Rats (6/group) were treated with codeine alone (10 mg/kg), with cannabidiol alone (10 mg/kg) and with three doses (5, 10 and 20 mg/kg) of Cod-CBD codrug (Fig. 3.14).

3.2.4 Chronic Constriction nerve injury (CCI, Neuropathic pain model)

Surgery

The rodent model of peripheral neuropathy (chronic constriction nerve injury, CCI) (Bennett and Xie, 1988) was used to characterize the antihyperalgesic effect of codeine and with the codeine- Δ^9 -THC codrug. This pain model involves the tying of four loose ligatures around the sciatic nerve, which results in the development of mechanical (tactile) allodynia in the ipsilateral hindpaw of the rat.

Mechanical hyperalgesia

Enhanced sensitivity to mechanical noxious stimuli (mechanical hyperalgesia) was evaluated using the paw pressure test (Randall and Selitto, 1957). This was done prior to surgery (pre-CCI baseline) and on the post-surgery day. The hind paw was placed between a blunt pointer and a flat surface and increasing pressure was applied to the dorsal side of the paw. Rats (6/group) were treated with codeine alone (4.9, 10, 20, 40 mg/kg doses), Δ^9 -THC alone (5.1 mg/kg dose) and Cod-THC codrug (2.5, 5 and 10 mg/kg doses). Drugs were administered via the oral route.

3.2.5 Statistical analysis

Responses were normalized for baseline values. Percent maximum possible effect was calculated at the time of peak response: %MPE = (TFL-baseline)/ (cut-off-baseline) * 100. ED₅₀ values were computed for Cod-THC codrug and codeine. The overall effects (antihyperalgesia) were presented as areas-under-the-time curves, calculated by the trapezoidal rule for baseline normalized responses. Data were analyzed using regression analysis, analysis of variance (ANOVA), post-hoc Student Newman Keuls test (SNK) and t-test. Level of significance was $P \leq 0.05$. All data were mean \pm SEM (n = number of rats).

3.3 Results

3.3.1 Cod-THC codrug antinociception (tail flick tests)

The antinociceptive effects of codeine alone and various doses of Cod-THC codrug were characterized after the oral administration in the tail-flick test. The present data provides evidence (Figs. 3.4, 3.5, 3.6, 3.7, 3.8) that a codrug consisting of codeine (low dose) and Δ^9 -THC (non-effective dose) significantly enhances codeine effectiveness against acute nociception. In preliminary experiments, one dose of Cod-THC codrug and one dose of codeine were given to the rats to check and compare the analgesic effect of the Cod-THC codrug with codeine. A 10 mg/kg dose of Cod-THC codrug and a 10 mg/kg codeine dose were chosen for this purpose (Fig. 3.4). Codeine and Cod-THC codrug tail-flick latency values were above baseline values, which indicate that both drugs exhibit an analgesic effect. On comparing the effect of codeine with the Cod-THC codrug, it can be observed that the analgesic effect of the codrug is much greater than that of codeine. Next, the time-response curve for three doses of the Cod-THC codrug (5, 10, 20 mg/kg) was generated to obtain a dose-response curve. Figs. 3.5 and 3.6 illustrate the time-response curve for the 5, 10, 20 mg/kg doses. In Fig. 3.5, the three doses of Cod-THC codrug were compared with codeine (10mg/kg) and in Fig. 3.6 the time-response curve for the three doses of the Cod-THC codrug is shown. Table 3.1 reports the area-under-the-curve (AUC) values for all the three doses of the Cod-THC codrug.

It can be seen that as the dose of the Cod-THC codrug is increased, the AUC also increases. This indicates that the drug exhibits a dose-response curve (Dose: $F_{5,23} = 11.1$, $P < 0.0005$). $F_{5,23} = 11.1$ indicates that the codrug is exhibiting a dose-response effect and the $P < 0.0005$ value proves the statistical significance of the data between each increasing dose. Post-hoc Student Newman Keuls (SNK) analysis indicates that the 10 and 20 mg/kg dose showed a significant analgesic effect when compared to vehicle alone ($P < 0.05$). The maximum analgesic effect was observed after 15 minutes with the 10 mg/kg dose, and after two hours with the 20 mg/kg dose of the Cod-THC codrug. This unusual result could be due to a solubility issue with the higher dose of codrug in the vehicle. The drug may be precipitating out in the gastrointestinal tract, probably in the stomach, after oral administration and then slowly dissolves as it passes through the gastrointestinal tract.

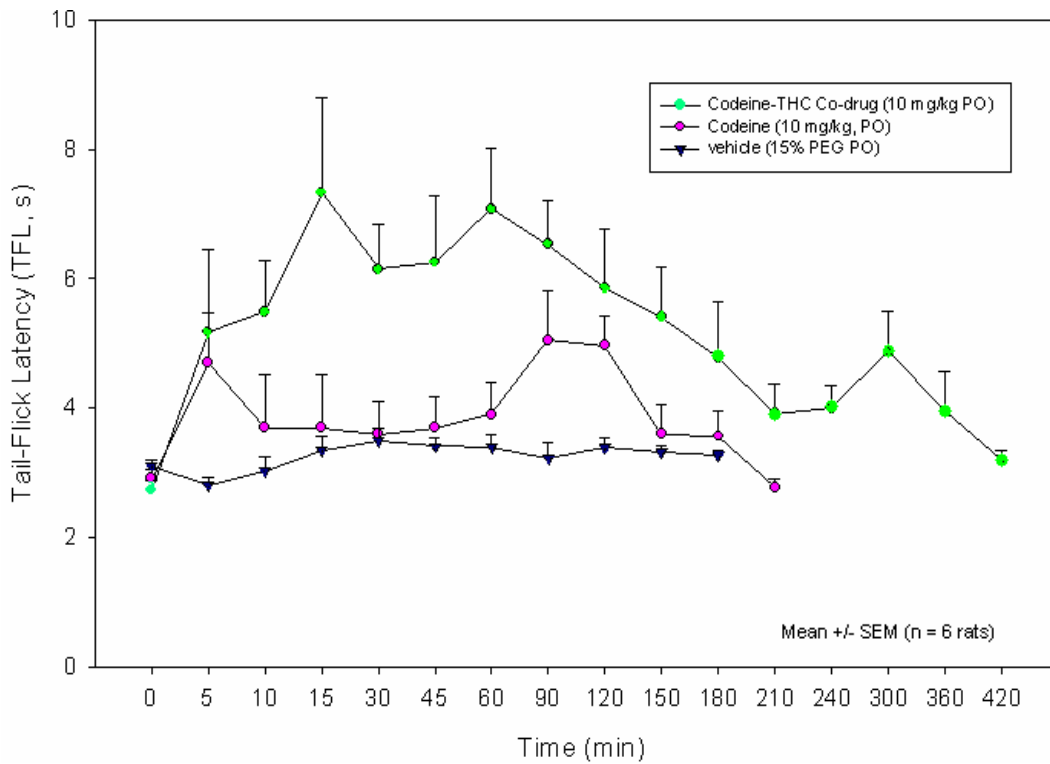


Fig. 3.4 Tail-Flick Latencies for Codeine and Cod-THC Codrug

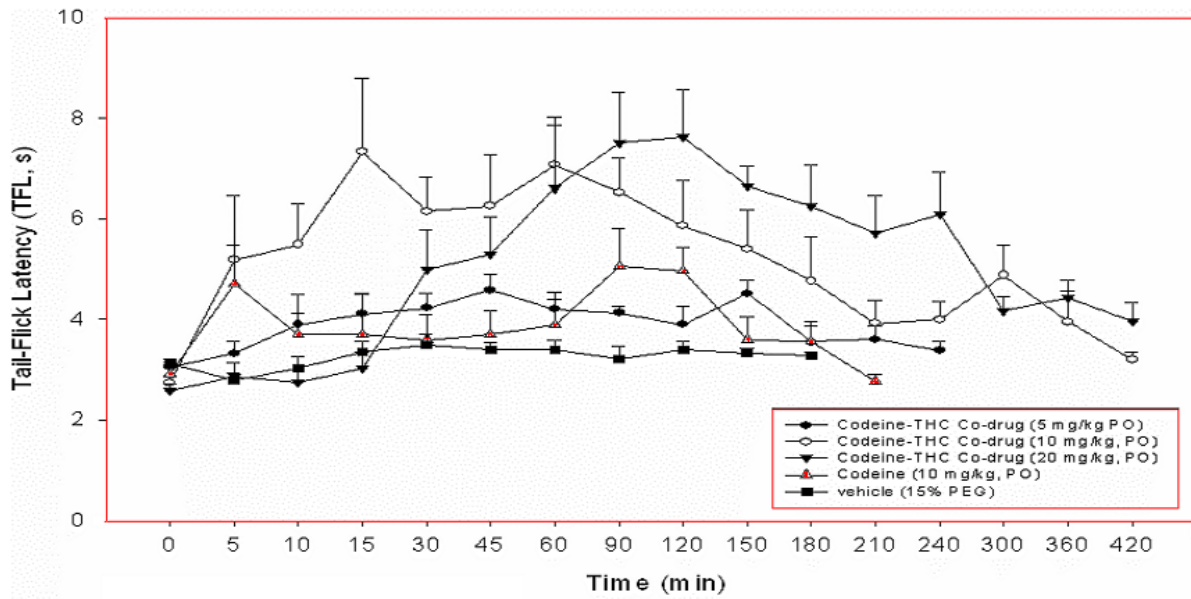


Fig. 3.5 Antinociceptive Effect of Codeine and Cod-THC Codrug (5, 10, 20 mg/kg doses) in the Tail-Flick Pain Model

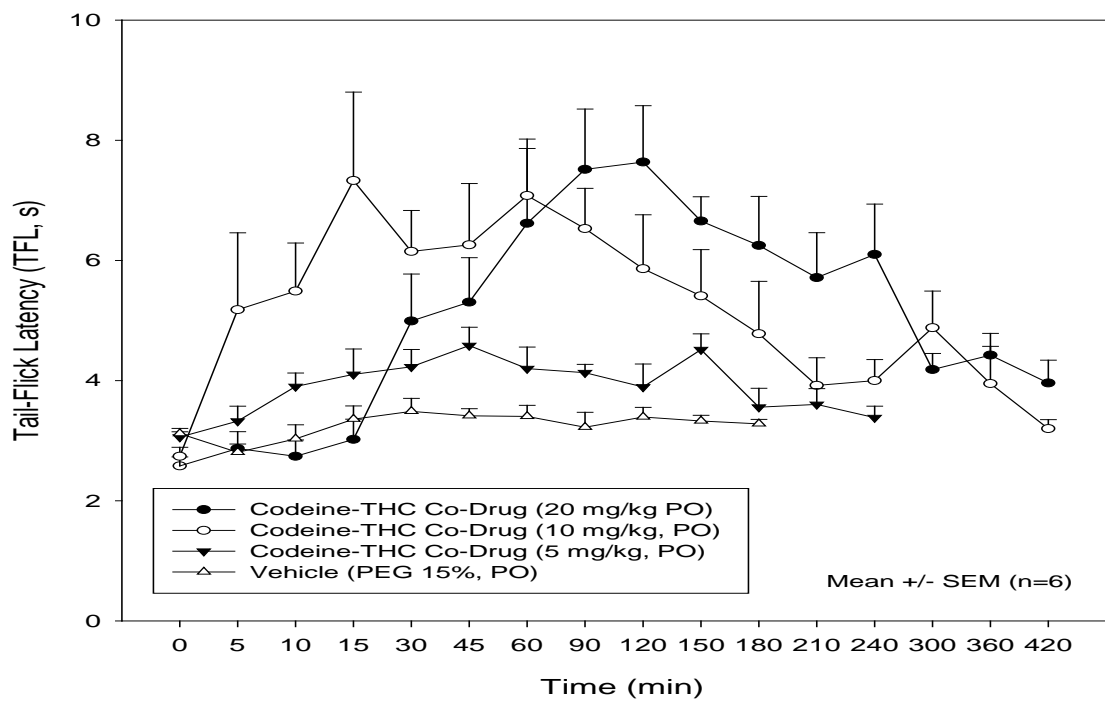


Fig. 3.6 Time-response Curves for the Cod-THC Codrug in the Tail-Flick Test

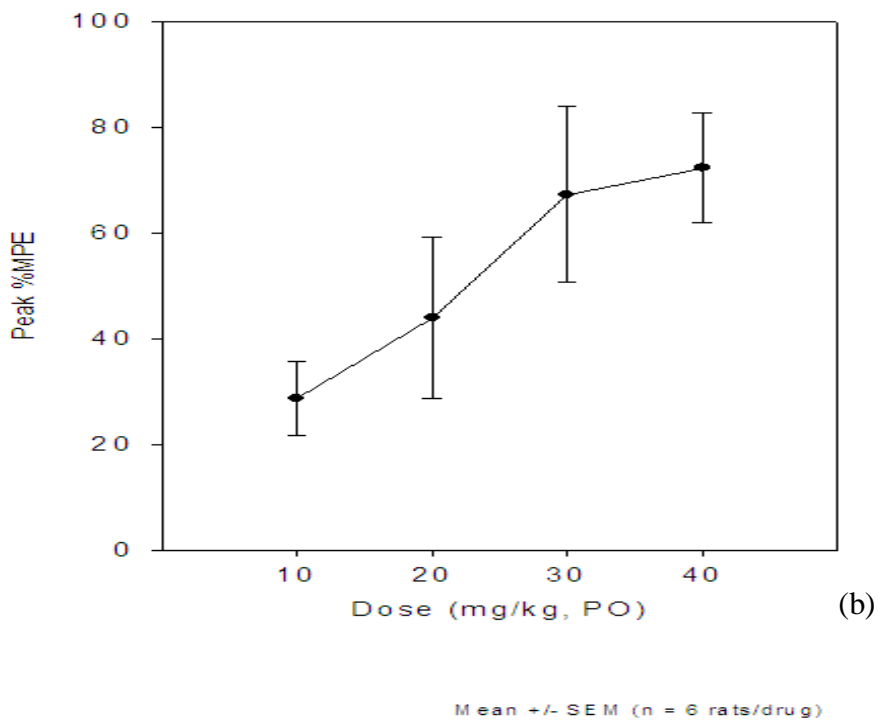
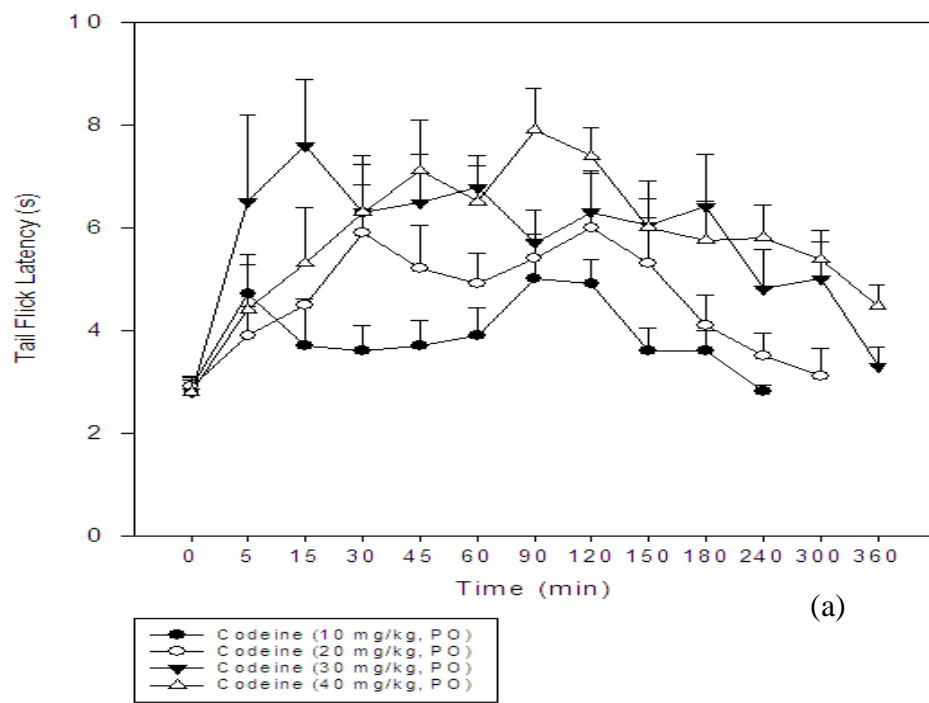


Fig. 3.7 Time-response (a) and dose-response (b) curves for Codeine in the Tail-Flick Model

Table 3.1 AUCs for 5, 10, and 20 mg/kg doses of Cod-THC Codrug

Cod-THC Codrug dose	AUC_{0-240 min.} (s * min)
5 mg/kg	190.5 ± 34.9
10 mg/kg	747.6 ± 144.6
20 mg/kg	1025 ± 171.1
Vehicle	8.5 ± 1.7

Fig. 3.8 illustrates the %MPE (Maximum Possible Effect) for the Cod-THC codrug and for codeine. % MPE can be related to the effectiveness of the drug. The greater the %MPE, the more effective the drug is. The highest %MPE achieved by codeine and the Cod-THC codrug is 70%. Increasing the dose further for both codeine and the Cod-THC codrug does not result in a further increase in the %MPE. The 20 mg/kg dose of the Cod-THC codrug produced the highest %MPE. The equi-effective dose of codeine was 40 mg/kg compared to a 20 mg/kg dose of the Cod-THC codrug. The 20 mg/kg dose of the Cod-THC codrug contains 9.8 mg/kg dose of codeine. Therefore, the analgesic effect shown by 9.8 mg/kg dose of codeine when given in the form of the Cod-THC codrug is equivalent to a 40 mg/kg dose of codeine alone. In conclusion, the present data demonstrates that combining codeine with Δ^9 -THC in the form of a codrug may enhance codeine effectiveness against acute nociception by decreasing the side effects associated with higher doses of codeine.

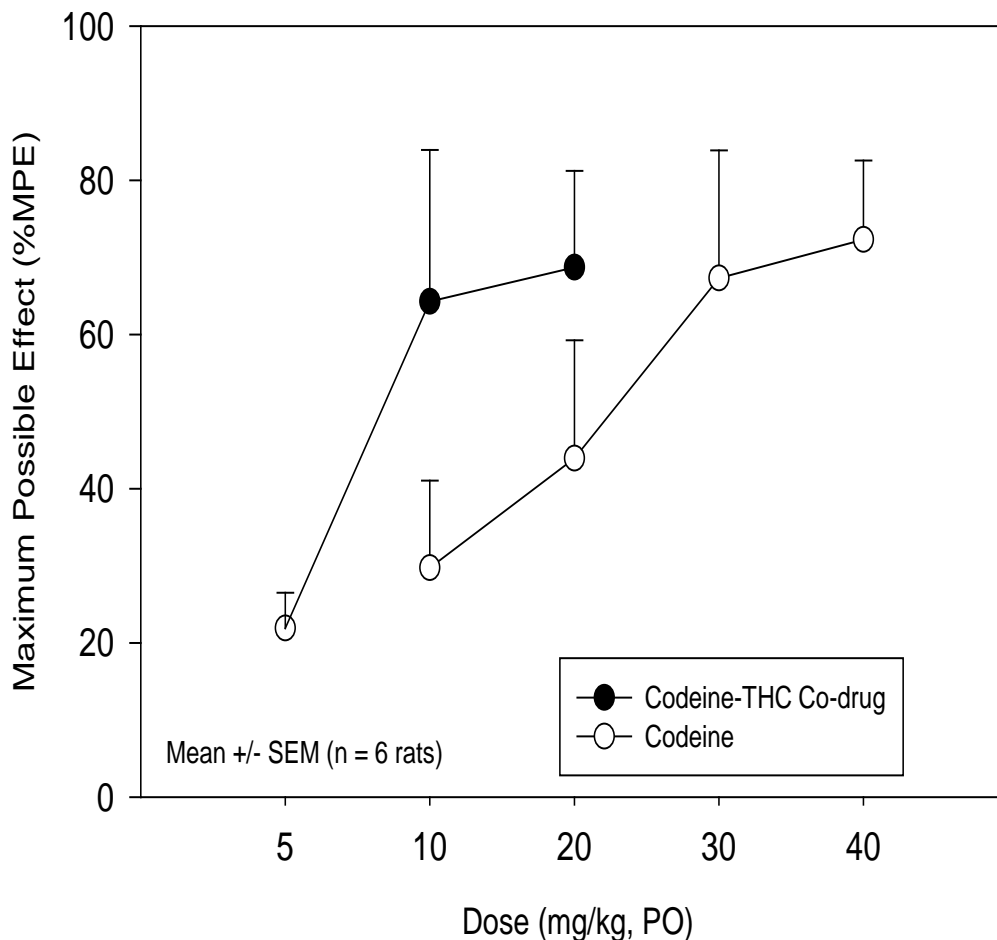


Fig. 3.8 Dose-Response Curves for the Antinociceptive Effects of the Codeine-THC Codrug and Codeine Alone in the Tail-Flick Test

3.3.2 Cod-THC codrug Antihyperalgesic effect (CCI model)

Chronic constriction nerve injury (CCI) results in significantly decreased thresholds to mechanical noxious stimuli (hyperalgesia) compared to the pre-surgical threshold. The paw withdrawal threshold (PWT) (pre-CCI) was 225 ± 3.5 g versus a PWT (post-CCI) of 112 ± 4.3 g. The antihyperalgesic effect of codeine alone, Δ^9 -THC alone and various doses of the Cod-THC codrug were characterized after administration via the oral route. The data obtained provides evidence (Figs. 3.9, 3.10, 3.11, 3.12, 3.13) that the Cod-THC codrug exhibits a synergistic antihyperalgesic effect. Fig. 3.9

demonstrates the time-response and dose-response curves for various doses of codeine alone (4.9, 10, 20, 40 mg/kg). Dose-response curves for codeine were generated to determine the dose of codeine that was equi-effective as the Cod-THC codrug. 65%MPE was exhibited by codeine. Figs. 3.10 and 3.11 show the time-response curves for various doses of the Cod-THC codrug (Dose: $F_{5,23}= 6.8$, $P<0.005$). $F_{5,23}= 6.8$ indicates that the codrug is exhibiting a dose-response effect and the $P<0.005$ value proves the statistical significance of the data. Post-hoc Student Newman Keuls (SNK) analysis indicates that the 5 and 10 mg/kg doses of the codrug showed an enhanced antihyperalgesic effect when compared to vehicle alone. The maximum possible effect was achieved around 1.7 hours post-dosing with the 5 mg/kg dose of the Cod-THC codrug, and at 3.5 hours post-dosing with the 20 mg/kg codrug dose. The enhancement of the analgesic response is evident at several points in the time-response curves, as well as in the overall effect (AUC) (Table 3.2).

The bar graph illustrated in Figs. 3.12, 3.13 indicate that the antihyperalgesic effect of the Cod-THC codrug is much more than just an additive effect of the two parent drugs. Both codeine and Δ^9 -THC at doses (4.9 mg/kg and 5.1 mg/kg) that did not produce a significant effects of their own, afforded an enhanced antihyperalgesic effect when each drug was incorporated into the Cod-THC codrug in their molar amounts(10 mg/kg Cod-THC codrug) (Fig. 3.11). One must consider the benefits of a synergistic relationship over an additive interaction. Additivity simply represents the addition of the expected effects of each dose of drug alone, whereas synergy describes a situation in which the combined effect greatly exceeds the expected simple addition. Clearly, synergistic drug interactions would be more significant, indicating that low doses of two drugs covalently tethered together in a codrug molecule could produce effects of high magnitude. The clinical benefits of such an enhancement can be easily imagined, as it would allow for the administration of much lower drug doses, which would still yield a potent analgesic effect yet hopefully induce fewer side effects. This is the first report of a synergistic interaction between Δ^9 -THC and codeine after administration of a Cod-THC codrug, since previous studies have only examined the physical mixtures of these two drugs.

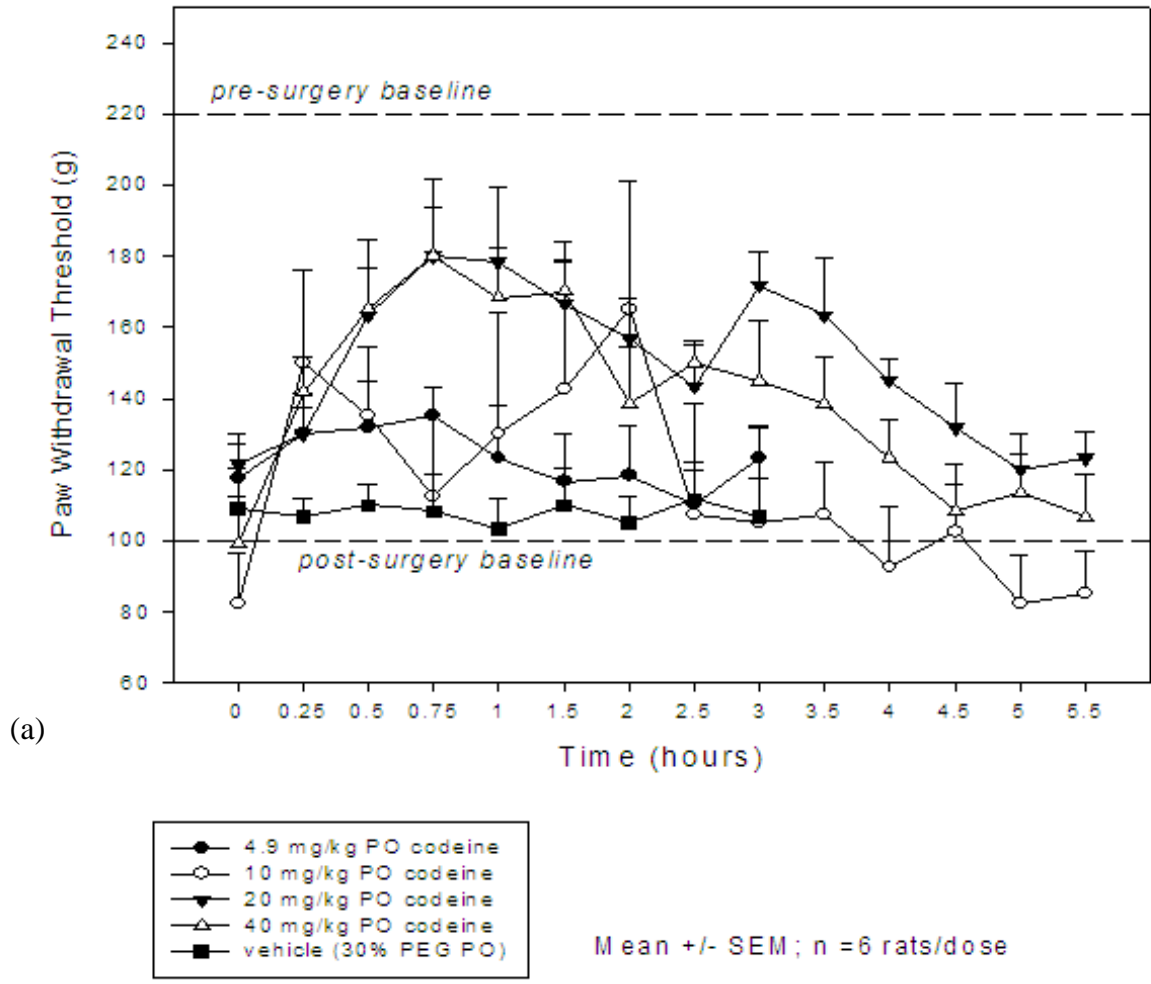


Fig. 3.9 (a) Time-response curve for Codeine in the CCI model

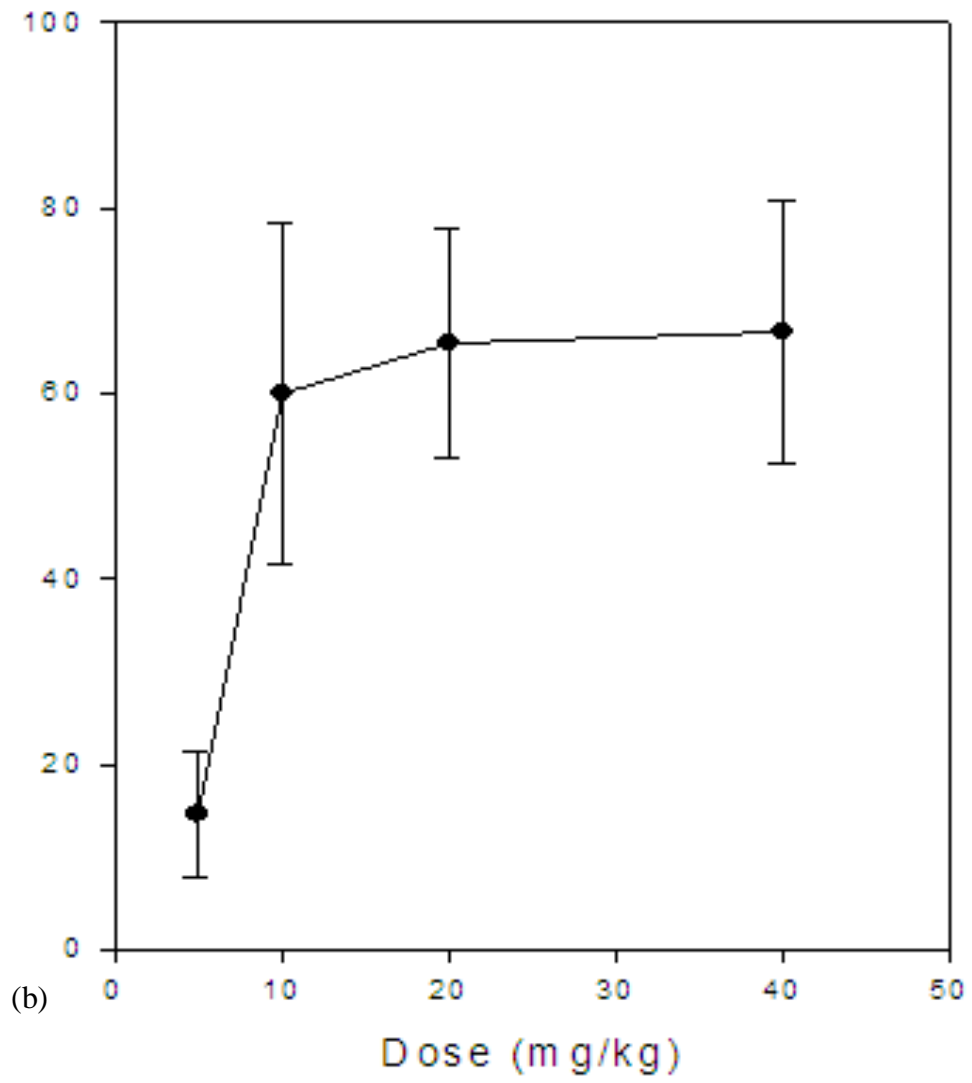


Fig. 3.9 (b) Dose-response curve for Codeine in the CCI model

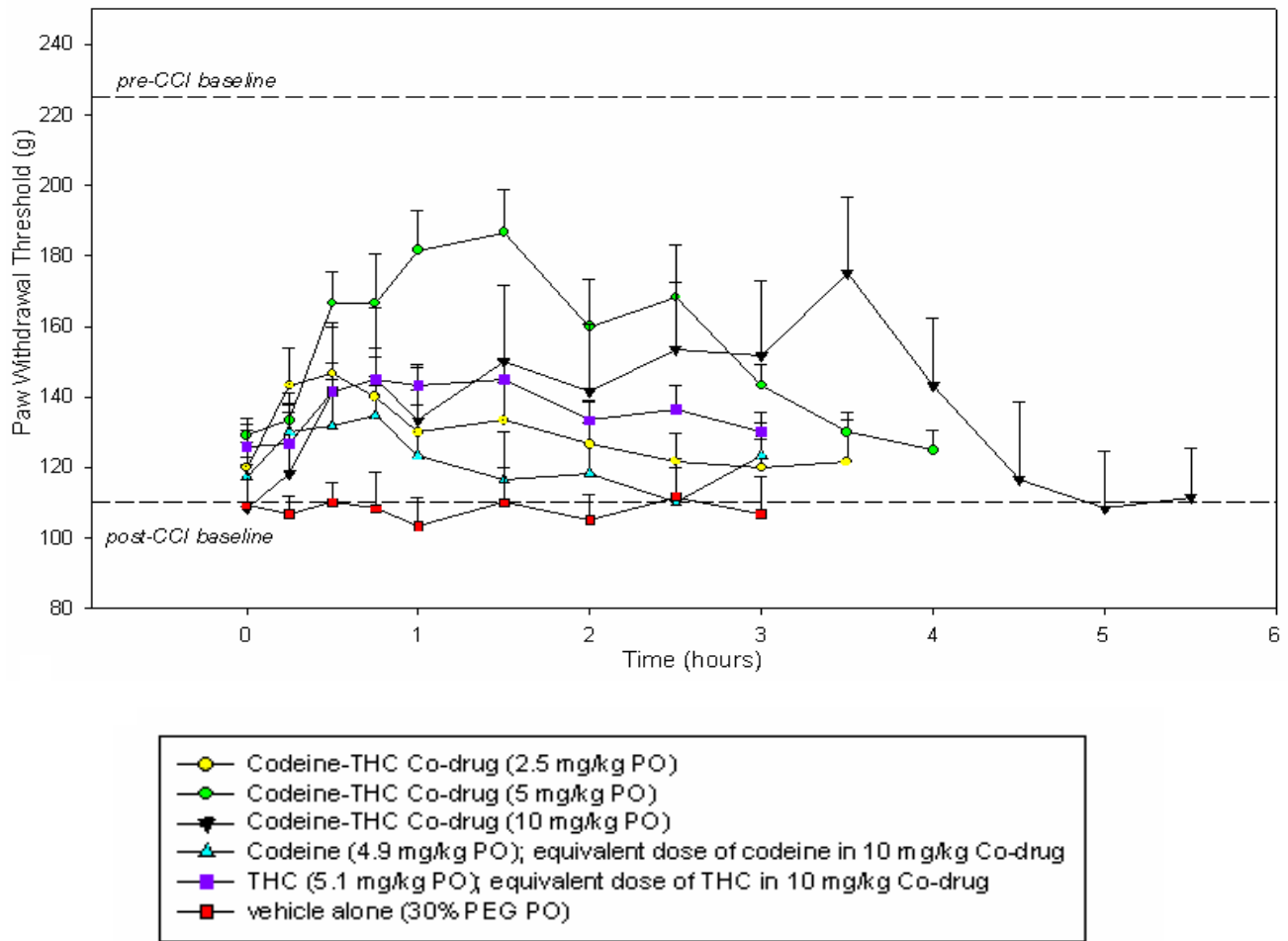


Fig. 3.10 Antihyperalgesic effect of the Cod-THC codrug in the CCI Model

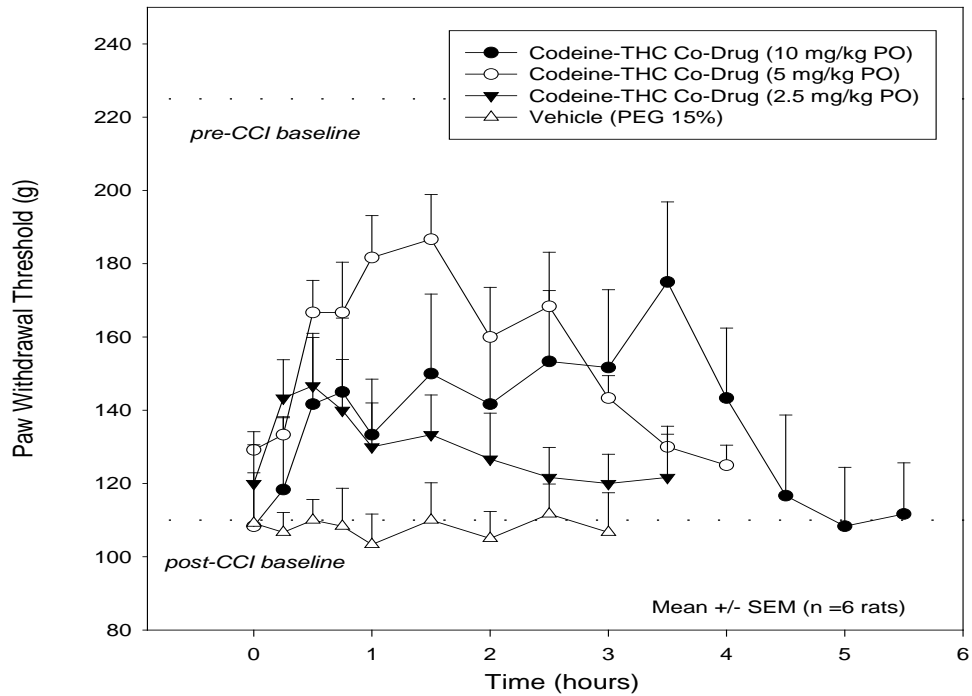


Fig. 3.11 Time-Action Curves for the Cod-THC Codrug in the Chronic Constriction Nerve Injury (CCI) Model

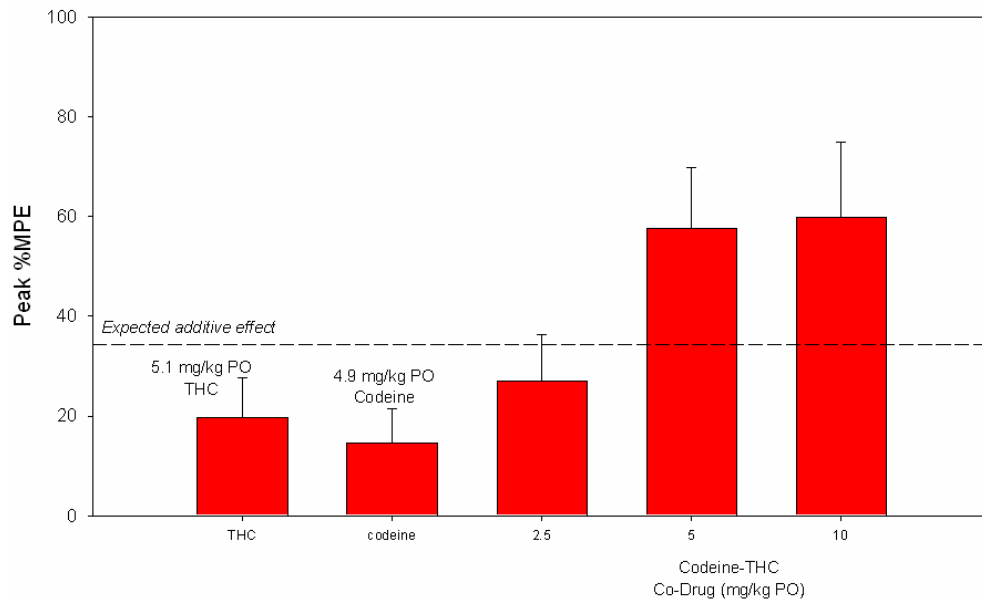


Fig. 3.12 Antihyperalgesic Effect of the Cod-THC Codrug in the Chronic Constrictive Nerve Injury (CCI) Model

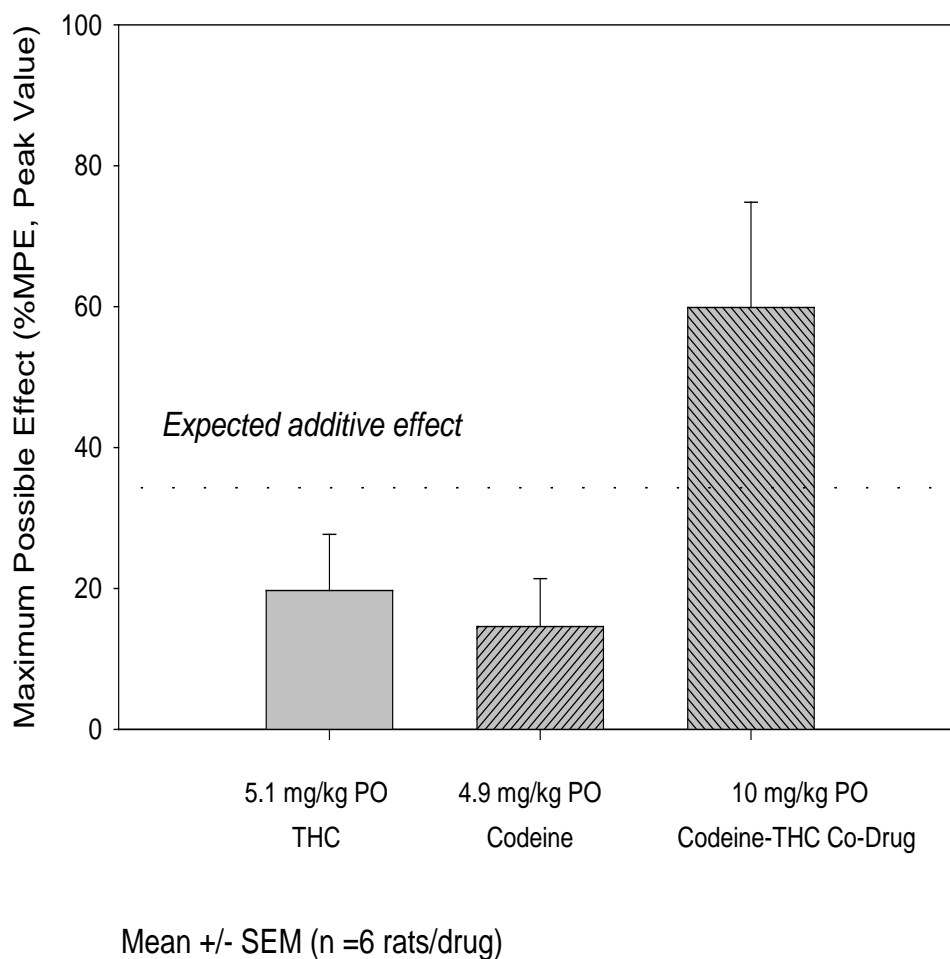


Fig. 3.13 Antihyperalgesic Effect of Codeine, THC and the Cod-THC Codrug in the Chronic Constriction Nerve Injury (CCI) Model

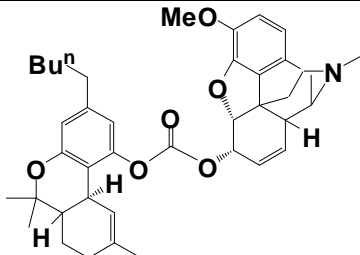
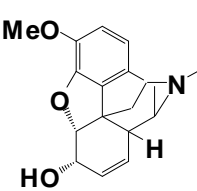
Table 3.2 AUCs for 2.5, 5, and 10 mg/kg Cod-THC Codrug (CCI model)

Cod-THC Codrug dose (mg/kg)	AUC _{0-180 min.} (g * min)
2.5	1925 ± 808.7
5	6406.3 ± 1663.9
10	9387.5 ± 2384.8

3.3.3 ED₅₀ values

The dose of a drug that is pharmacologically effective for 50% of the population exposed to the drug, or that shows a 50% response in a biological system that is exposed to the drug is defined as the ED₅₀ value of the drug. As can be seen in Table 3.3, the ED₅₀ value for the Cod-THC codrug in the Tail-flick test, as well as in the CCI pain model is much lower than the ED₅₀ value of codeine in either test, which suggests that the use of a low dose combination of these two analgesics in a codrug structure is a valid and effective approach for improved treatment of pain.

Table 3.3 ED₅₀ values for the Cod-THC codrug and codeine

 <p>The structure shows a morphine molecule with a morphine ring system, a methoxy group (MeO) at the 3-position, and a nitrogen atom with a methyl group. It is linked via an ester bond to a THC molecule, which has a butyl group (Buⁿ) at the 1-position and a hydroxyl group (OH) at the 2-position.</p>	 <p>The structure shows a morphine molecule with a morphine ring system, a methoxy group (MeO) at the 3-position, and a nitrogen atom with a methyl group. It has a hydroxyl group (HO) at the 6-position.</p>
<p>ED₅₀ = 6.42 mg/kg(Tail-flick) = (0.01 mmol/kg)</p> <p>= 3.99 mg/kg (CCI) =(0.0062 mmol/kg)</p>	<p>ED₅₀ = 12.5 mg/kg (Tail-flick) = 0.042 mmol/kg</p> <p>= 13.5 mg/kg (CCI) =(0.045 mmol/kg)</p>

3.3.4 Codeine-cannabidiol (Cod-CBD) codrug antinociception (tail flick test)

The antinociceptive effects of codeine alone (10 mg/kg), cannabidiol alone (10 mg/kg) and various doses of the Cod-CBD codrug (5, 10 and 20 mg/kg) were evaluated after oral administration in the Tail-flick test (Fig. 3.14, 3.15). Cannabidiol was chosen because it is a non-psychoactive cannabinoid. Fig. 3.14 shows the dose-response curve for the antinociceptive effect of the Cod-CBD codrug. The graph illustrates that 10 and 20 mg/kg doses of the Cod-CBD codrug exhibit an antinociceptive effect. A 10 mg/kg dose of codeine shows 30 %MPE, while a 10 mg/kg dose of cannabidiol shows 40 %MPE in the Tail-flick test. When given in the form of the Cod-CBD codrug, the %MPE produced by the 20 mg/kg dose is 70 %. This is an example of additive effect rather than synergistic effect (Fig. 3.15). The opioid dose can still be reduced even with the additive effect shown by the Cod-CBD codrug since less codeine is needed to show the same effect when given in conjunction with cannabidiol.

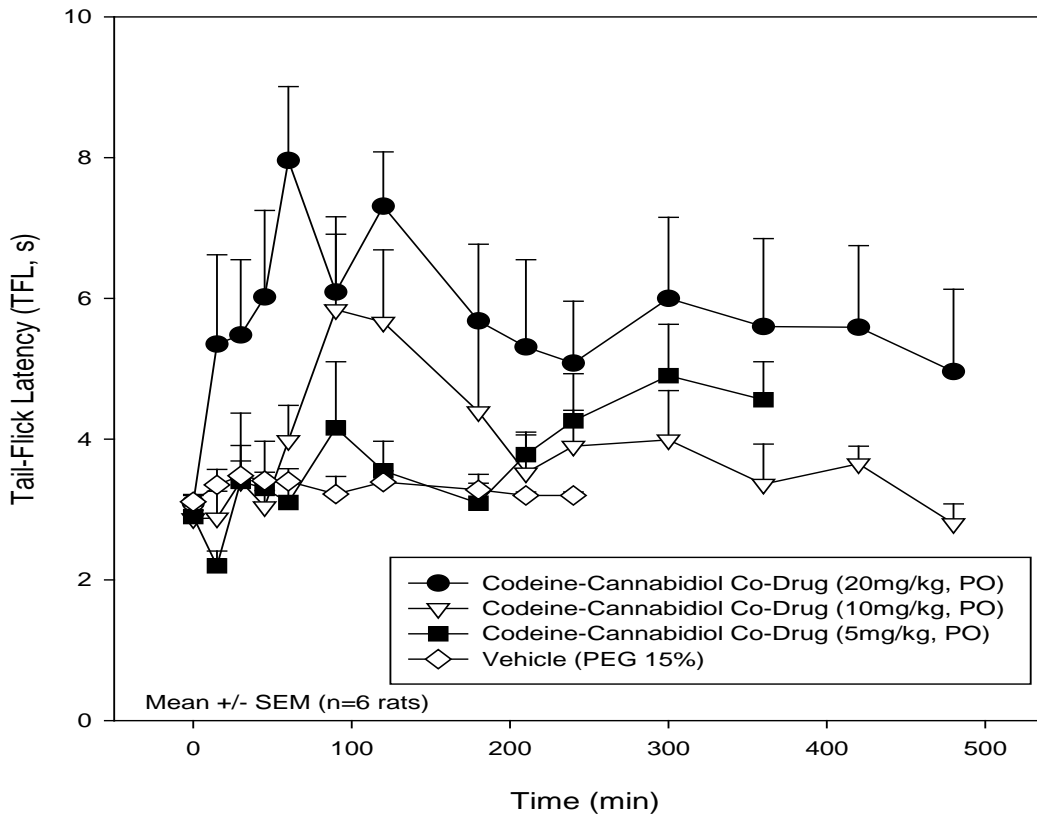


Fig. 3.14 Time-Response Curves for the Cod-CBD Codrug in the Tail-Flick Test

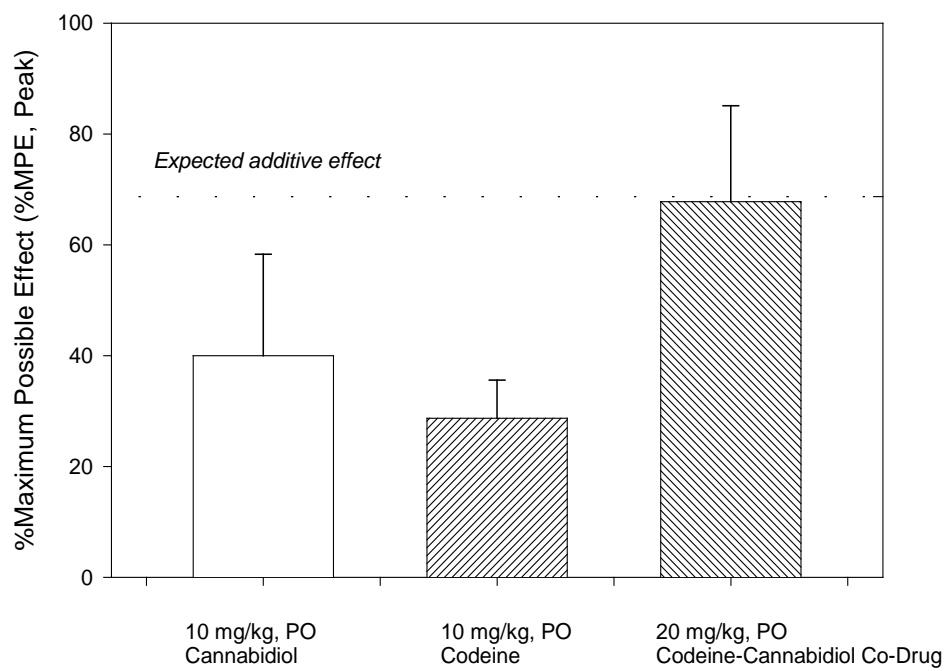


Fig. 3.15 Antinociceptive Effects of Codeine, Cannabidiol and the Cod-CBD Co-drug in the Tail-Flick Test

Chapter 4

***In-vitro* Stability Study of the Cod-THC Codrug**

4.1 Introduction

Compounds in drug discovery encounter a wide range of pHs when administered to patients. Oral dosing exposes compounds to pH 1 to 2 in the stomach, pH 4.5 at the beginning of the small intestine, pH 6.6 as an average pH for the small intestine, and pH 5 to 9 in the colon. The mean fasting stomach pH of an adult is approximately 2, and increases to 4-5 following ingestion of food. These are useful pHs for *in vitro* evaluation of the chemical stability of a drug candidate as it passes through the gastrointestinal tract (Kern and Di 2008).

Important insights can be obtained by studying the stability of the drug with simulated gastrointestinal fluids. These include simulated gastric fluid (SGF) and simulated intestinal fluid (SIF) (Piper et al., 1963; DeBeer et al., 1935). The recipe of preparing these gastrointestinal fluids are specified in the United States Pharmacopeia (USP) and described in chapter 1. The prime object of performing stability study of a drug in nonenzymatic and enzymatic assays is to predict stability of the drug in gastrointestinal tract after oral dosing. The obtained stability results can guide the structural modification of the drug to improve gastrointestinal stability for increasing bioavailability and for prioritization of compounds for subsequent *in vivo* pharmacokinetic studies (Patrick, 1995).

Blood contains a large number of hydrolytic enzymes such as cholinesterase, aldolase, lipase, dehydropeptidase, and alkaline and acid phosphatase. If the drug has a labile moiety, sensitive to one of these enzymes, it can be decomposed in the plasma. Many such enzyme sensitive groups are used to enhance the compound's pharmacological activity at the target protein. Rapid hydrolysis in plasma can be a major cause of a compound's rapid clearance, and pharmacologically efficacious concentrations

may not be achievable *in vivo* if this occurs. Exceptions are the issue of a prodrug or a codrug, which requires hydrolysis in plasma to produce the active parent drug(s). Prodrug strategy is mainly utilized to improve absorption of the prodrug from the gastrointestinal tract, since the prodrug will be designed to enhance gastrointestinal absorption by improvement on physicochemical properties compared to the parent drug. Similarly in a codrug strategy gastrointestinal absorption of the two parent drugs can be improved. Once in the plasma, the codrug is designed to be rapidly hydrolyzed to afford the parent compounds. Therefore, before the *in vivo* study of the codrug is performed, plasma stability data must be generated to determine if the codrug is stable in the gastrointestinal tract (Kern and Di 2008).

With the aim of improving the oral bioavailability of the parent drugs codeine and Δ^9 -THC, the codrug Cod-THC was initially evaluated for its stability in buffers ranging from pH 1 to pH 9 (Waterman et al., 2002), as well as in SGF, SIF, and rat plasma and brain. The following experiments were performed in aqueous solutions to model drug barriers:

- pH : Aqueous buffers (37 °C, pH 1-9)
- GI : Simulated gastric fluid (USP, 37 °C)
- GI : Simulated intestinal fluid (USP, 37 °C)
- Plasma : Rat plasma (37 °C)
- Brain : Brain homogenate (37 °C)

The molecular weight of the Cod-THC codrug is 639 g/mole. Since this value is above 500, the molecule might not cross the blood-brain barrier, but this cannot be concluded before carrying out the pharmacokinetic study of the Cod-THC codrug. If the codrug does cross the blood-brain barrier, then it is important to determine its stability in brain homogenate, to determine if it can be hydrolyzed by brain enzymes to release the parent drugs. Thus, a stability study of the Cod-THC codrug was also carried out in rat brain homogenate.

4.2 Materials and Methods

4.2.1 Drugs

The Cod-THC codrug and Δ^9 -THC were synthesized in the laboratory via the procedures reported in Chapter 2.

4.2.2 Sample preparation

Standard curve and quality control validation solutions:

Stock solutions of Cod- Δ^9 -THC, codeine, Δ^9 -THC and the internal standard (2-methoxynaphthalene) were prepared in methanol. A standard curve with eight points was prepared and utilized in the quantitative analysis of the unknown samples. Standard curve samples were prepared by spiking blank plasma/buffers/brain homogenate with Cod-THC, Codeine, or Δ^9 -THC working solutions. Calibration curves were obtained using quadratic least-squares regression of area-under-the-curve (AUC) ratios (analyte peak AUC/internal standard peak AUC) *versus* drug concentrations. The amount of codrug, or parent drugs, was then determined using the standard curves.

Kinetics of hydrolysis of the codrug in aqueous solutions (non-enzymatic):

A 0.02 M hydrochloric acid buffer, pH 1.3, as a non-enzymatic simulated gastric fluid; a 0.02 M sodium phthalate buffer, pH 5.2; a 0.02 M phosphate buffer, pH 7.4; and a 0.02 M boric acid and potassium chloride buffer, pH 9.7 was used in this study. The pH 5.2 simulates intestinal fluid and the pH 7.4 simulates rat plasma. pH 9.7 was utilized to check the chemical stability of the carbonate bond present in Cod-THC codrug. Reactions were initiated by adding 5mL of 1.0×10^{-3} M stock solution (in methanol) of the Cod-THC codrug to 5 mL of appropriate thermostated (37 ± 0.5 °C) aqueous solutions of the above buffer species. Aliquot-parts (300 μ L) were removed from the codrug-buffer solutions at various time intervals, mixed with 50 μ L of the 0.01M internal standard solution (2-methoxynaphthalene) and 20 μ L of the resulting solution was immediately

injected onto the HPLC-DAD analytical system for quantitative analysis. Experiments were run in triplicate (Omar, 1998).

Kinetics of hydrolysis of the codrug in simulated gastric fluid (SGF) and simulated intestinal fluid (SIF) (enzymatic conditions):

Reactions were initiated by adding 5mL of 1.5×10^{-3} M stock solution (in methanol) of the Cod-THC codrug to 5 mL of appropriate thermostated (37 ± 0.5 °C) SGF and SIF solutions. Aliquot-parts (300 μ L) of the resulting solutions were removed at various time intervals, mixed with 50 μ L of the 0.01M internal standard solution (2-methoxynaphthalene) and immediately analyzed by HPLC-DAD. Experiments were run in triplicate.

Kinetics of hydrolysis of the codrug in rat plasma (*in vitro*):

Plasma from male Sprague-Dawley rats was obtained by centrifugation of blood samples at 12000 rpm for 10-15 min. The supernatant plasma fractions (2 mL) were diluted with phosphate buffer to afford a total volume of 2.5 mL (80% rat plasma). Incubations were performed at 37 ± 0.5 °C in a water-bath with constant stirring. Reactions were initiated by adding 100 μ L of the Cod-THC codrug stock solution (0.06 M in methanol) to 2.5 mL of preheated (37°C) 80% rat plasma. Aliquot-parts (100 μ L) were removed at various times, mixed with 50 μ L of the 0.01M internal standard solution (2-methoxynaphthalene in methanol) and then deproteinized by mixing with 600 μ L of acetonitrile. After centrifugation for 10 minutes at 12,000 rpm, the supernatant was separated, dried under nitrogen gas, the residue reconstituted with 300 μ L of methanol, and the resulting solution was analyzed by HPLC-DAD.

Kinetics of hydrolysis of the codrug in rat brain homogenate:

Brain homogenate obtained from male Sprague-Dawley rats was obtained by homogenizing brain tissues with 3 volumes of 1.15% KCl/g brain tissue for 2 minutes in

a tissue homogenizer. Incubations were performed at 37 ± 0.5 °C in a water-bath with constant stirring. The reactions were initiated by adding 100 μ L of the codrug stock solution (0.06 M in methanol) to 2.5 mL of preheated (37°C) brain homogenate. Aliquot-parts (100 μ L) were removed at various times, mixed with 50 μ L of the 0.01M internal standard solution (2-methoxynaphthalene in methanol) and deproteinized by mixing with 600 μ L of acetonitrile. After centrifugation for 10 minutes at 12,000 rpm, the supernatant was separated, dried under nitrogen gas, the residue reconstituted with 300 μ L of methanol, and the resulting solution analyzed by HPLC-DAD.

4.2.3 HPLC analysis

HPLC analysis was carried out with an Agilent 1100 series Quatpump, equipped with a photodiode array detector and a computer integrating apparatus. A Waters Symmetry® C₁₈ (5 μ m, 3.9 x 150 mm) column protected with guard column (Nova-Pak® C₁₈; 3.9 x 20 mm; 4 μ) was used as the stationary phase; Methanol/6mM phosphate buffer containing 0.025% heptafluorobutyric acid (HFBA) with the pH adjusted to 6.9 with triethylamine was used as mobile phase. A 1.2 mL/min flow rate was used, and UV detection was carried out at 220 nm. The 20 min time gradient program was as follows :

0-4 min: 45% Buffer

4-7 min: 45% to 7% Buffer

7-14 min: 7% Buffer

14-17 min: 7% to 45% Buffer

17-20 min: 45% Buffer

Analytes were eluted out at 4.7 min (codeine), 6.7 min (2-methoxynaphthalene), 8.4 min (Δ^9 -THC), and 12.2 min (Cod-THC codrug) using a 20 min gradient time program.

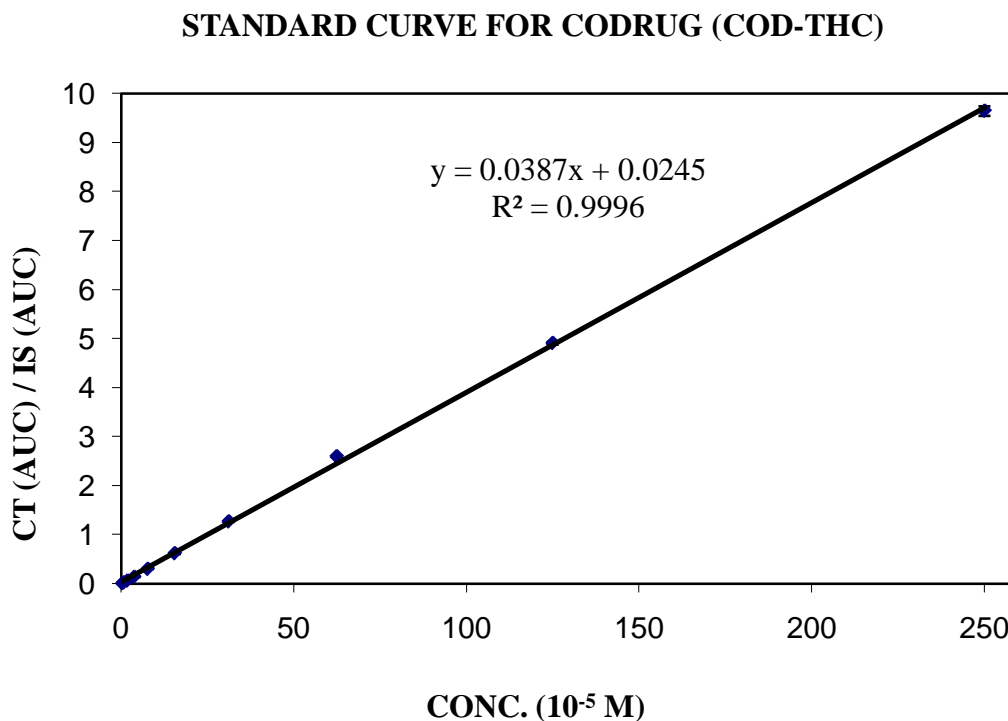
The ion-pairing agent HFBA was utilized since it afforded better resolution of analyte peaks. Ion pairing agents are ionic compounds that contain a hydrocarbon chain

that imparts hydrophobicity such that the resulting analyte ion pair can be better retained on the reversed-phase column. Ion-pairing agents are added at concentrations of between 0.01 to 0.2% w/v. Hydrophobic counter-ions such as trifluoroacetate (TFA) and heptafluorobutyrate, in addition to ion-pairing with positively charged solutes also increase the affinity of the solute for the hydrophobic stationary phase.

4.3 Results

4.3.1 Assay Validation

The calibration curves were linear over the concentration range of 4-2500 μM for Cod-THC, 5-2400 μM for Codeine and 1.0-2200 μM for Δ^9 -THC with $r^2 > 0.99$ for Cod-THC, codeine and Δ^9 -THC respectively (Fig. 4.1).



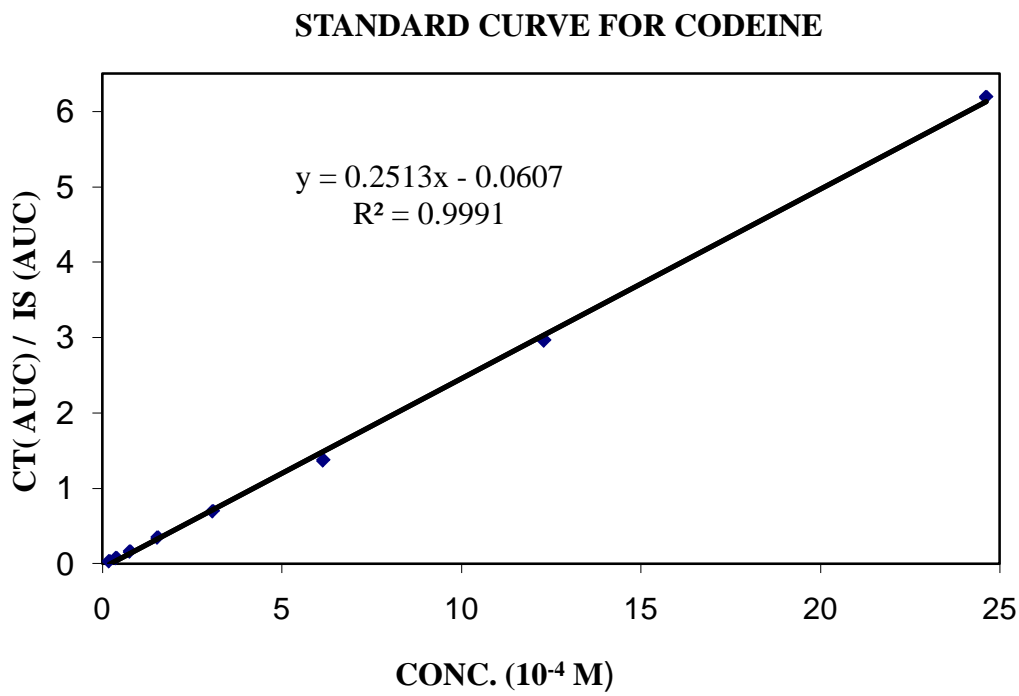
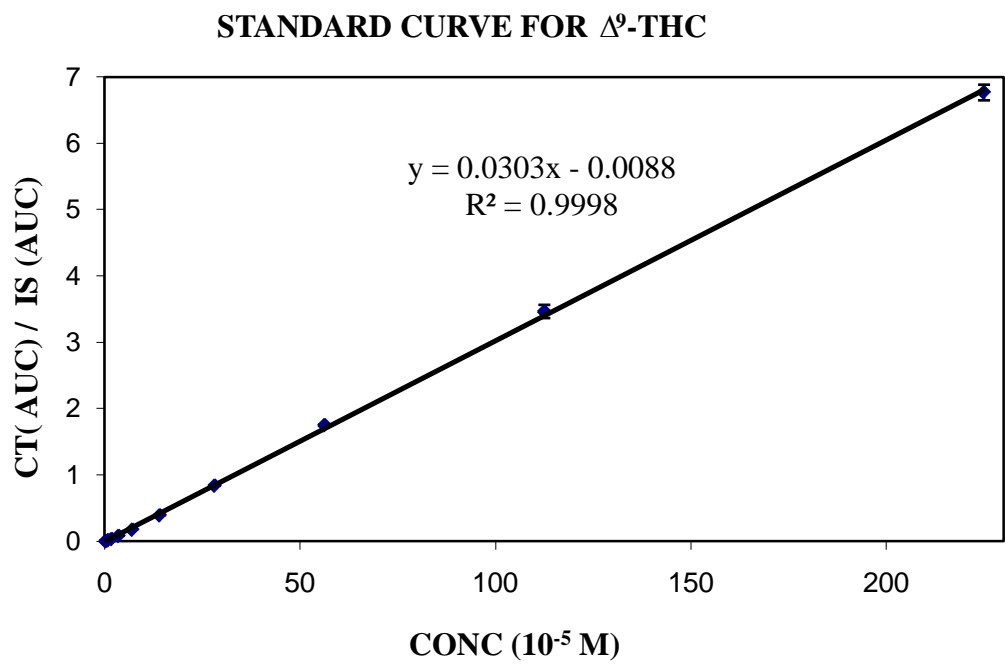


Fig. 4.1 Standard curves for Cod-THC codrug, Δ^9 -THC and codeine

4.3.2 Chemical and enzymatic stability study

Chemical and enzymatic stability studies on the Cod-THC codrug were carried out *in vitro*. Chemical hydrolysis was examined utilizing buffers at pH 1.3, 5, 7.4 and 9.7, and enzymatic hydrolysis was examined in simulated gastric fluid (SGF), simulated intestinal fluid (SIF), rat plasma and brain homogenate. Half-life values and the rate constant of the hydrolysis of the codrug in different media were obtained from slopes of semi-logarithmic plots of codrug concentrations *versus* time.

The data from the chemical hydrolysis studies at pH 1.3 and in SGF indicates that the Cod-THC codrug is stable in these media, and thus is not likely to undergo chemical or enzymatic hydrolysis in the stomach when given orally. In fact, no observable degradation of the codrug occurred in these media over 8 hours (Figs. 4.2, 4.3). Thus, the Cod-THC codrug should pass unhydrolyzed through the stomach after oral administration. Additionally, at pHs 5.0, 7.4 and in SIF, no degradation of the codrug was observed for 8 hours. Thus, the codrug should be absorbed intact from the intestine and reach the systemic circulation as a single molecular entity (Figs. 4.2, 4.3).

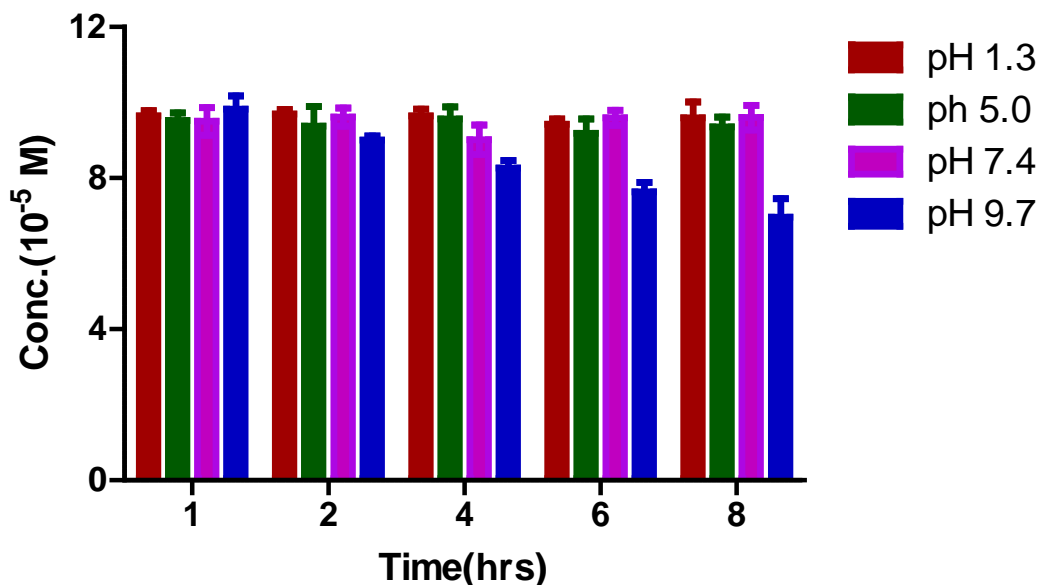


Fig. 4.2 Hydrolysis of the Cod-THC codrug at different pHs (non-enzymatic hydrolysis)

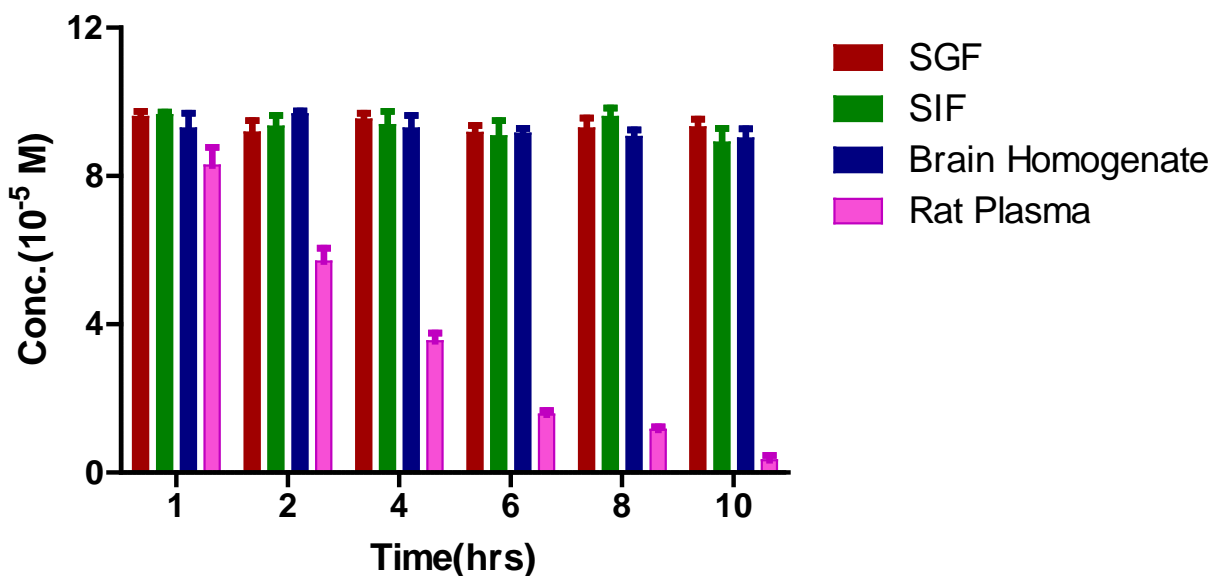


Fig. 4.3 Hydrolysis of the Cod-THC codrug in different enzymatic solutions

In rat plasma, significant hydrolysis of the Cod-THC codrug was observed and the kinetics of codrug disappearance with concomitant codeine and Δ^9 -THC appearance was determined by HPLC-DAD analysis. The disappearance of the Cod-THC codrug was correlated with pseudo first order kinetics (Figs. 4.3, 4.4). The same kinetic behavior was observed in buffer at pH 9.7 (Figs. 4.2, 4.5). Table 4.2 reports the hydrolytic rate constants and half-life values of the codrug obtained by regression analysis from slopes of semi-logarithmic plots of concentration *versus* time.

4.3.3 Stability study in brain homogenate

The stability study of the Cod-THC codrug in brain homogenate was carried out over 8 hrs and samples were analyzed by HPLC–UV assay. The data from the enzymatic hydrolysis study in brain homogenate indicates that the Cod-THC codrug is stable in brain, and thus is not likely to undergo enzymatic hydrolysis in the brain. In fact, no observable degradation of the codrug occurred over 8 hours (Fig. 4.3).

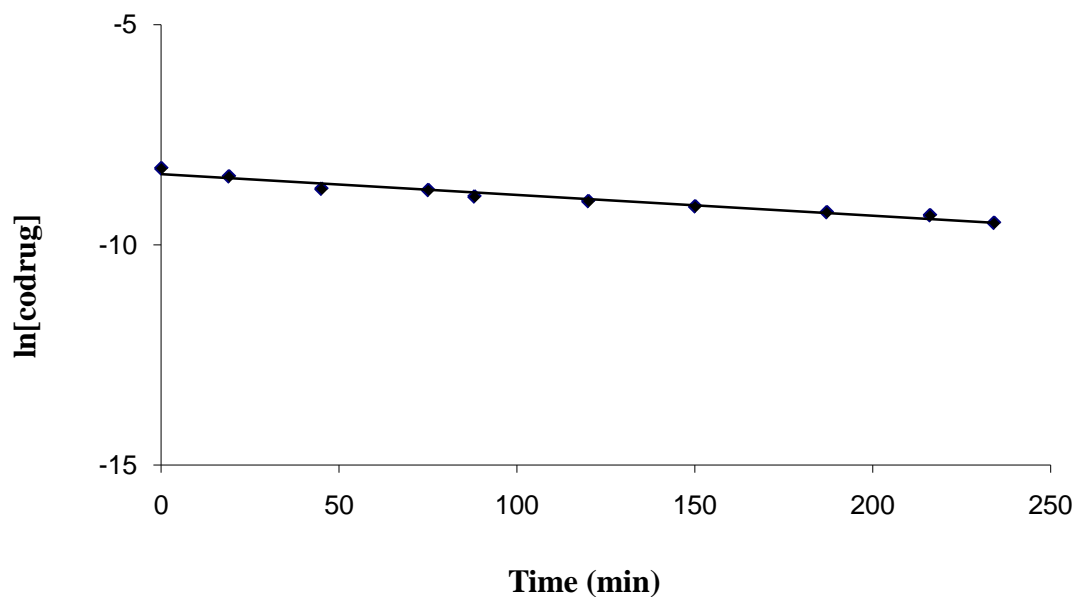


Fig. 4.4 Hydrolysis of the Cod-THC codrug in rat plasma

Table 4.1 Rate constants for the hydrolysis of the Cod-THC codrug in pH 9.7 buffer and 80% Rat plasma at 37 °C

	$t_{1/2}$ (hr)	K_{obs} (hr ⁻¹)
Rat plasma	2.46 ± 0.11	0.282 ± 0.012
pH 9.7	19.25 ± 1.21	0.036 ± 0.001

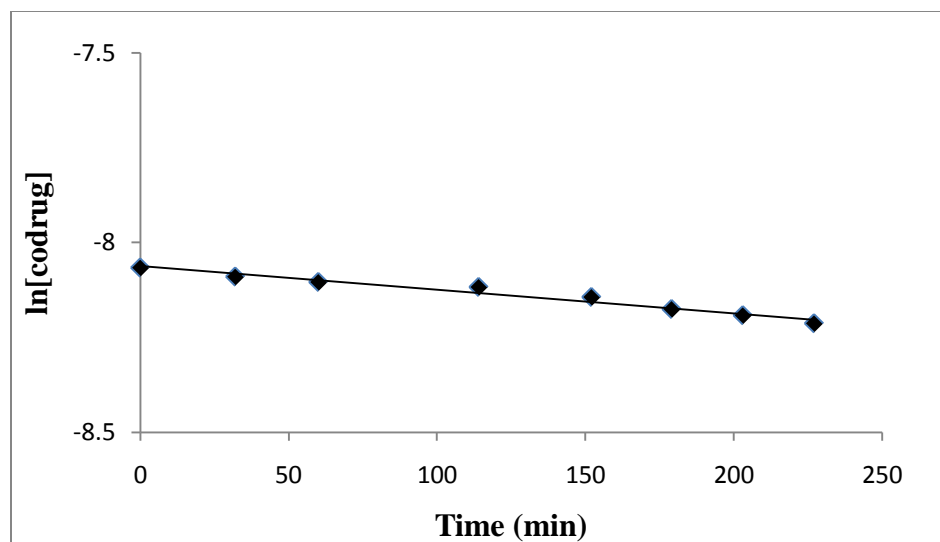


Fig. 4.5 Hydrolysis of the Cod-THC codrug at pH 9.7

Results of the comprehensive stability study of the Cod-THC codrug in different nonenzymatic aqueous buffers and biological media demonstrate that the carbonate ester linkage of the codrug is predicted to be stable in the gastrointestinal tract when the codrug is administered orally. Hydrolysis of the carbonate ester linkage in 80% rat plasma showed that the codrug is hydrolysed and generates the parent drugs, suggesting that after oral administration, and absorption from the gastrointestinal tract the codrug will generate both parent drugs in the systemic circulation. Linker design in codrug synthesis has to be carried out in a thoughtful way such that the linker is not too chemically labile or too stable. Codrugs with labile linkers will not survive the harsh conditions of the gastrointestinal tract, and thus will hydrolyze in the gastrointestinal tract before the codrug reaches the systemic circulation. Codrugs with very stable linkers may reach the systemic circulation, but may not be capable of generating the parent drugs in the plasma. Thus the choice of a carbonate ester linkage linking the allylic hydroxyl group of codeine and the phenolic group of Δ^9 -THC was found to be an ideal codrug linker design for oral administration. The stability of the Cod-THC codrug in rat brain homogenate indicates that the enzymes present in rat brain homogenate are incapable of cleaving the codrug into the parent drugs. This study predicts that any codrug entering the brain from the systemic circulation will not be transformed into the parent drugs. Thus, if

oral administration of the codrug to rats results in the presence of the parent drug molecules in brain, then these parent drugs must have entered the brain as the individual parent drug molecules from the systemic circulation, and did not originate through hydrolysis of the codrug in the brain.

Chapter 5

Pharmacokinetic Analysis of Cod-THC Codrug

5.1 Introduction

Pharmacokinetics is the study of the time course of a drug concentration in different body compartments such as plasma, blood, urine, cerebrospinal fluid, and tissues, and incorporates the processes of absorption, distribution, metabolism and excretion (ADME) after a specific route of administration of a drug (Smith et al., 2001).

The drug can enter the body in a variety of ways which have already been discussed in detail in Chapter 1. Drugs are mostly given orally for reasons of convenience and patient compliance. If the drug has been given orally, then it first enters the gastrointestinal tract, and gets absorbed through the gastrointestinal mucosal wall into the bloodstream. It is then shunted via the portal vein through the liver, where the “first pass effect” takes place, and then reaches the systemic circulation. The first-pass effect is a phenomenon of drug metabolism whereby the concentration of a drug is greatly reduced before it reaches the systemic circulation. It is the fraction of lost drug during the process of absorption which mainly takes place in liver and gut wall. Therefore, the oral administration of a drug involves an additional absorption step. The percentage of the administered dose reaching the circulation as the free drug is termed the bioavailability of the drug. The drug then gets distributed to various tissues and organs in the body. The extent of this distribution depends on the structural and physicochemical properties of the drug. Some drugs may enter the brain and the central nervous system by crossing the blood–brain barrier. Finally, the drug will bind to its molecular target, for example, a receptor or an ion channel, and exert its desired action. If the drug is injected directly into the bloodstream (e.g. by the intravenous route), then it is 100% available for distribution to the tissues. But if it is given orally, then its bioavailability will usually be less than 100% (Smith et al., 2001).

Once the drug is in the bloodstream, a portion of it is available to illicit its pharmacodynamic effect; the rest may bind to plasma proteins in an inactive reversible

protein-drug complex. Binding to plasma proteins is sometimes advantageous since the drug is continuously released from the protein-drug complex and this can result in a prolonged drug action (Smith et al., 2001). The unbound drug follows the concentration gradient and gets distributed into the peripheral tissues. These tissues contain specific or non-specific binding sites. The non-specific binding sites can act as reservoirs for the drug. This “total volume of distribution” determines the equilibrium concentration of drug after administration of a specific dose.

Pharmacokinetic parameters are derived from the measurement of drug concentrations in blood or plasma after administration. The key pharmacokinetic parameters are Volume of Distribution (V_d), Clearance (Cl), Absorption, Half-life ($t_{1/2}$) and Oral Bioavailability (F). Their importance for the dose regimen and dose size is shown in Fig. 5.1 (van de Waterbeemd and Gifford, 2003).

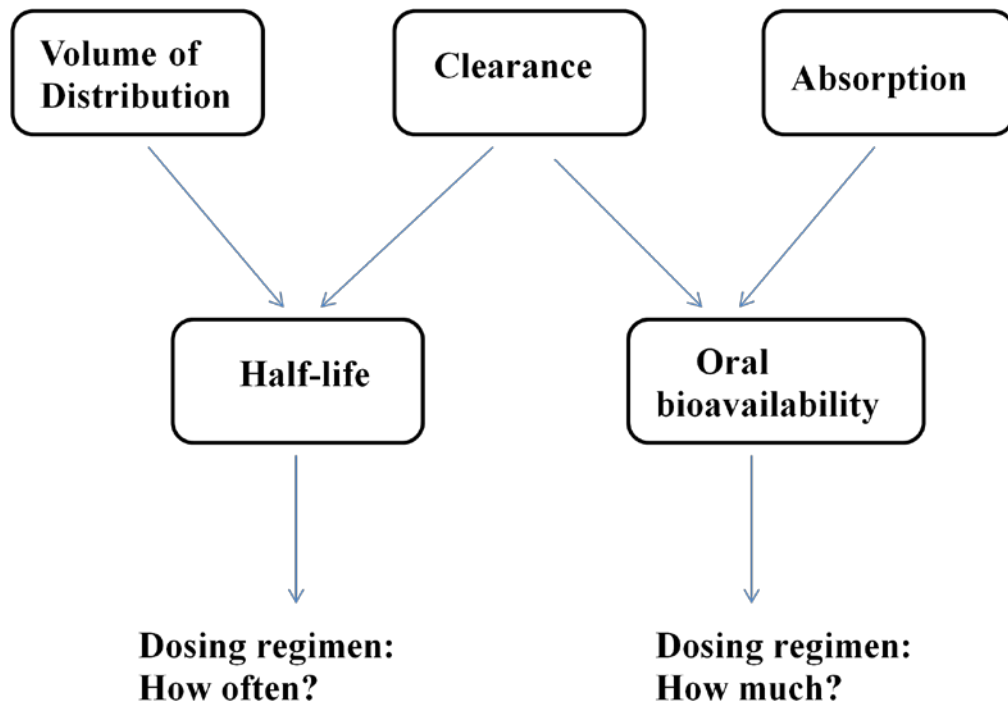


Fig. 5.1 Pharmacokinetic Parameters and their importance for dose regimen and dose size

Volume of Distribution (V_d) -- Volume of Distribution is defined as the apparent space or volume into which a drug distributes. It is a theoretical concept that connects the

administered dose with the actual initial concentration (C_0) present in the systemic circulation. If the drug is highly lipophilic in nature, then the drug will have a high volume of distribution, because the drug specifically or non-specifically binds to tissues and stays there.

$$V_d = \text{Dose}/C_0$$

Clearance (Cl) --Clearance of a drug from the body mainly takes place via the liver (hepatic clearance or metabolism, and biliary excretion) and the kidney (renal excretion).

By plotting the plasma concentration against time, the area under the curve (AUC) relates to dose, bioavailability (F) and clearance.

$$\text{AUC} = F \times \text{Dose}/\text{Cl}$$

Half-life ($t_{1/2}$) --Half-life is the time taken for the drug concentration in the plasma to be reduced by 50%. It is a function of the clearance and volume of distribution, and determines how often a drug needs to be administered.

$$t_{1/2} = 0.693 V_d/\text{Cl}$$

Intravenous (IV) bolus dosing (i.e, the entire drug dose is given as a rapid injection) captures the pure distribution and elimination processes.

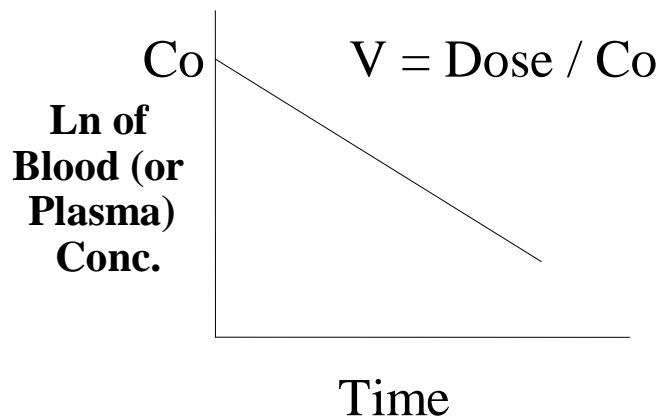


Fig. 5.2 Concentration *versus* time curve

In the “first pass effect” the liver metabolizes the drug into active or inactive metabolites, which can then be more easily excreted. Prodrugs are inactive chemical entities that get activated only after they are metabolized to the active drug. This is often a strategy utilized to improve pharmacokinetic properties and drug ability. Some drugs are excreted in the bile and eventually may pass out of the body in the feces, while some are filtered by kidney, where a portion undergoes reabsorption, with the remainder being excreted in the urine. Smaller amount of drugs are excreted in the tears, breast milk and sweat.

5.1.1 Pharmacokinetic profile of Codeine and Δ^9 -THC

There is a continuing need for novel analgesic medications that are able to provide high efficacy pain relief while providing more favorable pharmacokinetics and a reduction in undesirable side-effects. Several reports indicate the low bioavailability (2 to 6%) of Δ^9 -THC after oral administration in rats due to poor absorption. Δ^9 -THC is also biotransformed by the cytochrome P450 enzymes CYP 3A4, CYP 2C9 and CYP 2C11 to 11-hydroxy- Δ^9 -THC, which contributes to its psychotropic activity, and to the 11-nor-9-carboxy-THC glucuronide conjugate, an inactive major urinary metabolite (Gustafson et al., 2004; McGilveray, 2005). Codeine is mainly metabolized in liver. Approximately 50-70% of codeine is converted to codeine-6-glucuronide by UGT2B7 and approximately 10-15% of codeine is N-demethylated to norcodeine by CYP3A4 (Thorn, 2009). Codeine-6-glucuronide also binds to the mu opioid receptor similar to codeine.

Approximately 10-15% of codeine is N-demethylated to norcodeine by CYP3A4 (Thorn, 2009). Norcodeine and Codeine-6-glucuronide both have the affinity for the mu opioid receptor similar to codeine. Approximately 0-15% of codeine is O-demethylated by CYP2D6 to morphine, the most active metabolite, which has 200 fold greater affinity for the mu opioid receptor compared to codeine (Thorn, 2009).

Enhancement of the antinociceptive effect of opioids with cannabinoids has been previously described in literature (Cichewecz et al, 1999; Cichewecz et al, 2001; Cichewecz and McCarthy 2002; Cichewecz and Welch 2003; Cox et al., 2007; Smith et al., 2007; Smith et al., 1998; Welch and Eads, 1999; Williams et al., 2008)). These opioid and cannabinoid drugs work via opioid and cannabinoid receptors, which are found throughout the central and peripheral nervous system. In addition, these two classes of drugs produce similar effects on calcium levels and cyclic AMP accumulation through G protein-mediated pathways. However, appropriate combination dosing of these active agents to afford concentrations of both drugs at the site of action, e.g., the brain or spinal column, can be difficult because of their very different physico-chemical and pharmacokinetic properties. Therefore, there is a need to devise a way of administering opioids and cannabinoids concomitantly to provide a more favorable pharmacokinetic profile that will promote optimal synergism. The analytical study of a Cod-THC Codrug designed for this purpose has demonstrated chemical stability in gastrointestinal tract and susceptibility to hydrolysis in rat plasma to the parent drugs, codeine and Δ^9 -THC (Chapter 3). To compare the pharmacokinetic profile of the Cod-THC codrug with those of the parent drugs (both individually and as a 1:1 physical mixture) after oral administration physical mixture, following studies were carried out:

- ❖ To determine the pharmacokinetics of Cod-THC codrug at three different doses (5, 10, 20 mg/kg) and to determine the pharmacokinetics codeine, and Δ^9 -THC after oral administration of an equimolar physical mixture dose (4.9 mg/kg codeine + 5.1 mg/kg Δ^9 -THC) of the two parent drugs in the rat.
- ❖ To evaluate the relative ability of the Cod-THC codrug (10 mg/kg dose) and a 1:1 physical mixture of codeine and Δ^9 -THC (4.9 mg/kg codeine + 5.1 mg/kg Δ^9 -

THC) to deliver codeine and Δ^9 -THC to the plasma and brain after oral administration in the rat.

5.2 Materials and Methods

5.2.1 Chemicals and reagents

The Cod-THC codrug and Δ^9 -THC were synthesized in the laboratory (see Chapter 2 for details). The chemicals used in this study were of HPLC grade or equivalent quality. Acetonitrile and potassium chloride were obtained from Thermo Fisher Scientific (Pittsburgh, PA). Heparin sodium injection, 10,000 USP units/ml, was purchased from Baxter Healthcare Corporation (Deerfield, IL). Nembutal sodium (pentobarbital sodium injection, USP) was obtained from Abbott Laboratories (North Chicago, IL).

5.2.2 Animals

All procedures involving animals were performed in compliance with the guidelines of the University of Kentucky Institutional Animal Care and Use Committee established by the National Institutes of Health's *Guide for the Care and Use of Laboratory Animals* (1996). Male Sprague-Dawley rats (200–250 g) were obtained from Harlan (Indianapolis, IN) and housed two per cage with ad libitum access to food and water in the Division of Laboratory Animal Resources at the University of Kentucky College of Pharmacy. Body weights at the time of dosing were 300–360 g. Rats were anesthetized with pentobarbital (40 mg/kg i.p.) and surgically implanted with jugular and femoral vein cannulas for i.v. drug dosing and blood sampling, respectively. For the first 3 to 4 days after surgery, the rats were observed for signs of infection at the surgical sites, yellowing of hair and hair texture, presence of blood around the eyes or nose, indications of loss of appetite, and decreased or absent fecal activity before the start of i.v. dosing.

5.2.3 Instrumentation

Samples were analyzed for analyte-specific (640.359 m/z to 282.261 m/z, Cod-THC; 315.2 m/z to 193.1 m/z, Δ^9 -THC; 300.2 m/z to 215.2 m/z, codeine; 286 m/z to 201 m/z morphine) and internal standard-specific (342.4 m/z to 324.2 m/z, naltrexone) transitions by LC/MS/MS utilizing reverse-phase chromatography and positive-mode ionization. The instrumentation consisted of a Varian LC system (ProStar 210 pumps, Prostar 410 autoinjector) connected through an ESI source to a Varian 1200L triple quadrupole mass spectrometer with all components controlled by a Varian MS Workstation version 6.42. Individual analyte-dependent ESI-(+)-MS/MS parameters were optimized for signal intensity.

5.2.4 HPLC and mass spectrometric conditions

Individual analyte-dependent ESI-(+)-MS/MS parameters were optimized for signal intensity. These optimized parameters were subsequently used in the analysis of biological samples (CE = 32, 19, 20.5, 16.5, 10.2V for Cod-THC, Δ^9 -THC, codeine, morphine and naltrexone, respectively). Briefly, 10 μ L of the biological sample was injected onto a guard column protected (Nova-Pak® C₁₈; 3.9 x 20 mm; 4 μ) Nova-Pak® C₁₈ analytical column (3.9 x 150 mm; 4 μ m). Analytes were eluted at 8.09 min (morphine), 10.02 min (codeine), 10.22 min (naltrexone), 14.33 min (Cod-THC), and 21.37 min (Δ^9 -THC) using water: acetonitrile (82:18, containing 0.04 % HFBA) (Solvent A): acetonitrile (Solvent B) gradient and a 0.3 mL/min flow rate. The 33 min gradient program began with 97:3 Solvents A: B for 3 min followed by a 5.3 min linear ramp to 5:95 solvents A: B. This percentage was held constant for 14 min, and then returned to 97:3 solvents A:B over a 3 min linear ramp; it was then held at 97:3 solvents A:B for an additional 6 min. Argon was used as a collision gas at 2.0 m Torr, and nitrogen used as a drying gas at 300 °C. The needle voltage was 5000V, the shield voltage was 600V, and the capillary voltage was 40V. Independent plasma and brain calibration curves for Cod-THC, codeine, morphine and Δ^9 -THC were generated from plots of analyte concentration and analyte: naltrexone peak area ratios.

5.2.5 Plasma Pharmacokinetics

Cod-THC codrug solution was prepared in 15% PEG-400 solution in saline and filtered through a 0.2- μ m filter. Groups of rats (n=3) were then injected with either 5, 10, 20 mg/kg *p.o.* or 1 mg/kg *i.v.* via the jugular vein. Doses and route of administration were chosen on the bases of studies evaluating the analgesic effect of Cod-THC codrug. Blood samples (0.2 mL) were obtained at 1, 5, 10, 15, 30, 45, 60, 120, 180 min after *i.v.* dosing and at 15 min, 30 min, 1, 2, 4, 5, 7 and 8 hrs after oral dosing. The withdrawn blood was replaced with heparinized saline (0.2 mL). Blood samples were centrifuged at 1200 g for 15 min, and the plasma was separated. The separated plasma was frozen immediately on dry-ice and stored at -80°C prior to analysis. To compare the pharmacokinetics of the codrug with an equimolar physical mixture, 4.9 mg/kg of codeine and 5.1 mg/kg of Δ^9 -THC were mixed together and administered orally to rats. This dose of physical mixture was chosen based on the same molar proportion of codeine and Δ^9 -THC in the 10 mg/kg codrug dose.

5.2.6 Standard Curve and Quality Control Validation Solutions

Stock solutions of Cod-THC, codeine, Δ^9 -THC and internal standard (naltrexone) were prepared in methanol. Two stock solutions were prepared; one for generating the standard curve, and a second one for quality control (QC) and method validation. A standard curve with eight points was prepared for the analysis of unknown samples. Standard curve samples were prepared by spiking blank plasma with Cod-THC, codeine, or Δ^9 -THC working solutions. Calibration curves were obtained using quadratic least-squares regression of AUC ratio (analyte peak AUC/internal standard peak AUC) *versus* drug concentrations. The amount of codrug, or parent drug, was then determined. Three quality control samples with different concentrations were prepared to check the sensitivity of the instrument. The three concentrations chosen were: one towards the higher end of the standard curve concentrations, one towards the middle, and the third one towards the lower end of the standard curve concentrations. Standard curves for

analyzing brain samples were constructed in a similar way using brain homogenate. In brain homogenate, a morphine standard curve was also generated.

5.2.7 Extraction procedure

To isolate Cod-THC, codeine, and Δ^9 -THC from plasma or brain samples, 50 μ L of plasma/brain tissue was transferred to polypropylene tubes to which 10 μ l of working internal standard solution was added followed by vortexing for 1 min. The samples were then centrifuged for 15 min at 8000 rpm. The supernatant was transferred into silylated micro-serts and evaporated to dryness under nitrogen gas at 37°C. Following drying, the residue was dissolved in 80 μ l of mobile phase by vortexing for 1min; 10 μ l of the sample was then injected into the LC-MS/MS unit.

5.2.8 Brain Uptake Study

Studies were performed to determine the concentration of codrug/parent drugs present in brain after oral doses of 10 and 20 mg/kg of Cod-THC codrug. These doses were chosen based on their assessment in the tail-flick pain model. Cod-THC codrug solution was prepared in 15% PEG-400 solution in saline and filtered through a 0.2- μ m filter. Noncatheterized male Sprague-Dawley rats (300-360) were assigned randomly to one of five time points ($n=3$ per group) for the 10 mg/kg Cod-THC codrug dose and to one of two time points ($n=3$ per group) for the 20 mg/kg dose. Individual rats were euthanized at 0.5, 1, 1.5, 2, 2.5 hrs after p.o. administration of the 10 mg/kg Cod-THC codrug and at 2 and 2.5 hrs after p.o. administration of the 20 mg/kg Cod-THC codrug. The brain was quickly removed, cleaned of surrounding tissue and veins, washed, weighed, and homogenized (3 volumes of 1.15% KCl/g brain tissue) for 2 min in a tissue homogenizer (Bio-Homogenizer M133/1281-0; Biospec Products, Inc., Barlesville, OK). Brain homogenate (4 ml) was mixed with an equal volume of acetonitrile and centrifuged at 1200g and 37°C for 5 min. The supernatant was separated and evaporated to dryness under a stream of nitrogen. The residue was reconstituted in 80 μ L of HPLC mobile phase. After decapitation, blood from the trunk of each rat at the time of euthanasia was

also collected and centrifuged at 1200g and 37°C for 5 min to obtain matching brain/plasma samples. The plasma samples (50 µL ml) were extracted with 6 volumes of acetonitrile and centrifuged at 1200 g for 15 min at 37°C. The supernatant was separated and evaporated to dryness under a stream of nitrogen, and the resulting residue was reconstituted with 80 µL of mobile phase. The same protocol was followed for the physical mixture of codeine and Δ^9 -THC. To compare with the 10 mg/kg Cod-THC codrug dose, 4.9 mg/kg of codeine and 5.1 mg/kg of Δ^9 -THC was utilized as a physical mixture. Again, the time-concentration curve for this physical mixture was generated in a similar way to that for the codrug.

5.2.9 Assay Validation

Blank plasma samples were extracted and analyzed by reverse phase HPLC for potential interfering peaks within the range of the retention time for Cod-THC, codeine, morphine, Δ^9 -THC and the internal standard, naltrexone. The extraction efficiency was determined by spiking Cod-THC, codeine, and Δ^9 -THC at concentrations of 25 and 100 ng/ml into blank plasma, and comparing peak AUCs of the extracted and unextracted standards at the same concentrations. This was done to find the difference between the concentrations of extracted and unextracted samples.

5.2.10 Pharmacokinetic Analysis

The plasma pharmacokinetic parameters for the Cod-THC codrug in the rat were determined after both p.o. and i.v. administration. Data were analyzed with a standard noncompartmental model using the program WinNonlin Professional (version 5.2; Pharsight Corporation, Mountain View, CA). Both C_{\max} and T_{\max} were determined. The AUC_{0-t} for the plasma concentration-time profile was determined using the linear-trapezoidal method (Whittaker and Robinson, 1967). $AUC_{0-\infty}$ was calculated as $AUC_{0-t} + C_t/k$, where C_t is the last measurable concentration of drug. The terminal half-life ($t_{1/2}$) was calculated by dividing 0.693 by the terminal rate constant (k) obtained from the fitted concentration-time data.

5.3 Results

Morphine, codeine, naltrexone, Δ^9 -THC, and the Cod-THC codrug chromatograms are shown in Fig. 5.3. Morphine had the lowest retention time (8.09 min) followed by codeine (10.02 min), naltrexone (10.22 min), Cod-THC (14.33 min) and Δ^9 -THC (21.37 min).

5.3.1 Assay Validation

The calibration curves for the Cod-THC codrug were linear over the concentration range of 0.67-343.04 ng/mL, and for codeine and Δ^9 -THC were linear over the concentration range 1.45-371.2 ng/mL and 1.45-371.2 ng/mL, respectively, in rat plasma, with correlation coefficients r^2 of > 0.99 for Cod-THC, codeine and Δ^9 -THC (Fig. 5.4). The LLOQ was established at 0.67, 1.45 and 1.45 ng/mL for Cod-THC codrug, codeine and Δ^9 -THC, respectively.

Chromatogram Plots

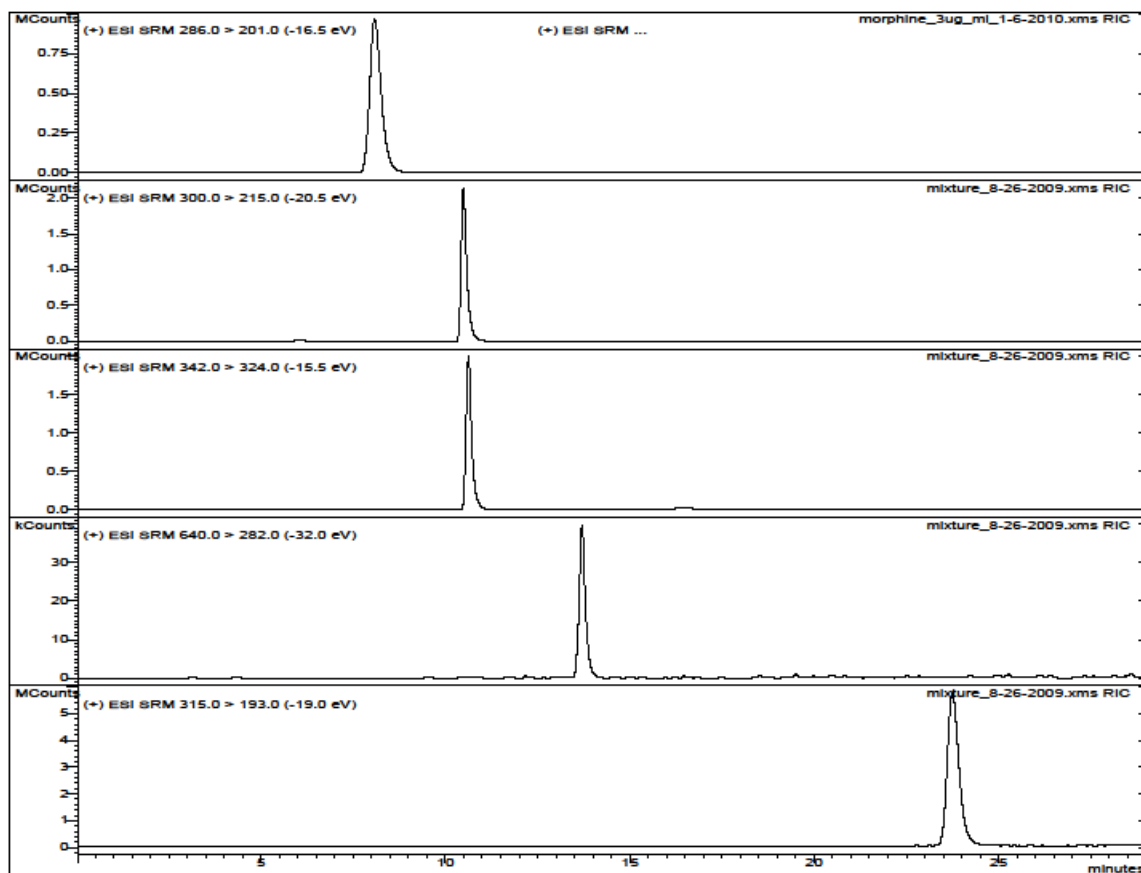
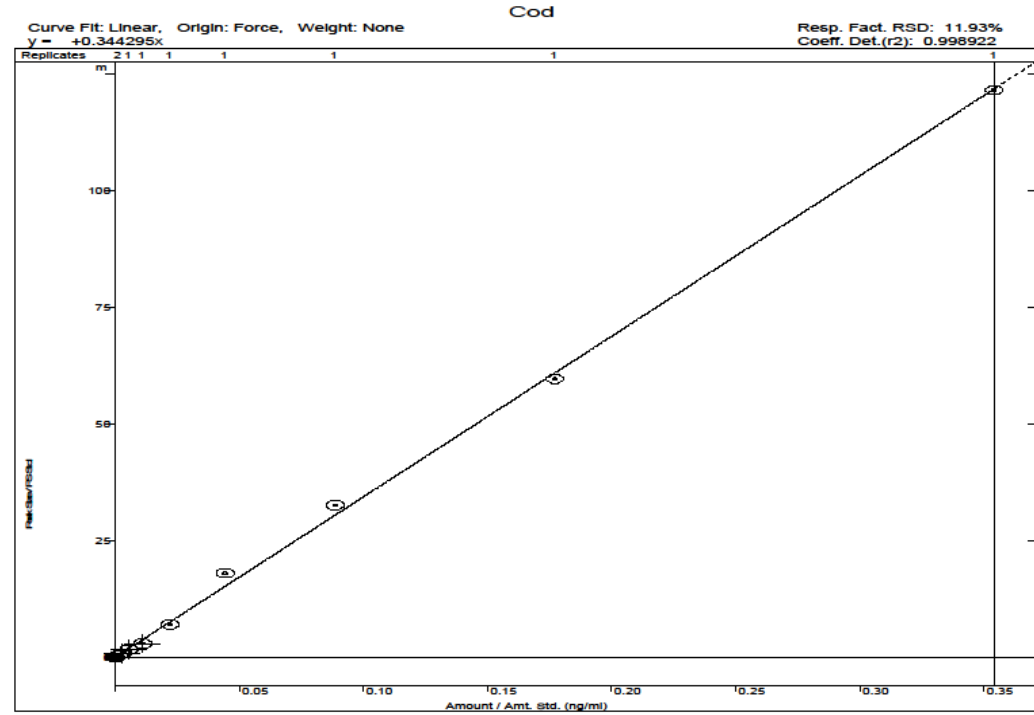


Fig. 5.3 Morphine, codeine, naltrexone, Cod-THC codrug and Δ^9 -THC Chromatograms

Print Date: 16 Jan 2010 13:37:52

Calibration Curve Report

File: c:\varian\ms\methods\harpreet\cod_the_plasma_hd_091609.mth
Detector: 1200 Mass Spec, Address: 42

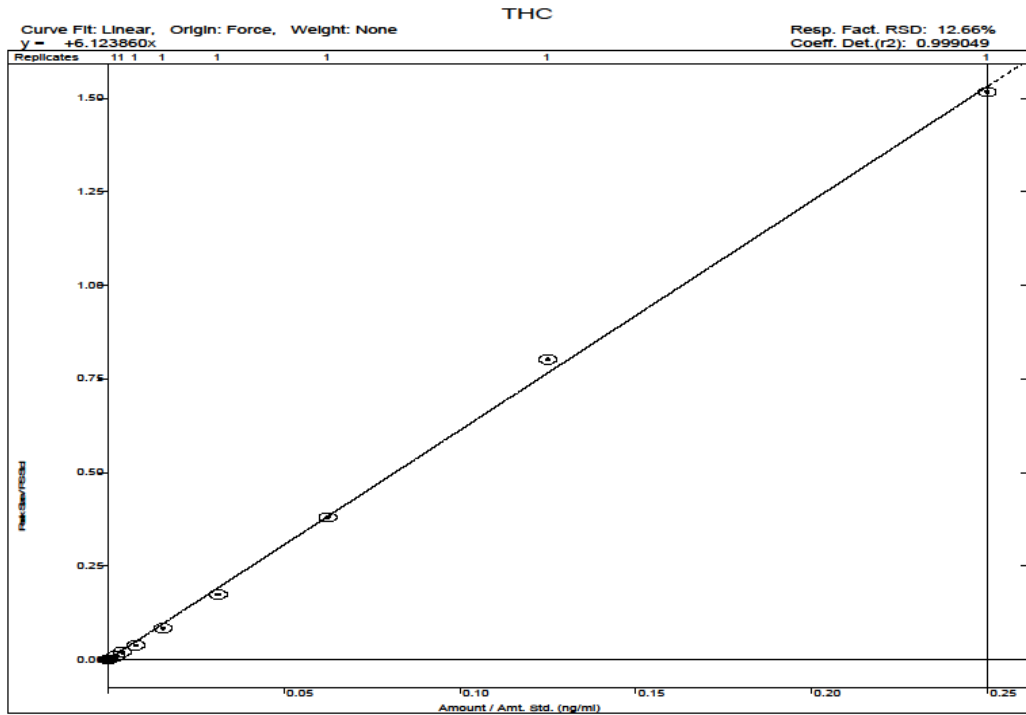


(a)

Print Date: 16 Jan 2010 13:38:55

Calibration Curve Report

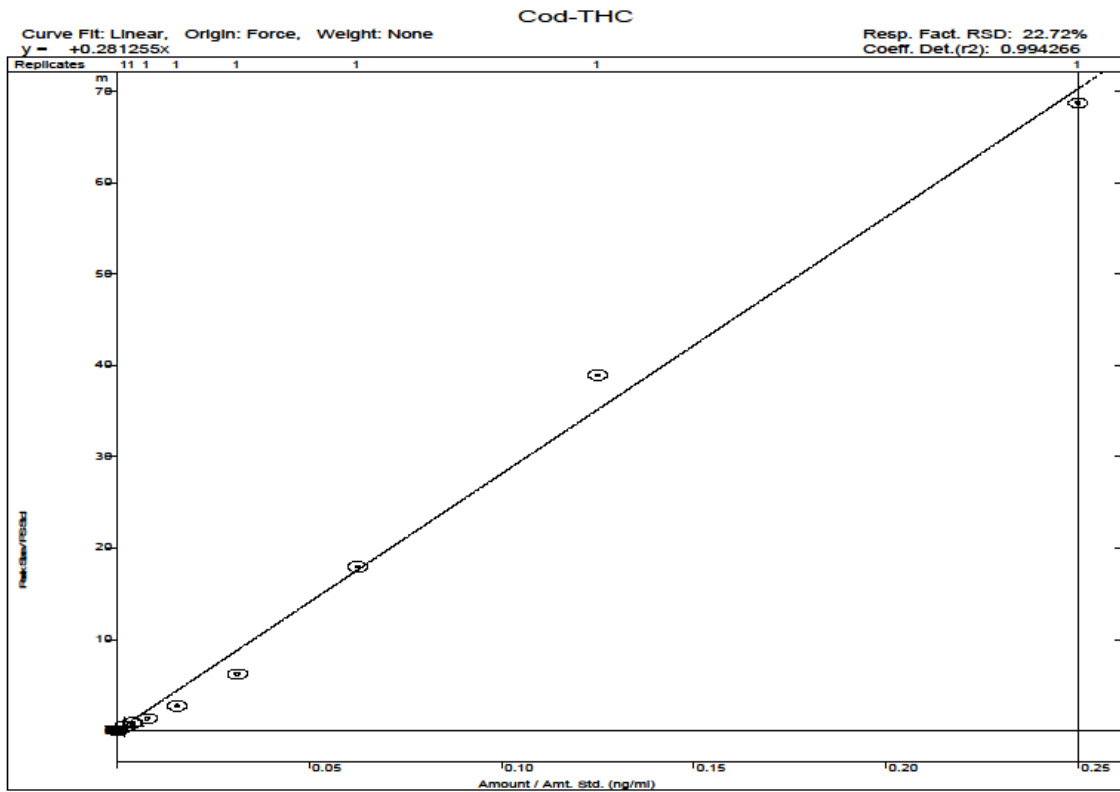
File: c:\varian\ms\methods\harpreet\cod_the_plasma_hd_091609.mth
Detector: 1200 Mass Spec, Address: 42



(b)

Calibration Curve Report

File: c:\varian\msd\methods\harpreet\cod_thc_plasma_hd_091609.mth
 Detector: 1200 Mass Spec, Address: 42



(c)

Fig. 5.4 Calibration curves for codeine (a), Δ^9 -THC (b) and Cod-THC codrug (c) in rat plasma

The calibration curves for Cod-THC, codeine, Δ^9 -THC and morphine were generated in rat plasma (from trunk blood) and also in rat brain homogenate (Figs. 5.5, 5.6). At the time of the brain homogenate study, the calibration curves for plasma (from trunk blood) were generated again to compare the concentration of the parent drugs in brain and plasma. The calibration curves generated in brain homogenate were linear over the concentration range 0.52-266.2 ng/mL for the Cod-THC codrug, linear over the concentration range 0.61-312.3 ng/mL for codeine, and linear over the concentration range 0.86-440.3 ng/mL for Δ^9 -THC and 6.13-196.2 ng/mL for morphine in rat plasma, with correlation coefficients $r^2 > 0.99$ for Cod-THC, codeine, Δ^9 -THC and morphine (Fig. 5.4). Fig. 5.7 shows the three chromatograms of morphine with three different

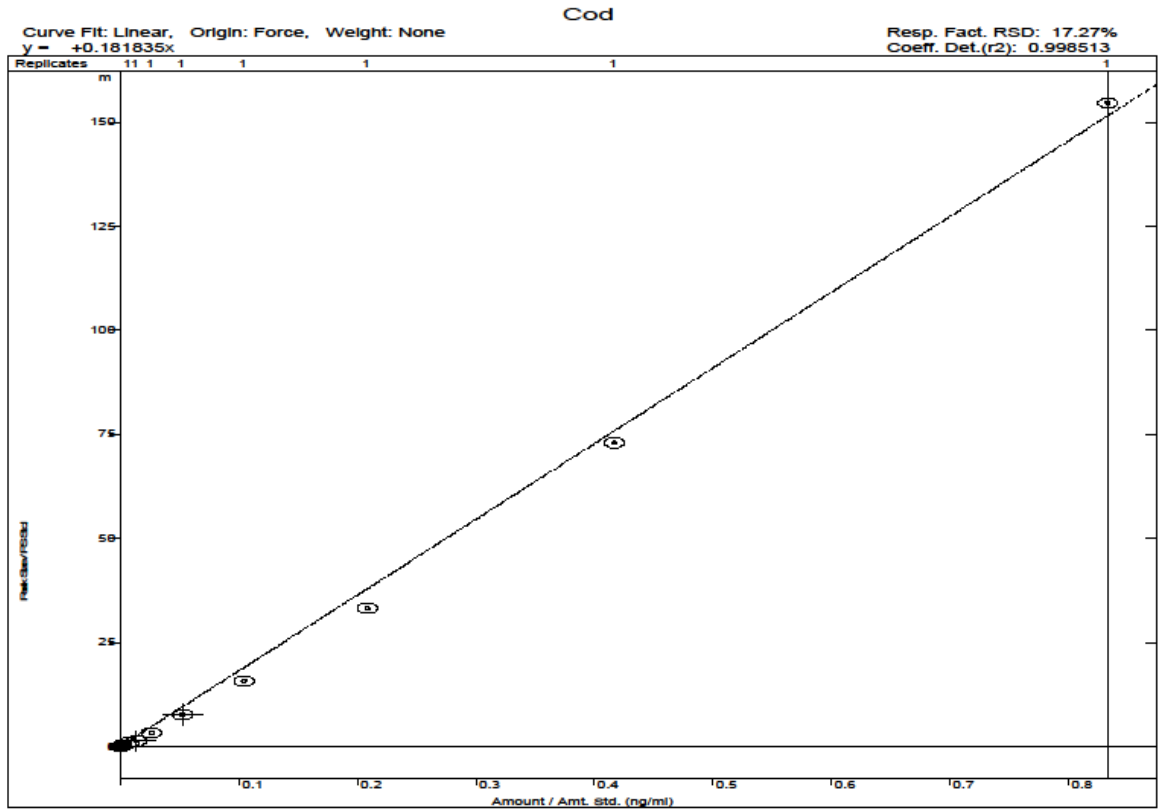
concentrations (3000, 300 and 3 ng/mL). The morphine peak was detectable only up to 3 ng/mL.

Print Date: 16 Jan 2010 13:32:11

Calibration Curve Report

File: ...arianws\methods\harpreet\cod_thc_morph_plasma_trunk_hd_121609.mth

Detector: 1200 Mass Spec, Address: 42

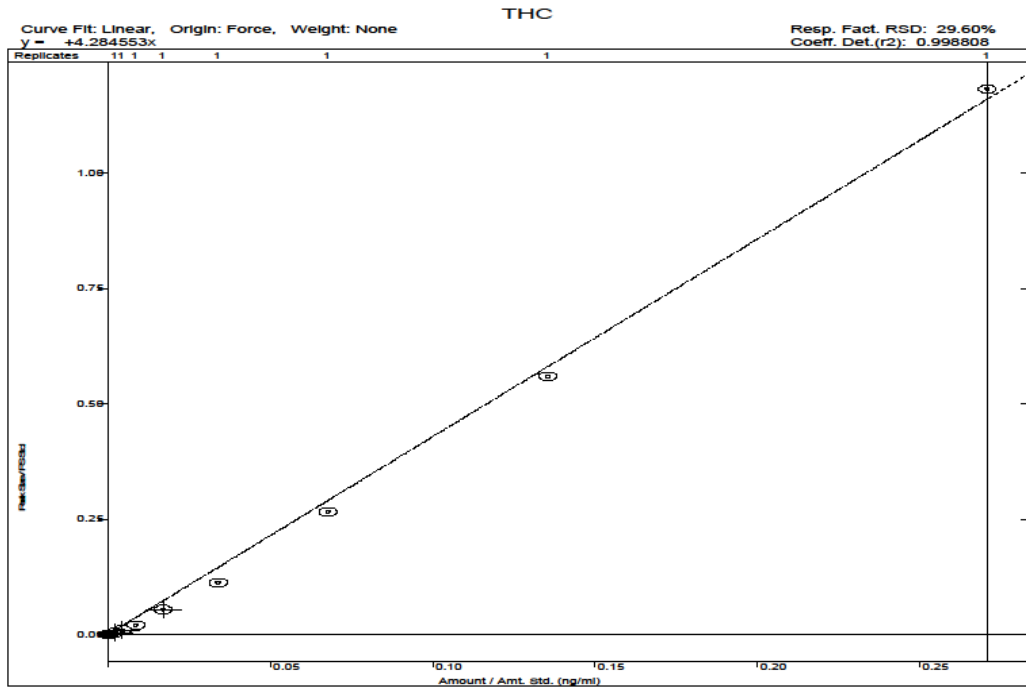


(a)

Print Date: 16 Jan 2010 13:30:17

Calibration Curve Report

File: c:\varian\ms\methods\harpreet\cod_thc_plasma_trunk_hd_092209.mth
Detector: 1200 Mass Spec, Address: 42

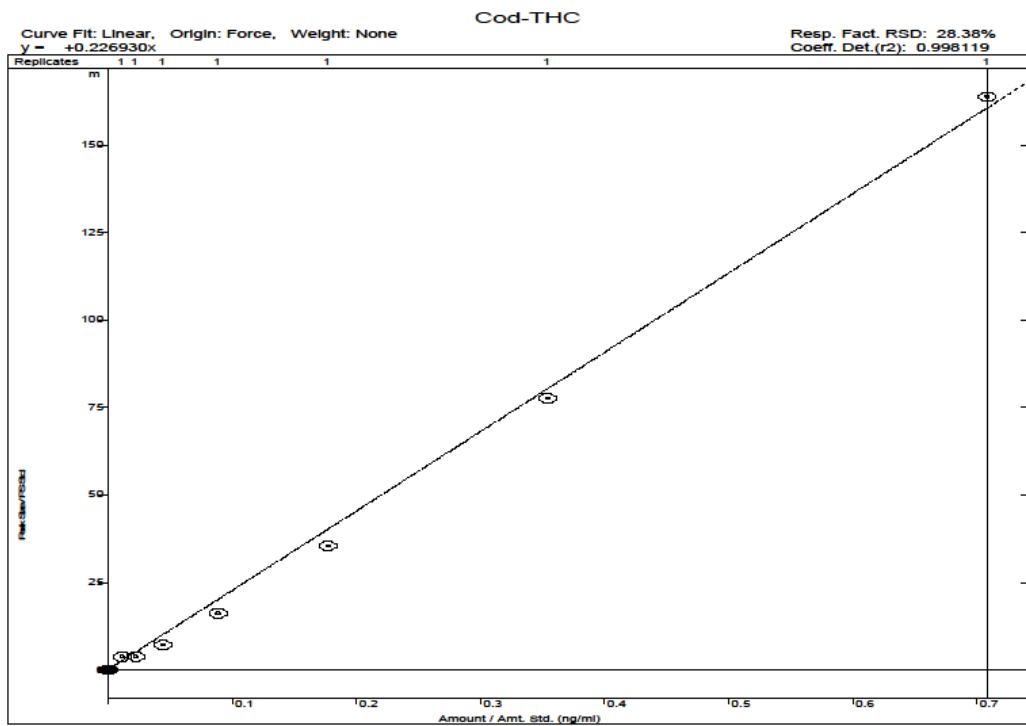


(b)

Print Date: 16 Jan 2010 13:32:30

Calibration Curve Report

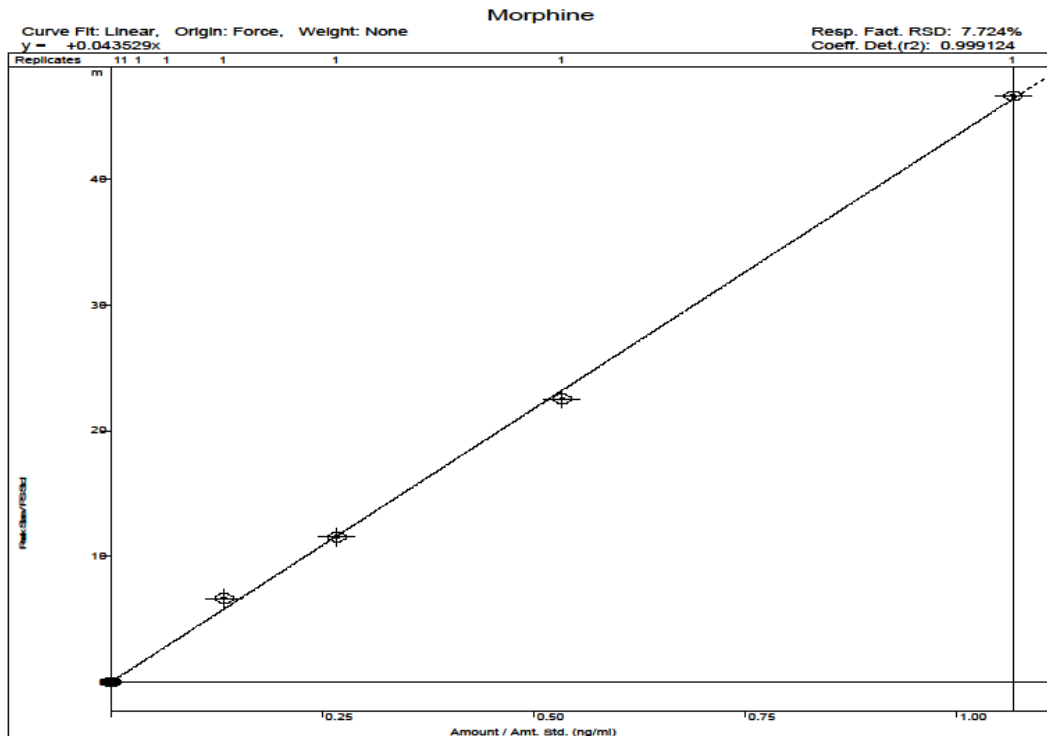
File: ...arian\ms\methods\harpreet\cod_thc_morph_plasma_trunk_hd_121609.mth
Detector: 1200 Mass Spec, Address: 42



(c)

Calibration Curve Report

File: ...arianws\methods\harpreet\cod_thc_morph_plasma_trunk_hd_121609.mth
 Detector: 1200 Mass Spec, Address: 42



(d)

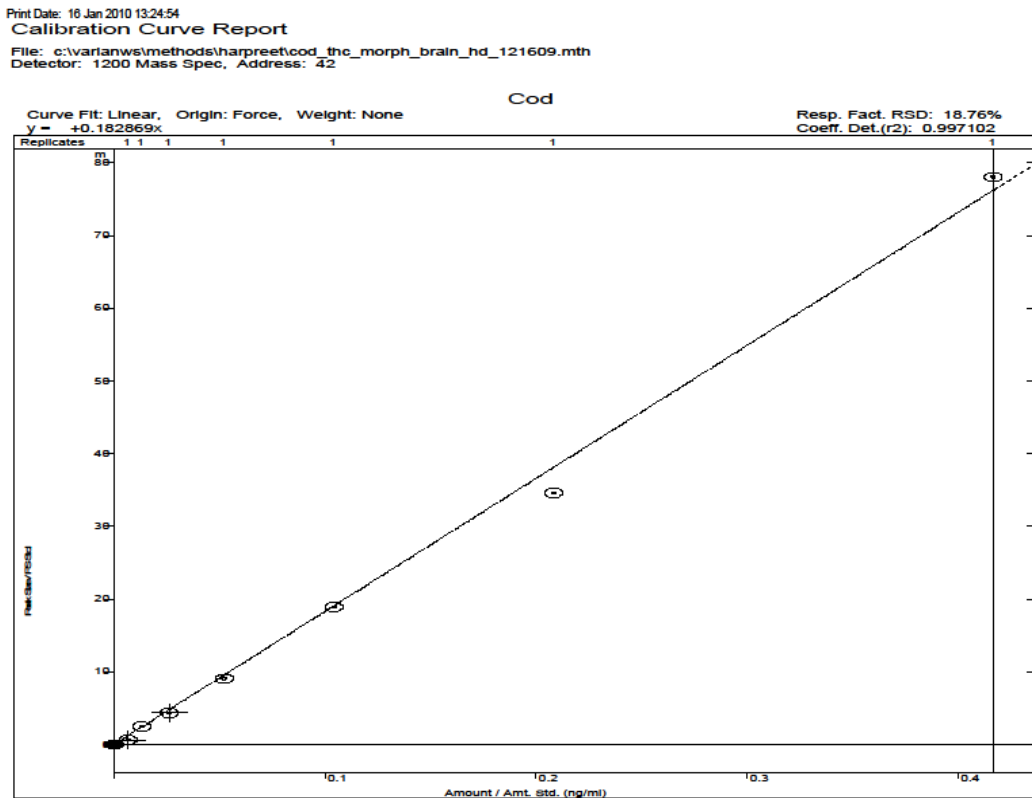
Fig. 5.5 Calibration Curves for codeine (a), Δ^9 -THC (b), Cod-THC codrug (c) and morphine (d) in rat plasma (trunk plasma)

5.3.2 Dose-response curve analysis for the Cod-THC codrug in plasma samples

The mean concentration versus time profiles for 5, 10 and 20 mg/kg doses of Cod-THC codrug after oral administration are shown in Fig. 5.8. As can be seen, in all the three doses, the Cod-THC codrug is hydrolyzed in the plasma to release the parent drugs. The hydrolysis is not complete, as codrug can be seen along with the parent drugs at all time points. These data also show a prolonged release of the parent drugs from the codrug over time. The release of the parent drugs from the codrug occurs in an equimolar ratio. At any time point in the time course, the codrug concentration is lower than that of

either of the parent drugs, indicating the presence of mainly parent drugs compared to codrug.

Since the codrug is being hydrolyzed in the plasma and releasing parent drugs in 1:1 ratio, this suggests that there is likely no stable intermediate codrug fragment being formed, and even if such an intermediate is forming, it is transient and is getting hydrolyzed very quickly to release the parent drugs concomitantly. The pharmacokinetic parameters for Cod-THC, codeine and Δ^9 -THC for the 5, 10, and 20 mg/kg doses are summarized in Table 5.1. Following oral administration of the 5 and 10 mg/kg doses of Cod-THC codrug, plasma levels of codeine and Δ^9 -THC reached C_{max} within 1 hr. For the 20 mg/kg dose there was a slight plateau from 2-4 hrs. This might be due to plasma enzyme saturation, which would decrease the rate of hydrolysis of the codrug. The data clearly show a dose-dependent relationship, since the AUC for the codrug, as well as for the parent drugs, increased linearly with increasing dose of codrug.

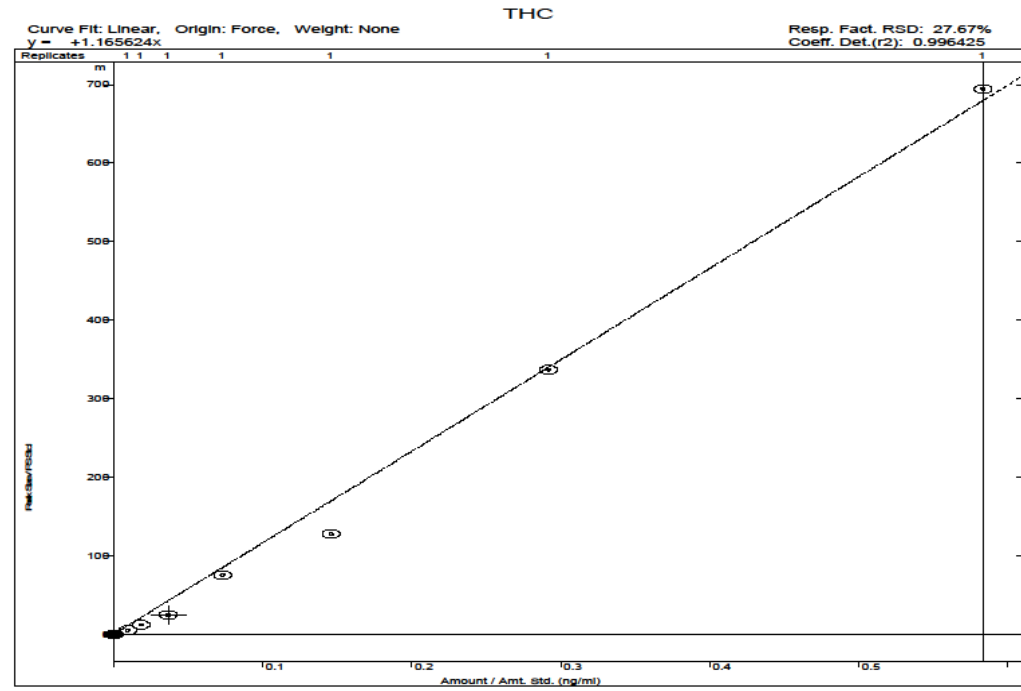


(a)

Print Date: 16 Jan 2010 13:27:11

Calibration Curve Report

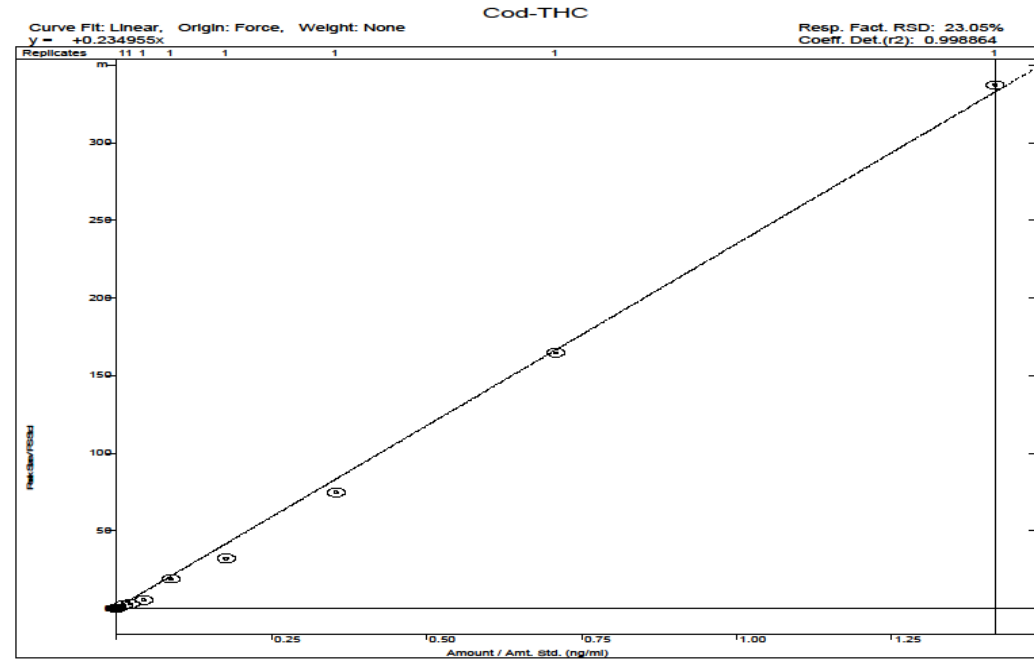
File: c:\varian\ms\methods\harpreet\cod_the_morph_brain_hd_121609.mth
Detector: 1200 Mass Spec, Address: 42



Print Date: 16 Jan 2010 13:28:41

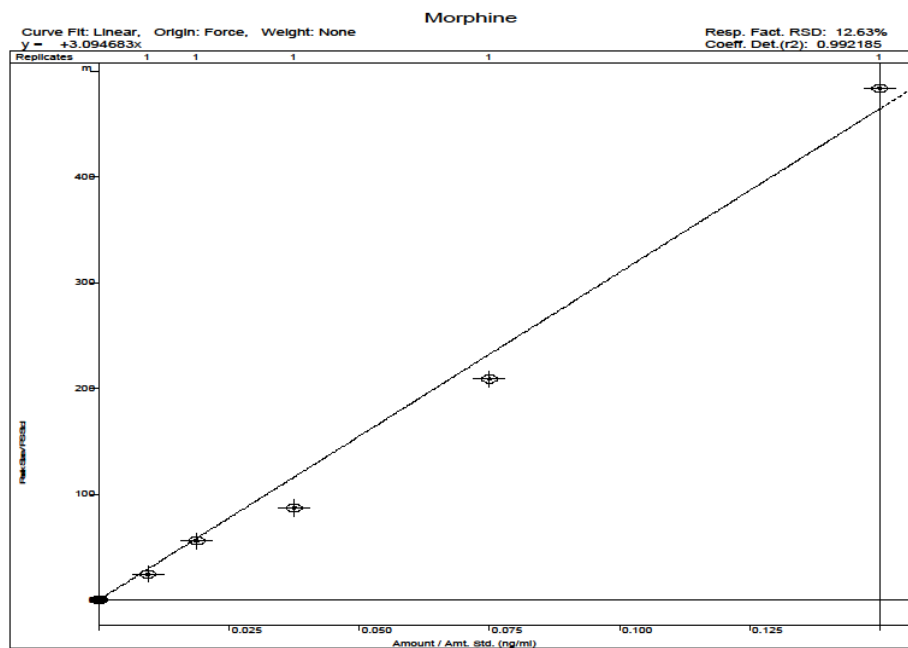
Calibration Curve Report

File: c:\varian\ms\methods\harpreet\cod_the_morph_brain_hd_121609.mth
Detector: 1200 Mass Spec, Address: 42



(c)

Print Date: 16 Jan 2010 13:36:08
Calibration Curve Report
File: c:\varian\sw\methods\harpreet\morph_brain_hd_010610.mth
Detector: 1200 Mass Spec, Address: 42



(d)

Fig. 5.6 Calibration Curves for codeine, Δ^9 -THC, Cod-THC codrug and morphine in brain homogenate

Chromatogram Plots

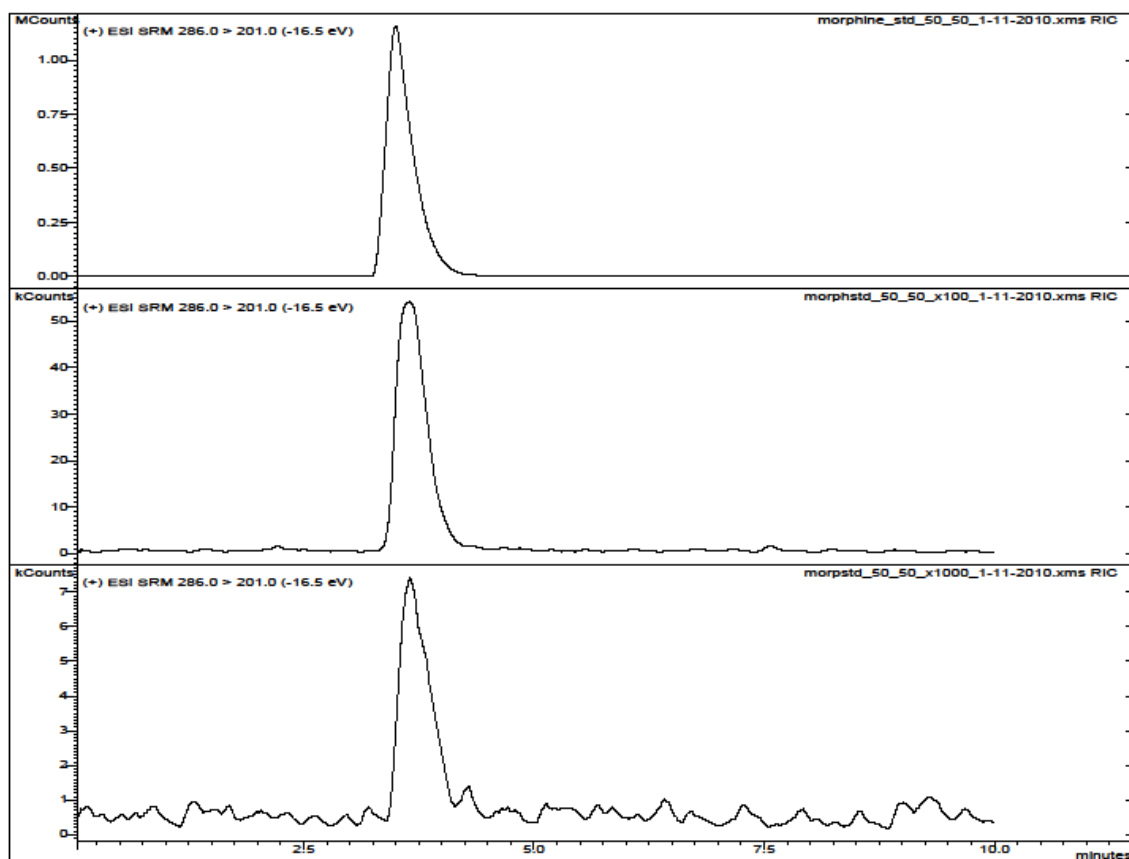


Fig. 5.7 Morphine peaks generated from different concentrations (3000, 300 and 3 ng/mL from the top) using slightly different LC-MS/MS method (0.05% of HFBA was added to both aqueous and organic solvents as compared to 0.025% in the previously described method).

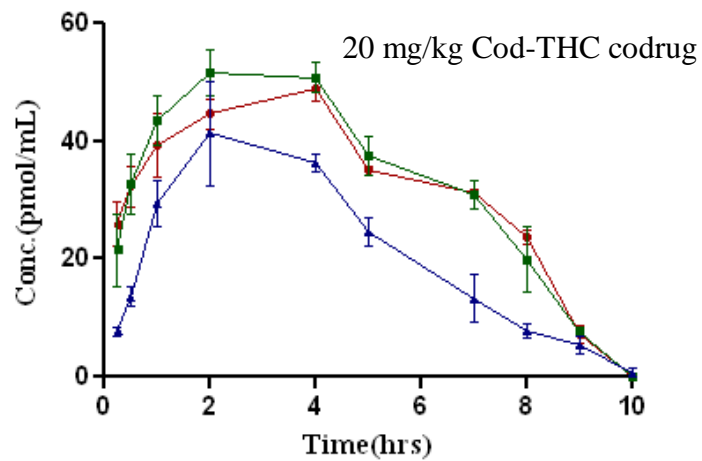
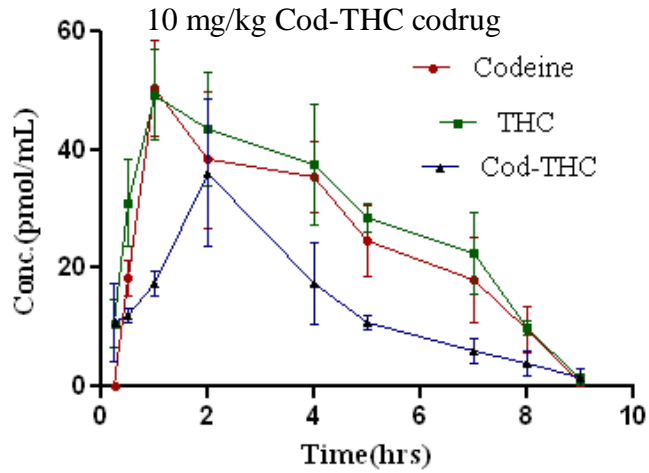
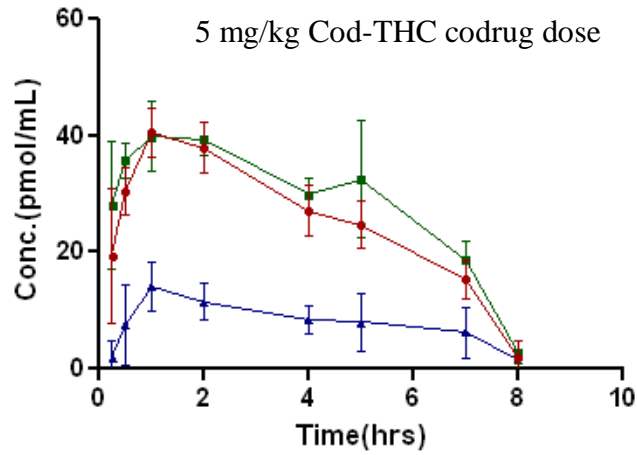


Fig. 5.8 Plasma concentration vs. time curve after oral administration of Cod-THC codrug (5, 10 and 20 mg/kg doses)

Table 5.1 (a) Pharmacokinetic parameters for the Cod-THC codrug, codeine and Δ^9 -THC after 5, 10, 20 mg/kg oral dosing

	Dose	AUC (hr* pmol/mL)	T _{max} (hr)	C _{max} (pmol/mL)	T _{1/2} (hr)
Codrug (Actual)	5 mg/kg	90.9 ± 17.4	1 ± 0.1	14.16 ± 4.64	4.24 ± 0.33
	10 mg/kg	199.7 ± 29.3	2 ± 0.1	24.4 ± 2.96	4.43 ± 0.25
	20 mg/kg	326.5 ± 37.4	4 ± 0.2	31.95 ± 6.14	4.57 ± 0.39
Δ^9- THC	5 mg/kg	281.7 ± 22.8	1 ± 0.1	39.8 ± 2.32	2.3 ± 0.37
	10 mg/kg	375.3 ± 18.2	1 ± 0.2	48.1 ± 3.18	4.0 ± 0.46
	20 mg/kg	474.2 ± 25.6	2.5 ± 0.3	56.4 ± 3.41	4.9 ± 0.44
Codeine	5 mg/kg	218.0 ± 19.6	1 ± 0.1	40.46 ± 2.75	2.4 ± 0.29
	10 mg/kg	318.0 ± 23.8	1 ± 0.3	49.17 ± 3.41	2.5 ± 0.38
	20 mg/kg	374.2 ± 28.3	3 ± 0.2	57.39 ± 3.97	4.1 ± 0.42

Table 5.1 (b) Calculated clearance values for the Cod-THC codrug, codeine and Δ^9 -THC

	Clearance (mL/min)
Cod-THC Codrug	35.3
Codeine	55.6
Δ^9 -THC	28.5

5.3.3 Codrug and physical mixture data comparison after oral administration

The mean concentration *versus* time profile for the 10 mg/kg dose of the physical mixture (i.e. 4.9 mg/kg codeine and 5.1 mg/kg Δ^9 -THC) after oral administration is shown in Fig. 5.9. For comparison, the 10 mg/kg Cod-THC codrug graph is also displayed in the same figure. The plasma concentrations of codeine and Δ^9 -THC are much higher after codrug administration compared to the plasma concentrations of these drugs after administration of an equimolar physical mixture. The parent drugs are clearly released from the codrug in 1:1 ratio, while administration of the physical mixture does not afford equimolar concentrations of codeine and Δ^9 -THC in plasma. This is likely due

to the different pharmacokinetic profiles of the two parent drugs and to the different pharmacokinetic profile of the Cod-THC codrug. The parent drugs are also present in plasma for longer period of time after oral administration of the codrug, probably due to the sustained release of the parent drugs from codrug in the plasma. When the pharmacokinetic parameters of an equimolar physical mixture of codeine and Δ^9 -THC were calculated and compared with that of an equimolar dose of codrug after oral administration, a significantly higher AUC for codeine and Δ^9 -THC was observed from the codrug than from the physical mixture of the parent drugs.

The oral bioavailability of codeine and Δ^9 -THC can be calculated from the AUC values from the oral dose (4.9 mg/kg codeine + 5.1 mg/kg Δ^9 -THC) and the AUC from the i.v. dose of the physical mixture (0.49 mg/kg codeine + 0.51 mg/kg Δ^9 -THC). The calculated bioavailability for codeine was 2.9 ± 1.4 % and the bioavailability for Δ^9 -THC was 3.0 ± 1.8 %.

Calculation of the oral bioavailability of the codrug is not straight-forward because of the time-dependent hydrolysis of the codrug to the parent compounds in the plasma. Thus, two bioavailability values for the codrug can be calculated, i.e. the “actual” codrug bioavailability, and the “total” codrug bioavailability. The actual codrug bioavailability is based on the amount of actual codrug present in the plasma; whereas the total codrug bioavailability is calculated assuming no hydrolysis of the codrug has taken place in the plasma. The total bioavailability value represents an approximation of the total amount of the codrug entering the systemic circulation after oral dosing. The actual codrug bioavailability was calculated to be 7.7 ± 3.8 %, and the total codrug bioavailability was found to be 21.1 ± 7.9 %. Since the total codrug bioavailability is much higher than the bioavailabilities of either of the parent drugs after oral administration of the physical mixture, this shows that more of parent drugs can be delivered orally in the form of the codrug than as a physical mixture. It should be noted that the total codrug bioavailability value may be underestimated, since the clearance parameters are not taken into account for the parent drugs (shown in Table 5.1 (b)).

Certainly, the data clearly indicates that the codrug has a superior pharmacokinetic profile when compared to the physical mixture of the two parent drugs.

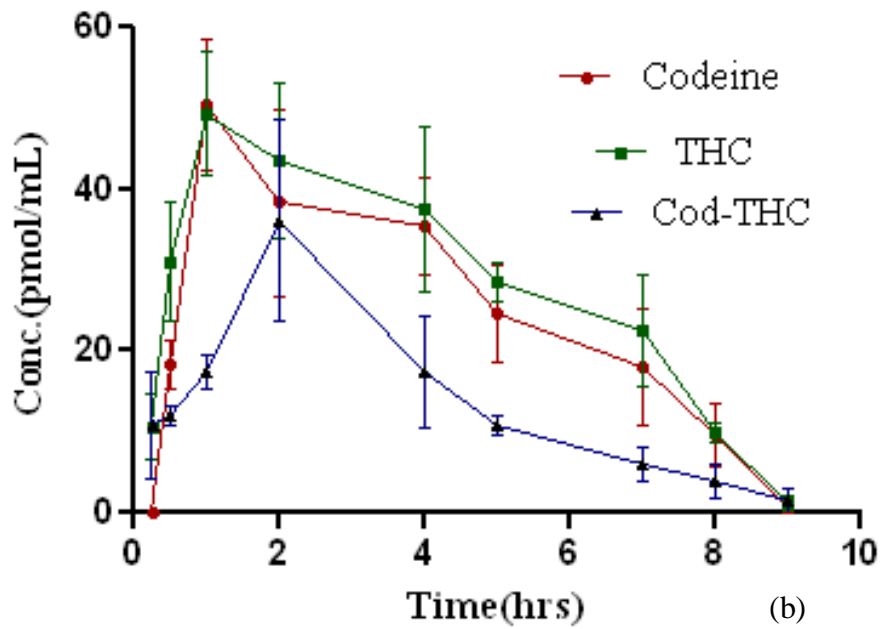
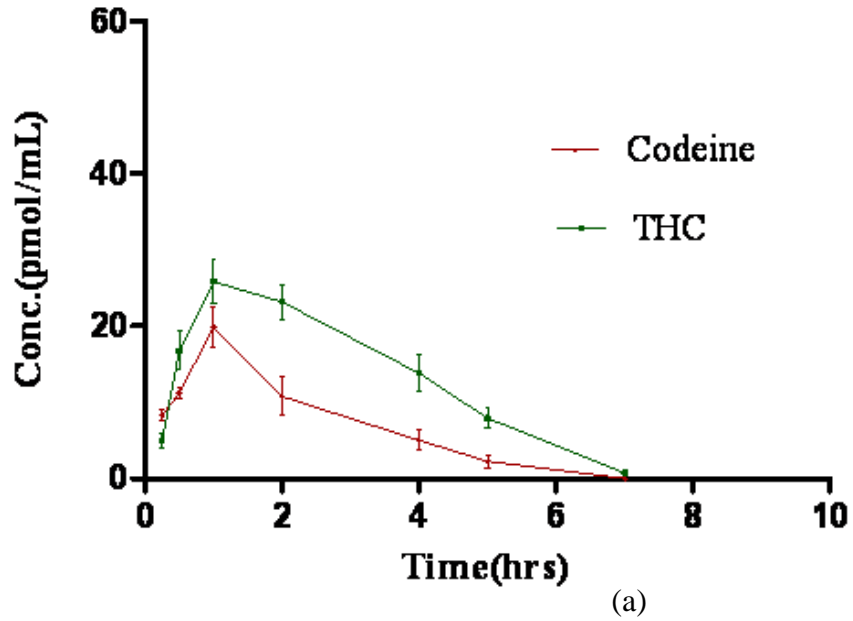


Fig. 5.9 Physical mixture of Codeine (4.9 mg) and Δ^9 -THC (5.1 mg) (a); Codrug 10 mg/kg (b)

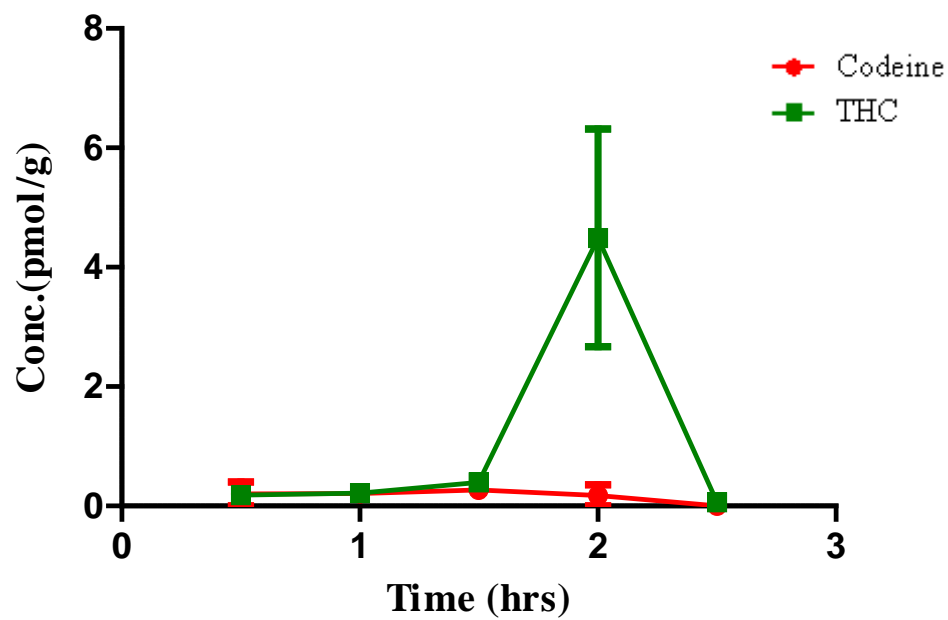
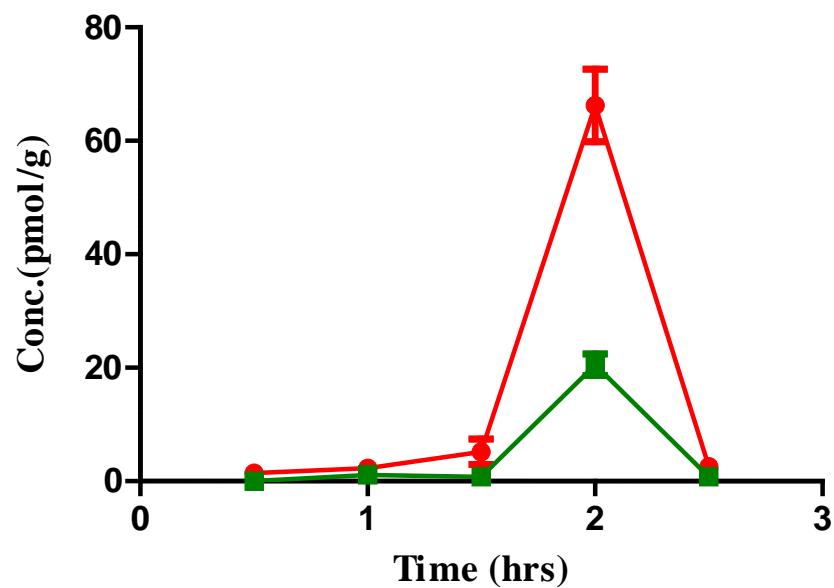


Fig. 5.10 Concentration vs. Time profile for Cod-THC (10 mg/kg dose) (a) and Physical mixture (Cod 4.9 mg/kg + Δ^9 -THC 5.1 mg/kg) (b) in brain after oral dosing

5.3.4 Brain Uptake Study Results

After oral administration of 10 mg/kg dose of the Cod-THC codrug, brain samples were analysed at different time points (0, 0.5, 1, 1.5, 2, and 2.5 hrs). The results of the analysis of the brain homogenate samples showed the presence of only the parent drugs; no codrug was present in brain at any time point measured after oral dosing of the Cod-THC codrug.

Fig. 5.10 shows the time *versus* concentration profiles for the Cod-THC codrug (10 mg/kg) and the physical mixture (4.9 mg/kg codeine and 5.1 mg/kg THC) after oral administration. The concentration of codeine and Δ^9 -THC is much higher in brain after oral administration of the Cod-THC codrug as compared to the brain concentrations of these drugs after oral administration of the physical mixture. The concentrations of codeine and Δ^9 -THC in the brain reach a maximum at two hours after oral administration; it is important to note that t_{\max} is same for both codeine and Δ^9 -THC. This correlates with the study of the codrug in rat tail-flick pain model. In the case of the physical mixture, the Δ^9 -THC concentration is significantly higher than the codeine concentration in brain after oral administration. This might be attributable to the higher plasma concentration of Δ^9 -THC compared to codeine in plasma samples after oral administration of the physical mixture.

Thus from the pharmacokinetic data, it can be concluded that Cod-THC codrug is much more efficient in terms of delivering higher concentrations of the two parent drugs in both plasma and brain when compared to the equimolar physical mixture of the two parent drugs. This also proves that combining two drugs with different physicochemical and pharmacokinetic profiles into a single chemical entity can improve the plasma and brain bioavailabilities of the two parent drugs. It is also noticeable that oral administration of the codrug produces the two parent drugs in molar ratio while the physical mixture fails to do that.

Chapter 6

Summary

There is a continuing need for analgesic medications that are able to provide high efficacy pain relief while providing more favorable pharmacokinetics and reducing the possibility of undesirable side effects. Enhancement of the analgesic effect of opioids with cannabinoids has been previously described (Cichewicz et al., 1999). These opioid and cannabinoid drugs work via opioid and cannabinoid receptors, which are found throughout the central and peripheral nervous system. Synergy between Δ^9 -THC and opioids is well documented in the literature (Bloom and Dewey, 1978; Cichewicz and McCarthy, 2002). In addition, these two classes of drugs produce similar effects on calcium levels and cyclic AMP accumulation through G protein-mediated pathways. However, appropriate dosing of these active agents to the site of action, e.g., the brain or spinal column, can be difficult because of their differential pharmacokinetics. Therefore, in the present dissertation, a codrug strategy is presented for orally administering opioids and cannabinoids concomitantly to provide a more favorable pharmacokinetic and analgesic profile than would be attainable by administering equimolar amounts of the parent drugs as a physical mixture.

Codrugs are designed to overcome various barriers to drug formulation and delivery, such as poor or extreme aqueous solubility, chemical instability, insufficient absorption after oral administration, rapid pre-systemic metabolism, inadequate brain penetration, toxicity and local irritation. The first chapter in this dissertation demonstrates the usefulness of the codrug strategy by discussing several reported examples. The codrug strategy is very useful when the physico-chemical and/or pharmacokinetic properties of two synergistic drugs are not favorable for delivery as a physical mixture, but can be improved by chemical combination of the two drugs.

A series of novel codrugs obtained by chemical conjugation of the opiate drug codeine with Δ^9 -THC, cannabidiol, and *abn*-cannabidiol, and of the opiate prodrug 3-*O*-

acetylmorphine with Δ^9 -THC, utilizing a carbonate linker moiety, were successfully synthesized. Before commencing the synthetic work with the expensive opiate and cannabinoid controlled substances, coupling reactions were initially carried out with model compounds, or chemical mimics of the drug molecules, in order to optimize the desired coupling chemistry. *p*-Nitrophenylchloroformate, which has been described in the literature as a useful reagent for the formation of unsymmetrical carbonates and carbamates (Anderson and McGregor, 1957) was found to be a useful reagent in these subsequent model coupling reactions. In the current work, an opiate was initially reacted with *p*-nitrophenylchloroformate to form the carbonate conjugate of the opiate and *p*-nitrophenol. This intermediate was then reacted with different cannabinoids to form the carbonate ester conjugate (codrug) of the opiate and the cannabinoid. In this second step, the good leaving group property of the *p*-nitrophenol is advantageous in the selective formation of the desired unsymmetrical carbonate ester.

Marketed for p.o. administration as dronabinol (Marinol[®]), Δ^9 -THC is a schedule II drug currently used as an appetite stimulant in acquired immunodeficiency syndrome-wasting patients, and as an anti-emetic for cancer chemotherapy when given orally. Although high doses of Δ^9 -THC are analgesic, they can be accompanied by side effects, such as anxiety, dry mouth or euphoria/dysphoria. The opiate codeine is commonly given p.o., primarily to ease pain. However, the continued administration of codeine can lead to tolerance, which can ultimately reduce the analgesic effect of the drug, necessitating the administration of high and potentially harmful doses to achieve effective pain control. Also, high doses of codeine can have undesirable side effects such as respiratory depression, constipation, nausea and vomiting. Given that mixtures of Δ^9 -THC and codeine are synergistic in the rat tail-flick test for antinociception (Williams et al., 2006), we hypothesized that when given in the form of codrug, the administration of codeine and Δ^9 -THC would have improved pharmacokinetics that would enhance the efficacy of codeine in managing pain. Also, since codeine shows little or no effect on neuropathic pain, we further hypothesized that a Cod-THC codrug would also exhibit an analgesic effect in neuropathic pain models. Thus, we investigated the effect of the Cod-THC codrug after oral administration in nociceptive and neuropathic pain models utilizing tail-

flick and chronic constriction injury pain models in the rat. The oral efficacies of each of the parent drugs, codeine and Δ^9 -THC were also compared with the Cod-THC codrug as pain modulators in the above pain models to determine their relative effectiveness. In both pain models, the codrug showed better effectiveness, as well as more prolonged pain management properties, when compared to the parent drugs. ED₅₀ values for the Cod-THC codrug were much lower in tail flick and CCI models as compared to codeine. Cod-CBD codrug was also analysed for its analgesic effect using tail-flick test.

The Cod-THC codrug was initially evaluated for its stability in buffers ranging from pH 1 to pH 9, as well as in simulated gastric and intestinal fluids (SGF and SIF, respectively), and in rat plasma and brain homogenate. SGF simulates stomach fluid and incorporates acidic and enzymatic hydrolysis conditions. SIF mimics the intestinal enzymes. The stability of the codrug was determined in the following media utilizing an HPLC-UV assay.

- pH : Aqueous buffers (37 °C, pH 1-9)
- Gastrointestinal tract : Simulated gastric fluid (USP, 37 °C)
- Gastrointestinal tract : Simulated intestinal fluid (USP, 37 °C)
- Plasma : Rat plasma (37 °C)
- Brain homogenate (37 °C)

The codrug was found to have a favorable drug stability profile for oral administration, being stable in aqueous solutions over a wide range of physiologically relevant pHs from 1 to 7.4, and was also stable in SGF, SIF and rat brain homogenate. In rat plasma, the codrug was hydrolyzed to the two parent drugs, codeine and Δ^9 -THC with a rate constant of 0.282 hr⁻¹.

Results of the comprehensive stability study of the Cod-THC codrug in different non-enzymatic aqueous buffers and in biological media demonstrate that the carbonate

ester linkage of the codrug is predicted to be stable in the gastrointestinal tract when the codrug is administered orally. Hydrolysis of the carbonate ester linkage in 80% rat plasma showed that the codrug is enzymatically cleaved to generate the parent drugs, suggesting that after oral administration, and absorption from the gastrointestinal tract the codrug will generate both parent drugs in the systemic circulation (plasma). Linker design in the codrug synthesis has to be carried out in a thoughtful way such that the linker is not too chemically labile or too stable. Codrugs with labile linkers will not survive the harsh conditions of the gastrointestinal tract, and thus will hydrolyze in the gastrointestinal tract before the codrug reaches the systemic circulation. Codrugs with very stable linkers may reach the systemic circulation, but may not be capable of generating the parent drugs in the plasma. Thus, the choice of a carbonate ester linkage linking the allylic hydroxyl group of codeine and the phenolic group of Δ^9 -THC was found to be an ideal codrug linker design for oral administration. The stability of the Cod- Δ^9 -THC codrug in rat brain homogenate indicates that the enzymes present in rat brain homogenate are incapable of cleaving the codrug into the parent drugs. Therefore, this study predicts that any codrug entering the brain from the systemic circulation will not be transformed into the parent drugs. Thus, if oral administration of the codrug to rats results in the presence of the parent drug molecules in brain, then these parent drugs must have entered the brain as the individual parent drug molecules from the systemic circulation, and did not originate through hydrolysis of the codrug in the brain.

The pharmacokinetic profile of the Cod-THC codrug was evaluated in the rat after oral administration and compared with the pharmacokinetic profile of the physical mixture of the parent drugs. Several groups have reported the low bioavailability of THC (2 to 6%) and codeine (4 to 8%) after oral administration in rats, due to poor absorption from the gastrointestinal tract (Chiang and Barnett, 1984; Shah and Mason, 1990). Therefore, rat plasma and brain concentrations, of the Cod-THC codrug were determined after oral and i.v. administration utilizing an LC-MS/MS analytical methodology. These properties were compared with those obtained after oral administration of an equimolar physical mixture of the two parent drugs, codeine and Δ^9 -THC.

The plasma concentrations of codeine and Δ^9 -THC were found to be much higher after oral administration of the codrug in the rat, compared to plasma concentrations of these drugs after oral administration of the equimolar physical mixture of the two parent drugs. The parent drugs were clearly released from the codrug molecule in 1:1 ratio in plasma, while administration of the physical mixture did not afford equimolar concentrations of codeine and Δ^9 -THC in the plasma. This is likely due to the different pharmacokinetic profiles of the two parent drugs, and to the different pharmacokinetic profile of the Cod-THC codrug. Also, the parent drugs were present in plasma for a longer period of time after oral administration of codrug, probably due to the sustained release of the parent drugs from the codrug in the plasma. The actual codrug bioavailability was calculated to be $7.7 \pm 3.8 \%$, and the total codrug bioavailability was found to be $21.1 \pm 7.9 \%$. Since the total codrug bioavailability is much higher than the bioavailabilities of either of the parent drugs after oral administration of the physical mixture, this shows that more of parent drugs can be delivered orally in the form of the codrug than as a physical mixture. It should be noted that the total codrug bioavailability value may be underestimated, since the clearance parameters are not taken into account for the parent drug. But still, the data clearly indicates the superior pharmacokinetic profile of a codrug as compared to the physical mixture of the two parent drugs.

The time versus concentration profiles for the Cod-THC codrug and the equimolar physical mixture were generated to determine the concentrations of the parent drugs in the brain after oral administration. The Cod-THC codrug was not detected in the brain, which indicates that the hydrolysis of the codrug is taking place in the plasma, and then the parent drugs cross the blood-brain-barrier to exert their effect. The concentrations of codeine and Δ^9 -THC were much higher in brain after oral administration of the Cod-THC codrug as compared to brain concentrations of these drugs after oral administration of the physical mixture. The concentrations of codeine and Δ^9 -THC in the brain reach a maximum at two hours after oral administration. This correlates with the study of the codrug in the pain models. The Δ^9 -THC concentration was found to be higher than the codeine concentration in brain after oral administration of the physical mixture while the concentration of codeine was higher in the brain after oral

administration of the codrug. This may be attributed to the higher plasma concentration of Δ^9 -THC compared to codeine in plasma samples after oral administration of the physical mixture.

The above data indicate that oral administration of a codeine- Δ^9 -THC codrug could be useful therapeutic delivery strategy to enhance the pain modulating properties of codeine. Thus, if extrapolatable to humans, following opioid administration in the form of an opioid-THC codrug, patients might require a lower dose of opioid, need fewer administrations of the opioid to control pain, and subsequently experience fewer side effects. Not only that, in cancer chemotherapy, where opioids show little or no effect in managing chemotherapeutically-induced neuropathic pain, the codrug approach of combining an opioid with a THC may be a better substitute for codeine alone, since it would be effective in managing a broader spectrum of pain.

Thus, this study proves the hypothesis that a codrug of an opiate and a cannabinoid can be synthesized, which is stable in gastrointestinal tract and shows a superior pharmacokinetic profile when compared to a physical mixture of the two parent drugs that make up the codrug. Also, an enhanced pharmacological effect of the codrug can be achieved compared to that of the two parent drugs.

References:

Anderson GW, McGregor AC (1957) *t*-Butyloxycarbonylamino acids and their use in peptide synthesis. *J Am Chem Soc* 79:6180-6183

Ascher JA, Cole JO, Colin JN, Feighner JP, Ferris RM, Fibiger HC, Golden RN, Martin P, Potter WZ, Richelson E (1995) Bupropion: a review of its mechanism of antidepressant activity. *J Clin Psychiatry* 56:395–401

Baltzer B, Binderup E, von Daehne W, Godtfredsen WO, Hansen K, Nielsen B, Sørensen H, Vangedal S (1980) Mutual pro-drugs of beta-lactam antibiotics and beta-lactamase inhibitors. *J Antibiot* 10:1183–1192

Bars DL, Gozariu M, Cadden SW (2001) Animal models of nociception. *Pharmacol Rev* 53:597–652

Bennett GJ, Xie YK (1988) A peripheral neuropathy in rat that produces disorders of pain sensation like those seen in man. *Pain* 33:87-107

Berenbaum MC (1989) What is synergy? *Pharmacol Rev* 41:93-141

Bidaut-Russell M, Howlett A (1988) Opioid and cannabinoid analgetics both inhibit cyclic AMP production in the rat striatum, in *Advances in the biosciences*. Pergamon Press, Oxford

Biewenga GP, Haenen G, Bast A (1997) The pharmacology of the antioxidant lipoic acid. *Gen Pharmacol* 29:315–331

Bloom AS, Dewey WL (1978) A comparison of some pharmacological actions of morphine and Δ^9 -Tetrahydrocannabinol in the mouse. *Psychopharmacology* 57:1432-2072

Bolla M, Almirante N, Benedini F (2005) Therapeutic potential of nitrate esters of commonly used drugs. *Curr Top Med Chem* 5:707-720

Burk RM, Roof MB (1993) Safe and efficient method for conversion of 1,2- and 1,3-diols to cyclic carbonates using triphosgene. *Tetrahedron Lett* 34:395-398

Chen J, Pettit, S, Fliri, H (2007) Abnormal cannabidiols as agents for lowering intraocular pressure. US Patent 2007/0249731A1

Chiang CN, Barnett, G (1984) Marijuana effect and delta-9-tetrahydrocannabinol plasma level. *Clin Pharmacol Ther* 6:234-238

Choi YH, Hazekamp A, Peltenburg-Looman AMG, Frederich M, Erkelens C, Lefeber AWM, Verpoorte R (2004) NMR assignments of the major cannabinoids and cannabiflavonoids isolated from flowers of *cannabis sativa*. *Phytochem Anal* 15:345-354

Cichewicz DL, Haller VL, Welch SP (2001) Changes in opioid and cannabinoid receptor protein following short-term combination treatment with Δ^9 -tetrahydrocannabinol and morphine. *J Pharmacol Exp Ther* 297:121–127

Cichewicz DL, Martin ZL, Smith FL, Welch SP (1999) Enhancement of μ opioid antinociception by oral Δ^9 -Tetrahydrocannabinol: dose-response analysis and receptor identification *J Pharmacol Exp Ther* 289:859–867

Cichewicz LD, McCarthy EA (2002) Antinociceptive synergy between delta(9)-tetrahydrocannabinol and opioids after oral administration. *J Pharmacol Exp Ther* 304:1010-1015

Cichewicz DL, Welch SP (2003) Modulation of oral morphine antinociceptive tolerance and naloxone-precipitated withdrawal signs by oral Δ^9 -tetrahydrocannabinol. *J Pharmacol Exp Ther* 305:812–817

Cichewicz LD (2004) Synergistic interactions between cannabinoid and opioid analgesics. *Life Sci* 74:1317-1324

Cooper BR, Wang CM, Cox RF, Norton R, Shea V, Ferris RM (1994) Evidence that the acute behavioral and electrophysiological effects of bupropion (Wellbutrin) are mediated by a noradrenergic mechanism. *Neuropsychopharmacology* 11:133–141

Copeland RL (2009) www.med.howard.edu/pharmacology

Cox ML, Haller VL, Welch SP (2007) Synergy between Δ^9 -tetrahydrocannabinol and morphine in the arthritic rat. *Eur J Pharmacol* 567:125–130

Crooks PA, Houdi AA, Kottiyil SG, Butterfield DA (2002) Morphine-6-sulfate analogues and their use for the treatment of pain. US Patent 6403602B1

Csont T, Ferdinandy P (2005) Cardioprotective effects of glyceryl trinitrate: beyond vascular nitrate tolerance. *Pharmacol Therapeut* 105:57-68

Cynkowska G, Cynkowski T, Al-Ghananeem A, Guo H, Ashton P, Crooks AP (2005) Novel antiglaucoma prodrugs and codrugs of ethacrynic acid. *Bioorg Med Chem Lett* 15:3524-3527

D'Amour FE, Smith DL (1941) A method for determining loss of pain sensation. *J Pharmacol Exp Ther* 72:74-79

de Abreu FC, Lopes AO, Pereira MA, De Simone CA, Goulart MOF (2002) Nitrooxyquinones: Synthesis, X-ray diffraction and electrochemical series. *Tet Lett* 43:8153-8157

DeBeer EJ, Johnston CH, Wilson DW (1935) The composition of intestinal secretions. *J Biol Chem* 108:113-120

de la Hoz A, Diaz-Ortiz A, Moreno A (2005) Microwaves in organic synthesis. Thermal and non-thermal microwave effects. *Chem Soc Rev* 34:164-178

Dunlap T, Chandrasena REP, Wang Z, Sinha V, Wang Z, Thatcher GRJ (2007) Quinone formation as a chemoprevention strategy for hybrid drugs: balancing cytotoxicity and cytoprotection. *Chem Res Toxicol* 20:1903-1912

Gasco A, Fruttero R, Rolando B (2005) Focus on recent approaches for the development of new No-donors. *Mini-Rev Med Chem* 5:217-229

Grinberg L, Fibach E, Amer J, Atlas D (2005) N-Acetylcysteine amide, a novel cell-permeating thiol, restores cellular glutathione and protects human red blood cells from oxidative stress. *Free Radical Biol Med* 38:136-145

Gu H, Kill-Gore JK, Duchek JR (2004) Process for preparation of (+)-p-Mentha-2,8-diene-1-ol. *International Patent* 2004/096740A2

Gustafson RA, Kim I, Stout PR, Klette KL, George MP, Moolchan ET, Levine B, Huestis MA (2004) Urinary pharmacokinetics of 11-nor-9-carboxy-delta⁹-tetrahydrocannabinol after controlled oral delta 9-tetrahydrocannabinol administration. *J Anal Toxicol* 28:160-167

Gutman AL, Nisnevich GA, Rukhman I, Tishin B, Etinger M, Fedotev I, Pertosokov B, Khanolkar R (2006) Methods for purifying trans(-)- Δ^9 -tetrahydrocannabinol and trans-(+)- Δ^9 -tetrahydrocannabinol. *International Patent* 2006/053766A1

Haenen G, Bast A (1991) Scavenging of hypochlorous acid by lipoic acid. *Biochem Pharmacol* 42:2244-2246

Hamad MO, Kiptoo PK, Stinchcomb AL, Crooks PA (2006) Synthesis and hydrolytic behavior of two novel tripartate codrugs of naltrexone and 6 β -naltrexol with hydroxybupropion as potential alcohol abuse and smoking cessation agents. *Bioorgan Med Chem* 14:7051-7061

Hammond CL, Lee TK, Ballatori N (2001) Novel roles for glutathione in gene expression, cell death, and membrane transport of organic solutes. *J Hepatol* 34:946–954

Hartley S, Wise R (1982) A three-way crossover study to compare the pharmacokinetics and acceptability of sultamicillin at two dose levels with that of ampicillin. *J Antimicrob Chemother* 10:49-55

Hogan Q (2002) Animal Pain Models. *Region Anesth and Pain M* 27:385-401

Hohmann AG, Briley EM, Miles H (1999) Pre- and postsynaptic distribution of cannabinoid and mu opioid receptors in rat spinal cord. *Brain Res* 822:17-25

Holtman JR, Crooks PA, Dhooper HK (2006) Novel synergistic opioid-cannabinoid codrug for pain management. US Patent 2008/0176885A1.

Horwitz LD (2003) Bucillamine: a potent thiol donor with multiple clinical applications. *Cardiovasc Drug Rev* 21:77–90

Howard M, Al-Ghananeem A, Crooks PA (2007) A novel chemical delivery system comprising an ocular sustained release formulation of a 3 α , 17 α , 21-trihydroxy-5 β -pregnan-20-one-BIS-5-Flouroucil codrug. *Drug Dev Ind Pharm* 33:677-682

Howard-Sparks M, Al-Ghananeem AM, Pearson AP, Crooks PA (2005) Evaluation of O^{3 α} -, O²¹-Di-(N¹-methyloxycarbonyl-2,4-dioxo-5-fluoropyrimidinyl)17 α -hydroxy-5 β -pregnan-20-one as a novel potential antiangiogenic codrug. *J Enzym Inhib Med Ch* 20:417–428

Howelett CA, Barth F (2002) International Union of Pharmacology XXVII. Classification of cannabinoid receptors. *Pharmacol Rev* 54:161-202

Hulsman N, Medema JP, Bos C, Jongejan A, Leurs R, Smit MJ, de Esch IJP, Richel D, Wijtmans M (2007) Chemical insights in the concept of hybrid drugs: The antitumor effect of nitric-oxide-donating Aspirin involves a quinone methide but not nitric oxide nor aspirin. *J Med Chem* 50:2424-2431

Jhaveri MD, Sagar DR, Elmes SJR, Kendall DA, Chapman V (2007) Cannabinoid CB2 receptor-mediated anti-nociception in models of acute and chronic pain. *Mol Neurobiol* 36:26–35

Joshi KS, Honore P (2006) Animal models of pain for drug discovery. *Expert Opin Drug Dis* 14:323-334

Kern EH, Di L (2008) *Drug-like properties: concepts, structure design and methods.* Elsevier, Oxford

Kiptoo PK, Hamad MO, Crooks PA, Stinchcomb AL (2006) Enhancement of transdermal delivery of 6-beta-naltrexol via a codrug linked to hydroxybupropion. *J Control Release* 113:137–145

Kiptoo PK, Paudel KS, Hammell DC, Hamad MO, Crooks PA, Stinchcomb AL (2008) *In vivo* evaluation of a transdermal codrug of 6-β-naltrexol linked to hydroxybupropion in hairless guinea pigs. *J Pharm Sci* 33:371–379

Leppanen J, Huuskonen J, Nevalainen T, Gynther J, Taipale H, Jarvinen T (2002) Design and synthesis of a novel L-Dopa–entacapone codrug. *J Med Chem* 45:1379-1382

Lipinski CA, Lombardo F, Dominy BW, Feeney PJ (2001) Experimental and computational approaches to estimate solubility and permeability in drug discovery and development settings. *Adv Drug Deliver Rev* 46:3–26

Martelli A, Rapposelli S, Calderone V (2006) NO-releasing hybrids of Cardiovascular drugs. *Curr Med Chem* 13:609-625

Martin MW, Newcomb J, Nunes JJ, McGowan DC, Armistead DM, Boucher C, Buchanan JL, Buckner W, Chai L, Elbaum D, Epstein LF, Faust T, Flynn S, Gallant P, Gore A, Gu Y, Hsieh F, Huang X, Lee JH, Metz D, Middleton D, Mohn D, Morgenstern K, Morrison MJ, Novak PM, Oliveira-dos-Santos A, Powers D, Rose P, Schneider S, Sell S, Tudor Y, Turci SM, Welcher AA, White RD, Zack D, Zhao H, Zhu L, Napier XS, Power E (2006) Novel 2-aminopyrimidine carbamates as potent and orally active inhibitors of Lck: synthesis, SAR, and in vivo anti-inflammatory activity. *J Med Chem* 49:4981-4991

Martínez M, Martínez N, Hernández AI, Ferrández ML (1999) Hypothesis: Can N-acetylcysteine be beneficial in Parkinson's disease? *Life Sci* 64:1253–1257

McGilveray IJ (2005) Pharmacokinetics of cannabinoids. *Pain Res Manag* 10:15A–22

Mogil JS (2009) Animal models of pain: progress and challenges. *Nat Rev Neurosci* 10:283-294

Nudelman A, Shpaisman IG, Terasenko I, Ron H, Savitsky K, Geffen Y, Weizman A, Rephaeli A (2008) A mutual prodrug ester of GABA and perphenazine exhibits antischizophrenic efficacy with diminished extrapyramidal effects. *J Med Chem* 51:2858-2862

Offen D, Ziv I, Sternin H, Melamed E, Hochman A (1996) Prevention of dopamine-induced cell death by thiol antioxidants: possible implications for treatment of Parkinson's disease. *Exp Neurol* 141:32–39

Omar FA (1998) Cyclic amide derivatives as potential prodrugs. Synthesis and evaluation of N-hydroxymethylphthalimide esters of some non-steroidal anti-inflammatory carboxylic acid drugs. *Eur J Med Chem* 33:123-131

Packer L, Witt EH, Tritschler HJ (1995) Alpha-Lipoic acid as a biological antioxidant. *Free Radic Biol Med* 19:227–250

Pan H, Wu Z, Zhou H, Chen S, Zhang H, Li D (2008) Modulation of pain transmission by G protein-coupled receptors. *Pharmacol Therapeut* 117:141-161

Pardridge WM (2001) *Brain Drug Targeting: The Future of Brain Drug Development*. Cambridge University Press, Cambridge

Patacchioli RF (2004) Neuropharmacology of cannabinoid system: From basic science to clinical applications. *Curr Neuropharmacol* 2:1-7

Patrick GL (1995) *An introduction to medicinal chemistry*. Oxford University Press, Oxford

Piera S, Iannitelli A, Cerasa SL, Cacciatore I, Cornacchia C, Giorgioni G, Ricciutelli, M, Nasuti C, Cantalamessa F, Stefano DA (2008) New L-dopa codrugs as potential antiparkinson agents. *Arch Pharm Chem Life Sci* 341:412-417

Pinnen F, Cacciatore I, Cornacchia C, Sozio P, Cerasa SL, Iannitelli A, Nasuti C, Cantalamessa F, Sekar D, Gabbianelli R, Falcioni LM, Stefano DA (2009) Codrugs linking L-dopa and sulfur-containing antioxidants: new pharmacological tools against Parkinson's disease. *J Med Chem* 52:559-563

Piper DW, Macoun ML, Builder JE, Fenton BH (1963) Nonproteolytic enzymes in gastric juice. *Digest Dis Sci* 8:701-708

Raffa RB, Clark-Vetri R, Tallarida RJ, Wertheimer (2003) Combination strategies for pain management. *4:1697-1708*

Randall LO, Selitto JJ (1957) A method for measurement of analgesic activity on inflamed tissue. *Arch Int Pharmacodyn* 61:409–419

Reche I, Fuentes AJ, Ruiz-Gayo M (1996) Potentiation of Δ^9 -tetrahydrocannabinol induced analgesia by morphine in mice: involvement of μ - and κ -opioid receptors. *Eur J Pharmacol* 318:11-16

Razdan RK, Dalzell HC, Handrick GR (1974) Hashish.¹ A simple one-step synthesis of (-)- Δ^1 -tetrahydrocannabinol (THC) from p-Mentha-2,8-dien-1-ol and olivetol. *J Am Chem Soc* 96:5860-5865

Rickards RW, Watson WP (1980) Conversion of (+)-(R)-Limonene into (+)-(1S,4R)-p-Mentha-2,8-dien-1-ol, an intermediate in the synthesis of tetrahydrocannabinoids. *Aust J Chem* 33:451-454

Rotha LB, Willins LD, Kroeze KW (1998) G protein-coupled receptor-GPCR trafficking in the central nervous system: relevance for drugs of abuse. *Drug Alcohol Depen* 51:73-85

Rukstalis MR, Stromberg MF, O'Brien CP, Volpicelli JR (2000) 6- β -Naltrexol reduces alcohol consumption in rats. *Alcohol Clin Exp Res* 24:1593–1596

Sanchez C, Hyttel J (1999) Comparison of the effects of antidepressants and their metabolites on reuptake of biogenic amines and on receptor binding. *Cell Mol Neurobiol* 19:467–489

- Scholz J, Woolf CJ (2002) Can we conquer pain? *Nature Neurosci* 5:1062-1067
- Silverman RB (2004) *The organic chemistry of drug design and drug action*. 2nd edn, Elsevier, Oxford
- Shah J, Mason DW (1990) Pharmacokinetics of codeine after parenteral and oral dosing in the rat. *Drug Metab Dispos* 18:670-673
- Slemmer JE, Martin BR, Damaj MI (2000) Bupropion is a nicotinic antagonist. *J Pharmacol Exp Ther* 295:321-327
- Smith DA, van de Waterbeemd H, Walker DK, Mannhold R, Kubinyi H, Timmerman H (2001) *Pharmacokinetics and Metabolism in Drug Design*. Wiley-VCH Verlag GmbH
- Smith PA, Selley DE, Sim-Selley LJ, Welch SP (2007) Low dose combination of morphine and Δ^9 -tetrahydrocannabinol circumvents antinociceptive tolerance and apparent desensitization of receptors. *Eur J Pharmacol* 571:129–137
- Smith FL, Cichewicz D, Martin ZL, Welch SP (1998) The enhancement of morphine antinociception in mice by Δ^9 -tetrahydrocannabinol. *Pharmacol Biochem Be* 60:559–566
- Stefano DA, Sozio P, Cocco A, Iannitelli A, Santucci E, Costa M, Pecci L, Nasuti C, Cantalamessa F, Pinnen F (2006) L-Dopa and dopamine-(R)- α -lipoic acid conjugates as multifunctional codrugs with antioxidant properties. *J Med Chem* 49:1486-1493 [1]
- Stefano DA, Sozio P, Cocco A, Iannitelli A, Santucci E, Costa M, Pecci L, Nasuti C, Cantalamessa F, Pinnen F (2007) Synthesis and study of L-dopa-glutathione codrugs as new anti-parkinson agents with free radical scavenging properties. *J Med Chem* 50:2506-2515

Stefano DA, Sozio P, Iannitelli A, Cocco A, Orlando G, Ricciutelli M (2006) Synthesis and preliminary evaluation of L-dopa/benserazide conjugates as dual acting codrugs. *Letters in Drug Design and Discovery* 3:747-752 [2]

Strasinger LC, Scheff NN, Stinchcomb LA (2008) Prodrugs and codrugs as strategies for improving percutaneous absorption. *Expert Rev Dermatol* 3:221-233

Tallarida RJ (2001) Drug Synergism: Its Detection and Applications. *J Pharmacol Exp Ther* 298:865–872

Thorn CF (2009) Codeine and morphine pathway. *Pharmacogenet Genomics* 19:556-558

van de Waterbeemd H, Gifford E (2003) ADMET in silico modelling: Towards prediction paradise? *Nature Reviews Drug Discovery* 2:192–204

Volpicelli JR, Alterman AI, Hayashida M, O'Brien CP (1992) Naltrexone in the treatment of alcohol dependence. *Arch Gen Psychiatry* 49:876–880

Wang D, Raehal KM, Bilsky EJ, Sadee W (2001) Inverse agonists and neutral antagonists at mu opioid receptor (MOR): possible role of basal receptor signaling in narcotic dependence. *J Neurochem* 77:1590–6000

Waterman KC, Adami RC, Alsante KM, Antipas AS, Arenson DR, Carrier R, Hong J, Landis MS, Lombardo F, Shah JC, Shalaev E, Smith SW, Wang H (2002) Hydrolysis in pharmaceutical formulations. *Pharm Dev Technol* 7:113-146

Welch SP, Eads M (1999) Synergistic interactions of endogenous opioids and cannabinoid systems. *Brain Res* 848:183–190

Williams J, Edwards S, Rubo A, Haller VL, Stevens DL, Welch SP (2006) Time course of the enhancement and restoration of the analgesic efficacy of codeine and morphine by Δ^9 -tetrahydrocannabinol. *Eur J Pharmacol* 539:57–63

Williams J, Haller VL, Stevens DL, Welch SP (2008) Decreased basal endogenous opioid levels in diabetic rodents: Effects on morphine and delta-9-tetrahydrocannabinoid-induced antinociception. *Eur J Pharmacol* 584:78–86

Woolf CJ (2004) Pain: moving from symptom control toward mechanism-specific pharmacologic management. *Ann Intern Med* 140:441-451

Woolf CJ, Salter MW (2000) Neuronal plasticity: increasing the gain in pain. *Science* 288:1765-1768

Vita

Born in New Delhi, India on March 5th, 1969

EDUCATION

Ph.D. in Chemistry, University of Kentucky, Lexington, KY.

Overall GPA: 3.57 Anticipated Graduation: May 2010

M.S. in Chemistry, Eastern Kentucky University, Richmond, KY.

Overall GPA: 4.0 Graduation: May 2005

Bachelor of Education in Teaching, Annamalai University, Madras, India.

Overall GPA: 3.5 Graduation: May 1992

Bachelor of Science in Chemistry, Delhi University, New Delhi, India.

Overall GPA: 3.7 Graduation: May 1990

COMPUTER SKILLS

Acrobat Reader, Microsoft Windows, Word, Excel, PowerPoint, Outlook, and Windows XP, Winonlin, Prism, Chemdraw, certification in Visual basic, Corel-draw, C language, COBOL

PUBLICATIONS

“Novel Synergistic Opioid-Cannabinoid Codrug for Pain Management”. By Joseph R. Holtman, Peter A. Crooks and Harpreet Dhooper, U.S. Patent Application Patent No. US2007176885, July 24th, 2008.

“Codrugs and Hybrid Drugs”. By Peter A. Crooks, Harpreet Dhooper and Ujjwal Chakraborty, in *Prodrugs and Targeted Delivery*, Edit Jarkko Rautio, Invited Chapter, Wiley-VCH, New York, 2009.

Synthesis, hydrolytic behavior and analgesic effect of Codeine and Δ^9 -THC codrug (in preparation)

Pharmacokinetic analysis of Codeine and Δ^9 -THC codrug using LC-MS/MS (in preparation)

PRESENTATIONS

“Preparation of a Synergistic Codrug of Codeine and Δ^9 -THC as a Potent Antinociceptive Agent”. Harpreet K. Dhooper, Joseph Holtman and Peter A. Crooks, *Twenty Second Annual Meeting and Exposition of the American Association of Pharmaceutical Scientists*, November, 2008, Atlanta, GA.

“Pharmacokinetic analysis of Opioid-Cannabinoid Codrug”. Harpreet K. Dhooper, Zaineb A. F. Albayati and Peter A. Crooks. *Twenty third Annual Meeting and Exposition of the American Association of Pharmaceutical Scientists*, November, 2009, Los Angeles, CA.

PROFESSIONAL AFFILIATIONS

AAPS American Association of Pharmaceutical Scientists

LICENSE AND CERTIFICATION

Kentucky Certified Science teacher